

Center for Integrative Physiology and Molecular Medicine  
Department of Physiology  
Faculty of Medicine  
University of Saarland, Homburg, Germany

# **Calcium-Dependent Activator Protein for Secretion Function in Murine Dorsal Root Ganglion Neurons**

**Dissertation zur Erlangung des Grades eines Doktors der Naturwissenschaften  
der Medizinischen Fakultät  
der UNIVERSITÄT DES SAARLANDES  
2016**

vorgelegt von: Ali H. H. Shaib  
Beirut - Libanon



## **Disclosure:**

This work was funded by:

The **Graduate school: Calcium Signalling and Cellular Nanodomains**

From: July 17, 2012 till June 30, 2015.

**CRC894**

From: July 1, 2015 till August 12, 2016.

All experiments were executed in the department of Cellular Neurophysiology, Prof. Dr. Jens Rettig, CIPMM – University of Saarland, 66421 Homburg; Germany.



UNIVERSITÄT  
DES  
SAARLANDES



Center for Integrative Physiology  
and Molecular Medicine



## Anlage I

### Erklärung gemäß § 7 Abs. 1 Nr. 4

Ich erkläre hiermit an Eides statt, dass ich die vorliegende Arbeit ohne unzulässige Hilfe Dritter und ohne Benutzung anderer als der angegebenen Hilfsmittel angefertigt habe. Die aus anderen Quellen direkt oder indirekt übernommenen Daten und Konzepte sind unter Angabe der Quelle gekennzeichnet.

Bei der Auswahl und Auswertung folgenden Materials haben mir die nachstehend aufgeführten Personen in der jeweils beschriebenen Weise unentgeltlich/entgeltlich geholfen:

1. PD Dr. Ute Becherer: War bei allen Experimenten und Planung beteiligt
2. Herr Ali Harb: War bei der Untersuchung von synaptischer Entwicklung und das Patchen von DRG Neuronen beteiligt.
3. Frau Margerete Klose: Hat bei der Preparation von zellulären Kulturen und Etablierung von Co-Kulturen mitgeholfen.
4. Herr Ahmed Shaaban: Half bei der durchführung von Western Blot.
5. Frau Angelina Staudt: und Frau Dr Becherer haben die STED daten aufgenommen und analysiert.
6. Prof. Dr. Ralf Mohrmann: War sowohl bei der Planung von Klonierungsstrategien als auch beim Schreiben von Makros in ImageJ zur Bildanalysebeteiligt.

Weitere Personen waren an der inhaltlich-materiellen Erstellung der vorliegenden Arbeit nicht beteiligt. Insbesondere habe ich nicht die entgeltliche Hilfe von Vermittlungs- bzw. Beratungsdiensten (Promotionsberater/innen oder anderer Personen) in Anspruch genommen. Außer den Angegebenen hat niemand von mir unmittelbar oder mittelbar geldwerte Leistungen für Arbeiten erhalten, die im Zusammenhang mit dem Inhalt der vorgelegten Dissertation stehen.

Die Arbeit wurde bisher weder im Inland noch im Ausland in gleicher oder ähnlicher Form in einem anderen Verfahren zur Erlangung des Doktorgrades einer anderen Prüfungsbehörde vorgelegt.

Ich versichere an Eides statt, dass ich nach bestem Wissen die Wahrheit gesagt und nichts verschwiegen habe.

Vor Aufnahme der vorstehenden Versicherung an Eides Statt wurde ich über die Bedeutung einer eidesstattlichen Versicherung und die strafrechtlichen Folgen einer unrichtigen oder unvollständigen eidesstattlichen Versicherung belehrt.

Ort, Datum

Thursday, April 18, 2016 - Homburg Saar

Unterschrift der/des Promovierenden



Digitally signed by:  
Ali Shaib

Unterschrift der die Versicherung an Eides statt aufnehmenden Beamtin bzw. Des aufnehmenden Beamten.



# Table of Contents

TABLE OF CONTENTS .....	I
LIST OF FIGURES.....	IV
LIST OF TABLES.....	VI
LIST OF ABBREVIATIONS .....	VII
ACKNOWLEDGMENTS.....	X
DEDICATION .....	XI
ABSTRACT .....	XII
ZUSAMMENFASSUNG.....	XIV
OPENING STATEMENT .....	XVI
<b>I. INTRODUCTION .....</b>	<b>1</b>
I.1 SPINAL CORD.....	2
I.2 DRG NEURONS.....	3
I.3 ASTROCYTES .....	5
I.4 SPINAL NEURONS.....	6
I.5 EXOCYTOSIS .....	7
I.6 CAPS.....	13
I.6.1 CAPS Isoforms.....	14
I.7 AIM OF THE THESIS .....	18
<b>II. MATERIALS AND METHODS .....</b>	<b>19</b>
II.1 MATERIALS:.....	19
II.1.1 Chemicals .....	19
II.1.2 Solutions .....	21
II.1.2.1 Base <sup>-</sup> 10x (Tobias) + 40 mM NH <sub>4</sub> Cl .....	21
II.1.2.2 Blocking Solution (50 ml) .....	21
II.1.2.3 S neurons Cell Culture Medium (50 ml) .....	21
II.1.2.4 DRG Intracellular Patch-Clamp Solution.....	21
II.1.2.5 DRG Extracellular Patch-Clamp Solution.....	22
II.1.2.6 DRG Extracellular Solution .....	22
II.1.2.7 DRG Cell Culture Medium .....	22
II.1.2.8 FUDR.....	22
II.1.2.9 HBS 2X Solution (100 ml).....	23
II.1.2.10 HEPES pH-Buffer Physiological Solution .....	23
II.1.2.11 HEK Cell Culture Complete-Medium (100 ml) .....	23
II.1.2.12 iB <sub>4</sub> Staining Solution.....	23
II.1.2.13 LB-Medium.....	23
II.1.2.14 Loading Buffer.....	24
II.1.2.15 Liberase S neurons Digestion Solution .....	24
II.1.2.16 Locke's 10x Solution .....	24
II.1.2.17 MES pH-Buffer Physiological Solution .....	24
II.1.2.18 Mounting Medium .....	24
II.1.2.19 Neurobasal A-Medium.....	24
II.1.2.20 Optimem .....	25
II.1.2.21 Paraformaldehyde (15% PFA, 10 ml) .....	25
II.1.2.22 PBS (1 l).....	25
II.1.2.23 Peptides-Blocking Solution.....	25
II.1.2.24 Permeabilization Solution (50 ml).....	26
II.1.2.25 PDL.....	26

II.1.2.26	Quenching Solution (50 mM Glycin).....	26
II.1.2.27	RPMI.....	26
II.1.3	Enzymes.....	26
II.1.4	Antibiotics.....	26
II.1.5	Bacteria and Cell Lines.....	27
II.1.5.1	Bacteria.....	27
II.1.5.2	Cell Lines.....	27
II.1.6	Mouse Strains.....	27
II.1.7	Kits.....	27
II.1.8	Cell Culture Products.....	27
II.1.9	Microscope Facilities.....	28
II.1.9.1	Total Internal Reflection Fluorescence Microscope.....	28
II.1.9.2	Confocal Laser Scanning Microscope.....	35
II.1.9.3	Structured Illumination Microscope.....	39
II.1.10	Devices.....	40
II.1.11	Consumables.....	41
II.1.12	Companies.....	42
II.1.13	Software.....	42
II.2	METHODS.....	44
II.2.1	Adult DRG Cell-Culture.....	44
II.2.2	Embryonic DRG Cell-Culture.....	46
II.2.3	DRG/S neuron Co-Culture.....	47
II.2.4	ICC.....	48
II.2.5	Double ICC.....	50
II.2.6	Calcium Phosphate-Lentivirus Production.....	51
II.2.7	RT PCR.....	52
II.2.8	Western Blot.....	53
II.2.9	iB4 Staining.....	54
II.2.10	Cloning.....	55
II.2.10.1	CAPS2b-mTFP.....	55
II.2.10.2	CAPS1-mTFP.....	59
II.2.10.3	CAPS1-TagRFP-T.....	60
II.2.10.4	VGLUT-mNectarin cloning.....	61
II.2.11	Analysis.....	65
III.	RESULTS.....	67
III.1	CAPS LOCALIZATION.....	67
III.1.1	CAPS Localization at mRNA Level.....	68
III.1.2	CAPS Localization at Protein Level.....	68
III.1.3	CAPS Localization at Cellular Level.....	69
III.2	STIMULUS PROTOCOL.....	72
III.2.1	Stimulating DRG Neurons.....	72
III.2.1.1	Stimulus optimization.....	73
III.2.1.2	LDCV Secretion.....	74
III.2.2	Stimulating Hippocampal Neurons.....	74
III.2.3	Stimulating DRG/S neuron co-cultures.....	75
III.3	CAPS ISOFORMS EFFECT ON LDCV SECRETION.....	75
III.3.1	CAPS Absence Hinders LDCV Secretion.....	76
III.3.2	CAPS Rescues LDCV Secretion in CAPS dKO Neurons.....	76
III.3.3	CAPS Overexpression Increases LDCV Secretion.....	77
III.4	HALF OF DRG NEURONS SECRETE LDCVS.....	78
III.5	PEPTIDERGIC AND NON-PEPTIDERGIC DRG NEURONS.....	79
III.6	CAPS ISOFORMS LOCALIZATION IN DRG NEURON SUBTYPES.....	80
III.6.1	CAPS1 Isoform Localization into DRG Subtypes.....	81
III.6.2	CAPS2 Isoform Localization into DRG Subtypes.....	83

III.7	LDCV SECRETION IN PEPTIDERGIC AND NON-PEPTIDERGIC NEURONS .....	84
III.7.1	<i>CAPS2 Mediates LDCV Secretion</i> .....	85
III.8	ESTABLISHING DRG/S NEURON CO-CULTURE.....	86
III.8.1	<i>DRG/S neuron Survival in Vitro</i> .....	86
III.8.2	<i>Synapses Form between DRG and S neurons</i> .....	87
III.8.3	<i>Synapses are Functionally Connected</i> .....	88
III.8.4	<i>Characterizing Synapses over Time</i> .....	88
III.9	CAPS1 LOCALIZATION AT SYNAPSES .....	91
III.10	MEASURING SYNAPTIC TRANSMISSION VIA V-GLUT mNECTARINE .....	93
III.11	MEASURING SYNAPTIC TRANSMISSION VIA SYNAPTOPHYSIN-PHFLUORIN .....	94
III.11.1	<i>CAPS1 Mediates SV Secretion in DRG/S neuron Co-Culture</i> .....	95
III.11.2	<i>A Role for CAPS2 in Synaptic Transmission?</i> .....	96
III.12	CAPS2 INDIRECTLY MODULATES SYNAPSES.....	98
<b>IV.</b>	<b>DISCUSSION .....</b>	<b>101</b>
IV.1	CAPS1 IS LOCALIZED TO ALL DRG NEURONS WHILE CAPS2 IS LOCALIZED TO THE PEPTIDERGIC SUBTYPES.....	102
IV.2	CAPS2 IS THE PRIMING FACTOR FOR LDCV SECRETION.....	104
IV.3	CAPS1 PRIMES SV SECRETION.....	106
IV.4	CAPS2 INDIRECTLY AFFECTS SYNAPTIC TRANSMISSION THROUGH PEPTIDE RELEASE.....	108
<b>V.</b>	<b>CONCLUSION AND PERSPECTIVES.....</b>	<b>111</b>
<b>VI.</b>	<b>APPENDIX.....</b>	<b>113</b>
VI.1	STIMULATING HIPPOCAMPAL NEURONS .....	114
VI.2	CAPS2 NEGATIVE CONTROL .....	115
VI.3	CAPS1 NEGATIVE CONTROL .....	116
VI.4	NPY-VENUS IS LOADED CORRECTLY INTO LDCVS .....	116
VI.5	VGLUT-mNECTARINE STRUCTURE .....	118
VI.6	LDCV SIZE IN PEPTIDERGIC AND NON-PEPTIDERGIC NEURONS – STED .....	118
VI.7	GOLGI STAINING .....	120
VI.8	LIFE ACT-RUBY EXPERIMENT .....	120
VI.9	LIST OF ANTIBODIES .....	122
<b>CURRICULUM VITAE .....</b>		<b>ERROR! BOOKMARK NOT DEFINED.</b>
<b>PUBLICATIONS.....</b>		<b>123</b>
<b>VII.</b>	<b>REFERENCES.....</b>	<b>124</b>

## List of Figures

Figure 1 Cross section of 4 of the spinal cord's 31 segments. ....	2
Figure 2 Astrocyte cells. ....	5
Figure 3 DRG neuronal connections to spinal neurons. ....	6
Figure 4 Spinal neurons in culture. ....	7
Figure 5 The constitutive and regulated secretory pathways. ....	8
Figure 6 The synaptic vesicle cycle. ....	9
Figure 7 SV exocytosis. ....	10
Figure 8 LDCV exocytosis. ....	12
Figure 9 CADPS gene map region. ....	14
Figure 10 Estimated protein expression level of CAPS1. ....	15
Figure 11 CAPS2 splice variants are present in adrenal glands. ....	16
Figure 12 Estimated protein expression level of CAPS2. ....	17
Figure 13 Total internal reflection fluorescence microscopy concept. ....	29
Figure 14 MicroProbes commercial field electrodes. ....	30
Figure 15 Magnified image of the original Tapered electrode compared to the custom eroded one. ....	31
Figure 16 Bright field image captured at 100x magnification of DRG neuron culture showing field electrode adjustment. ....	32
Figure 17 Stimulation protocol to induce LDCV release. ....	33
Figure 18 Synaptic transmission stimulus protocol. ....	34
Figure 19 Moiré pattern. ....	39
Figure 20 Schematic view of preparation of dissociated and explant DRG sensory neuronal cultures. ....	44
Figure 21 DRG isolation. ....	45
Figure 22 Image iT-FX Signal Enhancer effect on auto-fluorescence. ....	49
Figure 23 Spectral mixing of mTFP, eGFP and Venus. ....	55
Figure 24 ZraI check-digest. ....	56
Figure 25 1% Agarose analytical gel. ....	57
Figure 26 pSFV-mCAPS2b-IRES-mTFP vector map. ....	57
Figure 27 CAPS2b-mTFP co-expressed with NPY-Venus in DRG neurons. ....	58
Figure 28 pSFV-CAPS1-IRES-mTFP vector map. ....	59
Figure 29 CAPS1-mTFP co-expressed with NPY-Venus in DRG neurons. ....	59
Figure 30 pSFV-CAPS1-IRES-Tag RFP-T vector map. ....	60
Figure 31 Cloning strategy of vGlut-mNectarine. ....	61
Figure 32 Splicing by Overlap Extension. ....	62
Figure 33 vGlut-mNectarine cloning. ....	63
Figure 34 Tile confocal images showing overexpression of vGlut-mNectarine in DRG-S neurons co-culture. ....	64
Figure 35 Representative example of classical LDCV secretion. ....	65
Figure 36 RT-PCR from 2 weeks old mice. ....	68
Figure 37 CAPS developmental protein expression levels. ....	68
Figure 38 DRG neurons autofluorescence profile. ....	69
Figure 39 CAPS isoforms are found in DRG neurons. ....	70
Figure 40 CAPS1/2 and CAPS2 double-immunostaining. ....	71
Figure 41 CAPS isoforms localization to synapses in DRG/S neuron co-culture. ....	72
Figure 42 Electrical stimulus for DRG neurons. ....	73
Figure 43 Electrical stimulus for DRG/S neuron co-cultures. ....	75
Figure 44 CAPS1 and CAPS2 dKO effect on LDCV secretion. ....	76
Figure 45 CAPS1 and CAPS2 overexpression in dKO effect on LDCV secretion. ....	77
Figure 46 CAPS2 overexpression effect on LDCV secretion in DRG neurons. ....	77
Figure 47 CAPS1 overexpression effect on LDCV secretion in DRG neurons. ....	78
Figure 48 Percentage of secreting cells. ....	78
Figure 49 Percentage of peptidergic and non-peptidergic DRG neurons. ....	79
Figure 50 CAPS1 with iB <sub>4</sub> staining. ....	81
Figure 51 CAPS1 localization into peptidergic neurons. ....	82

Figure 52 CAPS2 with iB <sub>4</sub> staining.....	83
Figure 53 CAPS2 localization into peptidergic subtypes neurons. ....	84
Figure 54 Examining secretion in peptidergic and non-peptidergic DRG neuron subpopulations.....	85
Figure 55 DRG/S neuron co-cultured neurons morphology over time.....	87
Figure 56 Marking synapses between DRG neurons and S neurons. ....	87
Figure 57 DRG/S neuron Synapses are functional.....	88
Figure 58 Synapse formation over time. ....	90
Figure 59 CAPS1 colocalization at synapses in co-cultured DRG/S neuron. ....	92
Figure 60 Measuring synaptic transmission with vGlut-mNectarine. ....	93
Figure 61 NH <sub>4</sub> Cl mode of action on SyHy. ....	94
Figure 62 Exemplary traces of averaged synapses from individual recordings of DRG/S neuron co-cultures. ....	95
Figure 63 Synaptic transmission in DRG/S neuron co-culture. ....	96
Figure 64 Synaptic transmission synchronicity.....	97
Figure 65 Blocking CGRP, substance P and BDNF. ....	98
Figure 66 Peptides antagonists reduce active synapses and synchronize them. ....	99
Figure 67 CAPS localization into peptidergic and non-peptidergic neurons. ....	103
Figure 68 CAPS2 primes LDCV release. ....	105
Figure 69 CAPS differential role model. ....	107
Figure 70 CAPS2 indirect effect on synaptic transmission model.....	109

## List of Tables

Table 1 The sensory modalities represented by the somatosensory systems. ....	4
Table 2 Comparison between SSV and LDCV. ....	11
Table 3 Role of CAPS in LDCV and SV release across the different studied species in the literature. ....	14
Table 4 List of used antibodies. ....	122

## List of Abbreviations

	Symbols	Prefix
	° C	Degrees Celsius
	μ	Micrometer
	Ω	Ohm
	#	Number
	%	Percent
	^	Restriction site
A	A	Ampere
	ANOVA	Analysis of variance
	AOTF	Acousto optic tunable filter
	ApE	A-plasmid Editor
	Ar	Argon
	ATP	Adenosine triphosphate
	AU	Airy Units
	a.u.	Arbitrary units
	BDNF	Brain-derived neurotrophic factor
	Bp	Base pair
	BSA	Bovine serum albumin
C	CAPS	Calcium-dependent activator protein for secretion
	CGRP	Calcitonin gene-related peptide
	CNS	Central nervous system
D	dKO	Double knockout
	DMEM	Dulbecco's modified eagle medium
	DMSO	Dimethyl sulfoxide
	DNA	DeoxyriboNucleic Acid
	dNTP	DeoxyriboNucleotide TriPhosphate
	S neurons	Spinal neuron(s)
	DH5α	<i>Escherichia coli</i> competent cells: F– endA1 glnV44 thi-1 recA1 relA1 gyrA96 deoR nupG purB20 φ80dlacZΔM15 Δ(lacZYA-argF)U169, hsdR17(rK–mK+), λ–
	DRG	Dorsal Root Ganglion
	DRGn	Dorsal Root Ganglion neuron(s)
	DPBS	Dulbecco's phosphate buffered saline
E	E	Electric field
	E(number)	Embryonic developmental stage
	EBSS	Earle's balanced salt solution
	<i>E. coli</i>	<i>Escherichia coli</i>
	EDTA	Ethylenediaminetetraacetic acid
	EGTA	Ethylene glycol tetraacetic acid
	<i>et al.</i>	et alia
F	FCS	Fetal calf serum
	FUDR	Fluorodeoxyuridine
	FW	Forward primer
G	g	Gram

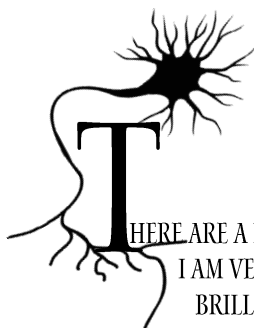
<b>H</b>	h	Hour
	HEK	Human embryonic kidney
	HEPES	4-(2-Hydroxyethyl)-1-piperazineethanesulfonic acid
	HPLC	High performance liquid chromatography
	HS	Horse serum
	Hz	Hertz
<b>I</b>	iB <sub>4</sub>	Isolectin GS-IB <sub>4</sub>
	ICC	Immunocytochemistry
	IgG	Immunoglobulin G
<b>K</b>	KO	Knockout
<b>L</b>	L	Liter
	LB	Loading buffer
	LB-medium	Lysogeny Broth-medium
	LDCV(s)	Large dense-core vesicle(s)
	LSM	Laser scanning microscopy
	LTD	Long-term depression
	LTP	Long-term potentiation
<b>M</b>	M	Mol/L
	m	Meter
	m-	Milli
	M-	Mega
	min	Minute(s)
	MW	Molecular weight
<b>N</b>	N	Number of mice
	n	Number of cells
	n-	Nano
	NA	Numerical aperture
	NBA	Neurobasal A
	NEAA	Non-essential amino acids
	NGS	Normal goat serum
	NPY	Neuropeptide-Y
	NSF	N-ethylmaleimide-sensitive factor
<b>O</b>	Osm	Osmol
<b>P</b>	<i>p</i>	Probability value
	P(number)	Postnatal developmental stage
	PBS	Phosphate buffered saline
	PCR	Polymerase chain reaction
	PDL	Poly D-Lysin
	Pen/Strep	Penicillin/Streptomycin
	PFA	Paraformaldehyde
	<i>Pfu</i>	<i>Pyrococcus furiosus</i> polymerase
	pH	Potential Hydrogen
	PKA	Protein Kinase A
	PNS	Peripheral nervous system
<b>R</b>	ref	Relative centrifugal force
	RNA	Ribonucleic Acid
	rpm	Round per minute



S	RPMI	Roswell Park Memorial Institute
	RV	Reverse primer
	s	Second(s)
	SAP	Shrimp alkaline phosphatase
	SDS	Sodium dodecyl Sulfate
	SEM	Standard error of the mean
	SFV	Semiliki Forest virus
	S neurons	Spine neurons
	SNAP-25	Synaptosomal-associated protein-25
	SNARE	Soluble N-Ethylmaleimide-sensitive factor attachment receptor
	Stbl3	<i>Escherichia coli</i> competent cells: F- glnV44 recA13 mcrB mrr hsdS20(rB-, mB-) ara-14 galK2 lacY1 proA2 rpsL20 xyl-5 leu mtl-1
	SV(s)	Synaptic vesicle(s)
	SybKI	Synaptobrevin/mRFP Knockin
	SypHy	Synaptophysin-pHluorin
T	sysy	Synaptic Systems
	<i>Taq</i>	<i>Thermus aquaticus</i>
	TIRFm	Total internal reflection fluorescence microscopy
	Tris	Tris(hydroxymethyl)aminomethane
U	t-SNARE	Target-SNARE
	U	Units
	UV	Ultra Violet
V	V	Volt
	VAMP	Vesicle-associated membrane protein
W	v-SNARE	Vesicular-SNARE
	WT	Wild type

## ACKNOWLEDGMENTS

---



HERE ARE A NUMBER OF PEOPLE WITHOUT WHOM THIS THESIS MIGHT NOT HAVE BEEN COMPLETED. I AM VERY GRATEFUL TO PROF. JENS RETTIG FOR GIVING ME THE OPPORTUNITY TO WORK IN HIS BRILLIANT LAB, HE PROVIDED EXCELLENT SUPPORT, SUGGESTIONS AND ROUTINELY FEEDBACKS. CALLING HIM “COMMANDER IN CHIEF” IS THE BEST DESCRIPTION TO SALUTE HIS OUTSTANDING SUPPORT.

I WOULD LIKE TO EXPRESS MY GRATITUDE FOR MY “EPIC” SUPERVISOR DR. UTE BECHERER, SHE WAS SPECTACULAR INSTRUCTOR WHO GUIDED ME THROUGH MY PHD THESIS. SHE PROVIDED ALL THE HELP AND TEACHING. SHE WAS SUCH A CARING FRIEND WHO TAUGHT ME THAT SCIENCE CAN BE ALSO FUN. SHE GAVE ME ALL THE SPACE TO DEVICE MY OWN WAY OF THINKING AND SHE WAS NEVER RELUCTANT TO OFFER HELP, EVEN ON EARLY SUNDAYS. UTE IS THE BEST “MOTHER DR.” EVER...

I WOULD LIKE TO EXPRESS MY DEEP AND SINCERE GRATITUDE TO MY MOM, DAD AND TO MY FAMILY AND WONDERFUL RELATIVES FOR SUPPORTING ME AND WAITING FOR ME AT BEIRUT INTERNATIONAL AIRPORT EVERY TIME I GO BACK FOR A VISIT. I WOULD LIKE TO THANK MY BROTHER ABED FOR HIS EXTRAORDINARY HELP IN THE EQUATIONS I NEEDED AND TECH-SUPPORT AS WELL AS DRAWING SOME MODELS FOR MY WORK. I WOULD LIKE TO THANK MY TALENTED COUSIN HUSSEIN ALAWIEH FOR DESIGNING THE COVER. I WOULD LIKE TO THANK MY BROTHER-FRIEND AHMED M. SHAABAN FOR BEING MY FRIEND, BUDDY AND ADVISOR. HE WAS SUCH A GREAT PERSON, FUNNY CO-TRAVELER AND A LOVING BIG BROTHER. SPECIAL THANKS FOR MY BROTHER ALI HARB. I KNEW HIM FOR YEARS AND FOR MANY ANOTHER COMING YEARS. I WOULD LIKE TO THANK MY SISTER HAWRAA BZEIH, “LE” WONDERFUL MARWA SLEIMAN AND THE INDEED “SPECIAL” MAZEN MAKKE FOR THEIR PRECIOUS FRIENDSHIP; WE WERE MORE LIKE A FAMILY IN GERMANY.

I WOULD LIKE TO THANK MADAM MARGERETE KLOSE FOR HER AMAZING WORK OF SUPERIOR QUALITY. SHE HAD THE MAJOR ROLE IN ESTABLISHING AND MAINTAINING OUR CULTURE SYSTEMS ALONG WITH OTHER GREAT SUPPORT IN ROUTINE LAB WORK.

I WOULD LIKE TO THANK DR. DAVID STEVENS FOR PROVIDING TREMENDOUS HELP. ONE ALWAYS LEARN A NEW THING WITH EVERY DISCUSSION HE GETS WITH DAVE. THANK YOU DAVID FOR SPENDING PART OF YOUR PRECIOUS TIME ON REVIEWING THIS THESIS, IT WAS OF GREAT HONOR TO ME.

I WOULD LIKE TO THANK PROF. RALF MOHRMANN AND EXPRESS MY GRATITUDE FOR TEACHING ME CLONING. RALF WAS SUCH AN EXCELLENT SOURCE FOR PROVIDING USEFUL MACROS THAT MADE LIFE EASIER. HE WAS ALWAYS PRESENT FOR HELP.

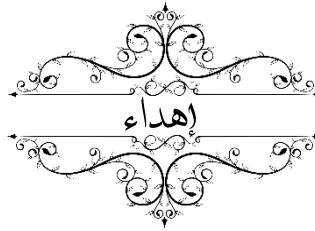
I WOULD LIKE TO THANK PROF. BARBARA NIEMEYER FOR HER ELEGANT INPUTS IN DEVISING SOME OF THE CLONING STRATEGIES. I WOULD LIKE TO THANK PROF. MARKUS HOTH FOR HIS WONDERFUL SUPPORT DURING THE GK PROGRAM.

THANK YOU ALL, YOU MADE MY STAY HERE IN HOMBURG WARM AND TOGETHER WITH GOD’S HELP MADE MY PHD THESIS A SUCCESSFUL STORY.

---



**T**HIS THESIS IS DEDICATED TO MY MOTHER AND FATHER, FAMILY AND MY TWO AUNTS, SECOND MOTHER RIMA AND HER HUSBAND BRIGADIER GENERAL WASSIM ALAWIEH, TO MY INSTRUCTOR AND SCHOOL DIRECTOR MR. AHMED M. SHEHADEH AND TO MY DEAR FRIENDS-BROTHERS ALI MOKDAD AND ALI KASSEM.



**ه**ذا الكتاب هو إهداء إلى كل من السيدة الوالدة والسيد الوالد، وأخوتي، وعماتي هدى وزينب شعيب ، وخالتي رima وزوجها المقدم الركن السيد وسيم علوية، والسيد المرني أحمد مهدي شحادي، وصاحبي العزيزين علي المقداد وعلي قاسم.

## Abstract

Dorsal root ganglion (DRG) neurons transmit sensory information to the central nervous system through glutamatergic synaptic transmission that can be modulated by diverse neuropeptides packaged in large dense core vesicles (LDCVs). LDCVs fuse at the cell somata and in afferent terminals along with synaptic vesicles, in response to a specific stimulus. Cultured DRG neurons are an appropriate system to investigate the role of Calcium-dependent Activator Protein for Secretion (CAPS) in the release machinery of these two different types of vesicles. CAPS has two isoforms that are known to be localized to different neurons in brain and DRGs. Hence DRG neurons are a good model to assess any possible differential roles of CAPS isoforms in LDCV and SV release. LDCV secretion can be studied in isolation or simultaneously with SV secretion once the DRG neurons are co-cultured with the spinal neurons.

Using RT-PCR, western blot and immunocytochemistry, we verified that both CAPS isoforms are expressed in DRGs. CAPS1 is expressed in all neurons while CAPS2 is present in half of the population. We visualized NPY-Venus labeled LDCVs in real time using total internal fluorescence reflection microscopy. LDCV release was stimulated by a field electrode inducing secretion in fifty percent of neurons. Double gene deletion of CAPS1 and 2 strongly reduced the number of secreting cells and significantly reduced the amount of exocytosed LDCVs per responding cell in comparison to control. Furthermore, CAPS1 or 2b overexpression raised the number of WT secreting neurons by 20%, and the responding cells released more than twice as many LDCVs in comparison to wild type (WT) controls. Since the density of LDCVs at the plasma membrane was not affected by CAPS expression level, our results indicate that CAPS is a priming factor for LDCVs in DRG neurons. Further investigation of secreting WT cells revealed that only peptidergic neurons secrete LDCV upon stimulation. Interestingly, Isolectin GS-IB4 (iB<sub>4</sub>) staining together with anti-CAPS2 antibody staining showed that eighty percent of peptidergic neurons express CAPS2. Overexpressing CAPS2b in non-peptidergic neurons induced secretion while CAPS2 KO neurons didn't secrete LDCVs. This strongly suggest that CAPS2 is the priming factor for LDCV release in WT DRG neurons. To address a possible role of CAPS in synaptic transmission we established DRG neurons co-cultured with spinal neurons (DRG/S neuron) to allow synapse formation. SypHy Lentivirus-based transfection was used to specifically label SVs

and visualize their exocytosis. We found that CAPS1 but not CAPS2 promotes synaptic transmission. Upon CAPS1 but not CAPS2 deletion, synaptic transmission is dramatically decreased. Surprisingly, in-depth analysis of the synaptic transmission suggested that CAPS2 indirectly affects synaptic transmission through peptide release. CAPS2 induced an unsynchronized secretion phenotype, while its absence synchronized synaptic transmission. Interestingly, blocking the receptors for the three major peptides, calcitonin gene-related peptide (CGRP), substance P (SP) and brain-derived neurotrophic factor (BDNF), led to the silencing of the majority of active synapses and induced synchronized synaptic transmission in the remaining active synapses. This suggests that the peptide antagonism might induce long-term depression, possibly by altering presynaptic calcium.

Taken together, these findings indicate that CAPS isoforms play differential roles due to their differential localization. CAPS2 is localized to DRG cell bodies and primes LDCV secretion, while CAPS1 is localized to synapses and primes SV secretion. Additionally, CAPS2 affects synaptic transmission by promoting the release of peptides which modulate SV fusion. We conclude that CAPS is an indispensable protein with multiple functions that regulate both LDCV secretion and synaptic transmission in dorsal root ganglions.

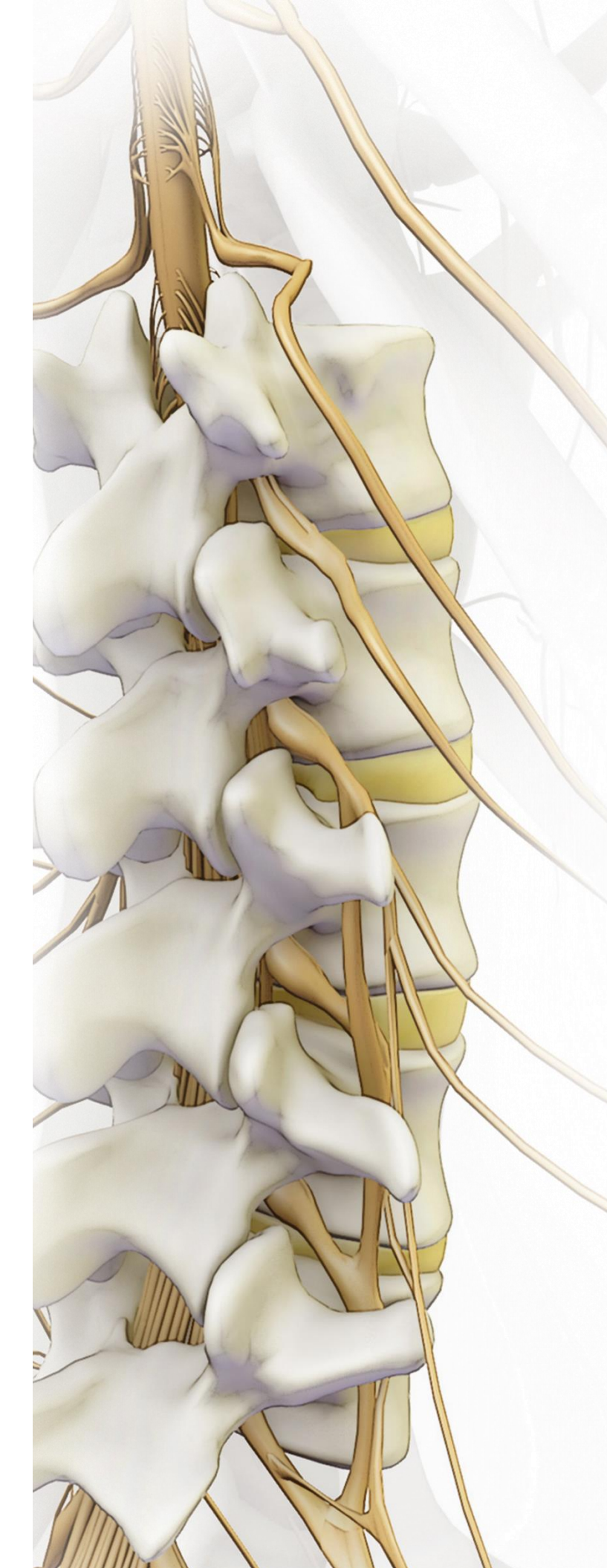
## Zusammenfassung

Spinalganglion (Eng: *Dorsal Root Ganglion (DRG)*) -Neurone übertragen sensorische Informationen an das zentrale Nervensystem durch eine glutamaterge synaptische Transmission, die durch verschiedene Neuropeptide moduliert werden kann und in großen dichten Kernvesikeln (Eng: *Large Dense Core Vesicles (LDCVs)*) verpackt sind. *LDCVs* werden als Reaktion auf einen spezifischen Stimulus an den Soma und in afferenten Termini zusammen mit synaptischen Vesikeln exocytisiert. Die Spinalganglion Kultur ist ein geeignetes System, um die Rolle des *Calcium-dependent Activator Protein for Secretion (CAPS)* in der Freisetzung zweier unterschiedlichen Arten von Vesikeln zu untersuchen. *CAPS* hat zwei Isoformen, die bekanntermaßen auf verschiedene Neuronen im Gehirn, und in *DRGs* lokalisiert sind. Daher sind *DRG* Neurone ein perfektes Modell, um mögliche Rollen der *CAPS* Isoformen in der *LDCV* und *SV* (Synaptic vesicle) Freisetzung zu bewerten. Die *LDCV*-Sekretion kann isoliert oder gleichzeitig mit der *SV*-Sekretion untersucht werden, sobald die *DRG*-Neuronen mit den Spinalneuronen co-kultiviert werden.

Unter Verwendung von *RT-PCR*, *Western-Blot* und *Immunzytochemie* konnten wir nachweisen, dass beide *CAPS* Isoformen in *DRGs* exprimiert werden. *CAPS1* wird in allen Neuronen exprimiert, während *CAPS2* nur in der Hälfte der Population vor liegt. Mit Hilfe des *Total Internal Reflection Fluorescence* Mikroskopie konnten *NPY-Venus* (Eng: *NeuropeptideY (NPY)*) markierte *LDCVs* in Echtzeit visualisiert werden. Die Freisetzung wurde durch eine Feldelektrode stimuliert, die eine Sekretion in fünfzig Prozent der Neurone induzierte. Die doppelte Gendeletion von *CAPS1* und 2 verminderte die Anzahl der sekretierenden Zellen stark und verringerte signifikant die Menge der exocytosierten *LDCVs* pro Reaktionszelle im Vergleich zur Kontrolle. Darüber hinaus erhöhte *CAPS1* oder 2b Überexpression die Anzahl der *WT* (Wildtyp) sezernierenden Neurone um 20%, und die reagierenden Zellen setzten mehr als doppelt so viele *LDCVs* frei im Vergleich zu *WT* Kontrolle. Da die Dichte der *LDCVs* an der Plasmamembran nicht durch das Expressionsniveau von *CAPS* beeinflusst wurde, legen unsere Ergebnisse nahe, dass *CAPS* ein *Priming* faktor für *LDCVs* in *DRG* Neuronen ist. Eine weitere Untersuchung des Prozentsatzes an sekretierenden *WT* Zellen ergab, dass nur peptiderge Neurone nach Stimulation *LDCV* sekretieren. Interessanterweise zeigte eine Antikörperfärbung von *Isolectin GS-IB4 (iB<sub>4</sub>)*

zusammen mit anti-CAPS2-Antikörperfärbung, dass achtzig Prozent peptiderger Neurone CAPS2 exprimieren. Überexpression von CAPS2b in nicht-peptidergen Neuronen induzierte Sekretion, während CAPS2 KO (*Knockout*) Neurone keine LDCVs sekretierten. Dies deutet stark darauf hin, dass CAPS2 der *Priming* faktor für die LDCV Freisetzung in WT DRG Neuronen ist. Um eine mögliche Rolle von CAPS bei der synaptischen Übertragung zu untersuchen, haben wir DRG Neurone mit spinalen Neuronen (*DRG/S Neuron*) co-kultiviert, und somit Synapsenbildungen ermöglicht. Eine *SypHy* (*Synaptophysin Phluorin*) *Lenti-Virus* basierte Transfektion wurde verwendet, um Synaptische Vesikel spezifisch zu markieren und ihre Exocytose zu visualisieren. Wir konnten zeigen, dass CAPS1, aber nicht CAPS2 die synaptische Übertragung fördert. Bei CAPS1, aber nicht CAPS2 deletion, wird die synaptische Übertragung drastisch verringert. Überraschenderweise zeigte eine eingehende Analyse der synaptischen Transmissionsexperimente, dass CAPS2 indirekt die synaptische Transmission durch Peptidfreisetzung beeinflusst. CAPS2 induzierte einen asynchronen Sekretions Phänotyp, während dessen Abwesenheit zu einer synchronisierten synaptische Übertragung führte. Interessanterweise führte die Blockierung von drei Hauptpeptiden, einschließlich *Calcitonin Gene-Related Peptide* (*CGRP*), *Substance P* (*SP*), und *Brain-Derived Neurotrophic Factor* (*BDNF*), zum *silencing* der Mehrheit der aktiven Synapsen und induzierte synchronische synaptische Übertragung in den verbleibenden aktiven Synapsen. Dies deutet darauf hin, dass die Peptidblockade eine Langzeit-Depression induzieren könnte, indem sie wahrscheinlich präsynaptisches Calcium verändert. Zusammengefasst zeigen diese Befunde, dass CAPS Isoformen aufgrund ihrer differentiellen Lokalisation differentielle Rollen spielen. CAPS2 ist in DRG Zellkörpern lokalisiert und ist für das *Priming* und die Sekretion von LDCV verantwortlich, während CAPS1 sich in Synapsen befindet und das *Priming* und Sekretion von SVs durchführt. Zusätzlich beeinflusst CAPS2 die synaptische Transmission durch die Förderung der Freisetzung von Peptiden, die an ihren präsynaptischen Rezeptor binden, wodurch die SV Exozytose induziert wird.

Wir fassen zusammen, dass CAPS ein leistungsfähiges unentbehrliches Protein mit Multifunktionen ist, das sowohl die LDCV Sekretion als auch die synaptische Transmission auf unterschiedliche Weise regulieren.



THE CHIEF  
FUNCTION OF THE  
BODY IS TO CARRY  
THE BRAIN  
AROUND.

Thomas A. Edison

THE CHIEF  
FUNCTION OF  
DRGs IS TO MAKE  
THE BRAIN AWARE  
OF ITS SURROUND.

Ali H. H. Shaib



# I. Introduction

It is vital for living organisms to sense the external world. The brain, through the anterior insular cortex, provides us with awareness of the feelings originating outside and inside the body (Craig, 2009). There are countless experiences that can be sensed in our world from the hugs of beloved people, to the rain drops splashing on your skin and the feeling of cool breath. Incredibly, we are able to differentiate and comprehend these inputs and substantialize them through our perception to make things matter for us. Information needed from our environment to maintain our awareness of events happening around us are conveyed by different nerve endings that innervate our skin and organs. These nerves collectively transfer the sum of information to the nervous system. The nervous system serves different major functions, some of which are the exteroceptive and interoceptive functions, then responds to stimuli originating outside or inside the body. Another function that is also needed for our perception is proprioception. It helps the nervous system keep good command over perception and control of body position and balance (Abraira and Ginty, 2013). These functions altogether involve the activation of primary neurons whose cell bodies are located in the dorsal root ganglion (DRG). DRG neurons act like a “*primitive brain*”; they can detect information from the periphery and send it to the central nervous system in order to be processed (Ibanez and Ernfors, 2007). The information is transmitted to the central nervous system via glutamatergic synaptic transmission that is subject to modulation via secretion of peptides contained in large dense core vesicles (LDCVs). The vesicular secretion of peptides and neurotransmitters is important in many neural and endocrine functions (Zhang and Zhou, 2002). Sensory inputs generate action potentials along the DRG axons which induce  $\text{Ca}^{2+}$ -dependent vesicle secretion (Huang and Neher, 1996; Zhang and Zhou, 2002). Secretion is controlled by a well-orchestrated exocytosis machinery and involves different vesicle pools and several fusion steps. Prior to fusion, vesicles undergo the membrane related maturation steps, docking, priming and a final fusion step that is calcium dependent. Fusion of the vesicle with the plasma membrane marks the release of the vesicular cargo, transmitting the chemical signal from the presynapse to the postsynapse (Becherer and Rettig, 2006). The exocytosis machinery has been examined in great detail for synaptic vesicles and to some extent for LDCV secretion in brain. However, it remains poorly understood in DRG neurons. Particularly, we are interested in the role

of CAPS in these neurons. It is widely accepted that CAPS regulates synaptic transmission and LDCV secretion in brain neurons (Eckenstaler et al., 2016; Farina et al., 2015; Fujita et al., 2007; Klenchin and Martin, 2000; Speidel et al., 2005; Speidel et al., 2003) and mutations in CAPS are associated with cerebellar disorders and autism (Okamoto et al., 2011; Sadakata et al., 2012; Sadakata et al., 2007a; Sadakata et al., 2007b) but its role in DRG neurons remains unknown. It is of great interest to understand how these sensory neurons transmit information and communicate with their surroundings and especially how pain is produced (Gu et al., 2010). Discovering how these sensory neurons work would help in providing potential treatment for sensory symptoms often associated to ataxia and pain.

### I.1 Spinal Cord

The spinal cord is defined by Cambridge dictionary as the set of nerves inside the spine that connect the brain to other nerves in the body. It is a very important structure that links the body to the foramen magnum part of the brainstem where it becomes continuous with the medulla oblongata (Ibanez and Ernfors, 2007). In humans, the spinal cord is divided into 31 segments that includes the cervical, thoracic, lumbar and sacral regions (Figure 1). The nervous tissue is composed of white and gray matter, together with supporting cells of the spinal cord. These tissues begin at the occipital bone

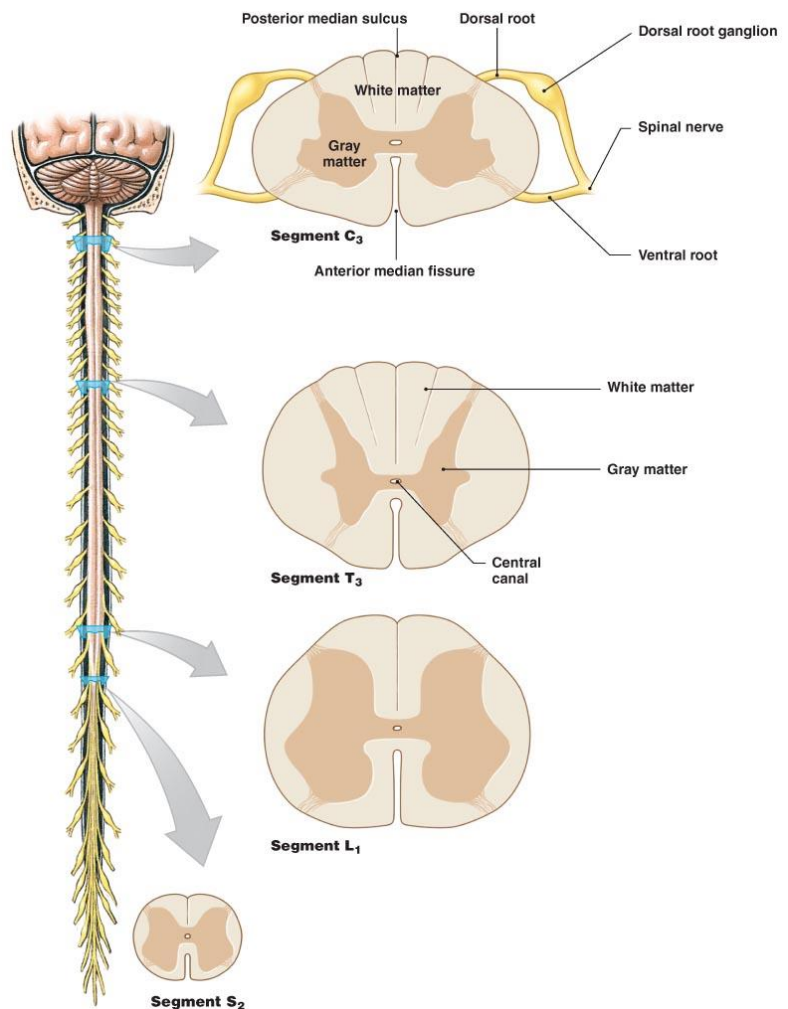


**Figure 1** Cross section of 4 of the spinal cord's 31 segments.

Source: Pearson Education Inc. © 2011

and extends to the second lumbar vertebrae reaching a length of around 45 cm in men and 43 cm in women. Its width varies from 13 mm thick in the cervical and lumbar regions to 6.4 mm thick in the thoracic part. In mice, the spinal cord is a white cylindrical slim structure that extends to a similar extent as in humans from the foramen magnum to the lower side of the vertebral column (Yaksh et al., 1999). Between the cranium and the sacrum end, there exist about 25 to 30 vertebrae (Green, 1941; MJ., 1965). The sensory information travels from the extremities of the body and goes through the spinal cord to the central nervous system (CNS) via afferent fibers. The CNS in return, can send motor orders via motor neurons located in the ventral horn. These neurons project their axons to the body parts, mediating CNS voluntary and involuntary reflexes through muscle innervation. The spinal cord connects the brain with the peripheral nervous system, controlling and tuning the flow of information. The spinal cord segments are associated with a pair of dorsal root ganglia that host the cell bodies of the primary sensory neurons. The central axons of these cells project into the spinal cord carrying the information into the CNS second order neurons.

### **I.2 DRG Neurons**

DRG neurons are pseudo-unipolar cells, with one axonal branch that extends all the way to the periphery and associates with peripheral sites. The second branch, which enters the spinal cord, forms synapses with second order neurons in the gray matter of the spinal cord, though few of these reach the dorsal column nuclei of the brainstem (Abaira and Ginty, 2013). A single DRG neuron nerve ending covers a receptive field of less than a 1 mm in diameter on the skin surface that often senses a range of different stimuli (Patapoutian et al., 2003). These neurons are very diverse and encompass different subsets that are distinct with respect to their cell body sizes, axonal morphologies, physiological properties, and expression of molecular markers. Some subsets respond to either thermal, tactile, proprioceptive, or nociceptive stimuli and are classified as thermoreceptors, mechanoreceptors, proprioceptors, and nociceptors, respectively (Ryan et al., 2007). The diversity of the receptive functions is extensive, for example somatosensory subset can be further divided into several modalities of somatic sensation that can be further divided into sub-

## INTRODUCTION

Modality	Sub Modality	Sub-Sub Modality	Somatosensory Pathway (Body)	Somatosensory Pathway (Face)
Pain	sharp cutting pain		Neospinothalamic	Spinal Trigeminal
	dull burning pain		Paleospinothalamic	
	deep aching pain		Archispinothalamic	
Temperature	warm/hot		Paleospinothalamic	
	cool/cold		Neospinothalamic	
Touch	itch/tickle & crude touch		Paleospinothalamic	Main Sensory Trigeminal
	discriminative touch	touch	Medial Lemniscal	
		pressure		
		flutter		
		vibration		
Proprioception	Position: Static Forces	muscle length		
		muscle tension		
		joint pressure		
	Movement: Dynamic Forces	muscle length		
		muscle tension		
		joint pressure		
		joint angle		

**Table 1 The sensory modalities represented by the somatosensory systems.**

DRG neurons are categorized into different somatic modalities that are further divided into sub-modalities (aka different types of sensation) and sub-sub-modalities. Each of these sensations are modality specific. For example, the somatosensory cold-sensation submodality is naturally stimulated by cold, the perceived sensation is then processed by a specific neuron which can not respond to warm or touch signals. Sensory receptors and their connections determine the modality specificity by which the responsible neuron will process the information and send it to the higher order of central nervous system neurons.

Source: Modified from Patrick Dougherty, Ph.D., Department of Anesthesiology and Pain Medicine, MD Anderson Cancer Center. Content available on: The University of Texas Health Science Center at Houston (UTHealth) website.

modalities. They are basically classified into four main categories that are presented in Table 1. A more general and easier classification is to group these neurons as peptidergic and non-peptidergic neurons that can be distinguished via isolectin labeling. The isolectin protein (iB<sub>4</sub>) isolated from an African shrub, binds to  $\alpha$ -D-galactose carbohydrate residues on small and medium sized neurons (Fullmer et al., 2004; Silverman and Kruger, 1990). The iB<sub>4</sub> can only bind the unmyelinated non-peptidergic or “*peptide poor*” primary neurons hence the name iB<sub>4</sub><sup>+</sup> neurons (Wang et al., 1994). Additionally this substance has been used to label the non-peptidergic neurons expressing the exposed isolectin P2X<sub>3</sub> receptors (Bradbury et al., 1998; Guo et al., 1999). By default, the “*peptide rich*” myelinated neurons were given the name iB<sub>4</sub><sup>-</sup> neurons. It is now widely accepted that these chemical differences on the surface of these neurons represent functionally distinct groups of DRG neurons (Snider and McMahon, 1998; Stucky and Lewin, 1999). DRG neurons carry out their functions with the help and maintenance provided to them by astrocytes (Fang et al., 2006).

### I.3 Astrocytes

Michael von Lenhossek introduced the term Astrocyte which translates literally into ‘Star-like cell’. They can be identified by staining against GFAP<sup>1</sup> (Figure 2). Astrocytes are highly heterogeneous in their morphology and the surface markers they express. Astrocytes are the most numerous and diverse glial cells in the nervous system (Nedergaard and Verkhratsky, 2012; Parpura and Verkhratsky, 2012). They create the micro-architecture allowing brain neurons to thrive and perform their functions. They store and distribute energy substrates, control development, synaptogenesis and maintenance of synapses and synaptic structures. (Kettenmann and Verkhratsky, 2011). These cells perform their supportive functions by establishing highly organized

anatomical domains that are extensively connected into networks, dramatically modulating the state of neurons (Belanger and Magistretti, 2009). While astrocytes maintain CNS integrity, they also do so for the PNS (Guenard et al., 1994). Astrocytes surround the pre- and postsynaptic structures in the PNS and stabilize them (Heikkinen et al., 2014). The idea of the functionality and participation of astrocytes at synapses became interesting when Alfonso Araque showed, using transmission electron microscopy, that astrocytes processes are in the direct proximity of synapses (Araque et al., 1999a; Araque et al., 1999b). Further studies revealed that astrocytes release molecules that are essential to sustain the maturation, structure and functionality of active synapses (Beattie et al., 2002; Pfrieger and Barres, 1997; Slezak and Pfrieger, 2003). The influence of astrocytes on synaptic survival, activity and plasticity can be exerted by glial-derived neurotrophins, cytokines and metabolites (Faissner et al., 2010). Astrocytes have proven to be essential for successful physiological studies involving CNS and PNS neurons. For this reason, we

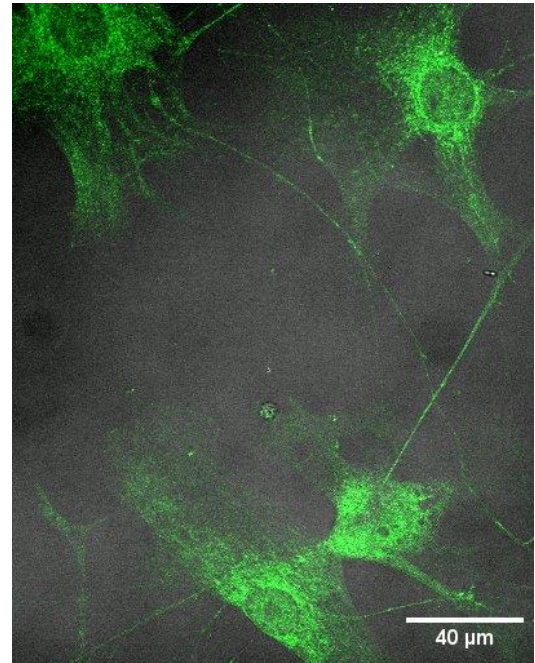


**Figure 2 Astrocyte cells.**

Astrocytes fixed with 4% and stained against rabbit GFAP and Alexa 488 secondary antibody. The displayed image is a bright field overlaid with 488 confocal acquisition.

---

<sup>1</sup> Glial fibrillary acidic protein, a common marker for astrocytes.

monitored and controlled the astrocyte numbers in such a way that there were adequate astrocytes for healthy DRG culture but not so many that imaging was impaired.

### I.4 Spinal Neurons

The primary afferents of different DRG subtypes that innervate the skin and body tissues, terminate in the spinal cord. The distribution pattern of this termination is determined by the sensory modality and the body region these afferents innervate (Sivilotti and Woolf, 1994). It is an orchestrated process that drives the modality specific terminations to the proper position inside the spinal cord grey matter. For instance, nociceptive neurons terminate in dorsal horn, mechanoreceptors neurons terminate in deeper laminae, while proprioceptive neurons terminate in the intermediate zone and in the ventral spinal cord horn (Figure 3). The grey matter encompasses the cell bodies of spinal neurons<sup>2</sup> that constitute a part of the CNS and is divided into several sections that include dorsal horn, intermediate column, lateral horn and ventral horn column. Spinal

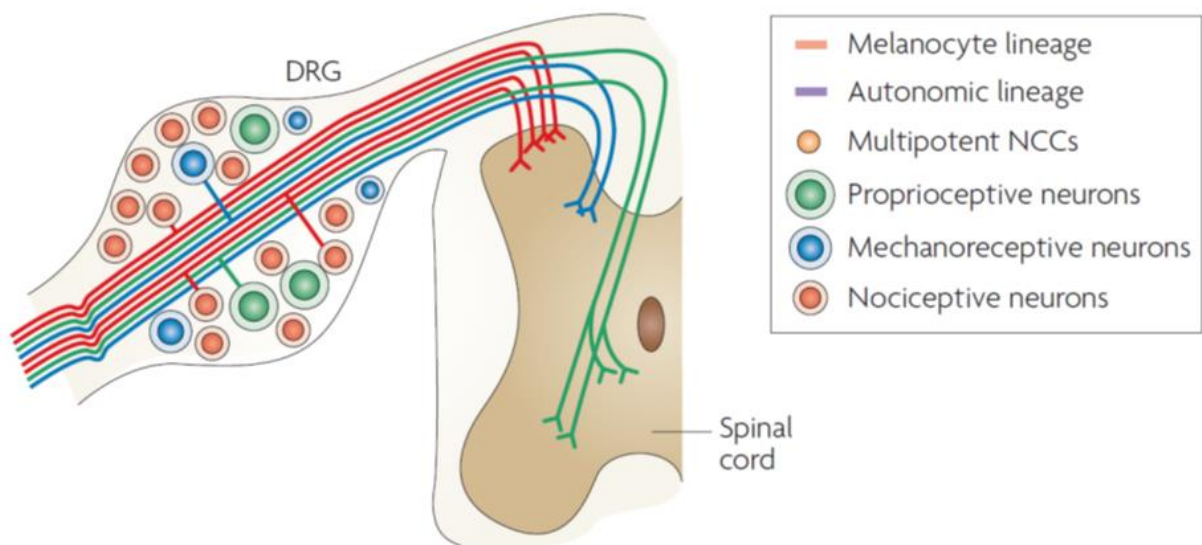


**Figure 3 DRG neuronal connections to spinal neurons.**

Modified from: Marmigère and Ernors. *Nature Reviews Neuroscience* 8, 114–127 (February 2007), doi:10.1038/nrn2057.

<sup>2</sup> In addition to spinal neurons, the grey matter encompass glial cells as well as astroglial and oligodendrocytes. These cells provide physical support and regulate the internal environment inside the grey matter



## INTRODUCTION

neurons process the information from DRG neurons through complex inhibitory and excitatory circuits (Todd, 2010). The information is then transmitted from spinal neurons to higher order neurons in the brain to be further processed. It was important for us to study synapses formed between DRG neurons and spinal neurons in order to assess the possible role of CAPS isoforms in synaptic transmission and for this reason we characterized these cells according to morphology. We noticed that spinal neurons were much smaller in size in comparison to DRG neurons and that they were morphologically different in terms of cell body shape (being more round) and having longer and thicker processes (Figure 4). It was relatively easy for us to distinguish both types of neurons once co-cultured. During the course of this PhD thesis we will present a detailed characterization of these cells and we will describe the time course of synapse formation and function.

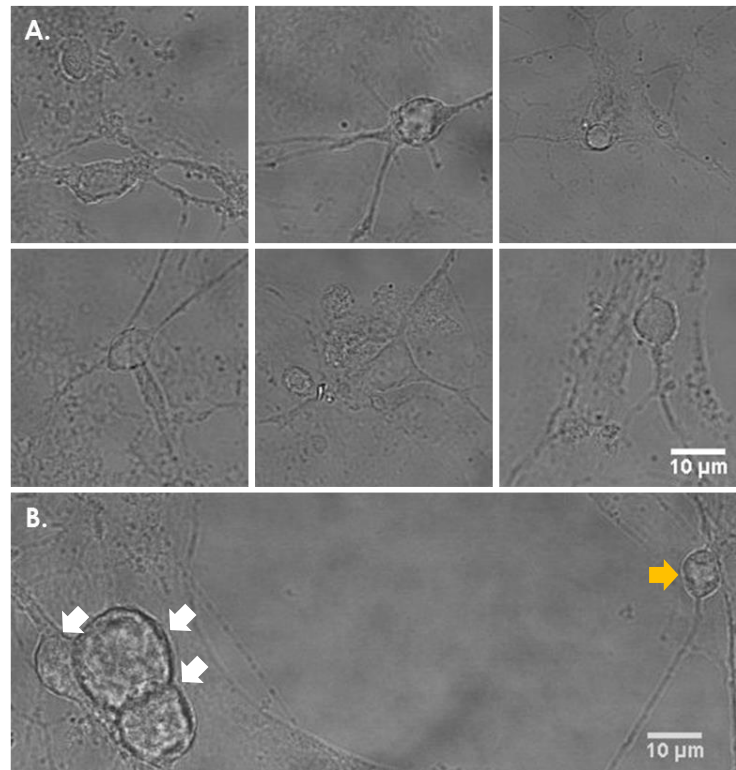


**Figure 4 Spinal neurons in culture.**

(A) Confocal bright field acquisition of dorsal horn neurons 6 DIV. (B) DRG/S neuron co-culture 6 DIV. S neuron can be distinguished from DRG neurons with their relatively smaller size. The white arrows point to DRG neurons while the yellow arrow points to S neuron.

### I.5 Exocytosis

The term exocytosis was conceived by the Belgian Nobel prize winner Christian de Duve by combining the Greek words Ἐξω, meaning "external" and κύτος, meaning "cell" (Blaschko; De Duve, 1963). As the meaning of the word implies, it is a process by which a vesicle fuses with the membrane of the cell, releasing its cargo to the outside (aka secretion). It is an essential mechanism for cells to accomplish their functions and maintain homeostasis (Alberts, 1989) For instance, the secretion of neurotransmitter serotonin is essential for brain function and mood regulation, the

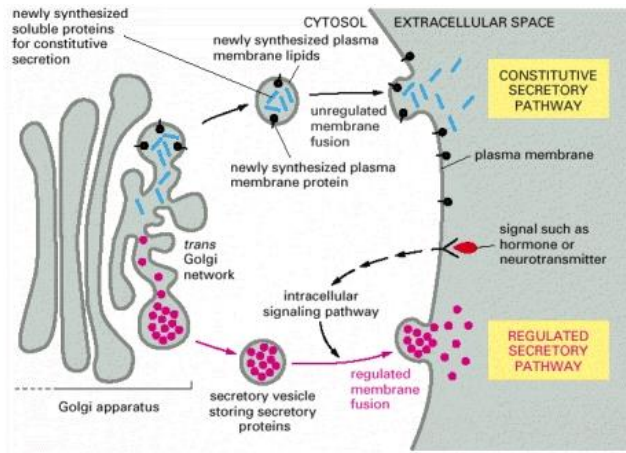


**Figure 5 The constitutive and regulated secretory pathways.**

The constitutive secretory pathway ensures the renewal of proteins located in the plasma membrane and the disposal of metabolites. The regulated secretory pathway takes place only in specialized cells whereby proteins in the *trans*-Golgi network are sorted into secretory vesicles, waiting a proper signal to drive their exocytosis.

Adapted from: Molecular Biology of the Cell. 4th edition. Alberts B, Johnson A, Lewis J, et al. New York. Garland Science; 2002.

secretion of peptides (for example NPY) and hormones (for example oxytocin) are important for regulating food intake/obesity and mental state (De-Miguel and Trueta, 2005; de Kock et al., 2003; Gehlert, 1999; Piekut, 1985). There are two modes of exocytosis, the constitutive pathway and regulated pathway of secretion (Frick et al., 2001). The first mode provides a continuous way of secretion of proteins that are packaged inside vesicles of which undergo direct secretion, delivering proteins to the extracellular matrix. Fusion of membrane organelles is also used to deliver proteins to the plasma membrane of the cell (Alberts B, 2002; Lacor et al., 2000; Lodish H, 2000). The second pathway occurs in specialized cells and is important for regulating peptide, neurotransmitter and hormone release. Regulated exocytosis is coupled to transient calcium increase in the cytosol which induces the fusion of secretory vesicles with the cell membrane, see figure 5 for more details (Alberts, 1989; Robert D. Burgoyne, 1993; Vitale et al., 2002). Exocytosis is a firmly regulated mechanism that involves vesicle trafficking, tethering, docking, priming and a final fusion step. Vesicle trafficking involves translocation of vesicles, often over long distances, from the Golgi apparatus to their destined site. Such translocation requires motor proteins and actin and/or microtubule cytoskeletal tracks (Johnson et al., 2012; Kuznetsov et al., 1992; Lang et al., 2000; Manneville et al., 2003). Once the vesicles are recruited to the intended site, they are tethered. A process known to happen before the interaction of vesicular Soluble N-Ethylmaleimide-sensitive factor attachment receptor (v-SNAREs) and transmembrane SNAREs (t-SNAREs). Tethering is defined as the first attachment of the vesicle with its target membrane and usually covers a distance half of the vesicle width ( $> 25$  nm). Tethering factors are known to share common characteristics, being either multi-subunit complexes or elongated coiled-coil proteins (Lowe, 2000) that stabilize the position of the vesicle long enough ensuring a successful docking for fusion (Toonen et al., 2006). Once the vesicles are strongly-tethered, they are subjected to tighter membrane positioning



bringing the vesicles in a proximity of 5 to 10 nm from the plasma membrane, a process called docking. Docking involves the integral vesicular proteins, synaptotagmin which interacts with two membrane proteins, syntaxin and SNAP-25 (Bennett and Scheller, 1994; Jahn and Sudhof, 1993; Pevsner et al., 1994). Tethering and docking establish physical proximity of membranes but are not enough to initiate vesicle fusion-competence. Prior to fusion, an additional biochemical process is

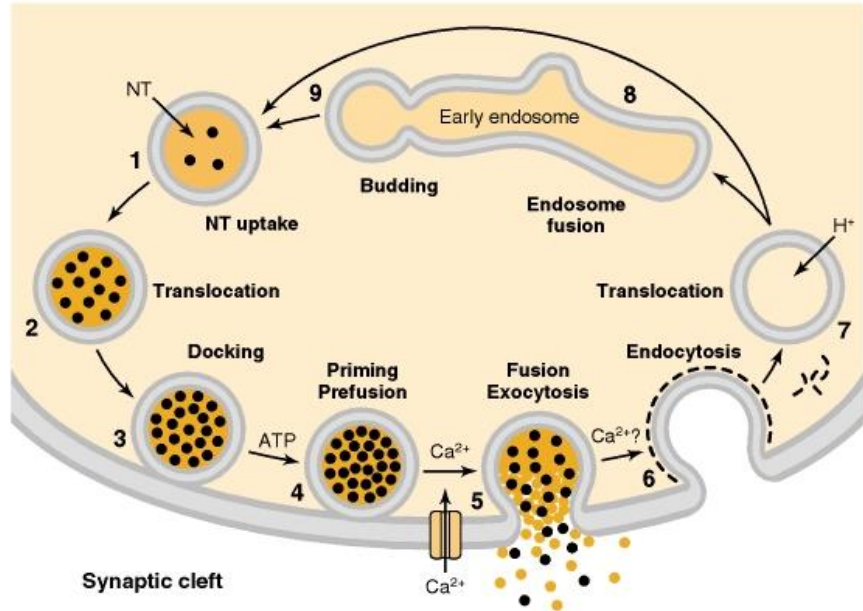


**Figure 6 The synaptic vesicle cycle.**

Synaptic vesicle exocytosis can be divided into several stages. 1: Synaptic vesicles are loaded with neurotransmitters by active transport. 2: Newly filled synaptic vesicles are then transported to the active zones of synapses, a process known as tethering. 3: The synaptic vesicles are then docked to the presynaptic membrane. 4: Synaptic vesicles status becomes fusion competent after a priming step awaiting calcium signal. 5: Calcium signal triggers fusion process. 6: Fused synaptic vesicles are then coated with Clathrin and are prepared for endocytosis. 7: Endocytosed synaptic vesicles shed the Clathrin coat and are acidified via proton pumps. 8: The synaptic vesicles later fuse with early endosomes. 9: Once ready, synaptic vesicles bud from endosomes. It is reported that some synaptic vesicles can skip the endosomal intermediate step and can go directly from step 7 to step 1.

Modified from: The Synaptic Vesicle Cycle in the Nerve Terminal. Basic Neurochemistry: Molecular, Cellular and Medical Aspects. 6th edition. Siegel GJ, Agranoff BW, Albers RW, et al., editors. Philadelphia: Lippincott-Raven; 1999.

needed that requires a set of proteins interacting with both the vesicle and the plasma membrane in an ATP-dependent fashion, rendering the vesicles fusion competent. This process is called priming whereby vesicles are now fusion competent and awaiting the calcium trigger to fuse (Klenchin and Martin, 2000; Martin and Kowalchyk, 1997). Fused vesicles are endocytosed and recycled for further rounds of fusion (Figure 6).

### I.5.1 SV Exocytosis

Synaptic vesicles are loaded with neurotransmitters, transferred to the active zones of pre-synaptic axonal terminal, docked then primed and await calcium signal to trigger fusion, a process called SV exocytosis. It takes about 100  $\mu$ s from the arrival of an action potential to the fusion of

## INTRODUCTION

SVs at the presynapse (Rizo and Rosenmund, 2008; Sudhof, 2004). Twenty years of accumulating research investigating neurotransmitter release shows that neuronal SNAREs that mediate exocytosis are the vesicular Synaptobrevin and the plasma membrane proteins SNAP-25 and Syntaxin. Synaptobrevin and Syntaxin-1 each have one SNARE motif before the C-terminal transmembrane domain while SNAP-25 has two SNARE motifs. The assembly of the four SNARE motifs into a tight SNARE complex consisting of a four-helix bundle (Lin and Scheller, 1997; Poirier et al., 1998; Rizo and Xu, 2015; Sutton et al., 1998) is required for the primed state (Sollner et al., 1993). The energy released by this assembly would trigger membrane fusion (Hanson et al., 1997) whereby Synaptobrevin binds to SNAP-25 and Syntaxin, drawing the vesicular and cell membranes into close proximity (Figure 7). The SNARE complex is disassembled right after fusion with the help of NSF and SNAPs (Sollner et al., 1993).

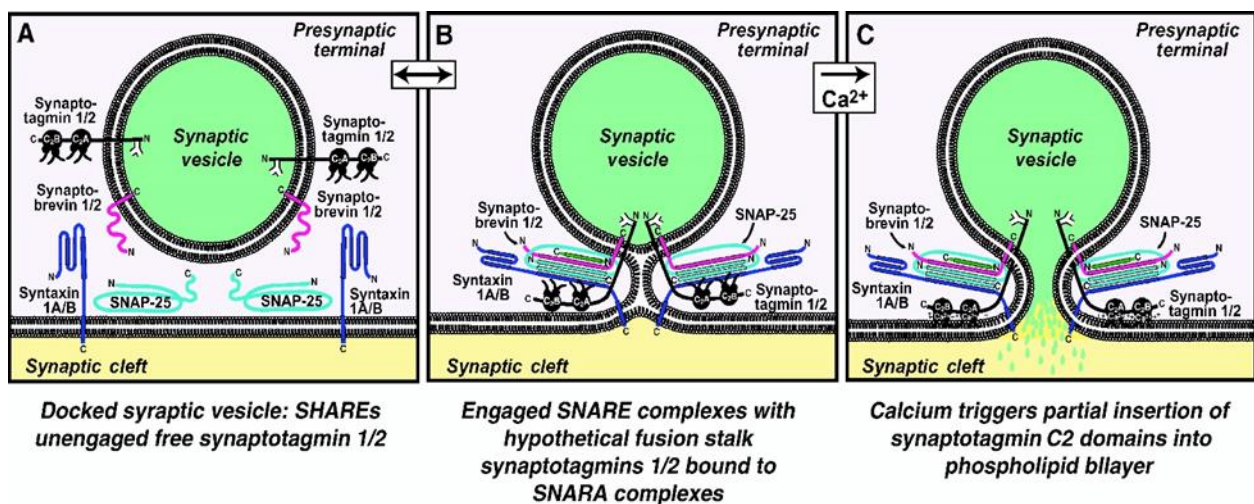


**Figure 7 SV exocytosis.**

SNARE proteins, complexins and synaptotagmin 1 and 2 interaction model during exocytosis. While vesicles are docked (panel A). There is no direct interaction of SNAREs and synaptotagmins while vesicles are docked (panel A). Upon priming (panel B), Complexins (green) bind to fully associated SNARE complexes, followed by association of synaptotagmins to the formed SNARE complex. Assembled SNARE complexes force the synaptic vesicle membrane and the plasma membrane into close proximity, resulting in an unstable intermediate as shown in the hypothetical fusion diagram. Calcium influx would trigger synaptotagmin C2 domains to partly insert into the phospholipids (panel C), destabilizing the fusion intermediate state. This causes mechanical perturbation that opens the fusion pore ending in full vesicle fusion.

Adapted from: Thomas C. Sudhof. The Synaptic Vesicle Cycle. Annu. Rev. Neurosci. 2004. 27:509–47.

## I.5.2 LDCV Exocytosis

Neurons and neuroendocrine cells secrete transmitters such as neuropeptides, neurohormones and amines that are contained in LDCVs (Bauerfeind et al., 1994; Liu et al., 1994; Park and Kim, 2009). Unlike, small EM clear core SVs (of about 50 nm in diameter), LDCVs are larger and have electron dense cores with vesicles of diameters from 100 to 300 nm. Whereas, neurotransmitters in SVs primarily bind to ligand gated ion channels to transmit the signal to the postsynapse in rapid way, neuropeptides contained in LDCVs target G protein-coupled receptors (GPCRs), hence modulating synaptic activity (Park and Kim, 2009) (see Table 2). LDCVs are secreted at the soma as well as near active zones of synapses (Zhao-Wen, 2008). The production of LDCVs can be quite a complex process for cells. Unlike SVs that can be locally produced at synapses to ensure fast recycling, immature LDCVs are de novo produced at the *trans*-Golgi network (Yang et al., 2001). Once formed, LDCVs undergo maturation steps allowing the transportation to the destined location and eventual docking at the plasma membrane, a process coordinated via Rab proteins (Grosshans et al., 2006) (Figure 8). Despite, the differences between the morphology and function of both SVs and LDCVs, they share common mechanisms of exocytosis whereby calcium is essential to trigger their release. In similar fashion to SV exocytosis, a synaptotagmin is required for calcium sensing in LDCV exocytosis (Schonn et al., 2008). In a very similar way to what was described in SV exocytosis section, the priming of vesicles into a fusion competent state involves the assembly of

	SVs	LDCVs
<b>Size (nm)</b>	~ 50	100–300
<b>Location</b>	Mainly CNS and clustered in nerve terminals	Mainly PNS and homogeneously distributed
<b>Endocytosis</b>	Local recycling by endocytosis	Slow endocytosis
<b>Morphology in EM</b>	Clear particle	Dense particle
<b>Neurotransmitters contained</b>	Classical neurotransmitters and ATP	Amines (catecholamine, serotonin, and histamine), peptide, and ATP
<b>Receptors stimulated</b>	Mainly ligand-gated channel (generating postsynaptic potential)	Mainly GPCR (modulating synaptic activity)
<b>Time delay between calcium influx and fusion</b>	~ 0.2 ms after single action potential	> 50 ms, longer latency after strong stimulation
<b>Distance from calcium channel to fused vesicle</b>	~ 20 nm	~ 300 nm

**Table 2 Comparison between SSV and LDCV.**

Adapted from: Yongsoo Park and Kyong-Tai Kim. Short-term plasticity of small synaptic vesicle (SSV) and large dense-core vesicle (LDCV) exocytosis. Volume 21, Issue 10, October 2009, Pages 1465–1470.

## INTRODUCTION

*trans*-SNARE complexes. This process that is further regulated with priming factors such as Munc13s. Interestingly, it was shown that Munc-13 does not play an essential role in LDCV exocytosis in contrast to the case of SV exocytosis (van de Bospoort et al., 2012). Exogenous Munc-13 facilitates LDCV secretion but its absence does not impair the ready releasable pool (RRP) (Figure 8) (Sieburth et al., 2007). Another important priming factor CAPS, a highly conserved protein through evolution with two isoforms that has been proven to play an important role in LDCV secretion (Walent et al., 1992). Most studies however focused on CAPS1, knowing that CAPS2 is expressed at eight fold higher than CAPS1 in endocrine cells (Sieburth et al., 2007; Speese et al., 2007; Zhou et al., 2007). Understanding the differences between CAPS isoforms should provide key insights to understand the differences in priming of SV and LDCV exocytosis. Through this thesis, we intended to decipher the role of CAPS isoforms in both SV and LDCV exocytosis.

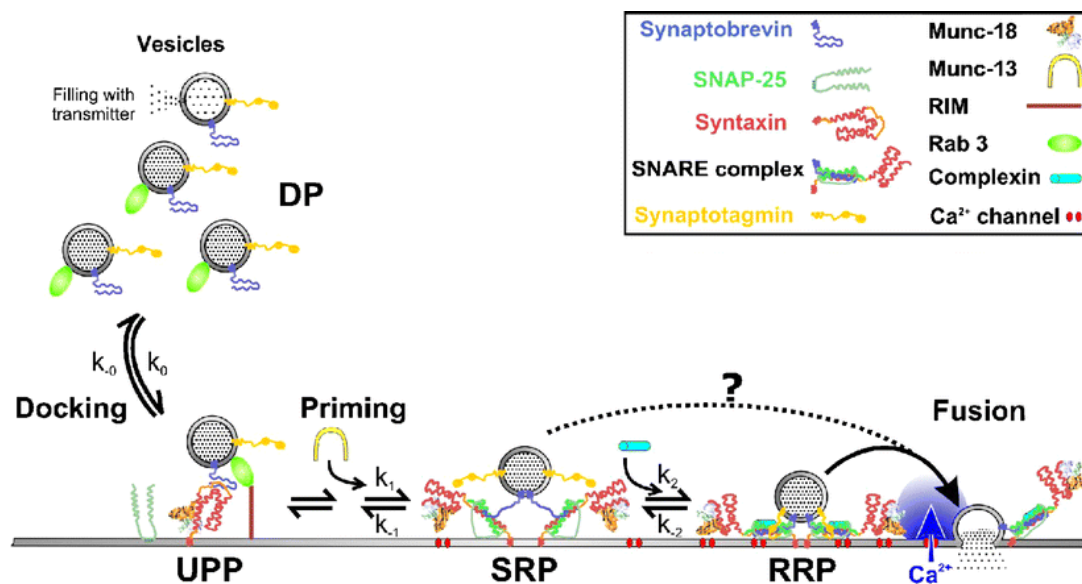


**Figure 8 LDCV exocytosis.**

Molecules that are involved in calcium-dependent exocytosis. Several molecular reactions occurs before calcium-dependent exocytosis. The transferring of vesicles from the depot pool (DP) to the unprimed pool (UPP) defines the docking step. Munc18 stabilize docked state of vesicles. Docking is followed by a priming step which corresponds to the transfer of vesicles from the UPP to the slowly releasable pool (SRP) because of the (partial) formation of the SNARE complex from the individual SNAREs SNAP-25, syntaxin, and synaptobrevin. Munc13 functions as a priming factor. Complexin modulates the equilibrium between SRP and RRP. The final fusion of vesicles is initiated by the binding of  $Ca^{2+}$  to synaptotagmin which acts as a calcium sensor.

Adapted from: Ute Becherer and Jens Rettig, 2006. Vesicle pools, docking, priming, and release.

### I.6 CAPS

In 1992, a novel brain protein first named p145 was identified by Thomas Martin's group. The protein was described as a dimer of 145 kd subunits that exhibited  $\text{Ca}^{2+}$ -dependent interaction with a hydrophobic matrix. It was suggested that p145 has a membrane-associated function because of its ability to bind phospholipids vesicles. The authors also proposed that the restricted expression of p145 suggests that this protein has a key role in the transduction of  $\text{Ca}^{2+}$  signals into vectorial membrane fusion events (Walent et al., 1992). It took the authors five years to give p145 the current name, CAPS ( $\text{Ca}^{2+}$ -binding protein) and they reported that  $\text{Ca}^{2+}$ -dependent triggering of vesicle fusion required CAPS as an additional cytosolic factor (Ann et al., 1997). A year later, CAPS got its final submitted name<sup>3</sup> which had a better descriptive meaning of its function. It was directly understood how important this novel protein is. CAPS was shown as a functional component of the exocytotic machinery that localizes selectively to LDCVs, and probably confers distinct regulatory features on neuropeptide and biogenic amine transmitter secretion (Berwin et al., 1998). As the attention towards CAPS further grew, more groups started studying it in different cell systems. The first study of CAPS effect on LDCV release was performed in calf chromaffin cells and showed that CAPS is critical for fusion of LDCVs with the membrane (Elhamdani et al., 1999). A second mammalian CAPS isoform was identified by Brose group; the localisation of both isoforms in the CNS as well as in other organs was then studied (Speidel et al., 2003). These studies reported among other findings that CAPS is expressed in DRG neurons but while CAPS1 was found in all DRG neurons, CAPS2 was found in an undefined subpopulation (Sadakata et al., 2006; Sadakata et al., 2007b). Later, CAPS<sup>4</sup> was studied in *Caenorhabditis elegans* where it was shown that it is required for LDCV but not SV exocytosis (Speese et al., 2007). In 2011, CAPS2 isoform was shown to promote BDNF release in the GABAergic interneuron network of the hippocampus and to be critical for the development of GABAergic interneuron network (Shinoda et al., 2011). CAPS2 was also shown to be essential for regulating LDCV trafficking by interacting with Class II ARF small GTPases (Sadakata et al., 2012). Rettig's group showed in 2014 that CAPS primes through its Pleckstrin homology domain and not through the Mun domain and that it doesn't interact with Syntaxin and surprisingly, that its function is not redundant with Munc13 (Nguyen

---

<sup>3</sup> Calcium-dependent Activator Protein for Secretion.

<sup>4</sup> CAPS homolog in *C. elegans* is named UNC-31.



Truong et al., 2014). Recently, it was shown that CAPS1 primes LDCV fusion at synapses in mammalian neurons and both CAPS1 and CAPS2 primes SVs (Jockusch et al., 2007). A more recent study showed that deletion of CAPS2 does not affect SV release (Farina et al., 2015), introducing some controversy to the field. CAPS isoforms play different roles in LDCV vs SV secretion among different species and cell types within species. It is not necessarily the case that CAPS acts as a priming factor in one cell type if CAPS does for another. For instance, the two powerful priming factors Munc13 and CAPS are not required for the molecular regulation of SV secretion in cochlear inner hair cells (Vogl et al., 2015).

The diverse effects of CAPS on LDCV and SV release among different species is illustrated in table 2. It is difficult to predict how CAPS would act in DRG neurons due to its unorthodox role as described in the literature. It was very interesting for us to investigate both isoforms in DRG and DRG/S neuron system as its roles remain yet unclear in these cells.

Species	LDCVs	SVs
<i>C. elegans</i>	<b>Yes</b> (Speese et al., 2007)	<b>No</b> (Speese et al., 2007)
<i>Drosophila</i>	<b>Yes</b> (Renden et al., 2001)	<b>Yes</b> (Renden et al., 2001)
Chromaffin cells	<b>Yes</b> (Elhamdani et al., 1999)	-
Hippocampal neurons	<b>Yes</b> (Shinoda et al., 2010)	<b>Controversial</b> (Jockusch et al., 2014) (Farina et al., 2015)
Hair cochlear cells	<b>No</b> (Vogl et al., 2015)	<b>No</b> (Vogl et al., 2015)
DRG neurons	?	?

**Table 3 Role of CAPS in LDCV and SV release across the different studied species in the literature.**

## I.6.1 CAPS Isoforms

The CAPS protein family is encoded by two CADPS genes that produce two isoforms, CAPS1 and CAPS2. The CADPS1 gene is located on chromosome 3 while CADPS2 gene is located on chromosome 7 (Figure 9).

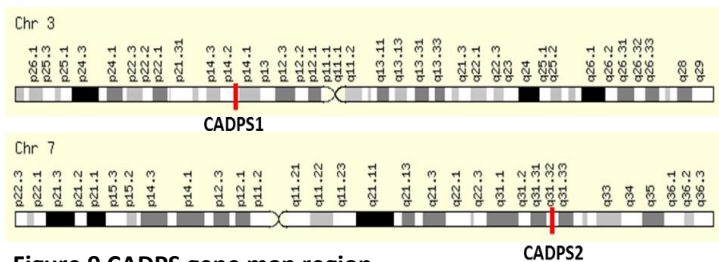


**Figure 9 CADPS gene map region.**

Source: Modified from GeneLoc Genome Locator.

CAPS proteins are widely expressed in all adult and fetal tissues examined, with the strongest expression in kidney and pancreas. In brain, it is expressed at high levels in cerebellum, to a lesser degree in cerebral cortex, occipital pole, and frontal and temporal lobes. CAPS is weakly expressed

## INTRODUCTION

in medulla, spinal cord and putamen (Cisternas et al., 2003). CAPS1 isoform is very important for neurons and is abundant among almost all neurons (Figure 10).



**Figure 10 Estimated protein expression level of CAPS1.**

Source: GeneReport for Unigene cluster for CADPS1 Gene Hs.654933.

CAPS1 deficiency affects the secretion of catecholamines, neuropeptides and peptide hormones (Berwin et al., 1998; Fujita et al., 2007; Speidel et al., 2008; Tandon et al., 1998). In the course of my thesis, I will study the effect of CAPS1 - as well as CAPS2 - on LDCV and SV release in DRG neuronal culture and DRG/S neurons co-culture, respectively.

Unlike CAPS1 where there are no known splice variants, CAPS2 isoform has 6 known splice variants 2b, 2a, 2c, 2d, 2e and 2f ranging from the longest to the shortest, respectively (Figure 11). CAPS2 isoforms are expressed right after birth with an expression peak around the first or second postnatal week. In several tissues the estimated expression level of CAPS2 is less important than CAPS1 (Figure 12). CAPS2 protein is concentrated in parallel fiber terminals<sup>5</sup> of the cerebellum

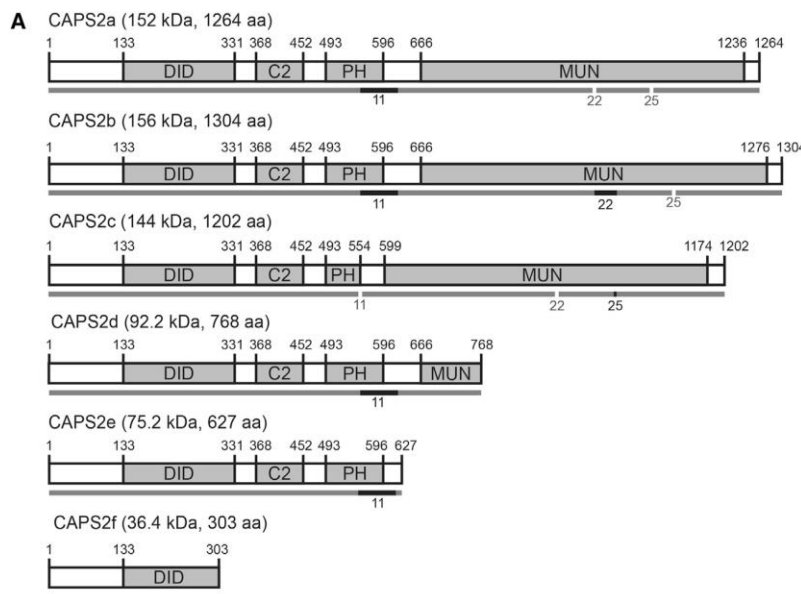
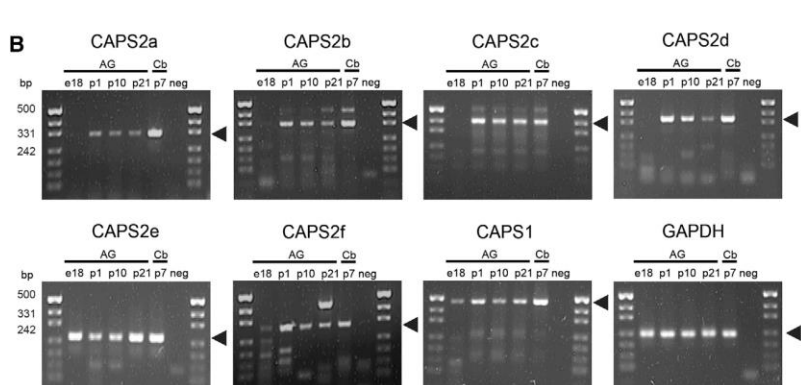


**Figure 11 CAPS2 splice variants are present in adrenal glands.**

(A) Domain structure of CAPS2 splice variants (Sadakata *et al.*, 2007). Domains are as follows: DID, C2 domain, PH domain, MUN domain. Numbers refer to the amino acids defining the respective domains. Alternatively spliced exons are indicated underneath. (B) RT-PCR of adrenal gland (AG) and cerebellum (Cb) using primers specific for CAPS2 splice variants. Lysates from adrenal glands obtained from mouse embryos at E18 and postnatal days 1, 10, and 21 were used as templates for lanes 1–4, and for lane 5, cerebellar lysate from postnatal day 7 mice was used as template. The outer lanes contain size markers.



<sup>5</sup> CAPS1 is enriched in Glomeruli and Climbing Fibers (Sadakata et al., 2007a).



## INTRODUCTION

where it is associated with vesicles containing BDNF. CAPS2 enhances release of BDNF, which is essential for normal cerebellar development (Sadakata and Furuichi, 2009).

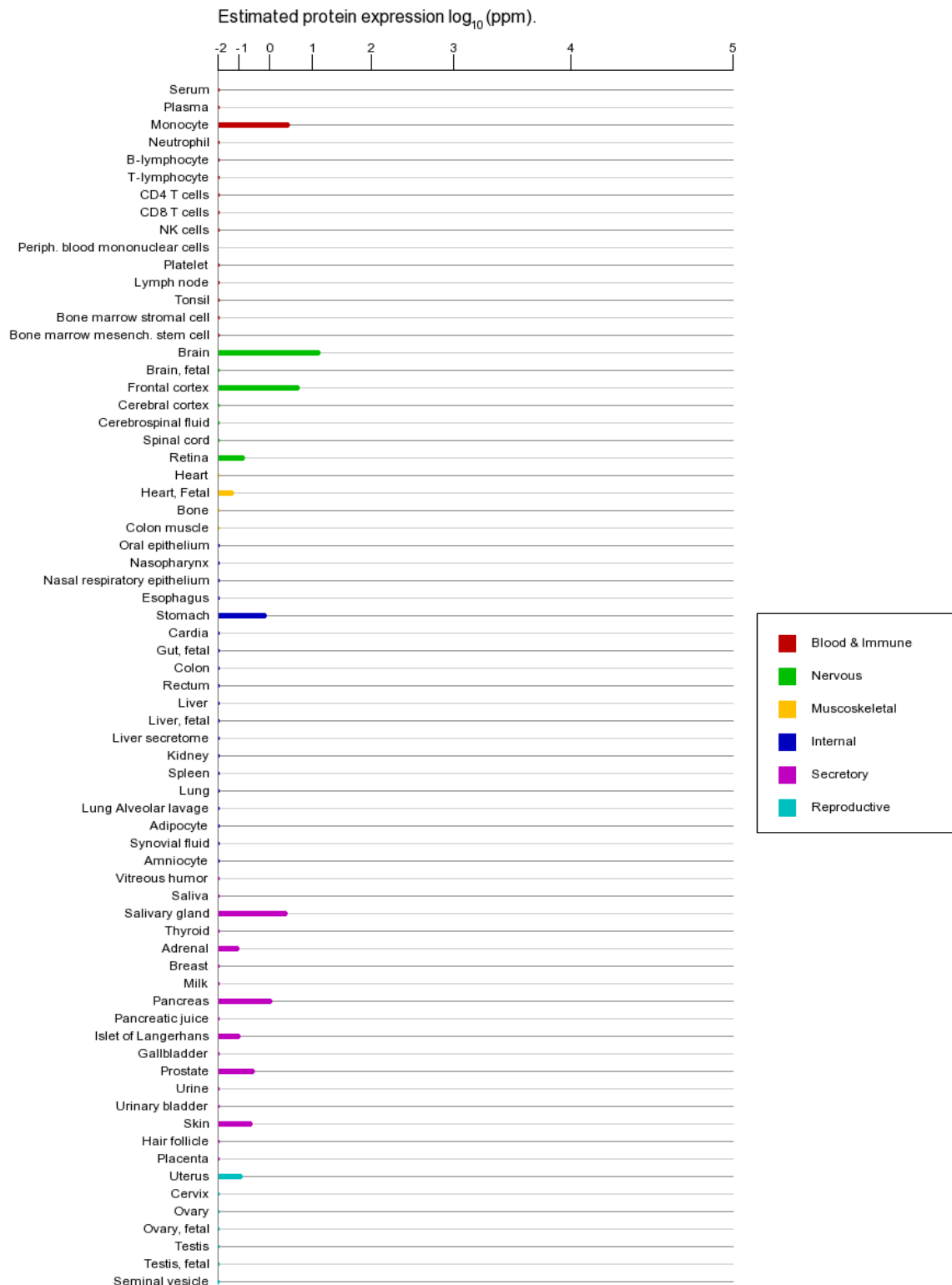


**Figure 12 Estimated protein expression level of CAPS2.**

Source: GeneReport for Unigene cluster for CADPS2 Gene Hs.649459

CAPS2 deficient mice exhibited autistic-like behavioral phenotypes such as impaired social interaction, hyperactivity and increased anxiety in an unfamiliar environment (Sadakata et al., 2007a).

### **I.7 Aim of the Thesis**

The secretion machinery that permits the release of both LDCVs and SVs in DRG neurons has not been studied. It is not clear which priming factors are involved. A quarter of a century time worth of CAPS studies made us understand that this protein plays different and sometimes opposite roles among mammalian and invertebrate systems. Due to the diverse and controversial roles of CAPS, it was of great interest to investigate whether it primes LDCV secretion or not. If CAPS does prime, the second question to address is which isoform is involved? According to (Sadakata et al., 2006; Sadakata et al., 2007b), CAPS1 is found in all DRG neurons while CAPS2 is localized to an unknown subpopulation. To which subpopulation does CAPS2 localize to and what role does it play? Since, DRG neurons are very diverse, this different localization might imply different roles of CAPS isoforms. To study whether CAPS primes SV release, it was necessary to establish DRG/S neuron co-culture in order to achieve functional synapses (Joseph et al., 2010) in-vitro and test at what time these synapses start to form and if they are functionally interconnected or not. We hypothesized that CAPS1 might be responsible for SV release because of its presence in all DRG neurons and it is known that all these cells form synapses with higher order CNS neurons. Would CAPS2 prime SV release as well? What would be the effect of absence of both isoforms on SV release? Another question was whether CAPS plays a role in synapses between DRG neurons and spinal neurons. The main aim of my thesis was to identify the role of CAPS isoforms in murine DRG neurons and to look deeper at the localization and investigate the idea of differential regulation at different levels. Unraveling the molecular exocytosis machinery of DRG neurons is relevant for controlling pain which is important in medicine.

## II. Materials and Methods

The used materials were mainly available at the department of Univ.-Prof. Dr. Jens Rettig and to lesser extent at the department of Univ.-Prof. Dr. Dieter Bruns.

### II.1 Materials:

#### II.1.1 Chemicals

Product	Company
Agar	Roth
B27-Supplement	Life Technologies
BSA	Sigma-Aldrich
CaCl <sub>2</sub> x 2H <sub>2</sub> O	Merck
Chloroform	Sigma-Aldrich
Cyclotraxin B	Tocris
DMEM	Life Technologies
dNTP-Mix	Fermentas
DPBS	Life Technologies
Ethanol 100%	Roth
EtBr	Life Technologies
EDTA	Sigma-Aldrich
EGTA	Sigma-Aldrich
FCS	Life Technologies
Formaldehyde	PolyScience
Fura-2 AM	Life Technologies
FUDR	Sigma-Aldrich
Glucose	Merck
Glutamax	Life Technologies
Glycerol	Roth
Glycin	Roth
HEPES	Sigma-Aldrich
HEPES-buffer	Sigma-Aldrich
HPLC water	Life Technologies
Isopropanol	Roth
Kanamycin K-1377	Sigma-Aldrich
KCl	Merck
λ Marker	Roche

## MATERIALS AND METHODS

---

Product	Company
MgATP	Sigma-Aldrich
NaCl	Merck
NaCHO <sub>3</sub>	Merck
Na <sub>2</sub> HPO <sub>4</sub> x 2H <sub>2</sub> O	Merck
NaH <sub>2</sub> PO <sub>4</sub> x H <sub>2</sub> O	Merck
NEAA	Life Technologies
Neurobasal A	Life Technologies
NGS	Panbiotech
Olcegepant	MedChem Express
Optimem	Life Technologies
PCR-buffer	Sigma-Aldrich
Penicillin	Life Technologies
Pepton	Roth
<i>pfu</i> -Polymerase Buffer	Fermentas
PDL	Sigma-Aldrich
Phenol	Sigma-Aldrich
RPMI	Sigma-Aldrich
Sodium pyruvate	Life Technologies
Streptomycin	Life Technologies
Sucrose	Merck
Trishydrochlorid	Roth
Triton X-100	Roth
Uridin	Sigma-Aldrich
Water	Sigma-Aldrich

### II.1.2 Solutions

#### II.1.2.1 Base<sup>-</sup> 10x (Tobias) + 40 mM NH<sub>4</sub>Cl

NH<sub>4</sub>Cl, 40 mM, (0.427 g/l)

NaCl, 1480 mM, (1.309 g/l)

KCl, 24 mM, (0.035 g/l)

HEPES, 100 mM, (0.0476 g/l)

MgCl<sub>2</sub> x 6H<sub>2</sub>O, 12 mM, (0.0487 g/l)

CaCl<sub>2</sub> x 2H<sub>2</sub>O, 25 mM, (0.0735 g/l)

#### II.1.2.2 Blocking Solution (50 ml)

NGS, 1.25 ml

PBS, 48.75 ml

#### II.1.2.3 S neurons Cell Culture Medium (50 ml)

NBA, 45 ml

FCS, 2.5ml

Horse serum, 2.5 ml

NGF, 100 µl

FUDR, 500 µl

#### II.1.2.4 DRG Intracellular Patch-Clamp Solution

L-Aspartat, 135 mM

MgCl<sub>2</sub> x 6H<sub>2</sub>O, 1 mM

HEPES, 10 mM

CaCl<sub>2</sub> x 2H<sub>2</sub>O, 3 mM

Cs-EGTA, 5 mM

MgATP, 2mM

Na<sub>2</sub>GTP 0.3 mM

pH: 7.2

Osmolarity: 300~315 mOsm

### **II.1.2.5 DRG Extracellular Patch-Clamp Solution**

NaCl, 131 mM

NaHCO<sub>3</sub>, 25 mM

KCl, 2.5 mM

NaH<sub>2</sub>PO<sub>4</sub> x H<sub>2</sub>O, 1.25 mM

MgCl<sub>2</sub> x 6H<sub>2</sub>O, 1 mM

CaCl<sub>2</sub> x 2H<sub>2</sub>O, 2 mM

Glucose, 10 mM

pH: 7.4 (5% CO<sub>2</sub> + 95% O<sub>2</sub>)

Osmolarity, ~300 mOsm (with glucose)

### **II.1.2.6 DRG Extracellular Solution**

NaCl, 147 mM

KCl, 2.4 mM

CaCl<sub>2</sub> x 2H<sub>2</sub>O, 2.5 mM

MgCl<sub>2</sub> x 6H<sub>2</sub>O, 1.2 mM

HEPES, 10 mM

Glucose, 10 mM

pH: 7.4

Temperature: 34 °C

Osmolarity: 300 mOsm (with glucose)

### **II.1.2.7 DRG Cell Culture Medium**

NBA medium

FCS 5%

FUDR 10 µl/ml

### **II.1.2.8 FUDR**

FUDR, 8.1 mM

Uridin, 20.5 mM

DMEM

### **II.1.2.9 HBS 2X Solution (100 ml)**

HEPES, 50 mM (1.19 g)

NaCl, 280 mM (1.64 g)

NaH<sub>2</sub>PO<sub>4</sub>, 1.5 mM (0.02 g)

### **II.1.2.10 HEPES pH-Buffer Physiological Solution**

NaCl, 30 mM

KCl, 100 mM

MgCl<sub>2</sub>, 2 mM

Glucose, 10 mM

HEPES, 20 mM

### **II.1.2.11 HEK Cell Culture Complete-Medium (100 ml)**

DMEM + 4.5 g/l Glutamax, 100 ml

Sodium pyruvate, 1.1 ml

NEAA, 1.1 ml

FCS, 10 ml

Penicillin/Streptomycin, 0.1 ml

### **II.1.2.12 iB<sub>4</sub> Staining Solution**

iB<sub>4</sub> conjugated to Alexa-568, 1 mg/ml (5 µl)

Extra cellular solution, 2 ml

### **II.1.2.13 LB-Medium**

Pepton, 8g

Hefextrakt, 4g

NaCl, 4 g

H<sub>2</sub>O, 800 ml

### **II.1.2.14 Loading Buffer**

Sucrose, 4g

Bromphenol blue

Sigma H<sub>2</sub>O, 10 ml

### **II.1.2.15 Liberase S neurons Digestion Solution**

Liberase DH, 2.3 U

NBA, 1 ml

### **II.1.2.16 Locke's 10x Solution**

NaCl, 1.54 M

KCl, 56 mM

NaH<sub>2</sub>PO<sub>4</sub> x H<sub>2</sub>O, 8.5 mM

Na<sub>2</sub>HPO<sub>4</sub> x 2H<sub>2</sub>O, 21.5 mM

D-Glucose H<sub>2</sub>O, 100 mM

### **II.1.2.17 MES pH-Buffer Physiological Solution**

NaCl, 30 mM

KCl, 100 mM

MgCl<sub>2</sub>, 2 mM

Glucose, 10 mM

HEPES, 20 mM

### **II.1.2.18 Mounting Medium**

Mowiol 4-88, 2.4 g

Glycerol, 6 g

H<sub>2</sub>O double distilled, 6 ml

Tris-Buffer, 12 ml

pH: 8.5

### **II.1.2.19 Neurobasal A-Medium**

NBA, 500 ml



B27, 5 ml

Glutamax, 5 ml

(This solution is either prepared with 1 ml of Penicillin/streptomycin or without antibiotics)

### **II.1.2.20 Optimem**

Optimem, 44 ml

Tryptosephosphate, 5 ml

HEPES buffer, 1 ml

Penicillin/Streptomycin, 50  $\mu$ l

BSA, 0.1 g

### **II.1.2.21 Paraformaldehyde (15% PFA, 10 ml)**

PFA, 1.5 g

Sigma H<sub>2</sub>O, 10 ml

NaOH, 15  $\mu$ l

pH: 7.4

### **II.1.2.22 PBS (1 l)**

Na<sub>2</sub>HPO<sub>4</sub>, 58 mM (10.3234 g/l)

NaH<sub>2</sub>PO<sub>4</sub>, 17 mM (2.345 g/l)

NaCl, 83 mM (4.850 g/l)

### **II.1.2.23 Peptides-Blocking Solution**

L-70,606 oxalate salt hydrate (10  $\mu$ M)

BIBN 4096BS Olcegepant (10 nM)

Cyclotraxin B (1  $\mu$ M)

NH<sub>4</sub>Cl, 40 mM, (0.427 g/l)

NaCl, 1480 mM, (1.309 g/l)

KCl, 24 mM, (0.035 g/l)

HEPES, 100 mM, (0.0476 g/l)

MgCl<sub>2</sub> x 6H<sub>2</sub>O, 12 mM, (0.0487 g/l)

CaCl<sub>2</sub> x 2H<sub>2</sub>O, 25 mM, (0.0735 g/l)

### **II.1.2.24 Permeabilization Solution (50 ml)**

Triton x-100, 50 µl

NGS, 1.25 ml

PBS 1x, 48.25 ml

### **II.1.2.25 PDL**

Poly-D-Lysin Hydrobromid, 0.5 mg/ml

Sigma H<sub>2</sub>O

### **II.1.2.26 Quenching Solution (50 mM Glycin)**

Glycin, 0.187 g

PBS, 50 ml

### **II.1.2.27 RPMI**

RPMI, 500 ml

FCS, 50 ml

Pen/Strep, 5.5 ml

HEPES, 5.5 ml

## **II.1.3 Enzymes**

Liberase DH Research Grade, Sigma-Aldrich from Roche  
Papain, Cellsystems, Worthington Biochemical Corporation

TrypLEE Express, Gibco from Life Technologies

Trypsin-EDTA, Invitrogen

## **II.1.4 Antibiotics**

Ampicillin Na-Salz, Zchl/Roth Carl, K029.1.

Pen/Strep, fisher scientific, 10452882.

Nigericin sodium salt, Zchl/Sigma Aldrich, N7143-10 mg.

Vancomycin, Zchl/Life Technologies, V-1644.

### II.1.5 Bacteria and Cell Lines

#### II.1.5.1 Bacteria

DH5 $\alpha$ : F<sup>-</sup> endA1 glnV44 thi-1 recA1 relA1 gyrA96 deoR nupG purB20  $\phi$ 80dlacZ $\Delta$ M15  $\Delta$ (lacZYA-argF) U169, hsdR17 (rK-mK+),  $\lambda$ <sup>-</sup>. Invitrogen, Life Technologies.

Stbl3: F<sup>-</sup> glnV44 recA13 mcrB mrr hsdS20 (rB<sup>-</sup>, mB<sup>-</sup>) ara-14 galK2 lacY1 proA2 rpsL20 xyl-5 leu mtl-1. Invitrogen, Life Technologies.

#### II.1.5.2 Cell Lines

HEK 293FT. Life Technologies.

### II.1.6 Mouse Strains

C57Bl/6N (Black 6), Stock No: 005304, The Jackson Laboratory

129/svj, Stock No: 000691 | 129X1. The Jackson Laboratory

### II.1.7 Kits

EndoFree Plasmid Maxi Kit, Qiagen

EndoFree Plasmid Mini Kit, Qiagen

QIAprep Spin Miniprep Kit, Qiagen

QIAquick Gel Extraction Kit, Qiagen

QIAquick PCR Purification Kit, Qiagen

### II.1.8 Cell Culture Products

Product	Lot #	Company	Size
NBA (1x)	10888022	Gibco	500 ml
B27 serum-free supplement (50x)	17504044	Gibco	10 ml
Pen/Strep	15070-063	Gibco	100 ml
FCS	10500-064	Gibco	500 ml
HS	P30-0701	PAN Biotech	100 ml
NGF	N-245	Alomone Labs	25 mg
FUDR	F0503	Sigma	100 mg
PDL	P0899	Sigma	50 mg
BSA	A8022	Sigma	1 g
EBSS (+Ca +Mg)	24010043	Gibco	1 g
Needle-Long (20 Gx2 <sup>3</sup> /4:0.9x70 mm)	NN2070S	Stoss Medica	
Needle-Thick (20Gx1 1/2 09x40 mm)	NN2038R	Stoss Medica	
Filter small-white (Acrodisc 13 mm 0.2 $\mu$ m)	PN4427T	Life Sciences	

Filter blue-green (32 mm 0.8/0.2 $\mu\text{m}$ )	514-4136	VWR
Filter white (0.2 $\mu\text{m}$ )	514-0061	VWR
Petri dish (150x20 mm)	821473	Sarstedt
Petri dish (92x16 mm)	821473	Sarstedt

### II.1.9 Microscope Facilities

#### II.1.9.1 Total Internal Reflection Fluorescence Microscope

Conventional epifluorescence microscopes are widely used to observe fluorescent samples. This technique comes at the cost of spatial resolution as the signal is highly affected by the sample brightness and the background fluorescence, which generates a fuzzy image. Meanwhile, confocal microscopes employ a Pinhole to limit the diffraction from backgrounds and foregrounds, it basically enables one to get specific emitted signals at specific depth but at the cost of speed. On the contrary, total internal reflection fluorescence microscopes (TIRFM) takes advantages of the properties of totally internally reflected lights which generates electromagnetic evanescent waves that illuminate fluorescent probes within a close proximity of the glass/water interface. With TIRFM, it is possible to achieve high spatial resolution with fast acquisition rates which enables high time resolution recordings, such as LDCV release from DRG neurons as well as synaptic transmission from DRG/S neurons co-cultures or any membrane-associated processes.

#### **TIRFM concept:**

TIRFM technique was initially developed by Danial Axelrod at the University of Michigan in beginning of 1980s (Axelrod, 1981). Whenever light passes through interface of two transparent media with different refractive indices it will be partially diffracted. Above a certain critical angle

of incidence, there will be total internal reflection inducing an electromagnetic field that pass through the interface forming an evanescent waves that decays exponentially with depth (Axelrod, 1981). Hence it excites fluorescent probes within the evanescent field and keeping the rest of the sample dark. The acquired images are therefore sharp and are not affected less by the fluorescence of other cell components or the background (Figure 13).

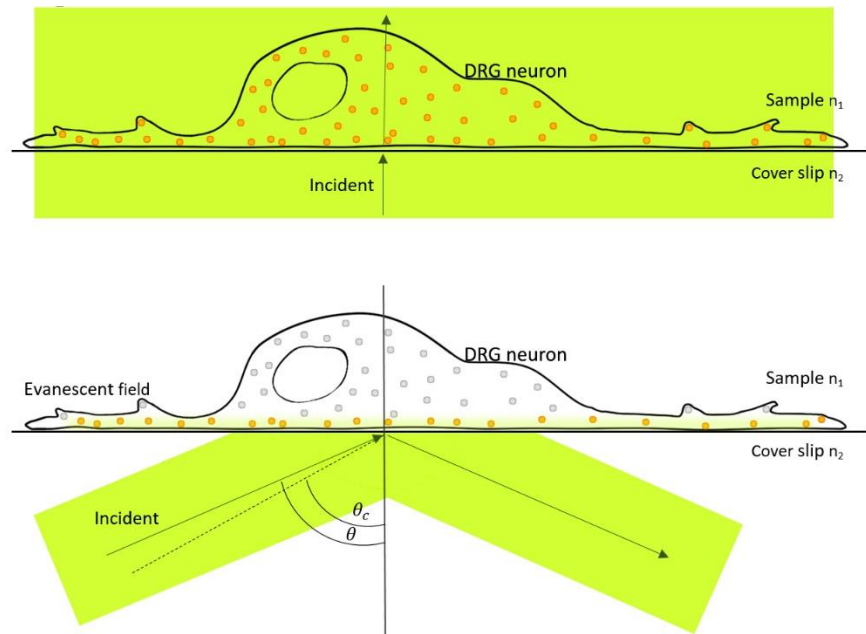


**Figure 13 Total internal reflection fluorescence microscopy concept.**

Unlike epifluorescence microscopes which covers the entire sample, Olympus TIRFM generates an evanescent field that penetrates to a restricted depth into the sample enabling to sharply visualize all the vesicles lying within this range. Graphical illustration: Abed Shaib.

### Microscope general information:

The Olympus TIRFM IX70 microscope setup is custom made with several enhancements that enable a wide set of electrophysiological experiments to be performed. For instance it is provided with two perfusion systems, one being automated and the other is manual; the manual was heated while the other was controlled via a Warner Instruments valve control (model VC-6 VALVE). The microscope is equipped with an 100x objective featuring a high numerical aperture (1.45 NA) that is equipped with a correction collar to adjust for the thickness of the coverslip. The laser light passes through the objective, the immersion oil ( $n = 1.52$ ), and is reflected at the interface between the glass coverslip and the extracellular solution ( $n \sim 1.33$ , Temp. 34 °C), achieving TIRF and an evanescent field that fades away exponentially with depth of 230 nm (Quintana et al., 2007). Excitation can be applied by two laser systems from Spectra-Physics (450, 488 and 514 nm – model 285-FA11) and a second red (561 nm) laser from Melles Riot (model 85-YCA-615); as well as through a high speed visichrome polychromator (model 2261). The laser wave length is modulated by an Acousto Optical Tunable Filter (AOTF) from Visitron Systems (model VS AOTF-2). The setup is equipped with different AHF filter sets (green/red, UV, mTFP and yellow/red) and a

QuantEM 512SC camera from Andor Technology Plc with Dual-View (565dcxr). The setup has 3 sets of objectives, the 10x, 40x and 100x NA 1.45 Apochromat TIRF objective. The setup is operated by VisiView version 2.1.2 software from Visitron Systems.

### Electrical stimulation components:

Electrical stimulus was applied via a Stimulator from AM Systems. The Stimulator is connected to a custom-made bipolar field electrode that is supported by a micro-manipulator model SM-8 from Luigs & Neumann Company. The original field electrode was purchased from MicroProbes (#PI2ST30.5B10) for Life Sciences, and was later subjected to manual enhancement by eroding the heated tapered end. Initially, the company produced only *Heat Tapered* field electrodes (H in Figure 14) that were not stable and air bubbles were generated whenever the applied stimulating voltage exceeds 2.5 V. At high voltage applied to a small surface area, the tip of the electrode heats which generates air bubbles that erode the tip. To counter this, I trimmed the tip of the electrode to approximately 60  $\mu\text{m}$  in diameter and then applied 4 V to induce maximum DRG cells response. The electrode was stable enough to handle up to 10 V at 100 Hz without generating air bubbles<sup>6</sup>. The impedance of the field electrode was 0.1  $\Omega$ . The company later reported that they added a more

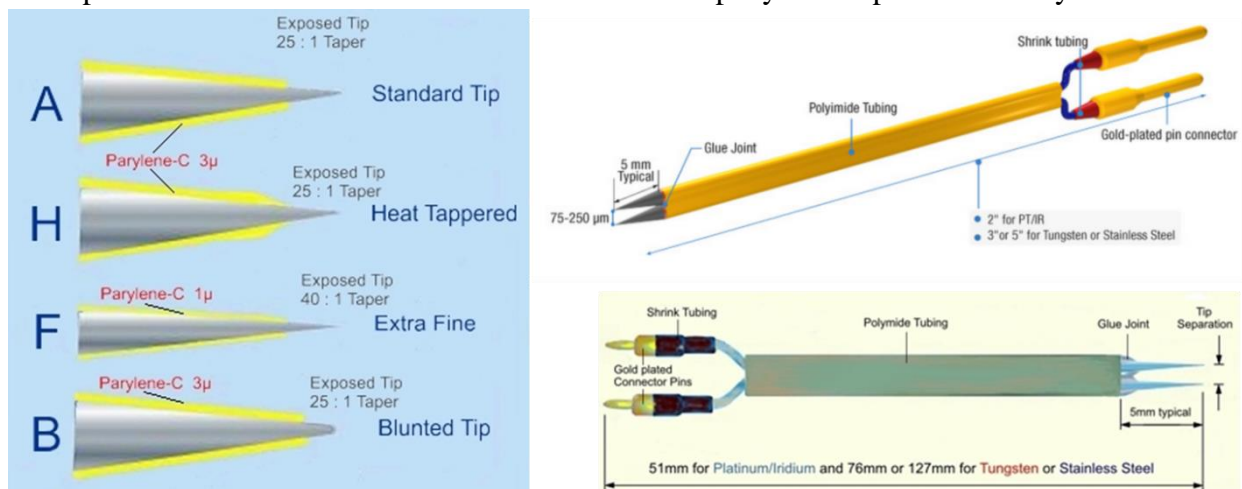


**Figure 14 MicroProbes commercial field electrodes.**

A - Standard tip profile (25:1 Taper). Tungsten - Platinum/Iridium - Pure Iridium - Stainless Steel.

H - Heat treated tapered tip profile (25:1 Taper). Tungsten - Platinum/Iridium - Pure Iridium Stainless Steel.

F - Extra fine tip profile (40:1 Taper). Tungsten only.

B - Blunted tip profile (25:1 Taper). Tungsten - Platinum/Iridium - Pure Iridium - Stainless Steel.

Source: MicroProbes for Life Technologies. Link: [www.science-products.com/Products/CatalogG/MPI-Electrodes/MPI.html](http://www.science-products.com/Products/CatalogG/MPI-Electrodes/MPI.html)

<sup>6</sup> My findings were supported by a study of A. Petrossians presented in SFN Chicago, 2015. Talk citation: Nanosymposium – Electrodes Arrays III: N227 (talk 565.08: In-vivo characterization of Platinum-Iridium electroplated dbs electrodes).

recent bullet-shaped electrode product to their inventory as a result of the numerous feedback from many scientists. The exposed length of the wider tip would be less than the sharp long electrode that makes it with almost same impedance. Hence isolation can be improved since the blunt pointed structure is more stable and less subject to fractures compared to the *Heat Tapered* end electrode; claiming that this provides greater selectivity and more stability of the field electrodes upon high voltage vigorous stimuli. The composed material in the selected field electrode was an alloy of Platinum and Iridium. Platinum is one of the best highly-unreactive precious conductors of electricity but it has a disadvantage that it is malleable. To overcome the malleability of Platinum, it was mixed with Iridium, the latter is well known for its high density, it is the second densest element after Osmium. Iridium is corrosion-resistant and it can handle temperatures as high as 2000 °C thus providing a good support to the good conductor Platinum, ensuring a stable break-resistant electrodes. The electrode was fixed to metal support exposing its tip and was eroded under 40x magnification using a sharp razor (Figure 15). The parylene layer was also removed from the tip to make sure it is well exposed so that the electricity is conducted to nearby cells. To test the electrode, a glass pipette with metal electrode connected to an oscilloscope was placed between the two field electrodes in a good conductor solution and 4 V stimulus was applied. Nearly, four volts

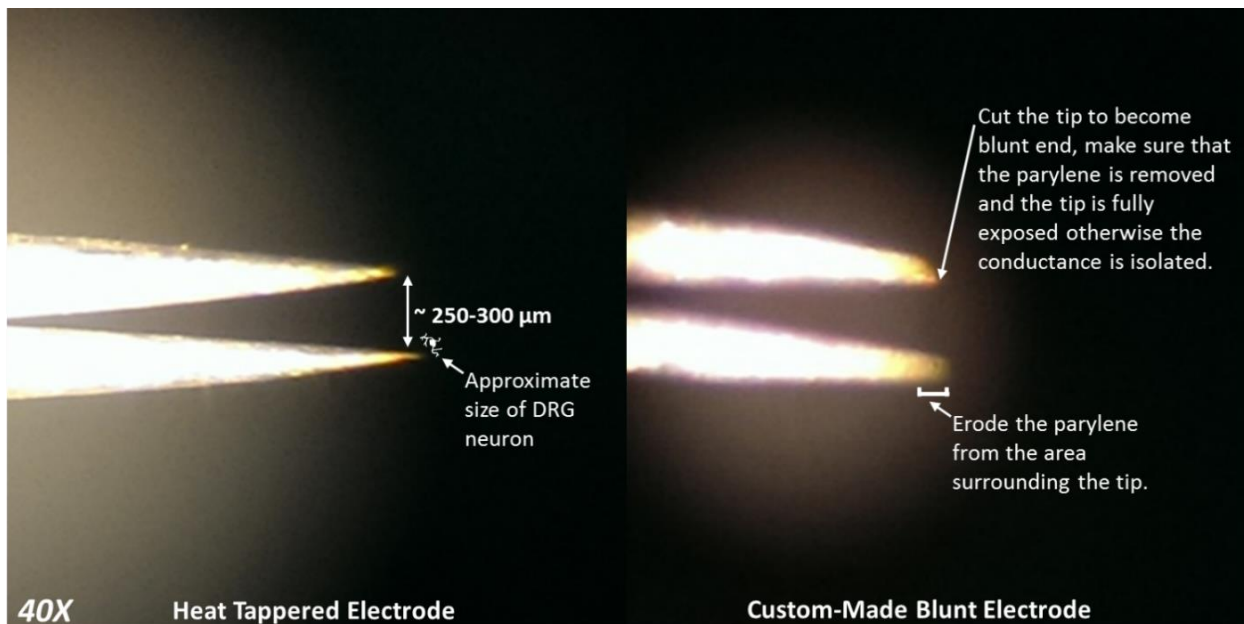


**Figure 15 Magnified image of the original Tapered electrode compared to the custom eroded one.**

In the first panel, the two tips of the field electrode are usually apart from each other with a distance ranging from 250 to 300 μm. In the second panel, the tip is manually eroded using a sharp razor to make it wider and the parylene insulating paint is removed away from the eroded part.

were detected by the oscilloscope hence confirming the effectiveness of the stimulus (Figure 16). However, the applied voltage decays over distance as it moves away from the electrode poles. In ideal condition, if the voltage is fixed, the surface area of the pointed tip of the electrode stays the same and considering the material as excellent conductor, the electric field  $E$  would equal to voltage divided by distance:

$$E = V/d$$

$$E = \frac{4}{150} = 0.0267 \text{ V}/\mu\text{m}$$

$$\Rightarrow 0.0267 = \frac{V}{50} \rightarrow V = 1.33 \text{ V for every } 50 \mu\text{m} \pm 1.33 \text{ V}$$

As a second way of confirming the functionality of the field electrode, a more physiological test was used, whereby DRG neurons were loaded with a calcium dye Fluo-4 AM and 4 V stimulus was conducted. Upon depolarization, voltage-dependent calcium channels open, allowing the entry of  $\text{Ca}^{2+}$ . Intracellular calcium concentration increase affecting the fluorescence intensity of Fluo-4. Cells in which the fluorescence intensity increased upon stimulation would be marked as responding cells to the electrical stimulus. The percentage of depolarized responding cells was measured (data is shown in *Results* chapter). A wider range of voltages were tested starting at 2.5 V to 7 V with 4 V having the highest number of responding cells.

### Recording of LDCV evoked release from DRG cultures:

DRG neurons were transfected with a Lentivirus encoding for NPY-Venus 6 days prior to physiological measurements. NPY-Venus is semi-pH sensitive protein that fluoresces weakly at

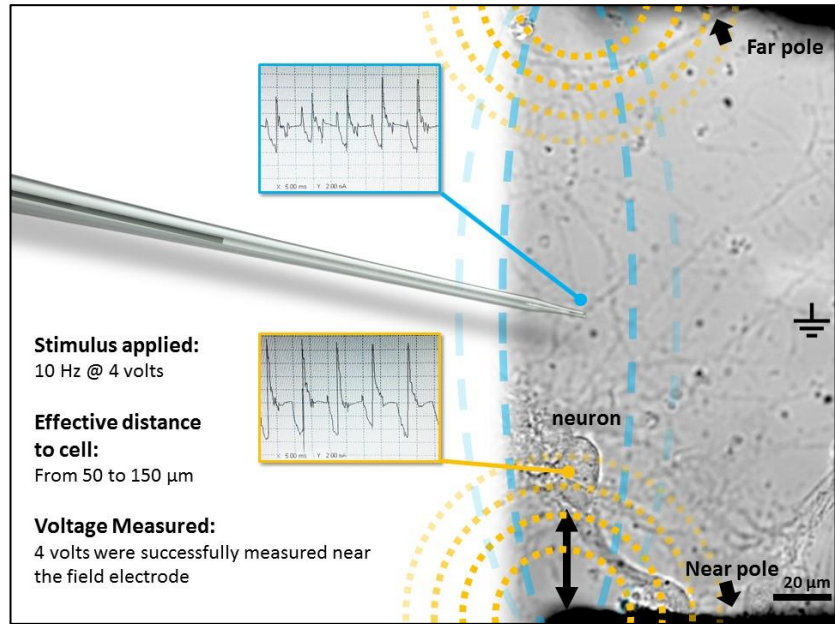


**Figure 16 Bright field image captured at 100x magnification of DRG neuron culture showing field electrode adjustment.**

The real image was edited for display purpose to present the place of the pipette that was used to measure the voltage between the two poles of the electrode. In the real settings the glass pipette is outside the camera detection field.



## MATERIALS AND METHODS

the acidic pH of the vesicle lumen. Upon fusion of the vesicle with the plasma membrane the pH lumen neutralises thereby dequenching the fluorescence of Venus. This fluorescence "flash" helped me to identify fusion events. A mild stimulus of 4 V at frequency of 10 Hz was applied to the cells for 30 s followed by a stronger stimulus of 4 V at 100 Hz to effectively evoke LDCV release (Figure 17). Fusion events were recorded in TIRF mode at 514 nm (2% laser) with EM Gain of 600 for 3 minutes. Exocytosis was essentially recognized by fast disappearance ( $>200$  ms) of NPY-Venus fluorescence. The number of fusion events were exclusively counted from DRG cell bodies. Fusion events may be underestimated as unclear fusion events were dropped in all measured sets. To assure the functionality of the field electrode, it was regularly tested every 3 to 4 months with calcium imaging and it was replaced with a new electrode every 8 to 9 months as it erodes with time.

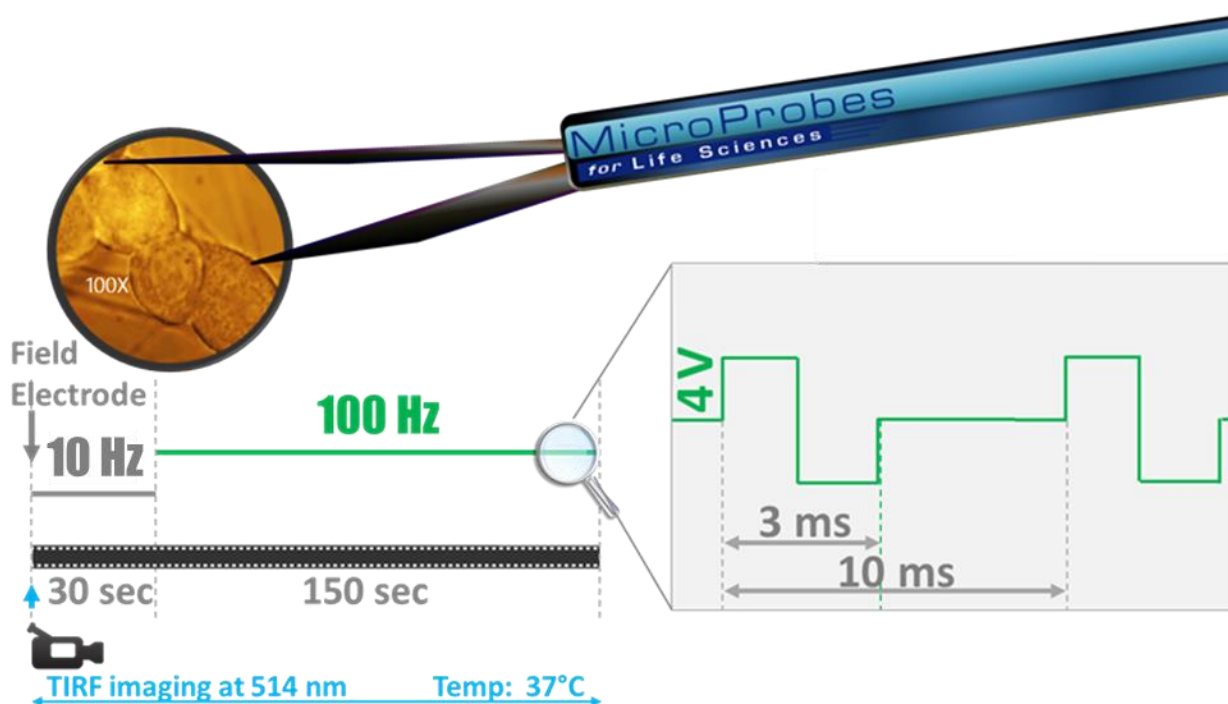


**Figure 17 Stimulation protocol to induce LDCV release.**

DRG neurons were transfected with NPY-Venus to visualize exocytosis using 100X objective and excited at 514 nm. TIRF movies were recorded for 3 minutes. Transfected DRG neurons were stimulated with bipolar field electrode to elicit LDCV secretion. The stimulation starts at 10 Hz for 30 sec and followed by 100 Hz, both of which are at 4 V intensity, having bipolar pulse width of 3 ms and inter-bipolar pulse duration of 10 ms. The recordings were made at 37 °C.

## SV evoked release recordings from DRG/S neuron co-cultures:

DRG/S neuron co-cultures were necessary for establishing functional synapses, more details would be provided in the *Results* and *Discussion* chapters. 24 hrs after taking the DRG neurons in culture, we added a Lentivirus encoding for Synaptophysin pHluorin (SypHy) BL-47 purchased from Viral Core Facility in Berlin. The superecliptic pHluorin was fused to the second intravesicular loop of synaptophysin (Granseth et al., 2006). On the third DIV, SypHy was removed

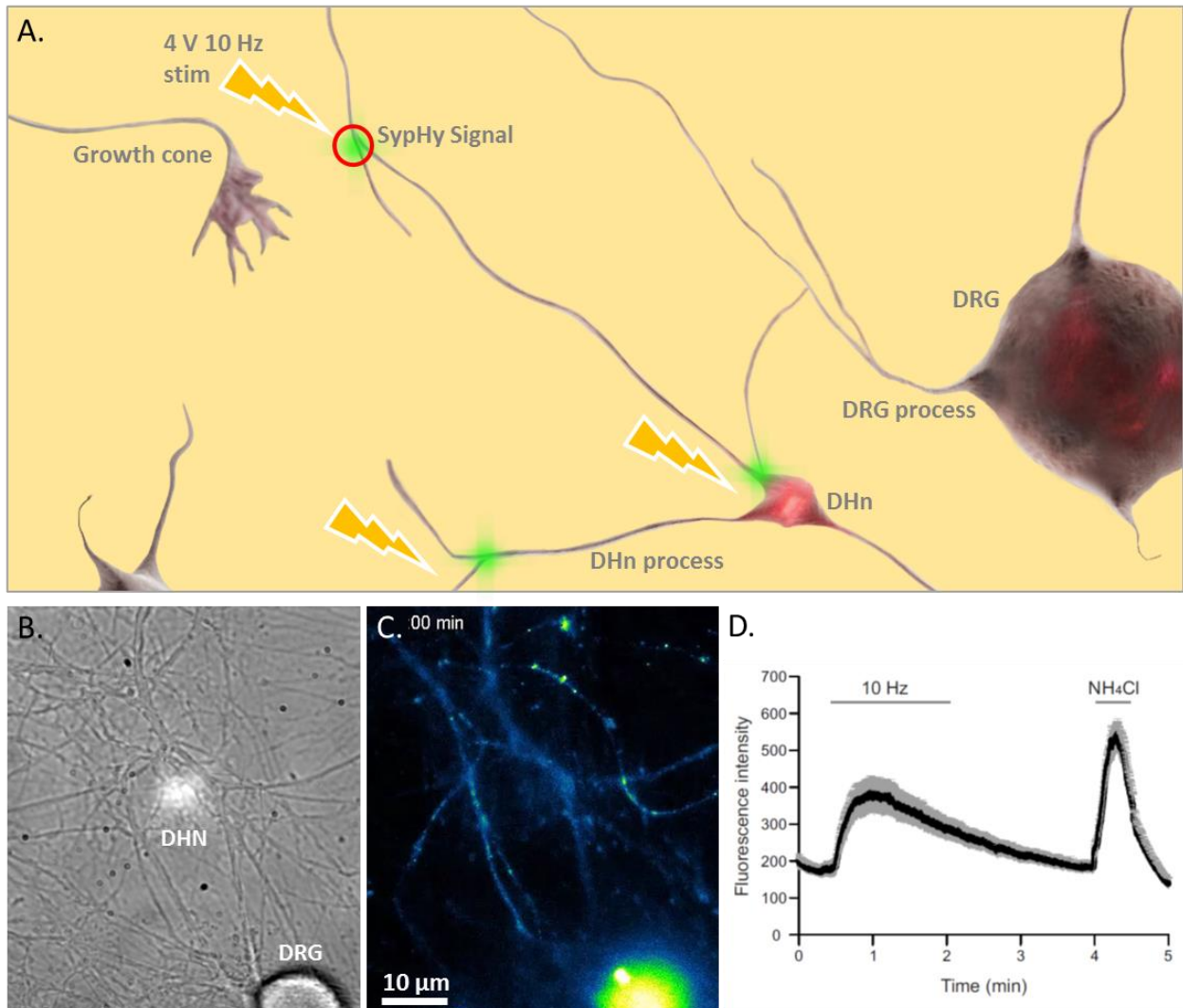


**Figure 18 Synaptic transmission stimulus protocol.**

(A) Graphical illustration of DRG/S neuron co-cultures. DRG neurons extend processes towards S neurons and form synapses on their cell bodies as well as on the processes. Upon applying 4 V at 10 Hz stimulus, synaptic vesicles fuse, SypHy is exposed to the neutral pH and hence the fluorescence signal increases. Single ROI (red circle) marks individual synapses to measure the mean gray value and plot their fluorescence over time. (B) Bright field image of DRG/S neuron co-culture acquired at 100x. (C) Snapshot from DRG/S neuron movie acquired at 488 nm in TIRFM. (D) Average fluorescent intensity graph of all the synapses displayed with SEM plotted against time. 4 V stimulus at 10 Hz was applied after 30 seconds of recording for 1 min, then the synapses were left to recover. After 4 min of recording,  $\text{NH}_4\text{Cl}$  was applied to deprotonate the vesicles at synapses and induce the maximum increase in fluorescence signal. Error bars in (D) are SEM.

and S neurons were added, thus ensuring that only synapses formed from DRG neurons onto S neurons were marked with SypHy, excluding the S neurons/S neurons synapses. DRG/S neurons were maintained 9 DIV together before any measurements were carried out. Five minutes recording in *semi*-TIRF mode (a border state between epifluorescence and TIRF acquisition, achieving higher signal to noise ratio) was performed. *Semi*-TIRF acquisitions were necessary to include processes and synapses outside the TIRF field. Thirty seconds were recorded prior to a 4 V at 10 Hz stimulus that was applied for 1 min. Then the synapses were allowed to recover for 3 min before NH<sub>4</sub>Cl was applied manually to deprotonate all the vesicles and highlight all synapses with maximum intensity. The maximum synapse fluorescence signal after NH<sub>4</sub>Cl application was used to normalize individual synapse response to the stimulus. A ten Hertz stimulus was previously in rat hippocampal neurons and cat superior cervical ganglion cells (Applegate and Landfield, 1988; Pysh and Wiley, 1974). The first reported usage of an external field electrode to stimulate DRG/S neuron co-cultures with 10 Hz stimulus date back to mid-80s whereby (Jahr and Jessell, 1985) showed that glutamate, or a glutamate-like compound is the excitatory transmitter that mediates fast excitatory postsynaptic potentials in these types of synapses. For carrying out the synaptic transmission experiments, I tested several stimuli, 5 Hz, 10 Hz, 20 Hz and 100 Hz in hippocampal and DRG/S neuron. I found that the best stimulus is 4 V at 10 Hz, as I had the maximum response with the smallest possible stimulus.

### II.1.9.2 Confocal Laser Scanning Microscope

Laser scanning microscopes (LSM) are able to scan samples either sequentially point by point, or multiple points at once whereby the information contained in electrical signals is digitized and is integrated into an acquired high optical resolution image. The microscope that I used is driven by *Zeiss Efficient Navigation* (ZEN) 2011 SP2<sup>7</sup> software that helps in setting the desired acquisition parameters to visualize samples.

#### LSM concept:

Sixty years ago, Hiroto Naora was the first to practically use confocal optics by direct supervision of Zyun Koana (Naora, 1951). They didn't generate images but rather used it in high

---

<sup>7</sup> Black edition, version 8.0

resolution micro-spectrophotometry. Ten years later, Marvin Minsky took advantage of that and added a scanning stage, building a microscope that can acquire images and filed a patent in 1957 without any scientific publications. LSM improved over time, but it took 30 years to become widely available as tool for obtaining High resolution optical images with depth selection, acquiring images focused to certain depth, a process called optical sectioning. Obtaining the data at different z-levels allows 3-D reconstructions of complex samples. The depth of scanning depends on the amount of light that can penetrate the tissues at a given time. Confocal LSMs send a laser beam that passes through aperture and then is focused by an objective lens within the surface of the fluorescent sample. The reflected laser and fluorescent light from the sample goes back through the objective lens and then into the beam splitter that sends part of the signal to a detection system. The original excitation wavelength is blocked and only the emitted signal is detected after passing through a Pinhole with desired Airy Units and finally to the photomultiplier tube (PMT); changing the emitted light signal into digital electrical one and hence digitizing an acquired data into high resolution image<sup>8</sup>.

### **LSM 780 microscope general info:**

The microscope is provided with several sets of objectives:

- 10x dry objective, NA 0.3, EC Plan-Neofluar, M27<sup>9</sup>, Yellow ring color.
- 20x multi-immersion objective, NA 0.8, Plan-Apochromat, M27, Red/Green ring color.
- 40x water immersion objective, NA 1.2, C-Apochromat, M27, Blue ring color.
- 63x oil immersion objective, NA 1.4, Plan-Apochromat, M27, Black ring color.
- 100x oil immersion objective, NA 1.45, Alpha Plan-Fluar, M27, White ring color.
- APO Calibration LSM.

### **Stage control:**

Controlling the loading and navigation through the sample can be done by an X-Y joystick. The focus can be adjusted through a side wheel and the desired focal plane can be saved so that it is possible to be loaded automatically for the next sample.

---

<sup>8</sup> Technical information was revised according to “Confocal Basic Concepts” lecture from Nikon by: Stephen W. Paddock - Laboratory of Molecular Biology, University of Wisconsin, Madison, Wisconsin 53706 and Thomas J. Fellers and Michael W. Davidson - National High Magnetic Field Laboratory, 1800 East Paul Dirac Dr., The Florida State University, Tallahassee, Florida, 32310.

<sup>9</sup> Thread type.

### **Fluorescence lamp and bright field:**

It is possible to choose between bright field and fluorescence view at the eyepieces while in 'Locate' configuration mode simply by turning on the X-Cite lamp 120PC Q and setting the desired filter. Open the lamp shutter with minimal lamp power of 12% to maximum 100% and the sample is ready for inspection. Once the intended area of acquisition is defined, hit the light-off to avoid photobleaching and switch the configuration mode into 'Acquisition'.

### **Acquisition configuration:**

It is possible through ZEN to devise acquisition parameters from scratch, reuse existing configuration or select 'Smart Setup' rather than using your own dyes mix with manual excitation/emission cut. Live scan settings provides the possibility to acquire at different wavelength excitations: Diode 405, Argon 458, HR Diode 488, HR Diode 514, HR DPSS<sup>10</sup> 561, HeNe 633 and HR Diode 642 nm lasers. For every laser, 'Gain Master', 'Digital Offset' and 'Digital Gain' can be defined as well as the addition of a bright field image (T-PMT) for every wave length while a uniform 'Pinhole' Airy Units is selected for all channels. Once the channels set, Zen also enables to define the 'Scan Mode', 'Frame Size', 'Line Step', 'Speed' and/or 'Pixel Dwell' time, 'Bit Depth' and the 'Averaging Number, Mode and Method'. The size of the scanned area can be defined by 'Scan Area' panel, a smaller area means lesser acquisition time, a feature than can be useful for fast acquisition purposes. There are four scanning possibilities: 'Live' as fast and continuous scan, 'Continuous' for high quality continuous scan but with lesser speed compared to 'Live', 'Snap' to acquire an image with the desired parameters and 'Do Experiment' to start the acquisition with the selected parameters for a defined number of cycles. While ZEN enables to acquire several cycles, it is also possible to do a Z-stack at several positions as a Tile scan at different selected positions with the option of correcting focus via infra-red adjustments of the focal plane. A slow feature (~ 17 sec) but recommended for long acquisition time to maintain the focal plane of interest during the recording. The 'Z-series' panel encompasses several options that enables the user to select the number of slices at which interval as well the last and first slice to be acquired. 'Tile' scan panel have several options to determine the regions of interest to be scanned as well the possibility of 'Live stitching' the acquired tiles with a certain percentage of image overlap. The acquired data can be represented in various ways and real time channel and color edit

---

<sup>10</sup> High Repetition rate Diode Pumped solid State Laser.

can be applied by stretching collective or individual channel stretch. Areas can be cropped and ROIs can be defined and pixel intensities can be measured and displayed in graphs while Live acquisition. 2-D or 3-D displays are available and there is a special panel for the metadata. Confocal imaging was mainly used during my study for ICC experiments, pH study experiments and real time long recording of growth cones movement analysis and synapse formation between DRG and S neurons.

### **LSM perfusion/suction system:**

The perfusion system was built by Dr. Elmar Krause and myself. The system was optimized in such a way to provide six solutions delivered sequentially or simultaneously. Four are automated and controlled with an electronic valve that can be switched on and off sequentially or simultaneously by a controller and two that are switched on manually by turning a knob independently. The perfusion is delivered to the specimen in glass pipette with a tilt angle that can be adjusted. The suction system end point is a glass pipette designed in such a way that keeps solution at its spherical bottom and sucks the extra solution out from a hole that is situated above the spherical bottom by 2 mm. This was necessary to eliminate desiccation of the sample due to surface tension and to reduce volume variation in the chamber which alter the focal plane and affect the recordings. The perfusion system specifications are as follows:

- Automated perfusion speed:  $144 \pm 5 \mu\text{l/s}$
- Manual perfusion speed:  $140 \pm 5 \mu\text{l/s}$
- Suction speed:  $404.4 \mu\text{l/s}$
- Dead-volume:  $\sim 241 \mu\text{l}$

Perfusion mixing was simulated in similar conditions of the built LSM perfusion system using water and Brilliant Black dye to ensure that the mixing covers the entire chamber and not just the surface as well as to test whether bubbles are generated or not.

### II.1.9.3 Structured Illumination Microscope

Hundred years ago, (Abbe, 1873) showed that optical microscopes have limited lateral resolution because of the finite wavelength of light. Unlike confocal microscopy, the super-resolution structured illuminated microscopy (SIM) can achieve a lateral resolution well beyond the classical limit without discarding light emission through a pinhole (Gustafsson, 1997; Heintzmann, 1998).

#### **SIM concept:**

SIM works in a very similar fashion to *moiré* effect. When two or more patterns are slightly tilted in angle and superimposed above each other, moiré fringes are formed (Figure 8). Similarly, in probes with fluorescent signal, SIM applies structured illumination locally at the place of interest. This generates a pattern that contains moiré fringes proportional to the original pattern but

much coarser in size because of the limit of light point spread function. But these fringes contain information about these structures that can resolve out high resolution information after processing the acquired raw data. Specialized algorithms, extract information thereby increasing the axial resolution - theoretically - up to 100 nm that is twice the light diffraction limit<sup>11</sup>. Images of Zeiss SIM microscopes can be acquired with up to 5 individual subsets (Grating 1 to 5) with a 60° rotation between every captured image set. The higher the grating the sharper the image one can get. As a consequence of higher grating, the acquisition speed is dramatically prolonged. SIM importance lies in its ability to generate high resolution images by its practical power in resolving signal to noise ratio. Starting with a wide-field microscope with inexpensive lasers and saturated structured-illuminated scanning, SIM microscopes in ideal world can surpass the diffraction limit and go up

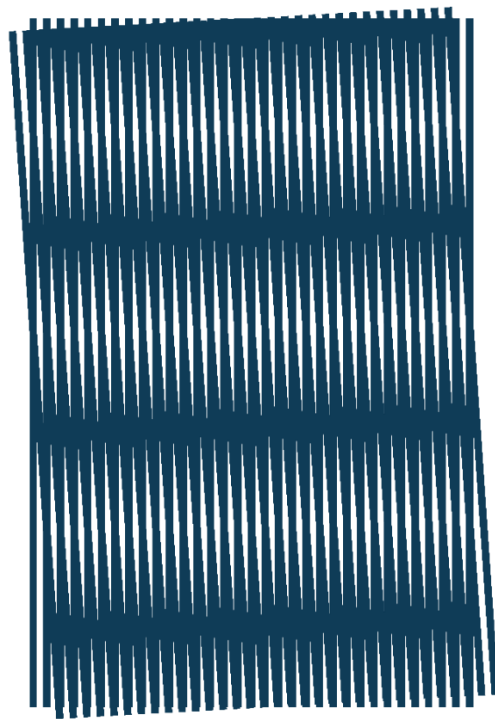


**Figure 19 Moiré pattern.**

Two sets of parallel lines with one set being slightly inclined and superimposed above the other creating a Moiré effect.

---

<sup>11</sup> Superresolution Structured Illumination Microscopy. Contributing authors: Tony B. Gines and Michael W. Davidson, National High Magnetic Field Laboratory, 1800 East Paul Dirac Dr., The Florida State University, Tallahassee, Florida, 32310.

to 50 nm in resolution whenever there is bright fluorescence and photostable probes (Gustafsson, 2000, 2005).

### **PALM<sup>12</sup>/ELYRA PS.1 microscope general info:**

The microscope is provided by 3 objectives:

- 63x oil immersion objective, NA 1.4, Plan-Apochromat, DIC<sup>13</sup> M27, Black ring color.
- 100x oil immersion objective, NA 1.46, alpha Plan-Apochromat, DIC M27 Elyra.
- 100x oil immersion objective, NA 1.57, alpha Plan-Apochromat, DIC Korr<sup>14</sup> M27 Elyra.

The setup is provided by ZEN 2011 SP3<sup>15</sup> to operate the microscope, the navigation is very much similar to the installed Zen on LSM 780. There are 4 different excitation wave lengths possible on ELYRA: HR Diode 405, 488 and 642 nm lasers as well as HR DPSS 561 nm laser. ‘Z-Stack’, ‘Time Series’, ‘Tile Scan’, ‘Positions’ and ‘Regions’ are adjustable very similarly as in ZEN SP2. Image ‘Bit Depth’ can go up to 16 Bit and ‘Averaging’ ranges from 2 till 16 and ‘Continuous’. ‘Grating’ is possible with 1, 2, 3, 4 or 5 rotations. Experiment acquisition is possible with 4 channels at a time, each having its ‘EMCCD<sup>16</sup> gain’, ‘Digital gain’ and laser wavelength and power. The previously mentioned LSM 780 setup is also equipped with ELYRA SIM; just by selecting the SIM panel in ZEN, the microscope is ready to acquire data in SIM mode.

### **II.1.10 Devices**

The devices were mostly used in Prof. Jens Rettig lab, otherwise it is stated.

Device	Company
Axiovert 200 microscope	Zeiss
Balance BP 1215	Sartorius
Bath incubator	Memmert
Centrifuge mini 3-1810	NeoLab
Centrifuge 5415 C	Eppendorf
Centrifuge 5415 D	Eppendorf

---

<sup>12</sup> Superresolution Photoactivated Localization Microscopy.

<sup>13</sup> Differential Interference Contrast.

<sup>14</sup> Correction Ring.

<sup>15</sup> Black edition version 8.1.5.

<sup>16</sup> EMCCD is a quantitative digital camera technology that is capable of detecting single photon events whilst maintaining high Quantum Efficiency, from Andor Technology Plc.



Centrifuge 5415 R Fast cool	Eppendorf
Centrifuge 5424	Eppendorf
Centrifuge 5702 R	Eppendorf
Centrifuge 5804 R	Eppendorf
Centrifuge Fresco 17	Thermo Scientific
Centrifuge Heraeus Labofuge 400 R	Thermo Scientific
Centrifuge mini spin plus	Eppendorf
Centrifuge small	Eppendorf
Combimag RCT	IKA
Eclipse TS 100 microscope	Nikon
Fluor chem M revelation machine	ProteinSimple
FT-14 UV screen	Fisher brand
Fridge 4 °C/-20 °C	Liebherr premium
Hera cell 150i CO <sub>2</sub> incubator	Thermo Scientific
Hera Freeze Heraeus -80 °C freezer	Thermo Scientific
Hera Freeze HFUB -80 °C freezer	Thermo Scientific
Hera guard eco	Thermo Scientific
Hera safe cell culture hood	Thermo Scientific
KL 1500 light source	Schott
Master cycler personal	Eppendorf
Master cycler gradient	Eppendorf
Micro-Forge	World Precision Instruments Inc.
Microwave	Sererin
MS2 minishaker	IKA
MSC-Advantage hood	Thermo Scientific
Peq Power	PeqLab
Peq Star	PeqLab
pH meter	Scaott
Power Pac	BioRAD
P-touch 2420 PC	Brother
Puller P-97	Shutter instruments
RCT basic	IKA
UV-chamber	Lab custom-built
Vortex mixer 7-2020	NeoLab
Wescor osmometer	Kreienbaum
Wild M3Z dissection microscope	Heerbrugg Switzerland

### II.1.11 Consumables

Product	Company
6-well plate	Becton Dickinson (BD)
6-well plate 3506	Corning Incorporated
Amicon Ultra-15 centrifugal filters (100,000 NMWL)	Merck Millipore
Cell-culture flask	Becton Dickinson (BD)

Coverslip (25 mm)	Fiser Scientific
Coverslip (25 mm) High Precision	Marienfeld
Eppendorf 1 ml tube	Eppendorf
Eppendorf safe-lock 2 ml tube	Eppendorf
Multiply $\mu$ strip 0.2 ml chain PCR tubes	Sarstedt
One-way pipette 2 ml and 25 ml	Falcon
One-way pipette 5 ml and 10 ml	Greiner bio-one
Petri dish (35 mm)	Becton Dickinson (BD)
Petri dish (92 mm, 150 mm)	Sarstedt
Plastic Pasteur Pipette (0.5, 2, 3 & 5 ml)	Ratiolab
Pipette tips (10 $\mu$ l) FilterTips	Clear Line
Pipette tips (2-20 $\mu$ l) Biosphere filter tips	Sarstedt
Pipette tips (1-200 $\mu$ l) Top-Lipe-Filter-Tips	Micro pore filter technology
Pipette tips (100-1000 $\mu$ l) Quality pipette tips	Sarstedt
Pipette tips 5 ml	Eppendorf

### II.1.12 Companies

**Abcam:** Cambridge, United Kingdom. **Adobe:** San Jose, California, United States. **AHF:** Tübingen, Germany. **Becton Dickinson:** Heidelberg, Germany. **Corel:** Ottawa, Canada. **Cell Signaling Technologies:** Danvers, United States. **Eppendorf:** Hamburg, Germany. **Fermentas:** St. Leon-Rot, Germany. **Fisher Scientific:** Schwerte, Germany. **Greiner Bio-One:** Frickenhausen, Germany. **HEKA:** Lambricht, Germany. **Life Technologies:** Darmstadt, Germany. **MedChem Express:** New Jersey, United States. **Merck:** Mannheim, Germany. **Microsoft:** Berlin, Germany. **New England Biolabs:** Frankfurt, Germany. **Olympus:** Hamburg, Germany. **Panbiotech:** Aidenbach, Germany. **Photometrics:** Tucson, United States. **QIAGEN:** Hilden, Germany. **Roche:** Grenzach Wyhlen, Germany. **Roth:** Karlsruhe, Germany. **Sarstedt:** Nümbrecht, Germany. **Sartorius:** Göttingen, Germany. **Schott:** Mainz, Germany. **Sigma Aldrich:** Steinheim, Germany. **Systat Software Inc.:** San Jose, California, United States. **Spectrapysics:** Darmstadt, Germany. **The Jackson Laboratory:** Bar Harbor, Maine, United States. **Thermo Fisher Scientific:** Schwerte, Germany. **Thomson Reuters:** Toronto, Canada. **Tocris:** Bristol, United Kingdom. **Visitron Systems:** Puchheim, Germany. **Warner Instruments:** Hamden, United States. **Wavemetrics:** Lake Oswego, United States. **Wescor:** Logan, United States. **World Precision Instruments:** Berlin, Germany. **Zeiss:** Jena, Germany.

### II.1.13 Software



Adobe Bridge CS5, version 4.0.0529, Adobe Systems Incorporated.

Adobe Photoshop CS5, Adobe Systems Incorporated.

A plasmid Editor (ApE), version 1.17, M. Wayne Davis.

CorelDRAW, version 16.1.0.843, Corel Corporation.

EasyTrack 2014, Detlef Hof.

## MATERIALS AND METHODS

---



ImageJ, National Institutes of Health, Federal Government of USA.



Igor, version 6.0.4.0, WaveMetrics Inc.



Metamorph, Molecular Devices.



Office 2013, Microsoft.



VisiView, Visitron Systems GmbH.



Pulse, HEKA Elektronik.



SigmaPlot Version 13, Systat Software, Inc.



SnapGene Viewer 2.8, GSL Biotech LLC



Zeiss Efficient Navigator (Zen) 2012, Carl Zeiss.

## II.2 Methods

### II.2.1 Adult DRG Cell-Culture

DRG neuronal cell culture is an excellent model to study the pathogenic mechanisms of the peripheral nervous system and establish new therapeutic compounds. These cultures provide a powerful tools to study neurodevelopment, neurite and axon formation, neuropeptides and neurotrophic factors release, neurotransmitter release, synapse formation, electrical signaling and exocytosis(Melli and Hoke, 2009). Adult DRG neurons are superior to embryonic and postnatal DRG neurons in terms of survival where they survive for 6 DIV and starts gradually to age and die while embryonic DRG neurons die much faster (Horie and Kim, 1984; Scott, 1977). Our group optimized mouse DRG neuronal culture whereby the adult cells can live up to 35 DIV, consistent with the results of others (Malin et al., 2007) and embryonic/postnatal DRG neurons can survive up to 15 DIV. We performed experiments with DRG neurons that were maintained for not

more than 11 DIV (data explaining why, is shown in the *Results* chapter). Therefore, we can safely assume that the current preparation protocol is fully optimized with the least stress possible on the cells to give reproducible results in our experiments. DRGs can be either dissociated by Trypsin enzyme or directly seeded onto culture dishes (Horie and Kim, 1984); we chose to dissociate them

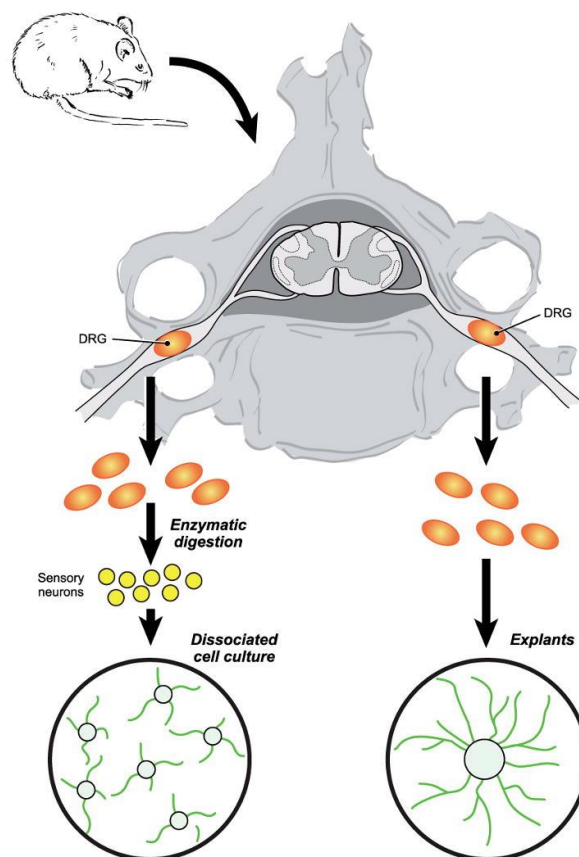


**Figure 20 Schematic view of preparation of dissociated and explant DRG sensory neuronal cultures.**

Source: Expert Opin Drug Discov. 2009 Oct 1; 4(10): 1035–1045. doi: 10.1517/17460440903266829.

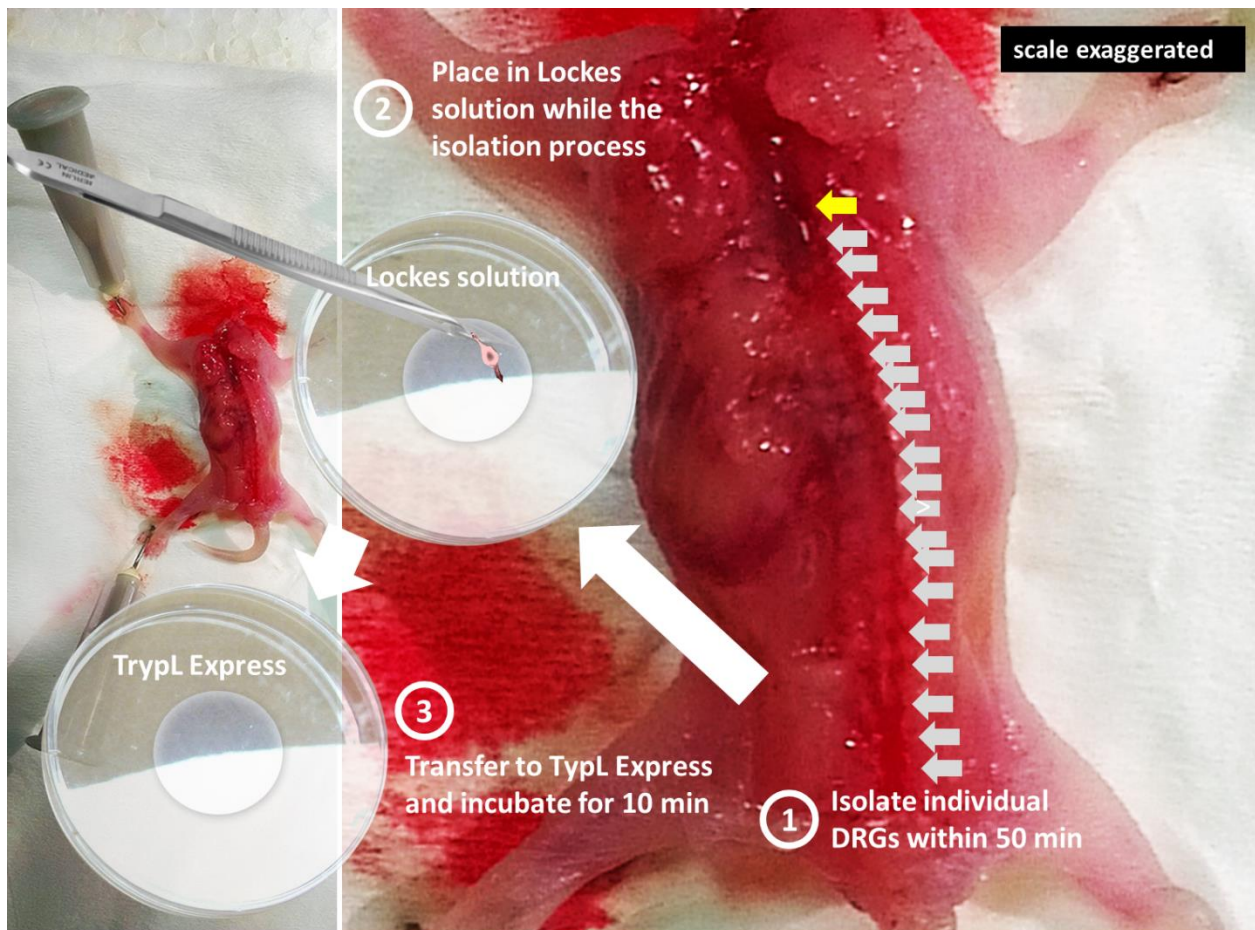


**Figure 21 DRG isolation.**

Individual DRG are isolated from bony foramen pocket-like structures (gray arrows) and transferred to a Petri dish with Lockes solution. The yellow arrow points to the the lumbar section after wich DRG isolation become nearly impossible because of their small size it gets. The entire isolation should be carried out within 50 min, to ensure good quality of cells. Afterwards DRGs are transferred to a Petri plate with TrypLE Express and incubated for 10 min before proceeding with digestion.

(Figure 20) to be able to study exocytosis of LDCVs and SVs at individual cell level. One day before the cell culture, coverslips were coated in a 6-well plates with a 3.3  $\mu$ M aqueous poly D lysine solution applied to their center. The 6-well plate is then placed in the incubator. The cell culture medium is prepared ahead of time and placed in the incubator so that it adjusts its pH to 7.4. On the day of cell culture preparation, the Poly-D-Lysine is washed away. PDL, might be toxic for the cells if used at high concentrations therefore it should be removed carefully by washing each coverslip 2 times with 300  $\mu$ l Sigma water. Both PDL and Poly-L-Lysine (PLL) promote neurite growth in low-density cultures but the D isomer minimizes the aggregation of neurons better than the L isomer (Brewer and Cotman, 1989). After washing, the 6-well plate is placed with an open lid in the UV chamber for 15 min. The enzymatic digestion solution was prepared with 1

ml NBA medium that was complemented with 2.31U/mg Unit Liberase and sterile filtered. Meanwhile a Petri dish with a 200 µl drop of Locke's solution and a Petri dish with 200 µl TrypLE Express were prepared and placed under the hood. When the UV sterilisation of the coated coverslip was over, the remaining water was washed out two times with 50 µl NBA-medium. Later, 2 ml of cell culture medium were added per well and the plate is placed in the incubator (37°C, 5% CO<sub>2</sub>). Adult mice were sacrificed according to the German Animal Welfare Act<sup>17</sup>. Animals were placed in transparent glass chamber and CO<sub>2</sub> was introduced gradually until the animal was unconscious. Unconscious animals were killed by decapitation (adult mice) or cervical dislocation (pregnant mice for caesarean-section). After ethanol disinfection, the skin over the spine is removed. The tissues surrounding the spine are also removed and the spine is incised at the level of the back legs as shown in figure 21. The posterior part of the spine is removed away along with the spinal marrow. DRGs are isolated and placed in a Petri dish with Locke's solution. The entire process was completed within 50 min. The DRGs were transferred into the prepared Petri dish with TrypLE Express solution to allow slow enzymatic dissociation of the DRG connective tissues capsule. DRGs are then transferred into a freshly prepared digestion solution and placed in water bath (37 °C) with gentle shaking. The DRG tissue was triturate 10 times with a 1 ml pipette. This step was repeated 4 times. In the last step the cells were triturated 15 times. Overall the digestion period was 20 to 22 min. Digestion was stopped by adding 100 µl FCS. The cell suspension was then centrifuged for 4 min at 3000 rpm. The supernatant is removed and the cells were washed by adding 600 µl of DPBS. They were centrifuged again for 4 min at 3000 rpm. The supernatant was removed and 600 µl of cell culture medium with Pen/Strep were added. The cells were plated onto the coverslips and placed in the incubator.

### II.2.2 Embryonic DRG Cell-Culture

All LDCV release experiments were done on adult DRG neurons, with the exception of CAPS1 and 2 dKO and CAPS 1 KO mice. Mice lacking either CAPS1 (Speidel et al., 2005) or both CAPS1 and 2 are not viable and they die right after birth. Genotypes were verified by PCR using primers as described in (Jockusch et al., 2007; Speidel et al., 2005). To study the effect of

---

<sup>17</sup> Adopted in May 25, 1998. Primary citation: Federal Law Gazette I, p. 1094.

the absence of both CAPS isoforms on LDCV release as well as synaptic transmission, it was necessary to carry out these experiments in embryonic DRGs. Embryonic DRG cell-cultures were prepared in very similar fashion to adult and postnatal DRG neurons protocol but with minor changes. Pregnant mice were sacrificed according to Animal Welfare Act and babies were removed by a C-section. All the cell culture procedures are similar to that of adult culture preparation until the isolation step, where 350  $\mu$ l of TrypLE is directly added onto the Petri dish having the DRGs in Lockes solution. After 5 min of incubation, with 1 ml tip pipette, DRGs are transferred into the Liberase digestion solution. Trituration is required during the entire digestion process which lasts between 2.5 to 3 min, depending on the age of embryo whether its E18 or almost P0 right before birth. Digestion is stopped by adding 200  $\mu$ l FCS. Cells are centrifuged and later washed with PBS as described in adult DRG prep. The cells were plated on the center of the coverslip and they were given 10 min under sterile hood to settle down. Then 2 ml of NBA with Pen/Strep was added and the culture was place in the incubator.

### **II.2.3 DRG/S neuron Co-Culture**

DRG neurons don't form synapses on their own in vivo or in cultures (Ransom et al., 1977a; Ransom et al., 1977b; Wake et al., 2015) rather, they do form synapses with their natural synapse-forming partner the dorsal and ventral horn neurons (Joseph et al., 2010). To study synaptic transmission, it was necessary to establish the DRG/S neuron co-culture system at our laboratory, because they are fundamental to study interactions between cell populations. Cell-cell interactions in co-cultures are affected by extracellular surrounding; for cell survival, the culture protocol needs to be given careful consideration (Goers et al., 2014). Amy MacDermott and her colleagues were among the first to study synaptic properties of DRG/S neuron co-cultures (Gu and MacDermott, 1997; Labrakakis et al., 2000). Because these co-cultures are very complex to establish, only very few laboratories based in New York, Wisconsin, Southern Illinois, London and Taketoyo have worked with (Cao et al., 2009; Hendrich et al., 2012; Joseph et al., 2011; Ohshiro et al., 2007; Yu et al., 2015). DRG/S neuron co-cultures are prepared in two separate steps. DRG prep was carried out as previously described. On the second day, DRG neurons are either transfected with the required Lentivirus of interest or not. On the third day, the S neurons were added on the DRG neurons and left together 9 DIV before carrying out synaptic transmission experiments. To extract

S neurons, P0 to P1 old mice were sacrificed by decapitation. The skin of the mice was sterilized with ethanol and the tissues on the back were cleared to expose the upper part of the spinal cord. The lower limbs of the pup were cut and a 21 G syringe capillary filled with EBS solution was placed on the upper part of the exposed spinal cord and a pressure was applied to eject the spinal cord tissue out. The spinal cord tissue was then transferred to a Carbogen-bubbled EBS solution to wash away the sucrose for optimized papain activity. Later on, the tissue was digested using enzymatic solution consisting of 5 ml DMEM, 10 mg L-Cystein, 100 mM CaCl<sub>2</sub> 0.5 ml, 50 mM EDTA and Papain 20 U/ml. The digestion was carried on at 37°C under constant oxygenation for 30 min. Mechanical dissociation was needed after the enzymatic treatment is over. To do so, 1 ml of S neurons cell culture medium was added to stop digestion. The solution was triturated gently 5 times and with slightly more pressure 2 times using 1 ml tip, then the tube was left upstanding for the precipitation of the tissue. Later, 1 ml of medium was added and then a 5 min centrifugation at 800 rpm was applied. The supernatant was discarded and 1 ml of filtered 1/1 solution containing Dnase, BSA, Trypsin inhibitor and EBSS was added. Trituration was applied 3-4 times and then centrifuged again for 5 min at 800 rpm. The previous step was repeated for a second time and the tissue was centrifuged again. The supernatant was again discarded the cells were resuspended fresh culture medium. The cells were plated on the coverslips (100 µl per well). The 6-well plate was placed in CO<sub>2</sub> incubator. On the next day, two thirds of the medium in the wells was discarded and replaced with a new fresh medium containing FUDR.

### II.2.4 ICC

Immunocytochemistry is a technique used to localize targets of interest at cellular level. In 1941, (Coons, 1941) published the first report describing immunofluorescence antibodies and till now this technique is widely used across different labs and is known as ICC. The idea is to use a specific primary antibody against the targeted substance and a secondary fluorescently labelled



## MATERIALS AND METHODS

antibody against the primary antibody to visualize it under the microscope (Ooij, 2009). The following ICC protocol was optimized for DRG cultures and DRG/S neuron co-cultures. Special steps were implemented to enhance the signal to noise ratio. To fix the cells, the medium was removed and the coverslips were washed one time with PBS containing 100 mM  $\text{CaCl}_2$  and 25 mM

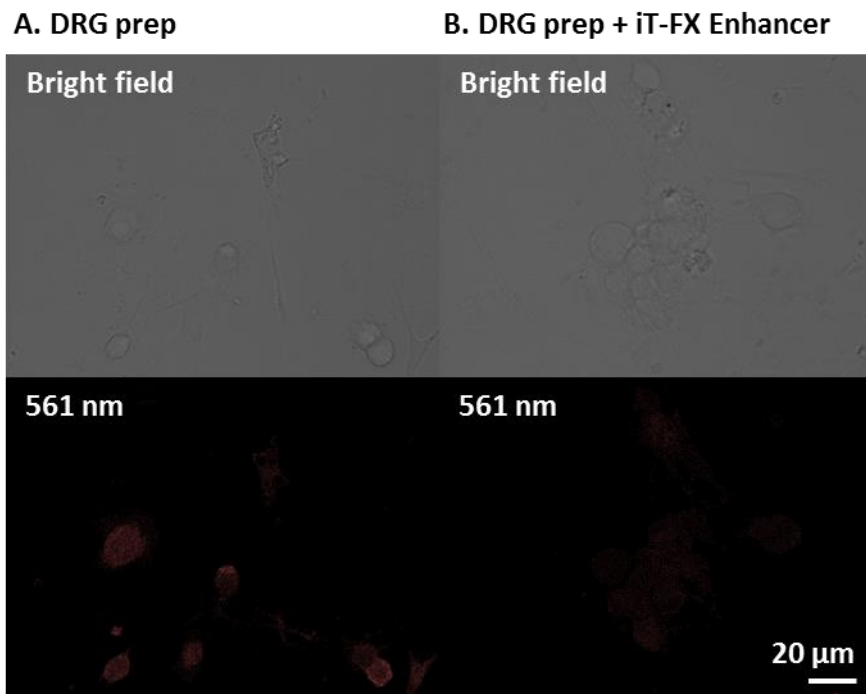


**Figure 22 Image iT-FX Signal Enhancer effect on auto-fluorescence.**

DRG culture was prepared from 2 weeks old WT mouse and cells were fixed after 7 DIV with 4% PFA for 20 minutes. Fixed DRGs were permeabilized with 0.1% Triton and stained with secondary antibody Alexa 561 and visualized at 561 nm wavelength using confocal microscopy. (A) DRG cells stained the classical way. (B) iT-FX Signal Enhancer was added during the permeabilization step for 30 min.

$\text{MgCl}_2$  to improve adhesion of the cells to the coverslip. This PBS was used for the rest of the ICC procedure. The cells were fixed in 4% ice-cold Paraformaldehyde in PBS of pH 7.4 for 20 min at room temperature or overnight at 4°C in the dark. Some experiments needed 2% PFA for 5 min to maintain the fragile structures of the fixed target of interest intact (such as synapses). Then the coverslips were washed three times with PBS for 2-5 min. All washing steps were done as quickly as possible, to prevent the cells on the coverslip from drying out. Samples were quenched with 50 mM Glycine in PBS for 10 min. Later, the Glycine is washed out with PBS three times for 2-5 min each. To permeabilize the cells, PBS containing 0.1% Triton-X-100 and 2.5% NGS was added for 30 min at room temperature. In an optional step, it is recommended to add 4 drops of iT-FX<sup>18</sup> to decrease background noise. iT-FX eliminates background staining therefore enhancing the signal-to-noise ratio of stained cells. It blocks nonspecific interactions of fluorescent dyes with cell constituents. I tested it separately to verify how effective it was and it did indeed significantly reduce the cell autofluorescence of DRG neurons when excited at 561 nm. Figure 17 shows the

<sup>18</sup> Image enhancer from Life Technologies.

autofluorescence of DRG neurons in comparison to DRG neurons that were treated for 30 minutes with iT-FX signal enhancer. To block unspecific free epitopes, the coverslips were washed two times with PBS/2.5% NGS for 2-5 min. The primary antibody was diluted to the working concentration in PBS containing 2.5% NGS. In a wet chamber, 100  $\mu$ L diluted primary antibody solution was placed on a piece of parafilm for each coverslip which was flipped on it with the cell side facing the antibody drop. The wet chamber was incubated for 1 h at room temperature or 4 °C over night. After the incubation was over, the coverslips were washed with PBS/2.5% NGS/0.1% Triton for 2-5 min. The secondary antibody (1:2000 Alexa 405/488/568/633/647-conjugated antibody) was diluted in PBS/2.5% NGS and kept in the dark. To avoid background, the diluted secondary antibody should be centrifuged at 13000g for 10 min at 4°C. The samples were incubated with the secondary antibody for 45 min in dark at room temperature and the cells were washed 5 times with PBS/2.5% NGS/0.1% Triton for 2-5 min after the incubation period is over. Additional 2 times washing steps with PBS is required. Finally, to mount the coverslip to the glass slide, 20  $\mu$ L mounting medium were added on the microscope slide. The coverslips were then dipped in distilled water to reduce salts and excess water was removed by gentle touching the coverslip to a fine tissue paper. The coverslips were then mounted upside-down whereby the cells were embedded in the mounting medium and left to dry for 3 hours at room temperature or 15 min at 37 °C while covered with Aluminum foil. The edges of the coverslips were then sealed with nail polish to protect the sample from over drying. The sealed samples were stored at -20 °C or 4 °C in dark. For all experiments, the samples were imaged at the same day or latest next day in the morning to maintain good quality. When 2% PFA fixation for 5 min was applied, the samples were exclusively imaged on the fixation and staining day as the samples were fragile and degrade within 10 to 15 hours.

### II.2.5 Double ICC

To be able to visualize co-distribution of two or more different targets in the same sample using primary antibodies raised in the same species, double ICC is needed with an intermediate 'blocking' step. Blocking of the free epitopes of the antibodies is carried out using anti-(against the secondary antibody raised in certain species) affinity Fab fragments. This procedure was divided into three parts. Part one is to label the first organelle with anti-x antibodies. To fix the cells, the

same procedure described in ICC section was performed. The second part involved blocking the free epitopes of previous secondary antibody. To do so, cells were incubated with 2.5% NGS in PBS for 1 h at room temperature. Three washing steps for 5 min each with PBS were applied. The cells were then incubated with *anti-x* affinity Fab fragments (1:50 dilution in PBS/2.5% NGS) for 1 h at room temperature, then, carefully washed 3 times for 10 min each with 1X PBS. The third part was to label for the second organelle with *anti-y* antibodies. The same procedure used for first organelle labelling was performed. And finally once the second labeling procedure is completed, coverslip were mounted on glass slides as described before. The samples were stored at -20 °C or 4 °C in dark.

### II.2.6 Calcium Phosphate-Lentivirus Production<sup>19</sup>

In order to produce Lentiviruses, human embryonic kidney cells (HEK 283FT) are transiently transfected with lentiviral transfer vector plasmid, packaging plasmid and envelope glycoprotein (Vigna and Naldini, 2000). Following transfection, lentiviral particles are released into HEK cells' culture medium (Tang et al., 2015). These particles are then harvested in Amicon Ultra-15 centrifugal filters (100,000 NMWL). This entire process takes 3 to 4 days depending on the Lentivirus generation and the size of protein encoded in the viral vector plasmid. The production process is divided into three main steps. On the first day in the morning, the medium of the HEK cells was changed to incomplete medium (DMEM + Glutamax) to starve and stress them. In the afternoon, the transfection procedure was started. Sterile 1.8 ml Sigma water was added to 15 ml Falcon tube, then the DNA-mix which contains 45 µg DNA of the vector to be produced and 10 µg of all the Helper Plasmids 12251 pMDLg/pRRE, 12253 pRSC-Rev and 12259 pMD2.G<sup>20</sup> (Dull et al., 1998) was added to the Falcon tube. Afterwards, 200 µL of freshly made calcium Chloride 2.5 M was added to the same Falcon tube. The mixture was vortexed. In a second Falcon tube, 2 ml HBS solution was added. The DNA solution was then moved from the first Falcon tube into the HBS Falcon tube 2 via a glass pipette. The transfer should be slow and in drop-wise manner directly into the center of the falcon tube without touching the plastic wall. The mixture is then incubated for 15 min at room temperature (up to 30 min) until a cloudy/milky mixture appear. To

---

<sup>19</sup> This procedure should be carried out entirely in S2- Laboratory. Wearing a lab coat is required.

<sup>20</sup> Third generation lentiviral packaging plasmid; Contains Gag and Pol; also requires pRSV-Rev (Addgene#12253) and envelope expressing plasmid (Addgene#12259) from AddGene – USA.

transfect the HEK cells, a new glass pipette was used and the mixture was carefully transferred in a drop wise manner along the entire cell culture flask while moving it in a gentle circular way. One to two cell culture flasks can be transfected with this 4 ml DNA/calcium/HBS mixture. Overnight incubation (14 – 16 hrs max) at 5% CO<sub>2</sub> / 37° C was required. In the second day, the medium was removed with a glass pipette. This used medium was discarded in 20% SDS. 8 ml of complete DMEM medium (+ Sodium Pyruvate, FCS and NEAA) was added. The flasks were left for 24 to 48 h in the incubator. NPY-Venus virus production needs 1.5 days incubation while VGLUT-mNectarin needs 3 days incubation before harvesting. On the third or fourth day, the color of the medium was checked, if it changed to yellowish-orange, the cells were inspected under the microscope. If clumps and floating cells were visible, the cells were excited with the specific wavelength against the fluorescent protein. Once a fluorescent signal was visible, harvesting is recommended as longer incubation periods might increase the apoptotic factors and free radicals that eventually will drastically affect the quality of cell cultures as well as the efficacy of transfection. The medium was then pipetted out from the flasks into a 50 ml falcon tube and centrifuged at 1200 rpm speed for 2 min (or up to 5 min). At this moment, it is possible to interrupt the procedure for 24 hrs and continue later; for this purpose, the medium was kept at 4° C. The harvested solution was poured in the Millipore Centrifugal Filter of 100,000 MWCO Falcon and centrifuged for 15 min at 4 ° C at 1,800 rpm. Once concentrating was done, the virus suspension was aliquoted into cryo-tubes and closed tightly before dipping into liquid Nitrogen for a brief while and stored directly at -80 ° C.

### **II.2.7 RT PCR**

Reverse Transcription-PCR technique was needed to detect whether CAPS1 and 2 were found in DRGs at mRNA level. DRGs were isolated from 5 adult mice and 170 mg of DRG tissue was collected and stored at -80 °C. The DRG tissues (50 – 100 mg) were transferred to a 50 ml Falcon tube containing 1 ml TRIzol reagent. The mixture was centrifuged at 1240 rpm for 10 min at 4 °C. The tissues were lysed by repetitive pipetting and grinding and then transferred to 1.5 ml Eppendorf tube. The mixture was then centrifuged at 11400 rpm for 10 min at 4 °C, the supernatant was transferred into a fresh Eppendorf tube and incubated for 5 min at room temperature. Afterwards, 0.2 ml of chloroform was added and the tube was shaken vigorously by hand for 15 s. The mixture was then centrifuged at 11400 rpm for 15 min at 4 °C and the resulting aqueous phase

was transferred into a new tube. Glycogen (1-5  $\mu$ l) and Isopropanol (0.5 ml) was added to precipitate the sample which was then incubated for 10 min at room temperature. Another centrifuging step at 11400 rpm for 10 min at 4 °C was required. The supernatant was removed and the remaining was mixed with 1 ml 75% ethanol mixed in Sigma water. The mixture was then centrifuged at 8900 rpm for 5 min at 4 °C. The RNA pellet was left briefly to dry and the resulting RNA was dissolved in 30  $\mu$ l Sigma water. In a second step, cDNA is to be produced from the resulting RNA whereby 1  $\mu$ g of RNA was mixed with 1  $\mu$ l dNTPs, 1  $\mu$ l random primers, and H<sub>2</sub>O. This mixture was incubated for 5 min at 65 °C and later 4  $\mu$ l of 5X strand buffer, 2  $\mu$ l of 0.1 M DTT, 1  $\mu$ l reverse transcriptase and 1  $\mu$ l RNase were added. Then PCR reaction was run and kept on hold at 4 °C. In the last step, the produced cDNA is screened with CAPS1 and CAPS2 primers. The PCR reaction components included: 1  $\mu$ l cDNA, 2  $\mu$ l 10X buffer, forward and reverse 0.2  $\mu$ l each, 1  $\mu$ l Taq Polymerase and 15.4  $\mu$ l Sigma water. The reaction was run for CAPS1 and CAPS2 separately in DRG cDNA and brain cDNA that was used as a positive control for both CAPS isoforms expression and a negative control with water instead of cDNA. The resulting PCR products were run in 0.1% agarose buffer with a PCR marker.

### II.2.8 Western Blot

Samples were collected from E18 and P7 pups and 11  $\mu$ g of each Sample was diluted with 5X sample buffer and homogenization buffer. The samples were then cooked for 5 minutes at 95 °C and were loaded into 8% SDS-polyacrylamide gel. The gel was run for 20 min at 100 V and then for 50 min at 160 V. The gels were blotted onto nitrocellulose membranes (wet blot 320 mA for 2 h) and blocked using 5% milk in TBST for 1 h. Membranes were then incubated with primary antibodies either against CAPS1 (1:500) or CAPS2 (1:3000) diluted in 1% milk TBST overnight. The membranes were washed the next day with 1% milk TBST 3 times for 15 min each. The secondary goat anti-rabbit antibody was used for both primary antibodies at a dilution 1:3000 in 1% milk plus TBST and was incubated for 1 h. Membranes were washed 3 times for 15 min each with TBST. They were then incubated in ECL detection reagent for 5 min and detected by FluorChem M system (Protein Simple).  $\beta$ -actin labelling was also performed to correct for the loading of the samples using a primary antibody (1:5000) and a secondary goat anti-mouse antibody (1:1000). Quantification of CAPS1 and CAPS2 protein signal in Western blot results were based on  $\beta$ -actin as a standard and normalized to protein expression level at P7.

### II.2.9 iB<sub>4</sub> Staining

Staining against Isolectin GS-iB<sub>4</sub> from *Griffonia simplicifolia*<sup>21</sup> coupled to Alexa Fluor 568 is used to mark the non-peptidergic unmyelinated DRG neurons. It is a common way as described in literature to differentiate between peptidergic myelinated DRG neurons and non-peptidergic neurons (Kubo et al., 2012). The advantage of using iB<sub>4</sub> over other markers like the NF200 antibody, is its ability to stain living cells without harming them. It's a perfect marker for live imaging while the NF200 is best optimized for fixed cells in ICC experiments. When iB<sub>4</sub> is applied, the non-peptidergic neurons are stained. To label the cultured DRG neurons, 5 µl (1 mg/ml) of iB<sub>4</sub> conjugated to Alexa-568 was added to 2 ml extra-cellular solution warmed chamber and incubated at 37 °C for 20 min. The coverslip was then dipped into another chamber that contains 4 ml of extra-cellular solution and later washed for 10 min with continuous extracellular solution perfusion. Neurons with bright red cell membrane staining when excited at 561 nm were defined as iB<sub>4</sub>-positive non-peptidergic neurons.

---

<sup>21</sup> Woody climbing shrub native to Central and West Africa. Isolectin GS-iB<sub>4</sub> is isolated from the seeds of this plant.

## II.2.10 Cloning

### II.2.10.1 CAPS2b-mTFP

The existing CAPS viral Semliki Forest constructs in the laboratory were all tagged with eGFP. Since we had to co-express each CAPS isoform with NPY-Venus to examine the effect of CAPS overexpression on LDCV secretion, we had to change pSFV1-CAPS2b-IRES-eGFP to pSFV1-CAPS2b-IRES-mTFP. It was nearly impossible to distinguish between DRG neurons co-expressing eGFP and Venus and those expressing either construct separately (or in isolation). This difficulty lies in the close spectral overlap of eGFP and Venus. Teal was our choice because of its reduced spectral overlap with Venus (Figure 23). The cloning strategy aimed at replacing the existing eGFP with Teal, but since there was no convenient direct restriction sites up and down-stream of eGFP, a more complex cloning strategy was developed

utilizing non-unique cutter enzymes. The strategy involved cutting the vector backbone with several restriction reactions - into three fragments, main vector backbone, eGFP fragment to be replaced by PCR mTFP product and a downstream smaller vector backbone fragment. The first cut involved ClaI and SpeI restriction enzymes to generate the vector backbone (fragment A). The second independent cut involves XhoI and SpeI to generate the second small vector backbone

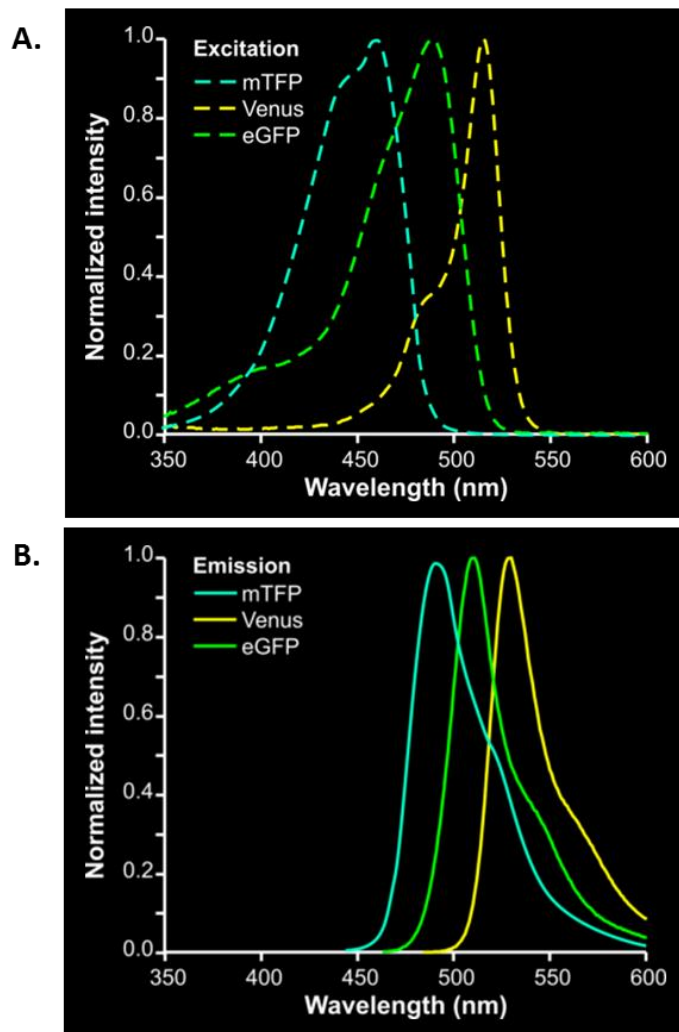
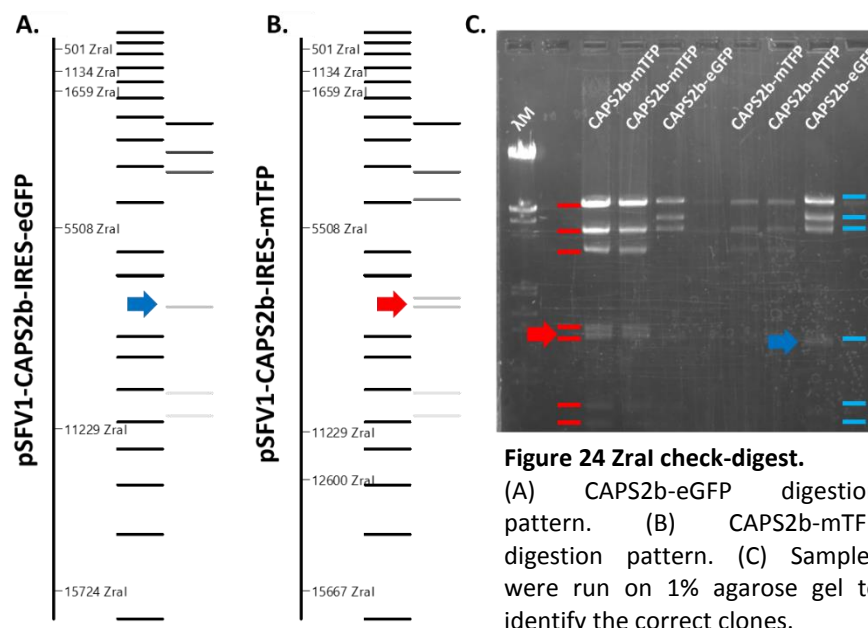


**Figure 23 Spectral mixing of mTFP, eGFP and Venus.**

(A) Normalized intensity of excitation wavelength of mTFP, eGFP and Venus. (B) Normalized intensity of emission of mTFP, eGFP and Venus.

## MATERIALS AND METHODS

fragment B. The third fragment (C) was a synthesized PCR mTFP product with unique inserted restriction sites. fragment A was generated by cutting 2 µl CAPS2b vector<sup>22</sup> with 2 µl of each ClaI and SpeI restriction enzymes and 5 µl of Buffer 4 mixed with 39 µl HPLC



water. The digestion mixture was incubated for 3 hrs at 37 °C and 1 µl SAP was added and incubated at 37 °C for another 1 hr. Heat inactivation followed the phosphorylation for 15 min at 75 °C. The product was then kept on ice. Fragment B was produced by adding 2 µl of CAPS2b vector DNA digested with 2 µl of each XhoI and SpeI restriction enzymes. Buffer 4 was convenient for both enzymes and 39 µl HPLC water was added to this reaction. The mixture was incubated at 37 °C for 3 hrs. Fragment C was produced by a PCR reaction whereby 0.3 µl of mTFP DNA<sup>23</sup> was mixed with 0.5 µl FW primer with ClaI Restriction site 5'AAAAAT^CGATGTGAGCAA GGGCG3' and 0.5 µl RV primer with XhoI Restriction site 5'AAAAC^TCGAGCTTG TACAGCTC3', 1 µl dNTPs, 1.2 µl Red Taq polymerase, 5 µl 10X PCR Buffer from Sigma and 51.5 µl of HPLC water. The PCR program started with 94 °C for 5 min followed by 25 cycles of 94 °C for 45 s, 60 °C for 45 s, 72 °C for 30 s and 72 °C for 7 min and kept on hold at 4 °C. Analytical gel with 1% agarose was used to estimate the amount of DNA to be used in the ligation reaction (Figure 24). Samples were extracted from gel using QIAquick Gel Extraction kit according to the protocol provided by the company<sup>24</sup>. According to the following formula: (Vector ng/ Vector bp x Insert bp = Insert ng for 1:1 ratio), it was estimated that the concentration of the vector is 60 ng/µl, 6 ng/µl for fragment B and 7 ng for fragment C. The ligation reaction was followed

<sup>22</sup> Lab reference number #284.

<sup>23</sup> Lab reference number #718.

<sup>24</sup> www.qiagen.com/handbooks - Cat. Nos. 28704 and 28706 - Protocol of September 2010



## MATERIALS AND METHODS

according to ratio 1:3:4-4.5 (V:I:P) which included 0.5  $\mu$ l of fragment A, 1  $\mu$ l of fragment B and 1  $\mu$ l of fragment C mixed with 2  $\mu$ l T<sub>4</sub> ligation buffer and 2  $\mu$ l of T<sub>4</sub> Ligase. Water up to 20  $\mu$ l was added to dilute the glycerol content that was used to preserve the enzyme. The ligation control included the same components of the ligation reaction but without fragment B and C. Both the ligation reaction tube and the control tube content were separately transformed in DH5 $\alpha$  bacterial cells. Ring transformation was carried out by thawing the 100  $\mu$ l bacteria slowly on ice for 20 min, and the 20  $\mu$ l of the ligation reaction mixture was added and incubated on ice for 30 min. The mixture is then transferred to 37 °C and then back on ice for 10 min to shock the bacteria. Afterwards 300  $\mu$ l of LB-medium is added and the entire mixture is kept at 37 °C with gentle shaking at 300 rpm. The content is then streaked on a pre-warmed agar Petri dish near fire source and incubated at 37 °C for 12 to 16 hrs. Colonies were picked and amplified overnight in the presence of Ampicillin. DNA was extracted using QIAprep Spin Miniprep kit<sup>25</sup>. To quickly verify whether the cloning reaction worked, check-digest reaction was carried out with ZraI restriction enzyme for its

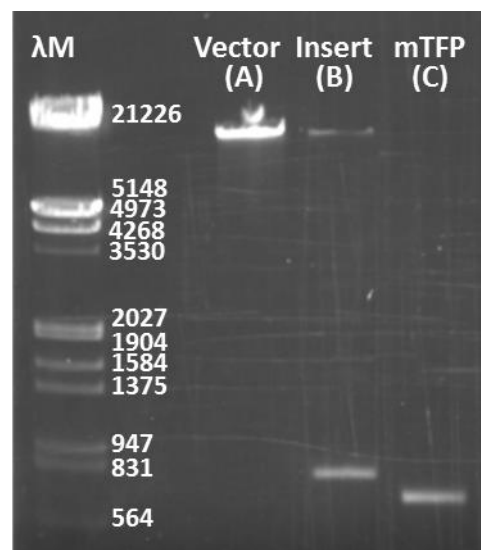


**Figure 25 1% Agarose analytical gel.**

Fragment A (1  $\mu$ l) was mixed with 1  $\mu$ l LB + 3  $\mu$ l water. Fragment B (2.5  $\mu$ l) was mixed with 1  $\mu$ l LB + 1.5 water. Fragment C (3  $\mu$ l) was mixed with 1  $\mu$ l LB mixed with 1  $\mu$ l water. The sample was run at 80 mV for 60 min.

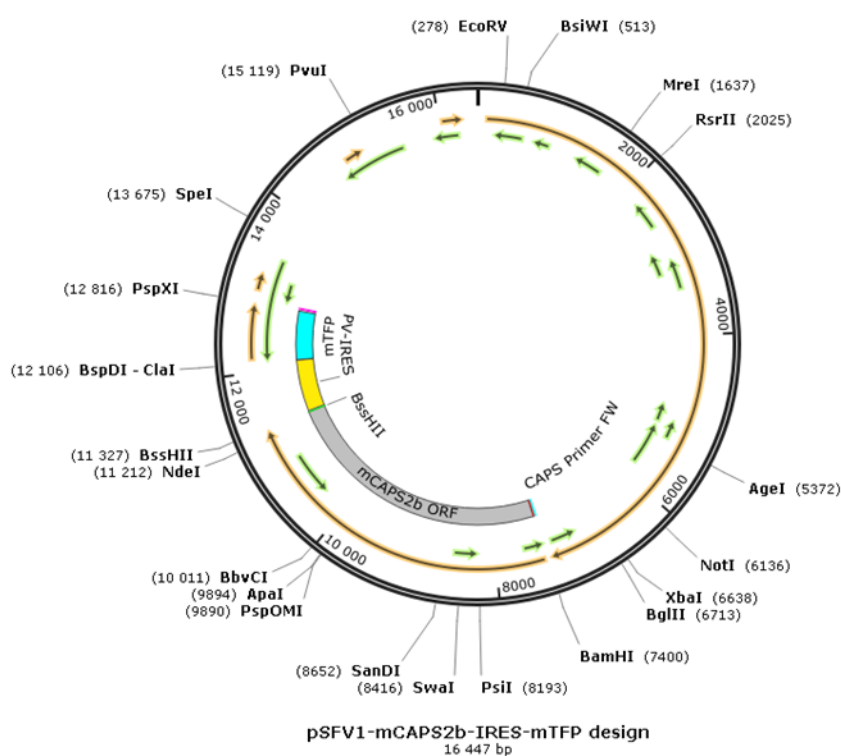


**Figure 26 pSFV1-mCAPS2b-IRES-mTFP vector map.**

The construct was added to the lab DNA and assigned a reference #294.

<sup>25</sup> www.qiagen.com/handbooks - Cat. Nos. 27104 and 27106 - Protocol of October 2011

## MATERIALS AND METHODS

unique cutting site in eGFP and two cutting sites in mTFP. The resulting DNA (10  $\mu$ l) from the minipreps was digested with 1  $\mu$ l ZraI in the presence of 2  $\mu$ l Buffer 4, 2  $\mu$ l BSA and 5  $\mu$ l water. The reaction was allowed to proceed for 2 hrs at 37 °C and then the samples were loaded along with LB at 1% agarose gel and run for 85 min at 80 mV (see Figure 25). The clones with the correct digestion pattern were sequenced using mTFP primers to eliminate the possibility of mutations during the PCR reaction. Once the sequencing results showed that the sequence is correct (Figure 26), Maxiprep was performed. The virus was later produced and tested on DRG neurons to verify whether it's functional and to check whether overexpressing it together with Lentivirus encoding for NPY-Venus is viable. Cells were imaged at 4 hrs of transfection and 4.5 hrs. The transfection efficacy was less than 20%. Cells expressing both CAPS2b and NPY-Venus can be clearly distinguished from cells expressing one of them (Figure 27). Hence the idea behind switching the fluorescent proteins was valid hence the next step was to apply this strategy to CAPS1 vector.

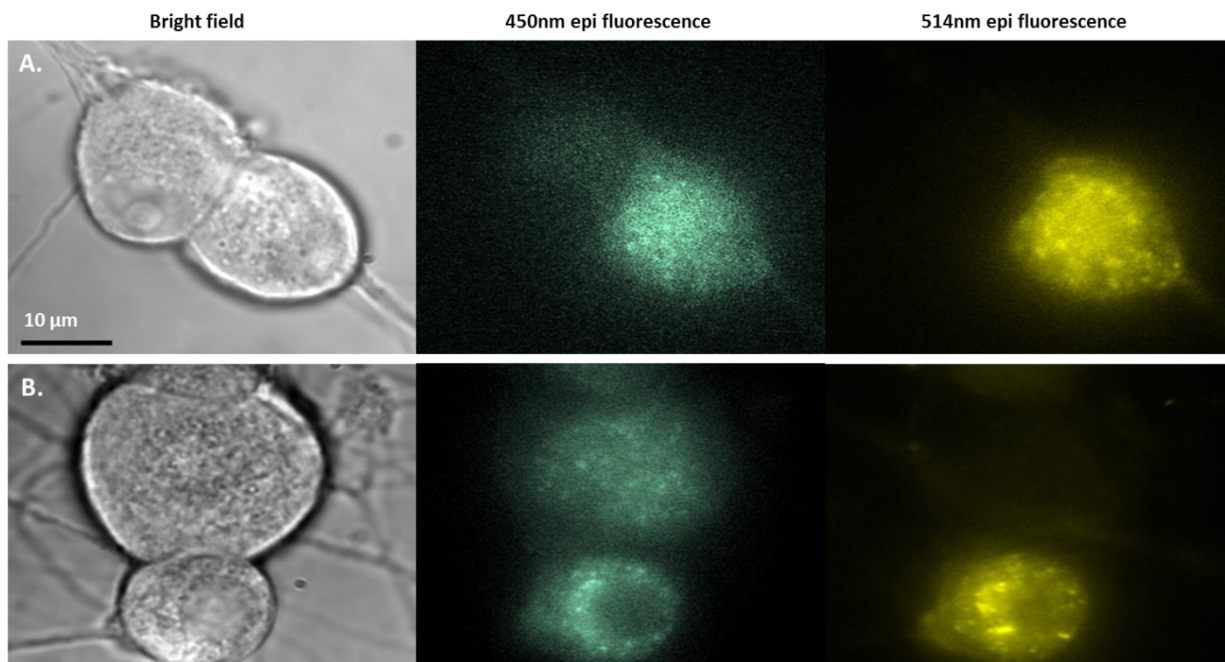


**Figure 27 CAPS2b-mTFP co-expressed with NPY-Venus in DRG neurons.**

(A) Two DRG neurons where one of them was double transfected with CAPS2b-mTFP and NPY-Venus imaged after 4 h of CAPS2b overexpression. (B) Two DRG neurons where both of them are overexpressing CAPS2b-mTFP and only the lower one is transfected with NPY-Venus imaged after 4.5 h of CAPS2b overexpression.

## II.2.10.2 CAPS1-mTFP

CAPS1 cloning was a more straight forward strategy. It involved replacing the recently cloned CAPS2b in pSFV1-mCAPS2b-IRES-mTFP with CAPS1. The mCAPS2b-IRES segment was cut out from pSFV1-mCAPS2b-IRES-mTFP by adding 2 µl of ClaI and 2 µl of BamHI mixed with 5 µl Buffer 4, 2.5 µl vector DNA and 39 µl HPLC water. The reaction was allowed for 3 h at 37 °C and SAP was added

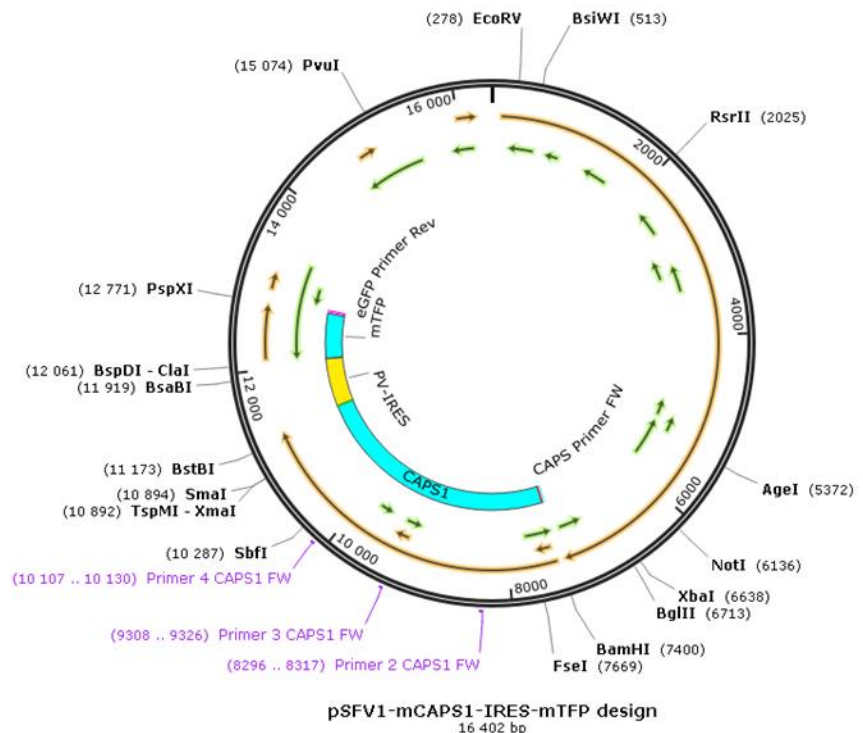


**Figure 28 pSFV-CAPS1-IRES-mTFP vector map.**  
The assigned reference #293.

for 1 h at 37 °C. Later on, the reaction was heat inactivated for 15 min at 75 °C. To produce the CAPS1 insert, mCAPS1-IRES was cut out from pSFV1-CAPS1-IRES-eGFP<sup>26</sup> using 2 µl of the vector DNA mixed with 2 µl of BamHI and 2 µl of ClaI, 5 µl of Buffer 4 was added and HPLC water up 50 µl. The reaction took place for 3 hrs at 37 °C. The vector and the insert was ligated in

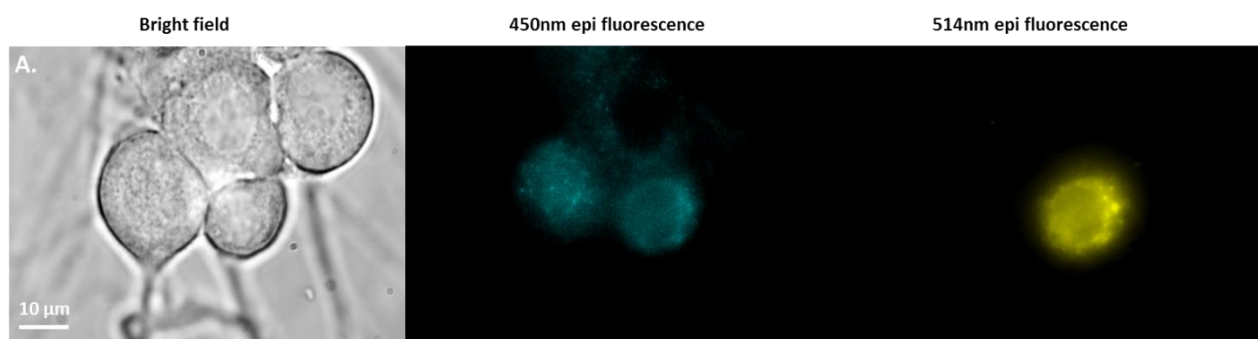


**Figure 29 CAPS1-mTFP co-expressed with NPY-Venus in DRG neurons.**

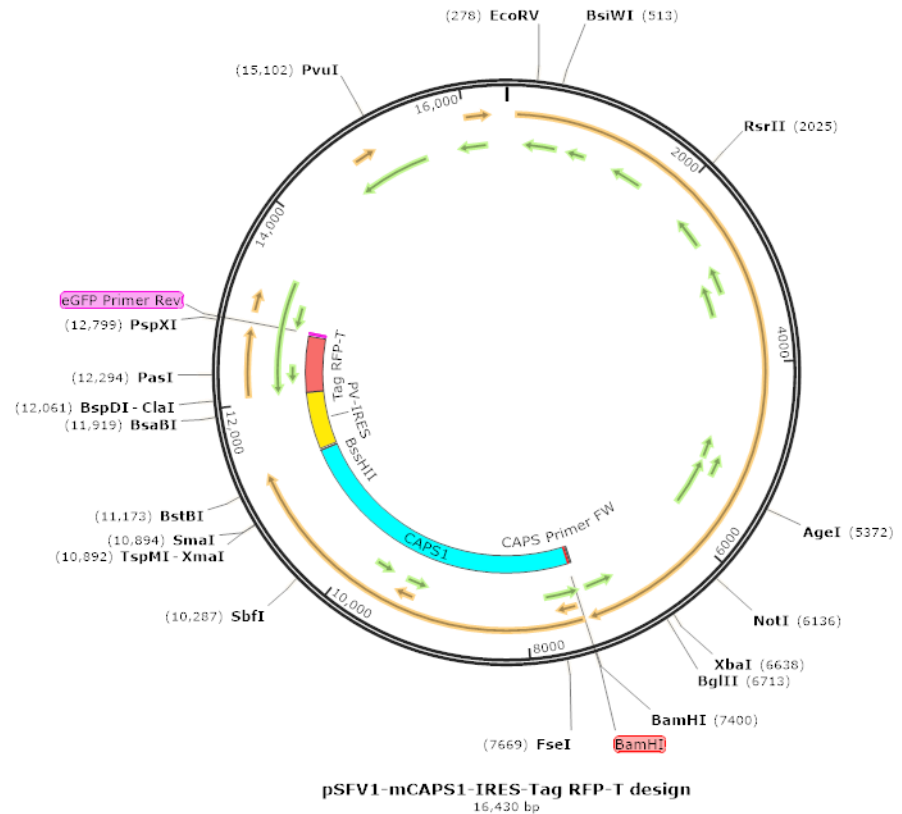
Two DRG neurons are transfected with CAPS1-mTFP. The lower left cell is transfected with NPY-Venus as well. No spectral mixing between mTFP and Venus was visualized when imaged at 3% 450 nm laser intensity. Upon higher laser intensity, Venus would be weakly excited and hence confused by the signal from CAPS-mTFP. Laser intensity lower than 3%, was not enough to visualize the mTFP signal because of the high autofluorescence of DRG neurons at that wavelength.

<sup>26</sup> Lab reference number #175.

1:3 ratio and the cloning was validated by using primers for CAPS1 shown in figure 17 and by sequencing. The virus was then produced and tested on DRG neurons (Figure 29) after 4.5 hrs of transfection. The transfection efficacy was about 20%.

### II.2.10.3 CAPS1-TagRFP-T

To measure synaptic activity, it was necessary at some point to co-express CAPS1 together with SypHy. This combination of TFP with pHluorin nm was not doable, hence we decided to switch the mTFP with Tag-RFP-T<sup>27</sup>. Roger Tsien developed a highly photostable Tag-RFP which is a monomeric derivative of eqFP578 from *Entacmaea quadricolor* which is very stable. **Figure 30 pSFV-CAPS1-IRES-Tag RFP-T vector map.**



This fluor-escent protein maintain most of the beneficial qualities of the original proteins and perform as reliably as *Aequorea victoria* GFP derivatives in fusion constructs (Shaner et al., 2008). The construct pSFV1-CAPS1-IRES-eGFP was used for exchange of eGFP with Tag-RFP. The eGFP was removed out by ClaI and PspXI restriction enzymes and the vector backbone was subjected to SAP to prevent the re-ligation on its own. TagRFP was synthesized by PCR to insert the ClaI and PspXI restriction sites using FW primer 5'TAGCAT^CGATCCTAGGCACC ATGGTGTCTAAGGGCGAAGAG3' with ClaI site and RV primer 5'TTACCC^TCGA GCGGCCGCTTTACTTGTACAGCTCGTCCATG3' with PspXI site. The FW primer had additional restriction site for AvrII that would be used to verify the exchange of fluorescent

<sup>27</sup> Lab reference number #1623.

proteins. The PCR reaction was carried out at 20 cycles to decrease the probability of generating mutations. The ligation reaction was carried with a 1:3 ratio and the transformation and DNA purification was made as previously described. Resulting samples were digested with BamHI and AvrII. Selected clones showed two bands corresponding to the vector backbone and CAPS1-IRES fragment. Further verification was performed with sequencing and the virus was produced and tested.

### II.2.10.4 VGLUT-mNectarin cloning

VGLUT-pHluorin obtained from T. A. Ryan could not be used with NPY-Venus because both are excited at 488 nm. For this reason, we replaced the fluorescent protein with mNectarine<sup>28</sup> enabling us to study both LDCV and SV exocytosis at the same time. The red fluorescent pH biosensor mNectarine was first describe by (Johnson et al., 2009) and its spectral characteristics were tested in HEK 293 cells. It was proven to be pH-sensitive with highest fluorescence at

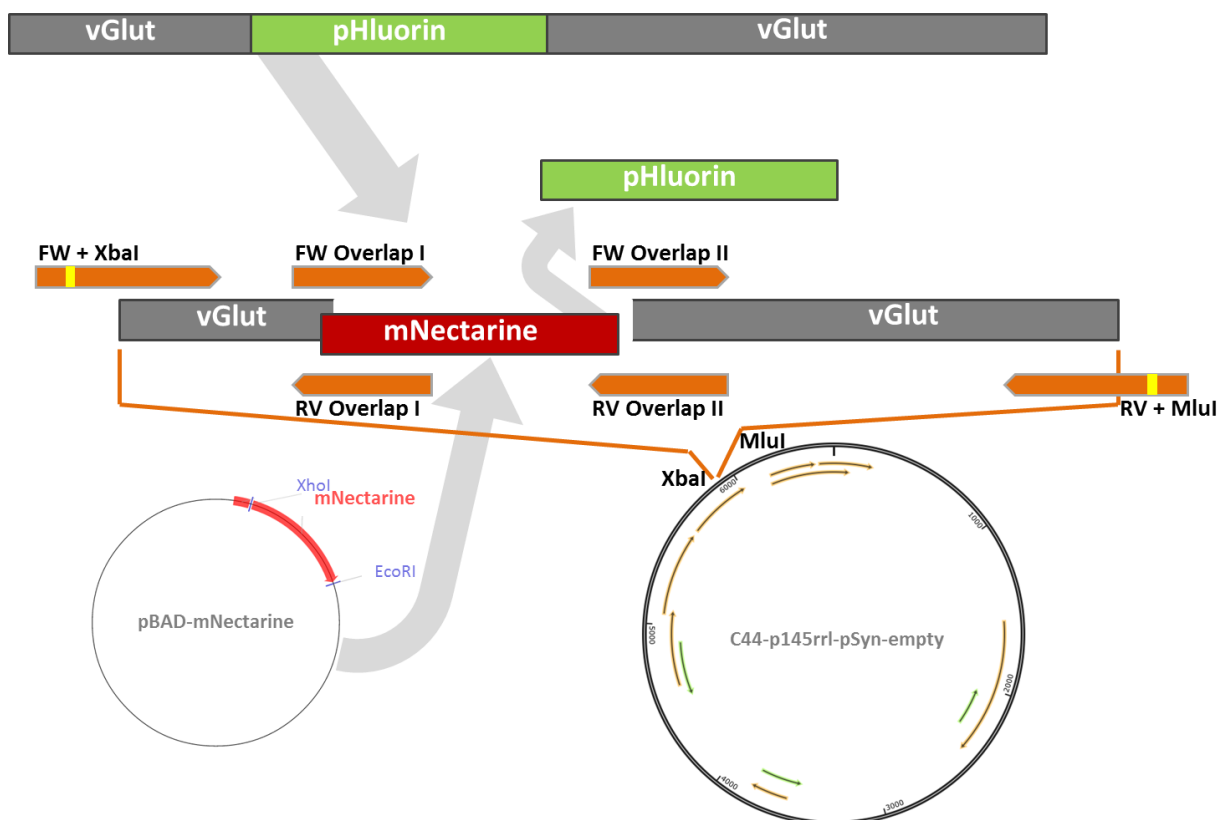


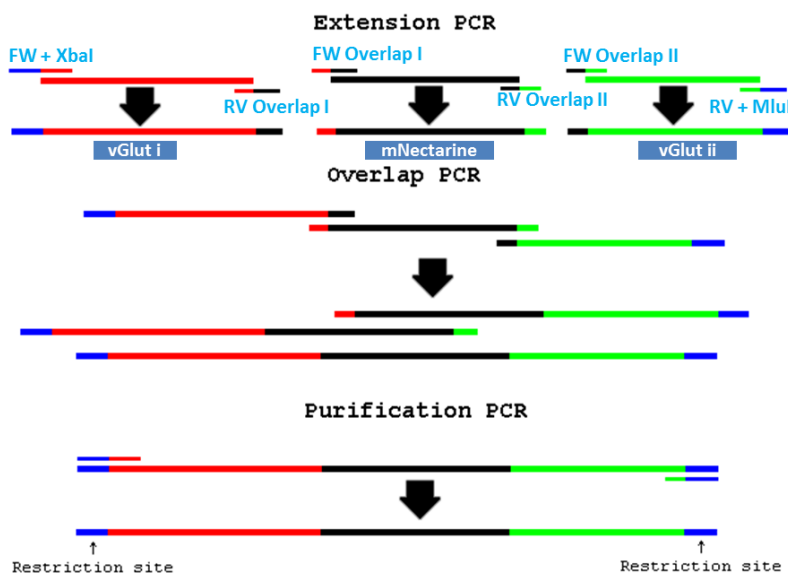
**Figure 31 Cloning strategy of vGlut-mNectarine.**

Splicing by overlap extension PCR removed out pHluorin and replaced it with mNectarine. Later VGLUT-mNectarine was cloned into second generation Lentivirus.

<sup>28</sup> pH-sensitive monomeric mNectarine red fluorescent protein. GenBank ID: FJ439505.



pH = 7.5. The most convenient way to clone mNectarine into the luminal part of VGLUT was to remove pHluorin with splicing it out by overlap extension PCR (Figure 31). The strategy involves constructing inner primers that bridge different pieces together. These primers should have close annealing temperatures for successful PCR. Two end primers with specific restriction enzymes are needed to insert the product in the viral vector of interest. The first step is to do the extension PCR by which the fragments are separately amplified. In this case its VGLUTi, mNectarine and VGLUT



Link: [http://openwetware.org/wiki/PCR\\_Overlap\\_Extension](http://openwetware.org/wiki/PCR_Overlap_Extension)

**Figure 32 Splicing by Overlap Extension.**

The procedure involves designing overlapping primers and two end primers with restriction site each. Using the proofreading Polymerase, 'Extension PCR' amplifies the segments of interest at the right annealing temperature. The resulting PCR products are used in 'Overlap PCR' reaction, whereby the template will act as primers for each other. To finalize the PCR product, use the end primers with the restriction sites for 'Purification PCR'. The correct size fragments are extracted and cloned into the vector.

Source: Modified from OpenWetWare website, Michael A. Speer, September 2011.

three independent extension PCR reactions were carried out in order to get the 3 different fragments. Fragment VGLUTi was produced by adding FW primer 5'CGTGT^CTAGAGCCACCATG GAGTTCCGGCAGG with XbaI restriction site, RV overlap I primer 5'CCTTGC TCCACCTGTCCCGC CGCTTC3', VGLUT-pHluorin 1.3 µl, dNTPs1 µl, Red Taq polymerase 1.2 µl, PCR buffer 5 µl and Sigma water 41 µl. Fragment mNectarine with the overlaps was produced by adding FW overlap I primer 5'GGGACAGGTGGAGTGAGCAAGG GCGAGGAG3', RV overlap II primer 5'TGCCTCCGCTCTTGTACAGCTCGTCCATGC3', mNectarine 1 µl, dNTPs1 µl, Red Taq polymerase 1.2 µl, PCR buffer 5 µl and Sigma water 41 µl. The third fragment VGLUTii PCR was done by adding FW overlap II primer 5'3 GAGCTGTACAAGAG CGGAGGCACAGGTGGC', RV primer 5'AGGCA^CGCGTTCAAGT AGTCCCGGACAGGG GGTG3' with MluI restriction site, VGLUT-pHluorin 1.3 µl, dNTPs1 µl, Red Taq polymerase 1.2 µl, PCR buffer 5 µl and Sigma water 41 µl (see Figure 33a). Once the

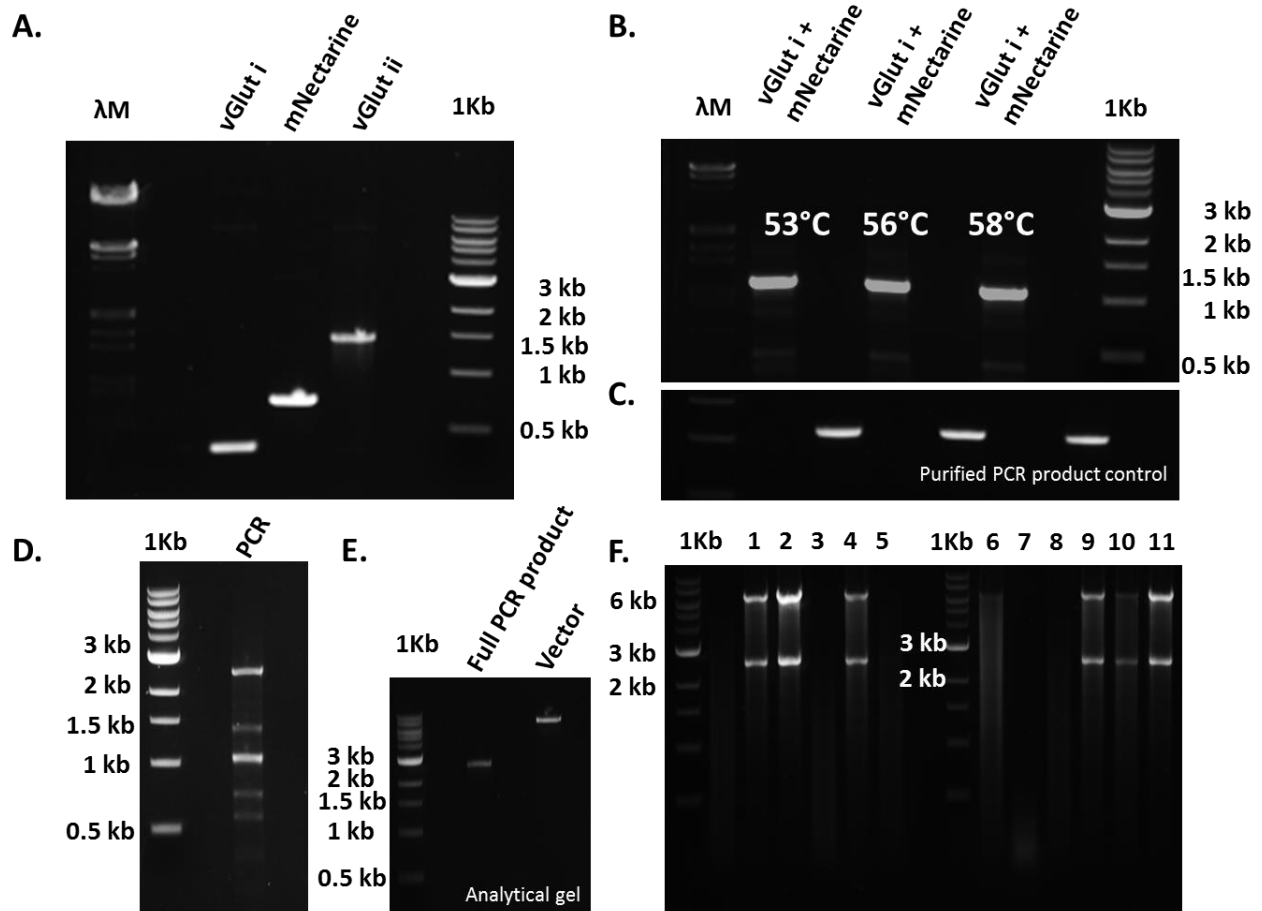


**Figure 33 vGlut-mNectarine cloning.**

(A) vGlut I, mNectarine and vGlut ii are produced with extension PCR. The produced products have overlapping ends. (B) First fusion gradient-PCR with 3 different extension temperatures whereby vGlut I is fused to mNectarine. (C) The correct fragment size was purified and part of it was loaded on a control gel. (D) Second fusion PCR between vGlutI-mNectarine and vGlut ii fragment. The expected size approximately 2600 bp. (E) Analytical estimation of the insert and the vector backbone in order to estimate the DNA ligation ratio. (F) The resulting clone's DNA from the ligation reaction were digested with XbaI and MluI. The insert was cut out in clone 1, 2, 4, 9 and 11, indicating that these were the correct clones. All gels were 1% agarose gel. Samples were run at 80 mV for 60 min.

products were purified, a first fusion PCR was applied to the first two fragments. Gradient PCR was the choice because we were not certain at which temperature we should carry this reaction, we chose 53, 56 ad 58 °C. It turned out all were as efficient (Figure 33 B). Fragment VGLUTi PCR product 0.5 µl was mixed with mNectarine PCR product 0.5 µl together with FW primer, RV overlap II primer, dNTPs1 µl, Red Taq polymerase 1.2 µl, PCR buffer 5 µl and Sigma water 40 µl. The PCR product was purified (Figure 33 C) and extracted. The VGLUTi-mNectarine (0.5 µl) product was then used in a second fusion PCR reaction mixed with VGLUTii PCR product 1 µl, dNTPs1 µl, Red Taq polymerase 1.2 µl, PCR buffer 5 µl and Sigma water 40 µl. At this step, no primers were added and the PCR was run for 10 cycles at 40 °C to allow the fragments to anneal.

## MATERIALS AND METHODS

Later, 0.5  $\mu$ l of FW primer and RV primer each were added and the PCR was run for 20 cycles at 60 °C (Figure 33 D). The obtained fusion PCR product was then purified and digested with XbaI and MluI. Analytical gel was performed to estimate the amount of products needed for successful ligation reaction (Figure 33 E). The ligation reaction involved 0.5  $\mu$ l of vector, 2  $\mu$ l insert, 2  $\mu$ l T<sub>4</sub> buffer, T<sub>4</sub> ligase, and 13.5  $\mu$ l water. A control reaction involved the same components but without insert. The first DNA transformation was carried in DH5 $\alpha$  cells. We failed to produce correct clones. To overcome this problem, different antibiotic concentrations, the agar quality and bacteria used (Tiscornia et al., 2006) were separately tested and none managed to produce successful resistant clones. (Bichara et al., 2000; Kang and Cox, 1996) Multiple direct repeats in Lentiviral vectors cause problems when transformed into DH5 $\alpha$ . On the contrary, instability-prone Lentiviral vectors are remarkably stable when cloned in *Escherichia coli* Stbl3 (Faisal A. Al-Allaf, 2012). Invitrogen Stbl3 is a chemically stable competent bacteria that reduce the frequency of homologous recombination of LTRs in big expression vectors. The company reported that the yielded DNA is ten-fold higher than that of DH5 $\alpha$ . Unlike DH5 $\alpha$ , Stbl3 can be harmful and cause irritation if it touches the skin. The transformation carried out in stbl3 worked from the first time and 5 out of 11 clones showed correct DNA once digested with MluI and XbaI (Figure 33 F). One of the clones

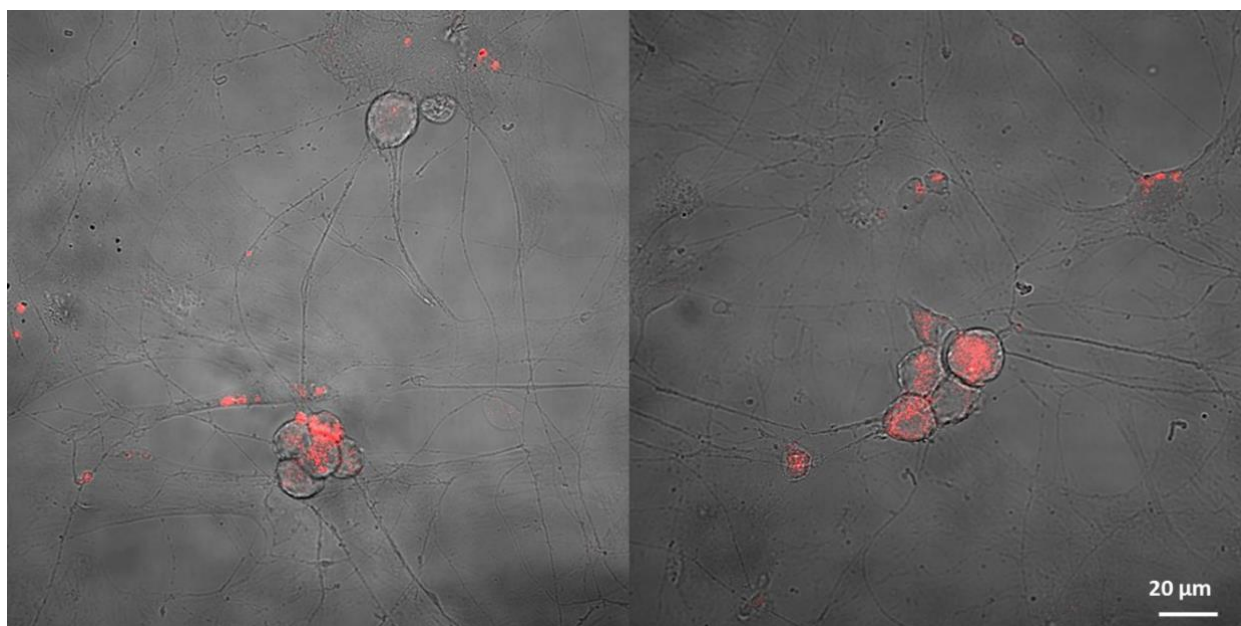


**Figure 34** Tile confocal images showing overexpression of vGlut-mNectarine in DRG-S neurons co-culture.

DRG culture was transfected with the Lentivirus encoding for vGlut-mNectarine and then S neurons were later added and left together for 5 DIV. The cells were then fixed with 4% PFA and excited at 561 nm and acquired *in tiles*. The resulting images were overlaid with bright field. The transfection efficacy was around 60%.



was successfully sequenced and the Lentivirus was produced. The virus was effectively tested in DRG/S neuron co-culture (Figure 34).

## II.2.11 Analysis

ICC experiments performed on SIM microscopes were processed using previously mentioned ZEN software. The background was subtracted and co-localization was performed using JACoP plugin on ImageJ to get Manders' coefficient (Bolte and Cordelieres, 2006). ICC experiments performed on confocal microscope and the data was analyzed in ImageJ v1.49i, the background was subtracted and the mean gray value was quantified to compare the true signal with that of control. Manders' coefficient was also calculated through ImageJ. LDCV secretion graphs were displayed as cumulative increase of released vesicles normalized to the surface area of individual cells. To analyze exocytosis, LDCV secretion was counted as fast disappearance of vesicles within 200 ms time while slower disappearance indicates that the vesicles are leaving the plasma membrane. The figure below is a representative classical example that demonstrates LDCV secretion where a vesicle approaches the membrane and fuses completely with it (Figure 35). The graph in figure 35 E depicts fluorescence intensity time course of the vesicle approaches the membrane, and hence its fluorescence is increased and then fuses inducing a fast disappearance of the signal. We also included all other forms of LDCV secretion that encompass kiss and run, kiss and stay and these vesicles that are docked at the membrane and fuses, inducing an increase

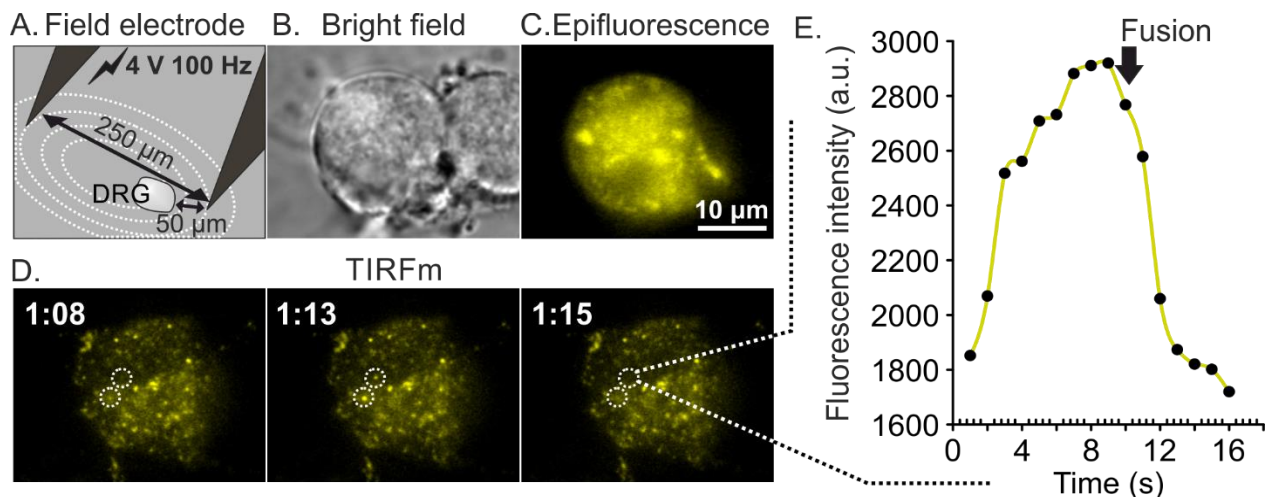


**Figure 35 Representative example of classical LDCV secretion.**

Cultured DRG neurons were transfected with a Lentivirus encoding for NPY-Venus and left to stay in culture for 7 days. The cells were then transferred to a special metal holder and are incubated with *Tobias* physiological solution and placed on the TIRFM setup. The field electrode is placed next to the cells as shown in (A) and images were acquired in bright field (B.), epifluorescence (C) as well as TIRF (D.). (E) Exemplary fluorescence intensity trace during fusion.

fluorescence intensity and fast disappearance of the signal because of the dispersion of the NPY-Venus cargo (Bost et al., 2017). Acquired data was analysed with ImageJ and secretion events were documented with specific regions of interest (ROIs). The LDCV secretion curves were displayed as average cumulative curves whereby individual cells were normalized to their own surface area and multiplied by the average area of all cells. In order to analyze synaptic formation, synapses were marked by ROIs and counted via special ImageJ macro written by Dr. Ralf Mohrmann who also wrote a second macro to measure distances between individual synapses and neurons. Mature synapses were defined by the co-localization of Bassoon, PDS95 and Synaptobrevin (SybKI). The number of synapses were normalized to the area of the acquisition, hence the displayed numbers in the graph represent synapse per unit of area. The synaptic transmission experiments were analyzed through ImageJ. Synapses were defined as SypHy labelled structures and responded to the 4 V at 10 Hz electrical stimulus. The background was subtracted by using a macro which calculated the average mean grey value over an ROI that selected an empty part of the coverslip and subtracted the value frame by frame for the entire acquisition. Synapses were marked by ROIs and the mean gray value was measured as a function of time. The displayed graphs were normalized to the maximum signal upon  $\text{NH}_4\text{Cl}$  application. The time at which maximum fluorescence was reached was different between recordings due to the manual application of  $\text{NH}_4\text{Cl}$ . For display purpose, I corrected for this shift. For each recording, the row contains the maximum values as determined and an index offset correction was applied. This offset function shifted the cells automatically in such a way that all maximums started at the same time point, before normalizing to it. Error bars were standard error of mean and were calculated through Excel or by SigmaPlot. Mann Whitney, t-test, one way ANOVA and two way ANOVA were calculated with SigmaPlot 13. Graphs were generated by SigmaPlot and rarely by Igor or Excel. The graphs were formatted with CorelDRAW X6.

### III. Results

Since the description of p145 aka CAPS1 in 1992 by Thomas Martin (Walent et al., 1992) and the discovery of the second isoform CAPS2 by Nils Brose (Speidel et al., 2003), there has been controversy concerning their function. Contradicting roles of these isoforms are ever growing in the literature. The two isoforms and the splice variants of CAPS2 with their different domains as well as their developmental expression over time add several layers of complexity. We chose DRG and DRG/S neuronal culture and co-culture, respectively to address the role of CAPS in LDCVs and SVs in one system. This neuronal culture enables us to study LDCV and SV release either individually or simultaneously. The first experiments investigated whether CAPS isoforms are found in DRG neurons at the mRNA and protein developmental expression levels as well as its localization at the cellular level.

#### III.1 CAPS Localization

CAPS1 and CAPS2 are distributed among various tissues and cell types in mice. For instance, CAPS1 and CAPS2 were shown to be widespread in mouse at mRNA level (Sadakata et al., 2004; Speidel et al., 2003). The cellular distribution was well examined by (Sadakata et al., 2006), whereby he showed that CAPS1 and CAPS2 were complementarily expressed in embryonic nervous system. CAPS1 was distributed at different levels while CAPS2 was localized to distinct cell types and fibers in various brain regions including olfactory bulb, cerebrum, hippocampal formation, thalamus, mesencephalic tegmentum, cerebellum, medulla and spinal cord. Using IHC experiments on spinal cord splices, the authors found that while CAPS1 was distributed in all DRGs, CAPS2 was in subpopulation only. Though this study gave us a hint about CAPS distribution in PNS neurons but it lacked the percentages at which each isoform was distributed and it was not providing the distribution of these isoforms at the level of different DRG neuron subtypes.

## III.1.1 CAPS Localization at mRNA Level

We sought to identify the presence of CAPS by using Reverse transcription-PCR on complete DRGs. RT-PCR semi-quantitative results indicate that CAPS1 and to lesser extent CAPS2 isoforms are found in DRGs isolated from 2 weeks old mice. This finding fits well with the previous findings described by (Sadakata et al., 2006). We next wanted to investigate the expression of CAPS isoforms at protein level and during development. This was of particular importance because some experiments in this work were carried out with adult WT or CAPS2 KO mice while others were made with CAPS dKO mice at embryonic day 18 because they die at birth (Speidel et al., 2008).

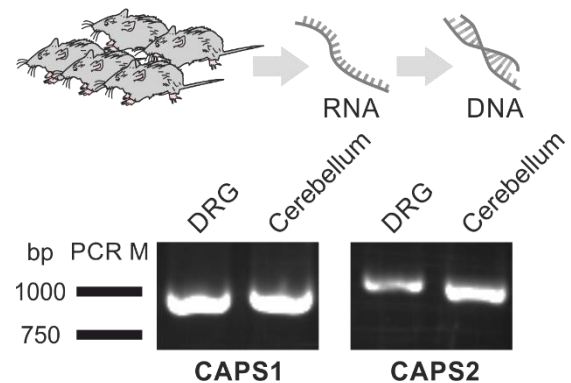


**Figure 36 RT-PCR from 2 weeks old mice.** mRNA was produced from 5 adult mice (170 mg of tissue) and converted to cDNA by PCR reaction.. In a second PCR reaction, screening for CAPS1 and CAPS2 was mediated by primers specific against each isoform. Cerebellum was used as a positive control for both isoforms (Sadakata et al., 2006; Sadakata et al., 2007a).

## III.1.2 CAPS Localization at Protein Level

To investigate the presence of CAPS isoforms at the protein level in DRG neurons, WT DRGs were isolated from 12 mice separately and Western blot<sup>29</sup> was carried out. To validate the specificity of the antibodies we used, dKO mice were used. The age of the mice from which the DRGs were isolated was E18 and P7. We chose P7 old mice because for imaging experiments on CAPS dKO cells, we waited for the Lentivirus expressing NPY-Venus 7 days before measuring

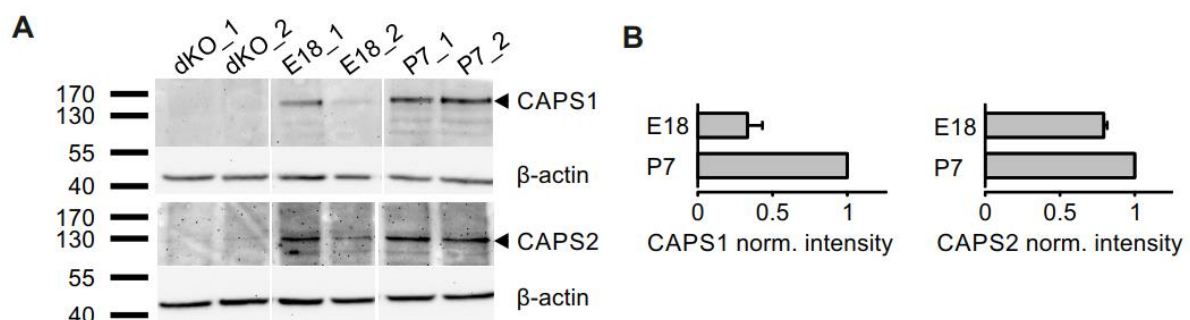


**Figure 37 CAPS developmental protein expression levels.**

<sup>29</sup> The Western blot was carried out by Mr. Ahmed M. Shaaban.

## RESULTS

**Continuing Figure 37...** (A) CAPS developmental protein expression levels was examined by western blot. DRGs were isolated from WT and CAPS dKO E18, and WT P7 old mice and the samples were run. Actin was used to standardize the protein expression levels. (B) The graph shows actin-based corrected protein expression levels normalized to the signal from P7. Results indicate that both CAPS1 and CAPS2 proteins are present prenatal mice and the expression levels is elevated in postnatal mice.

LDCV exocytosis. Both CAPS1 and CAPS2 isoforms were found at the protein level in E18 pups (Figure 37 A). To correct for sample loading errors,  $\beta$ -actin labelling was also performed. Interestingly, CAPS1 expression levels doubled as pups grew older. CAPS2 embryonic expression levels were high compared to that of CAPS1. While RT-PCR and Western blot experiments confirmed the existence of CAPS isoforms in DRGs, they also contain cells other than neurons such as astroglial cells and fibroblasts. Therefore, we screened for CAPS at the cellular level to exclude the possibility that CAPS was localized to cells other than our neurons.

### III.1.3 CAPS Localization at Cellular Level

ICC experiments to localize CAPS in DRG neurons involves primary antibodies against CAPS isoforms that are detected through secondary antibodies coupled to IgG Alexa Fluorophore. To make sure that the signal from such experiments is correct, control samples are essential to prove that the primary antibody is specific to the antigen, the secondary antibody is specific to the used primary antibody and the obtained signal is a result of the added label and not due to endogenous autofluorescence (Burry, 2011). Furthermore, we investigated the autofluorescence profile of these cells in order to be able to distinguish the real signal from noise that usually arises from cell components and free radicals and to choose the appropriate fluorophore of the secondary antibody. To do so, an adult DRG cell culture was fixed with 4% PFA at 1, 7 and 14 DIV. The cells were excited with 405, 458, 488, 514, 561 and 633 nm lasers and the

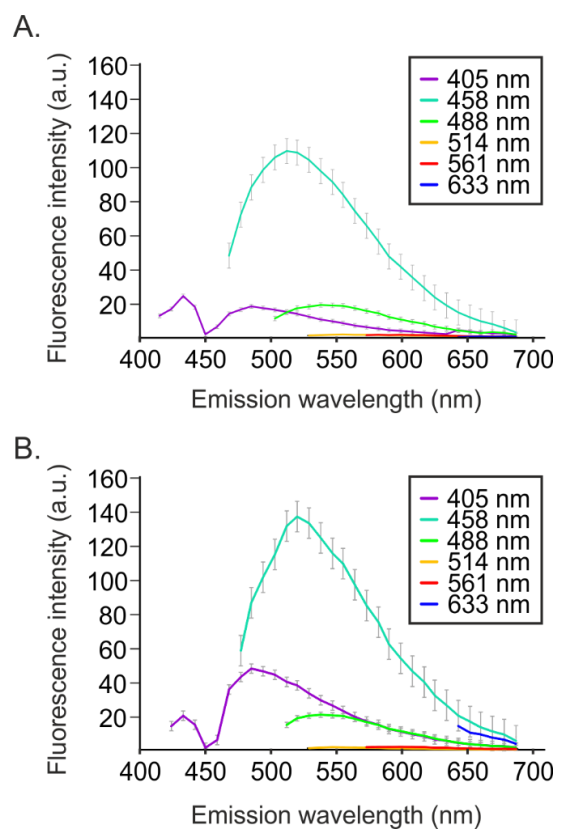


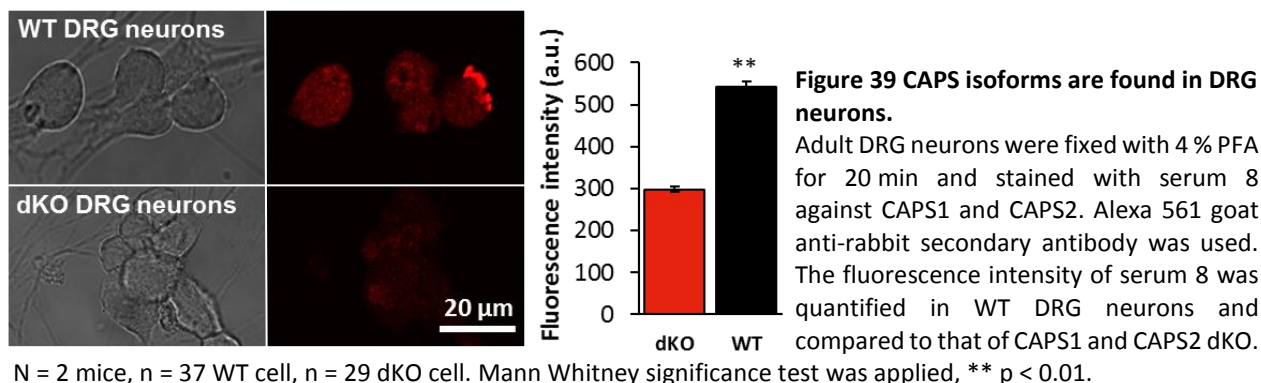
**Figure 38 DRG neurons autofluorescence profile.**

DRG neurons were fixed with 4% PFA for 20 min and images were acquired using confocal microscope. (A) Autofluorescence emission intensity was measured upon exciting with different wavelengths in 1 day old DRG culture, and 7 days old culture in (B.).

## RESULTS

emission spectrum was plotted in figure 31. We found that one day old fixed DRG neurons exhibits autofluorescence at 405, 458 and 488 nm and very low autofluorescence at 561 and 633 nm (Figure 31 A). The longer the neurons stay in culture the stronger the autofluorescence got. The autofluorescence was highest with excitation at 458 nm (Figure 31 B). Living DRG neurons showed a milder but similar autofluorescence pattern compared to fixed cells. Taking into consideration this autofluorescence pattern of DRG neurons both in living cultures and fixed preps, all upcoming experiments were optimised accordingly.

Thus, to localize CAPS isoforms, E18 DRG neurons of WT and CAPS dKO genotype were separately produced and left to stay in culture for seven<sup>30</sup> days. Then the cells were fixed according to the previously described protocols and CAPS isoforms were screened using home produced antibodies in collaboration with Dr. Martin Jung. To detect both CAPS isoforms, a 1347/48 – serum 8<sup>31</sup> was used. Results indicate that CAPS1 and CAPS2 are found in DRG neurons in both diffuse cytoplasmic and punctate staining (Figure 32). It was possible to purify from this serum the antibodies that recognize CAPS2 only. Several purified serums were produced, I tested 1403b – serum 4, 6 and 10 to finally use serum 6. Controls that ensured the specificity of serum 6 were carried out in CAPS2 KO background, to rule out any cross-reactivity with CAPS1 isoform (*Appendix VI.1*). We took advantage of this newly generated serum to perform double immunostaining together with serum 8 which recognizes both isoforms and managed to determine the distribution of individual isoforms. The results showed that half of the cells were positive for CAPS2 (Figure 39) which means that rest of the signal comes either entirely from coexistence of CAPS1 in all cells and CAPS2 in half of the population or by random distribution of each isoform



<sup>30</sup> DRG neurons are transfected with a Lenti-virus encoding for NPY-Venus to label LDCVs to monitor exocytosis. The virus is incubated for seven days in order to achieve a bright labeling of LDCVs.

<sup>31</sup> 1347/48 – serum 8 was produced by injecting the full length CAPS2e protein into the rabbit and due to the high similarity between CAPS1 and CAPS2 isoforms, this serum can detect both isoforms.



## RESULTS

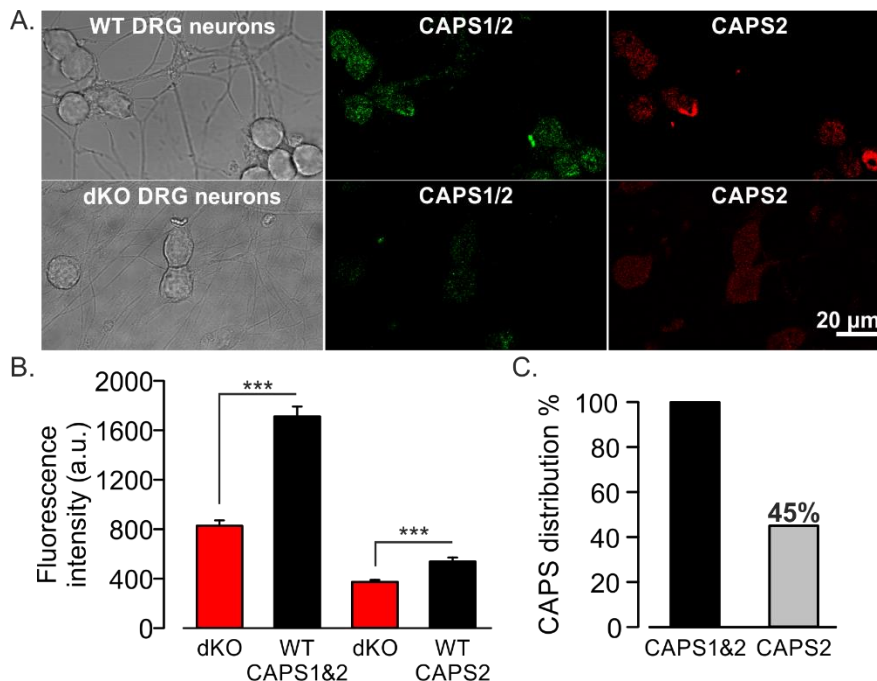
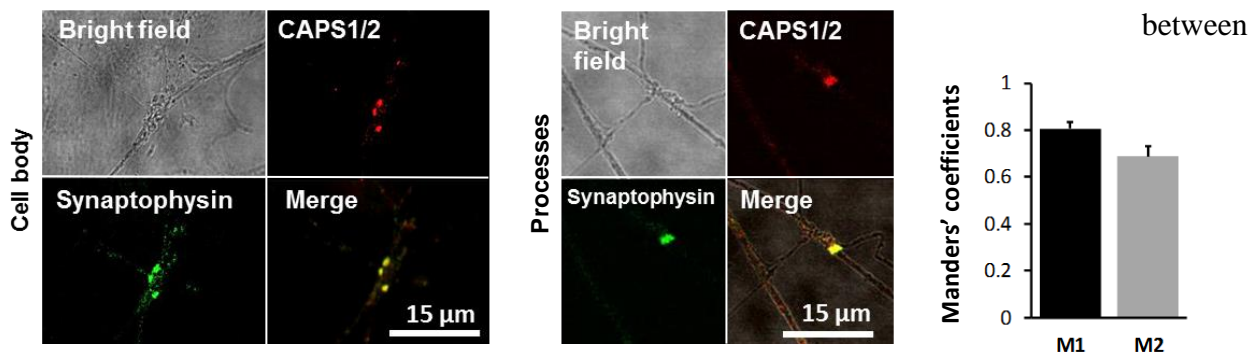


**Figure 40 CAPS1/2 and CAPS2 double-immunostaining.**

Adult DRG neurons were fixed and stained with serum 8 against CAPS1 and CAPS2. Alexa 561 goat anti-rabbit was used as secondary antibody was. Fab fragments were used to block serum 8 active sites before carrying out the second staining with purified serum 6 against CAPS2. Alexa 488 goat anti-rabbit secondary antibody was applied against purified serum 6. The images were acquired by confocal microscope and the signal from WT DRG neurons was compared to dKO neurons. (A) Bright field and confocal images acquired at, 561 and

488 nm of DRG neurons were compared to dKO cells. (B) Graph displaying the fluorescence intensity of serum 8 and serum 6 compared to dKO signal. (C) Distribution of CAPS isoform among cells in percentage. N = 2 adult mice, n = 28 WT and n = 94 dKO cell. Mann Whitney significance test was applied, \*\*\* p < 0.001.

and not necessarily being expressed together. However, the second possibility is unlikely because previous data indicates that CAPS1 is found in all DRG neurons while CAPS2 in a subpopulation (Sadakata et al., 2006). CAPS2 staining was remarkably diffuse, suggesting that the punctate staining from serum 8 comes from CAPS1. We were also interested to know the subcellular localization of CAPS to get a hint about its function, whether it is localized to synapses, in order to test its possible effect on SV secretion, using the advantage from DRG/S neuron co-culture system. We used serum 8 and carried out double ICC together with anti-synaptophysin antibody in DRG/S neuron co-culture. Results showed that CAPS fluorescence signal was intensified at synapses between DRG neurons and spinal neurons (Figure 41). Manders' coefficient of  $0.8 \pm 0.02$  from synaptophysin to CAPS suggests that the majority of synapses have either CAPS1 or 2 or both isoforms, while the lower Manders' coefficient of  $0.6 \pm 0.03$  from CAPS to synaptophysin suggests that CAPS is also found in processes and not just at the synapses. Further analysis of the position of synapses indicates that 40% of synapses were found between DRG processes and S neurons cell body and about 60% of the synapses were between processes of these neurons. This shows that CAPS is indeed found at synapses and confirms that the DRG/S neuron co-culture can be used to study the possible differential roles of CAPS isoforms in secretion of LDCVs and SVs. However, DRG neurons are silent in culture (Ransom et al., 1977b) and synapses don't exist



DRG

**Figure 41 CAPS isoforms localization to synapses in DRG/S neuron co-culture.**

Adult WT DRG neurons were co-cultured with dKO S neurons for five days and were fixed with 4 % PFA for 20 min and marked with serum 8 against CAPS1 and CAPS2 which was labelled with Alexa 561 goat anti-rabbit secondary antibody was used against serum 8. Fab fragments were used to block serum 8 antibodies active sites before carrying out the second staining against synaptophysin. Alexa 488 goat anti-rabbit secondary antibody was used against synaptophysin. The images were acquired using confocal microscope. They were subjected to uniform threshold to compute Manders' coefficients that are shown in the adjacent graph. M1 = Fraction of synaptophysin overlaying with CAPS isoforms, M2 = Fraction of CAPS isoforms overlaying with synaptophysin. N = 2 animals for DRG neuronal preparation, N = 8 P0 pups for S neurons preparation, n = 82 cell.

subpopulations (Joseph et al., 2010; Wake et al., 2015), so it was a prerequisite to establish and optimize and stimulation protocol to induce secretion of both LDCVs and SVs in DRG and DRG/S neuron cultures, respectively.

### III.2 Stimulus Protocol

Stimulating LDCV and SV secretion was carried out the previously described field electrode but at different frequencies. The concept was to pick the mildest stimulus that can induce the highest number of cells responding to the stimulus.

#### III.2.1 Stimulating DRG Neurons

The electrical stimulus of four Volts at hundred Hertz to induce LDCV secretion was applied via a custom-made bipolar Platinum-Iridium field electrode. The establishment and the concept behind the field electrode is explained in details in the *Materials and Methods* chapter.



## RESULTS

### III.2.1.1 Stimulus optimization

To test and optimize the electrical stimulus, cultured DRG neurons were incubated with the fluorescent calcium sensor Fluo 4 AM<sup>32</sup> for 15 min and then washed. Several voltage intensities at different frequencies were tested and fluorescence intensity change was recorded. Results showed that a minimum stimulus of 2.5 V induced a slight increase in intracellular calcium, while at 4 V about 70% of DRG neurons displayed a strong increase in intracellular calcium (Figure 42), going below 2.5 V or above 4 V did not change the percentage of responding cells (*data not shown*), hence we picked 4 V at 100 Hz. The frequency of 100 Hz was chosen because it was shown that BDNF release from LDCVs in hippocampal neurons was not evoked at stimulus lower than 50 Hz

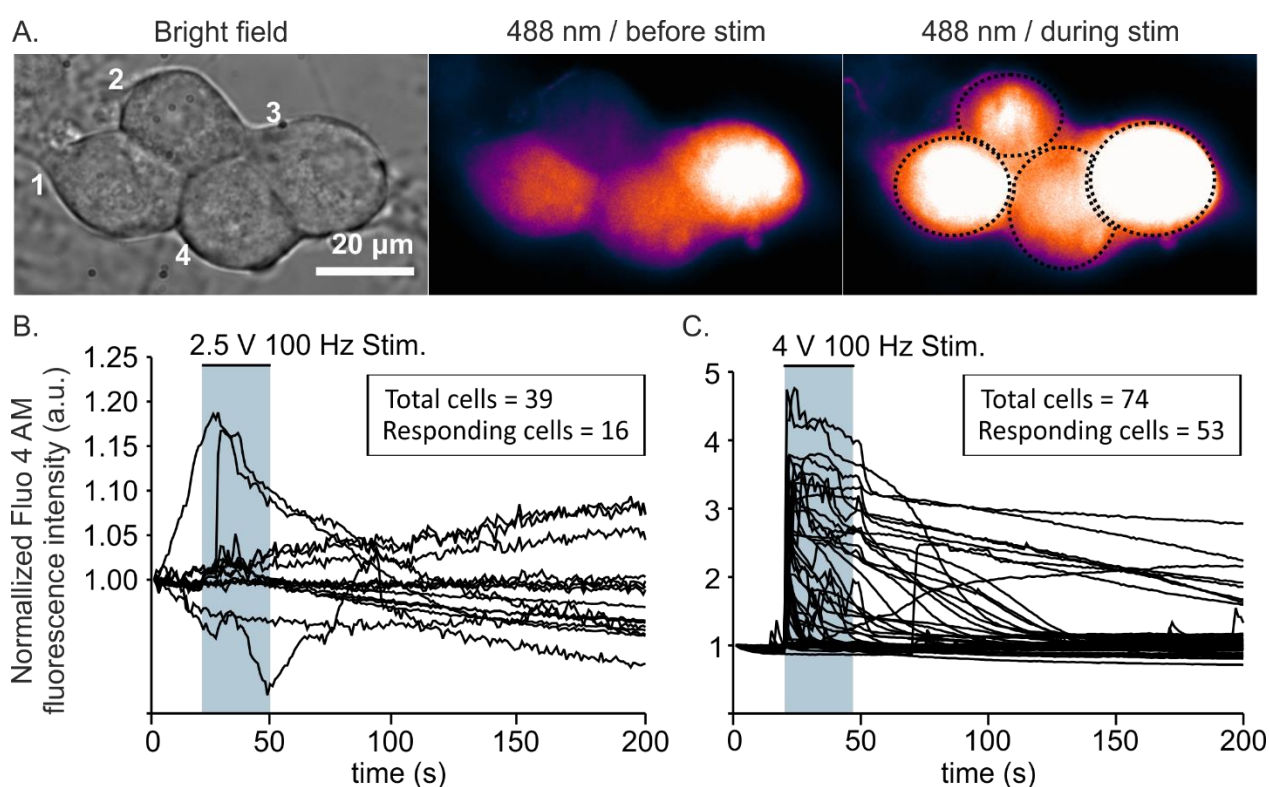


**Figure 42 Electrical stimulus for DRG neurons.**

DRG neurons were loaded with Fluo 4 AM dye for 20 min before recording. The cells were stimulated by custom-made bipolar Platinum-Iridium field electrode at different voltages and the increase of Fluo 4 fluorescence intensity was imaged in epifluorescence mode. (A) Representative four DRG neurons are shown in bright field (left), epifluorescence at 488 nm before the electrical stimulus (middle) and upon the electrical stimulus (right). Three cells showed an increase in fluorescence intensity while the fluorescence in DRG number 4 didn't change, hence this cell didn't respond to the stimulus. ROIs marked the individual neurons and the fluorescence curves were plotted as a function of time in the lower graphs. (B) The graph shows the fluorescence intensity normalized to the baseline of individual DRG neurons subjected to 30 seconds stimulus of 2.5 V at 100 Hz as a function of time. (C) DRG neurons were stimulated with 4 V at 100 Hz and the fluorescence intensity was plotted against time.

<sup>32</sup> Fluo 4 AM from ThermoFisher is a fluorescent calcium assay. Upon binding calcium, its structure is modified inducing an increased fluorescence once excited at 488 nm.

(Gartner and Staiger, 2002). It was notable that DRG neurons didn't exhibit measurable calcium signal before the stimulus, supporting the argument that these cells are silent in culture and needs stimulus in order to secrete. The field electrode was entirely renewed every six month and calcium measurements were carried out every 3 months to ensure the consistency and efficacy of the electrical stimulus.

### **III.2.1.2 LDCV Secretion**

To visualize secretion, DRG neurons were transfected with NPY-Venus. Venus was tagged to NPY to ensure its localization into LDCVs. NPY-Venus was driven by a Lentiviral expression system, it was essential to test if NPY-Venus was sorted correctly into LDCVs although Lentiviruses are gentle on cells and ensure a high survival rate after infection (Mao et al., 2015). NPY-Venus expressing DRG neurons were fixed and stained against Chromogranin A, a marker for LDCVs. Colocalization analysis showed that overexpressed NPY-Venus is loaded correctly into LDCVs (see *Appendix VI.3*).

### **III.2.2 Stimulating Hippocampal Neurons**

To further verify the efficacy of the stimulus, we tried to stimulate hippocampal neurons with 10 Hz according to what is described in the literature (Balkowiec and Katz, 2002; Jacobs and Meyer, 1997). Eight days old hippocampal neurons<sup>33</sup> were loaded with Fluo 4 AM and stimulated with 4 V at 10 Hz and 4 V at 100 Hz. The recordings showed that both stimuli had similar effect of about 70% of the neurons exhibited an increase in intracellular calcium (see *Appendix VI.1 A. & B.*), proving the efficacy of the customized field electrode. Unlike DRG neurons, hippocampal neurons were active before the stimulus which is normal for neurons that form active synapses in culture (Basarsky et al., 1994; Fletcher et al., 1994). This activity was evident in the first thirty seconds before the stimulus, as fluctuations of calcium concentration were visible. This, was not the case in DRG neurons calcium recordings (see *Appendix VI.1 B.*).

---

<sup>33</sup> Hippocampal neuronal cultures were kindly provided by Mr. Ali Harb.

### III.2.3 Stimulating DRG/S neuron co-cultures

To study the effect of CAPS on SV secretion, we tested which stimulation frequency should be used to evoke reliable SV exocytosis. DRG neurons were infected with synaptophysin-pHluorin one day before adding the S neurons. Co-cultured neurons remained 9 days in culture to give enough time for synapses to form. Results showed that a 10 Hz stimulus was enough to evoke SV secretion at synapses. A 100 Hz stimulus following the first 10 Hz didn't evoke further SV release, and one 100 Hz stimulus alone didn't managed to evoke higher SV secretion as compared to 10 Hz (Figure 43 A, B & C). Consistent with hippocampal neurons results, a 10 Hz stimuli is enough to evoke SV secretion. Now that the stimulus protocols to evoke SV and LDCV release were established, we could start studying the effect of CAPS on the exocytosis machinery.

### III.3 CAPS Isoforms Effect on LDCV Secretion

Unlike central nervous system neurons, the exocytosis machinery in DRG neurons is not thoroughly studied. For instance it is known that exocytosis from the somata of DRGs is calcium- (Huang and Neher, 1996) and voltage-dependent (Liu et al., 2011) but how it is regulated at the molecular level remains poorly understood. Based on the differential localization of CAPS in DRG

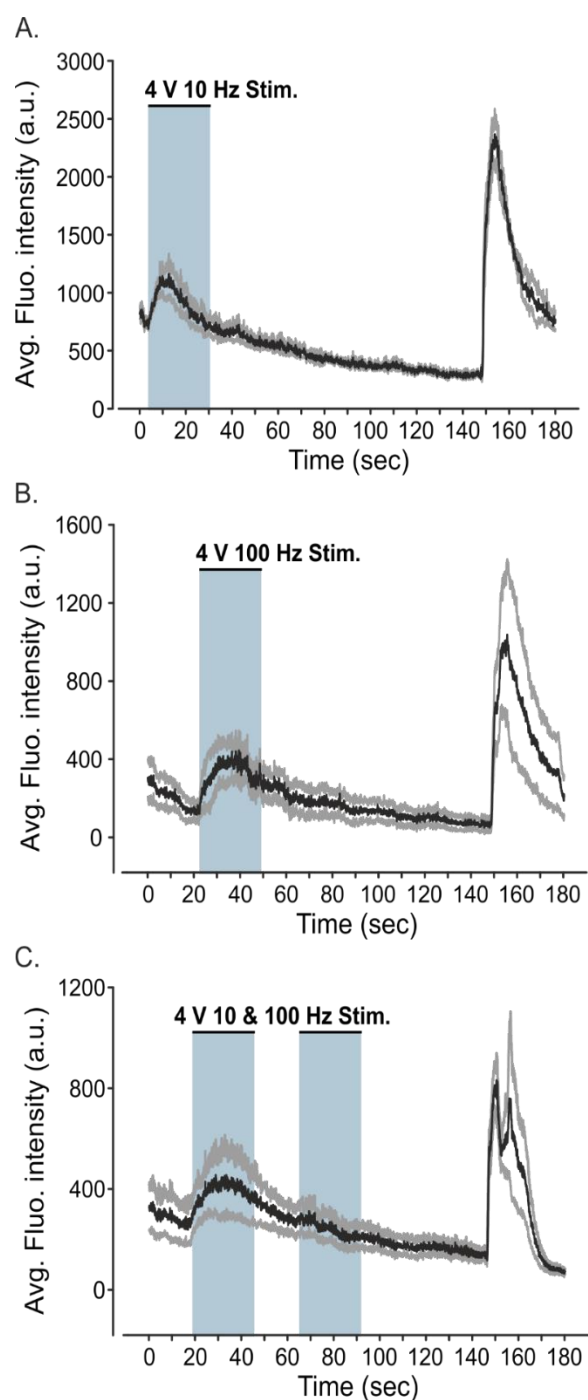


**Figure 43 Electrical stimulus for DRG/S neuron co-cultures.**

(A) DRG/S neuron co-cultured neurons were transfected with synaptophysin pHluorin and stimulated at 10 Hz. Fluorescence intensity was quantified as a function of time. A stronger stimulus was applied in (B) at 100 Hz and a 10 Hz stimulus followed by a 100 Hz stimulus was tested in (C).

## RESULTS

neurons (see Figure 40 & 41), we speculated that CAPS isoforms might play a role in the secretion machinery of LDCVs and SVs. To test this hypothesis, we prepared DRG neuron cultures from CAPS1 and CAPS2 dKO E18 mice, monitoring their LDCV release and compared it to neurons of WT E18 mice.

### III.3.1 CAPS Absence Hinders LDCV Secretion

DRG neuronal cultures of CAPS1 and CAPS2 dKO mice were made at E18 because these mice were not viable and died at birth. LDCV secretion was measured in dKO and WT neurons that were prepared simultaneously and measured on the same day. The cumulative normalized secretion to individual cell surface area in WT cells was in average two vesicles per cell. This was significantly decreased to an average of one vesicle being secreted in dKO cells (Figure 44 A). To test whether CAPS1 and CAPS2 dKO had an effect on tethering of LDCVs to the plasma membrane, the vesicles in the TIRF plane were counted in WT and compared to dKO condition. No significant difference was measured (Figure 39 B & C). These results suggest that CAPS has a role in LDCV secretion in DRG neurons through priming but not tethering.

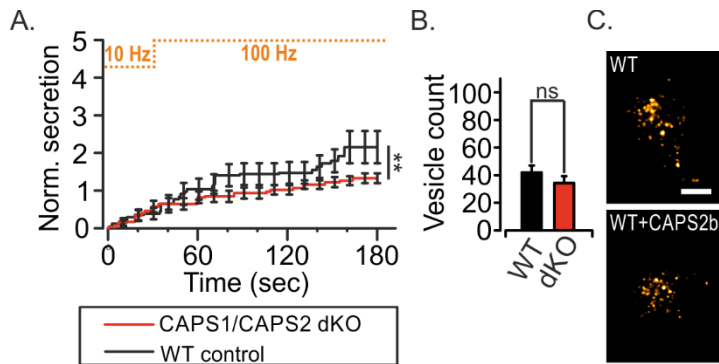


**Figure 44 CAPS1 and CAPS2 dKO effect on LDCV secretion.**

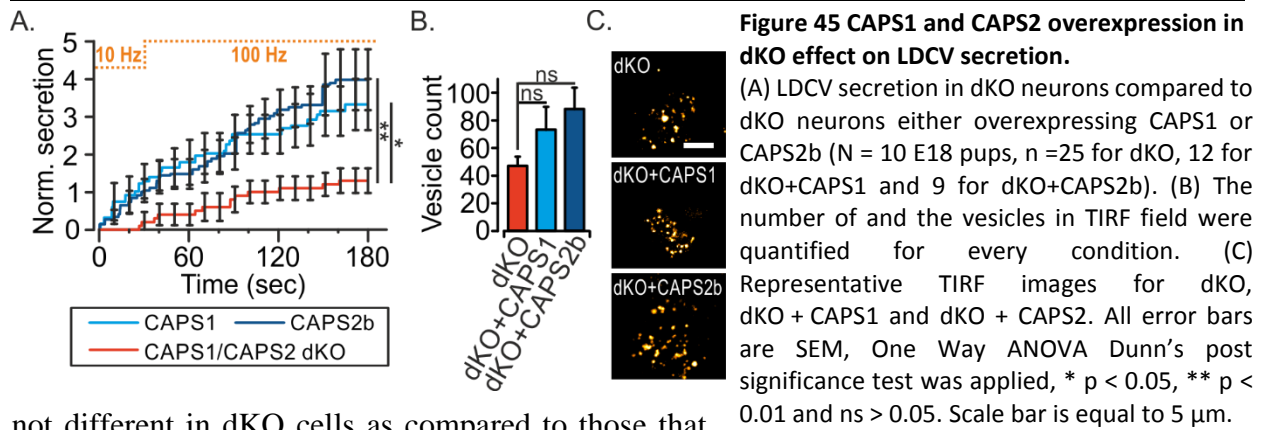
(A) Cumulative secretion of LDCVs normalized to cell surface area in WT compared to CAPS1 and CAPS2 dKO neurons. (N = 11 E18 pups, n = 29 for WT and 74 for dKO). (B) Vesicles in the TIRF field were counted in both WT and CAPS1 and CAPS2 dKO neurons and depicted in the graph. (C) Representative TIRF image of WT neurons and CAPS1 and CAPS2 dKO neurons expressing NPY-Venus. Scale bar is equal to 5  $\mu$ m. All error bars are SEM, Mann Whitney

significance test was applied, \*\* p < 0.01 and ns p > 0.05.

### III.3.2 CAPS Rescues LDCV Secretion in CAPS dKO Neurons

Rescue experiments were performed to test whether the dKO secretion phenotype can be reversed by CAPS expression. Both CAPS1 and CAPS2 isoforms were able to restore LDCV secretion in CAPS dKO DRG neurons exceeding the WT level. CAPS dKO DRG neurons transfected with CAPS1 secreted in average  $3.3 \pm 0.8$  LDCVs in the time of the recording comparable to neurons transfected with CAPS2 that secreted in average  $3.9 \pm 0.3$  LDCVs, but significantly more than in dKO DRG neurons (Figure 40 A). The number of tethered vesicles were

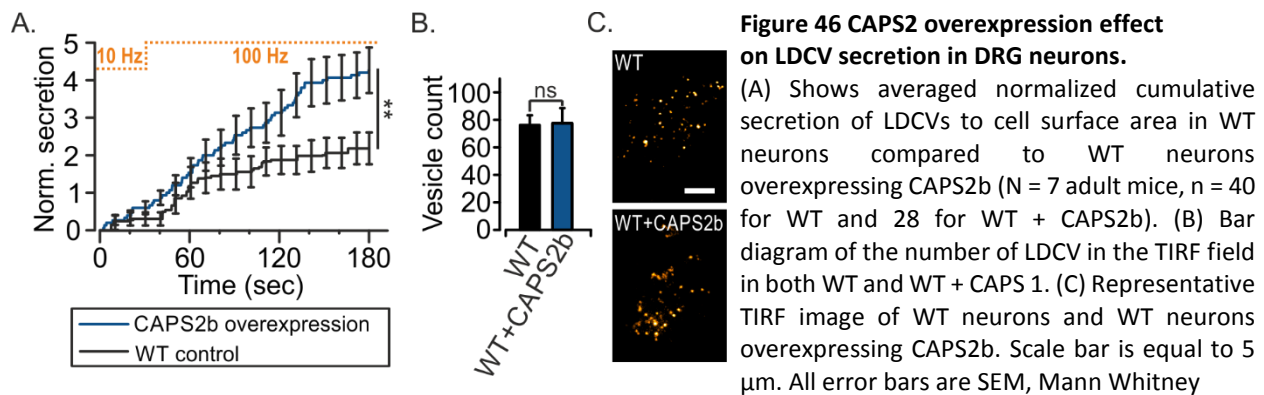
## RESULTS



not different in dKO cells as compared to those that overexpress either CAPS1 or CAPS2 with no evident significant change (Figure 40 B & C). These data indicate that the reduction of secretion in CAPS1 and 2 dKO neurons is solely due to the deletion of the protein and not to some downstream series of effects.

### III.3.3 CAPS Overexpression Increases LDCV Secretion

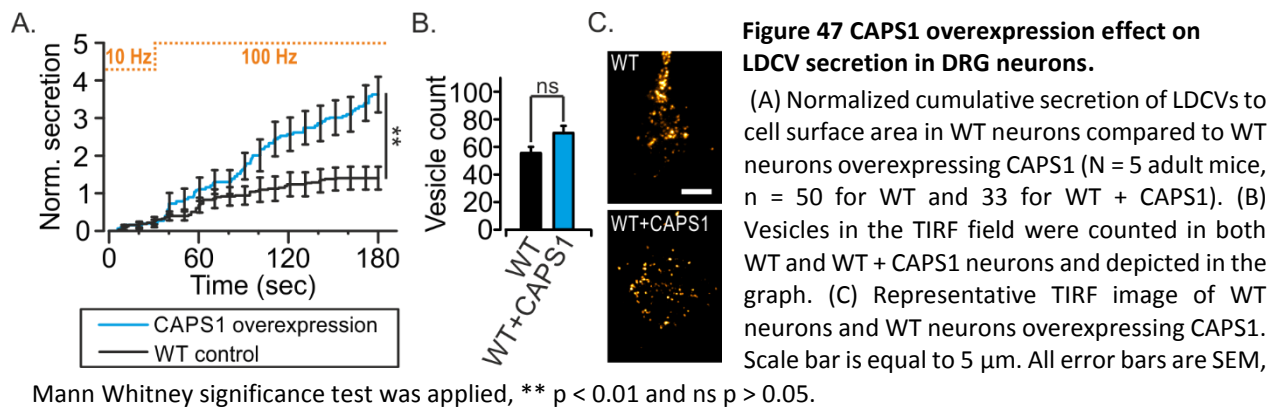
CAPS dKO neurons rescued with either CAPS isoform secreted more LDCV than WT neurons. In chromaffin cells, however, LDCV secretion of CAPS dKO cells is rescued by CAPS2 transfection only to WT level and in WT cells CAPS1 or 2 overexpression failed to increase LDCV



Whitney significance test was applied, \*\* p < 0.01 and ns p > 0.05.

exocytosis (Liu et al., 2010). Thus we tested if CAPS overexpression in WT DRG neurons would affect the LDCV secretion. First, CAPS1 was overexpressed and secretion was compared to WT cells. CAPS1 overexpressing neurons secreted  $3.6 \pm 0.4$  LDCVs while control neurons secreted  $1.4 \pm 0.3$  LDCVs (Figure 46 A) without affecting the number of vesicles tethered to the plasma membrane (Figure 46 B & C). This suggests that CAPS1 has no function at the level of tethering of vesicles and the effect on secretion is rather due to enhanced LDCV priming. In similar fashion, CAPS2 overexpression increased secretion till  $3.9 \pm 0.3$  LDCVs compared to  $2.1 \pm 0.4$  LDCVs in WT condition (Figure 47 A) without affecting the overall number of tethered vesicles to the plasma

## RESULTS



membrane (Figure 47 B & C). Altogether, this data indicates that CAPS isoforms can affect LDCV secretion through priming and not tethering.

### III.4 Half of DRG Neurons Secrete LDCVs

The secretion from dKO neurons was intriguing, as we noticed while doing the experiments that only a very small population secreted from the entire measured cells. Further analysis of the data showed that half of the neurons would respond to the stimulus and secrete LDCVs in WT system while this percentage is significantly decreased to 30% in CAPS1 and CAPS2 dKO

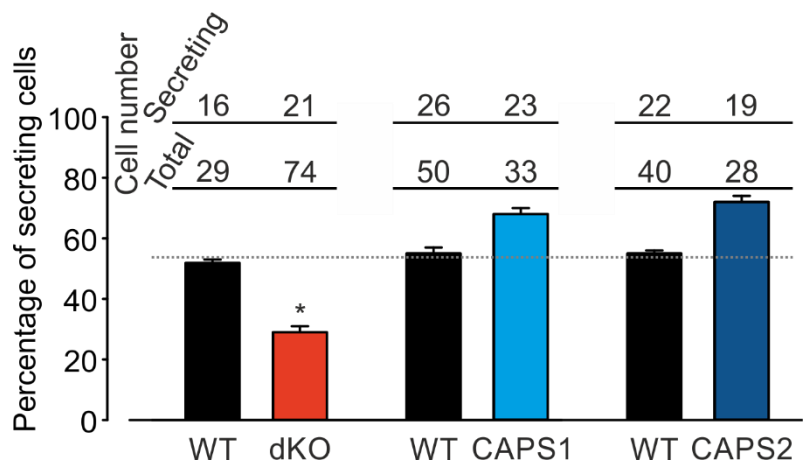


**Figure 48 Percentage of secreting cells.**

Percentage of secreting cells was counted in CAPS1 and CAPS2 dKO, CAPS1 overexpressing and CAPS2 overexpressing neurons and compared to those of WT neurons. Mann Whitney significance test was applied, \* p < 0.05.

system. Upon overexpressing of either CAPS isoform in WT cells, there was a tendency to have more cells that secreted LDCVs. This data emphasize the strong effect of CAPS by showing that CAPS not only affects the number of secreted LDCVs but also the number of secreting cells.

We were also puzzled by the fact that whatever electrical stimulus we applied even with higher voltage (*data not shown*), the number of secreting cells in WT was not changed. Therefore, we investigated whether stimulated LDCV secretion is limited to a certain subset of DRG neurons.



### III.5 Peptidergic and Non-Peptidergic DRG Neurons

DRG neurons constitute a very heterogeneous population depending on their sensory input or morphological characteristics. Despite this diversity, they can be classified into two main categories, the peptidergic myelinated neurons and the non-peptidergic un-myelinated neurons (Saeed and Ribeiro-da-Silva, 2012). Peptidergic neurons can be marked by anti-CGRP antibody (Barabas et al., 2012), anti-NK-1<sup>34</sup> (McLeod et al., 1998; Takeda et al., 1991; Todd et al., 2002), anti-Chromogranin A (Adams et al., 1993; Schafer et al., 2010) and anti-TRKB<sup>35</sup> receptor (Dykes et al., 2010; Scott et al., 2011). Often, NF-200<sup>36</sup> is used as a

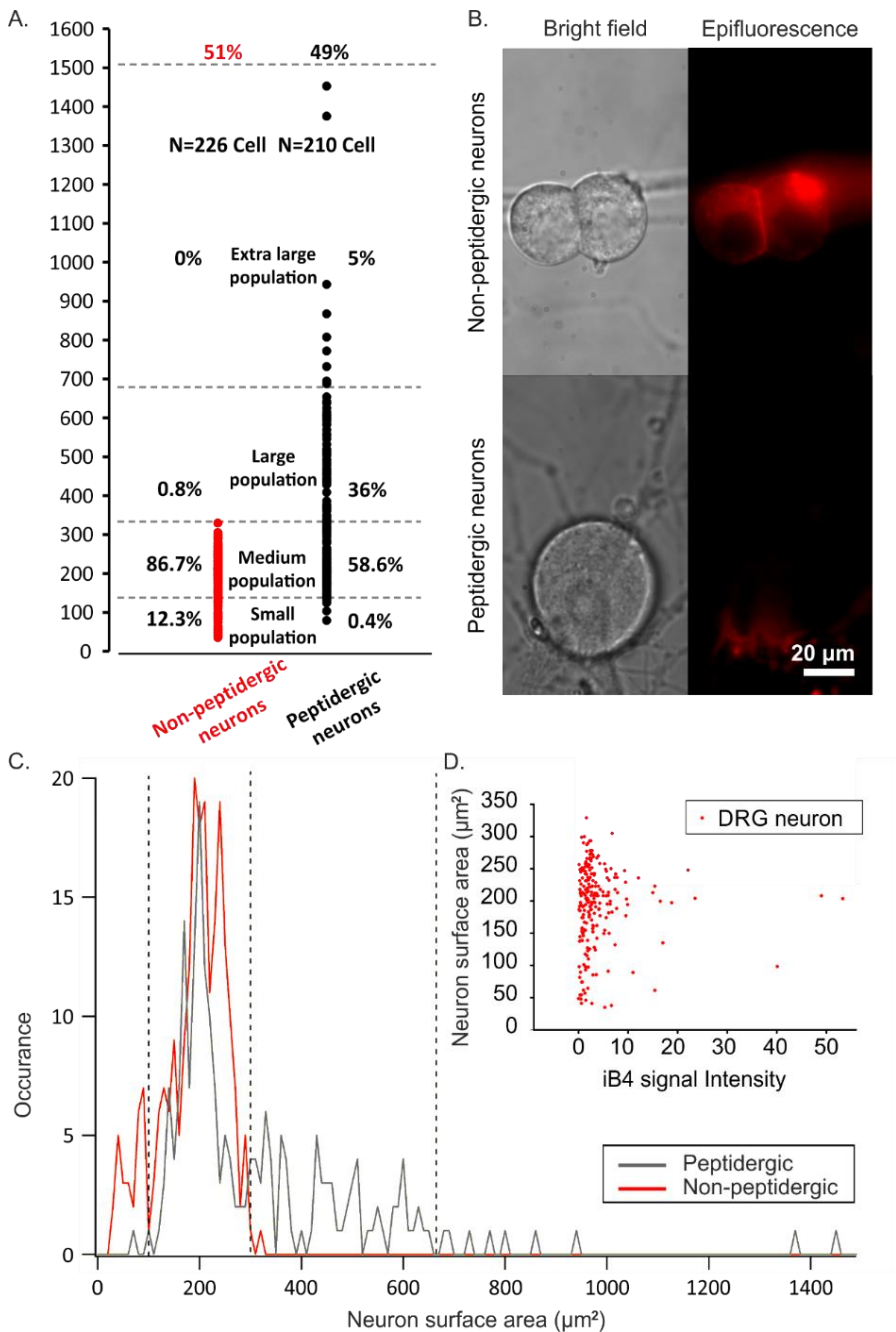


Figure 49 Percentage of peptidergic and non-peptidergic DRG neurons.

<sup>34</sup> Neurokinin-1 receptor for substance P, is a G protein coupled receptor that is a product of TACR1 gene and found in CNS and PNS (Takeda et al., 1991).

<sup>35</sup> Tyrosine Kinase B receptor that has high specificity to BDNF.

<sup>36</sup> Neurofilament-200 is anti-heavy neurofilaments of around 200-220 kDa that are major component of neuronal cytoskeleton.

## RESULTS

---

global marker to label all peptidergic neurons (Ishikawa et al., 2005; Pierce et al., 2006; Second von Banchet et al., 2002). Non-peptidergic neurons are collectively labelled by isolectin B<sub>4</sub> (Hunt and

**Continuing figure 49...** (A). Cultured WT DRG neurons were fixed with 4% PFA and stained against Isolectin receptor using GS-iB<sub>4</sub> coupled to Alexa-561 and incubated for 1 hr. Fixed cells were imaged using confocal microscopy and cells were counted and screened against positive and negative staining. Positively stained cells are non-peptidergic neurons and the unstained cells are the peptidergic DRG neurons. N = 436 cells were imaged from two DRG neuron cultures. (B) Representative images showing in the upper panel two positively medium-sized stained non-peptidergic neurons imaged at 561 nm laser and in the lower panel, one larger DRG peptidergic neuron that is not stained. (C) Occurrence of DRG neuronal subpopulations versus neuron surface area. (D) Plot of the signal intensity of iB<sub>4</sub> positive neurons against their surface area, N = 226.

Mantyh, 2001; Molliver et al., 1997; Stucky and Lewin, 1999; Wang and Zylka, 2009; Woolf and Ma, 2007) according to the protocol that was described by Kubo et al. (2012). Because iB<sub>4</sub> can be applied to living cells, we chose this method to identify different neuron subtypes while carrying out physiological experiments. To characterize DRG neuronal populations, two adult mice preparations were fixed after 7 DIV with 4% PFA and stained with iB<sub>4</sub>. Extensive washing steps were applied with the addition of iT-FX image enhancer. To account for the high diversity of neuronal populations, about 436 cells were imaged using confocal microscope. The acquisition parameters were set in such a way to increase the signal-to-noise ratio with 1 AU pinhole, low digital gain and 2% laser power. Results showed that 49% of the DRG neurons in culture are peptidergic neurons and 51% are non-peptidergic neurons. The peptidergic neurons were mainly of medium, large and extra-large sized population while non-peptidergic neurons were of medium and small size (Figure 49 A & B). The two subtypes were grouped according to size (Figure 44 C). We further investigated whether there is a correlation between the strength of iB<sub>4</sub> and the size of DRG neurons. The fluorescence intensity of iB<sub>4</sub>-positive cells were plotted against the size in Figure 44 D, and the results suggest that there is no correlation. Now that we were able to group these cells according to peptidergic and non-peptidergic classes, we screened for CAPS isoforms among these two subpopulations and checked whether they have a preferential localization.

### III.6 CAPS Isoforms Localization in DRG Neuron Subtypes

CAPS isoforms were localized to DRG neurons subtypes using ICC experiments involving primary antibodies against CAPS1 and CAPS2.



### III.6.1 CAPS1 Isoform Localization into DRG Subtypes

To localize CAPS1, experiments to ensure the specificity of a new commercial anti-CAPS1<sup>37</sup> antibody were carried out involving WT cells that were compared to CAPS1 KO cells (*Appendix VI.2*). WT DRG neurons were fixed with 4% PFA for 20 min and stained against CAPS1 together with iB<sub>4</sub> labelling. Image stacks were acquired using a confocal microscope with 2% laser intensity for both 488 and 561 nm wavelength and 500 digital gain. Taking a stack helps in judging whether the neuron is peptidergic or not, because some red processes from non-peptidergic neurons were wrapped around the base of other neurons, falsifying the identification. A non-peptidergic neuron should be entirely outlined with the red signal from the base to its top. CAPS1 fluorescence intensity was analysed in iB<sub>4</sub> positive and negative neurons. Results indicate that CAPS1 is distributed randomly across peptidergic and non-peptidergic neurons. Nevertheless, some peptidergic DRG neurons showed brighter CAPS1 fluorescence but it didn't impact significantly the average fluorescence when compared to the non-peptidergic neurons (Figure 50). To further characterize CAPS1 localization in peptidergic neurons subtypes, we stained DRG neurons against NK-1r and TRKB receptor together with anti-CAPS1. The fluorescence intensity of CAPS1 was quantified and we compared it between cells that expressed NK-1r or not. CAPS1 expression was

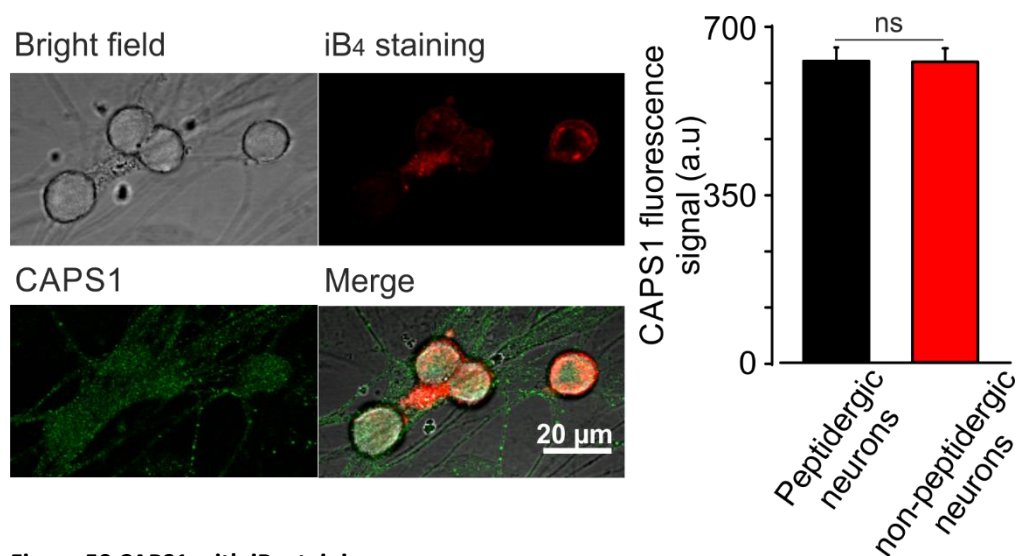


**Figure 50 CAPS1 with iB<sub>4</sub> staining.**

Embryonic WT DRG neurons were fixed with 4% PFA for 20 min then stained against CAPS1 (1:1000) and iB<sub>4</sub>-Alexa 561. The left panel shows confocal images of DRG neurons in bright field, 561, 488 nm and all 3 channels merged. The graph to the right shows CAPS1 fluorescence intensity in peptidergic and non-peptidergic DRG neurons. N = 2 animals. N = 118 cell. Mann Whitney significance test was applied, ns p > 0.05. All error bars are SEM.

<sup>37</sup> Polyclonal rabbit anti-CADPS1 antibody from Synaptic Systems, cat. no. 262 013

## RESULTS

significantly higher in NK-1r positive cells (Figure 51 A). The same analysis was done for TRKB positive cells and there was no significant preferential localization of CAPS1 to this subtype of peptidergic neurons (Figure 51 B). About 22.7%<sup>38</sup> of adult DRG neurons are NK-1r positive (Hall et al., 1997; Tuchscherer and Seybold, 1985), this probably explains why there is no significant difference of CAPS1 expression levels among peptidergic and non-peptidergic neurons. Next we examined CAPS2 distribution among different DRG subtypes.

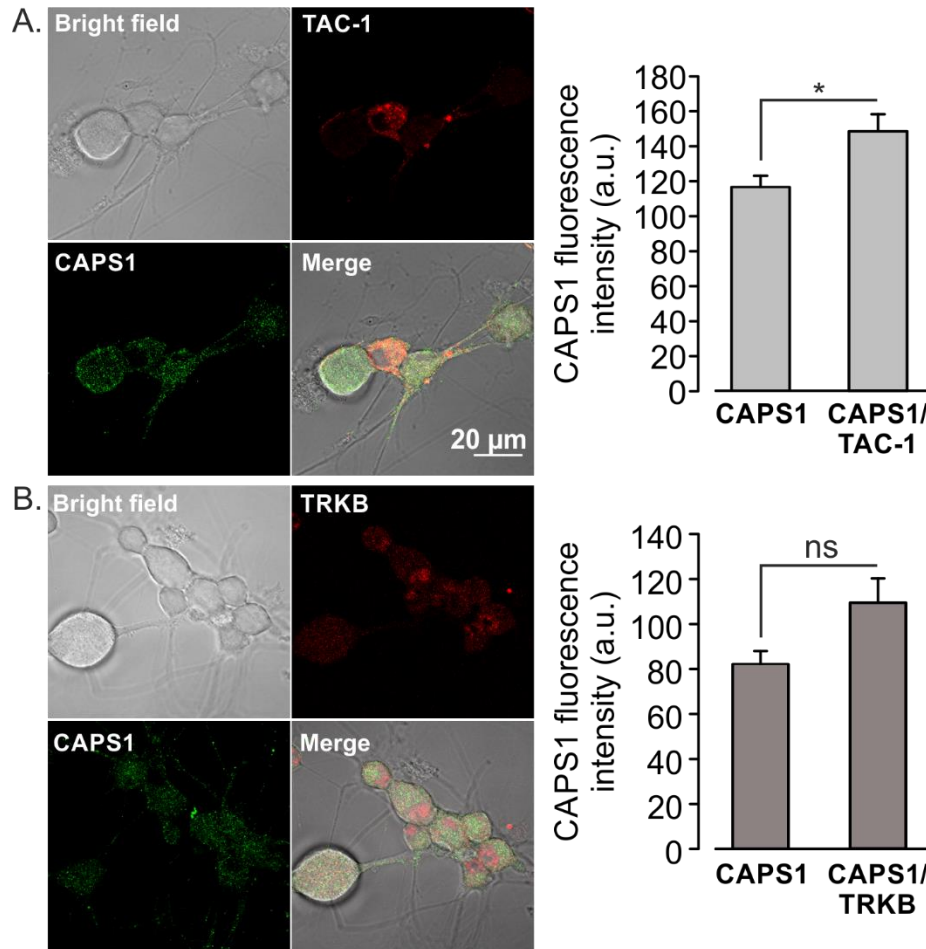


**Figure 51 CAPS1 localization into peptidergic neurons.**

Embryonic WT DRG neurons were fixed with 4% PFA for 20 min then stained against CAPS1 and stained either against TAC-1, which is an antibody recognizing NK-1 receptors, or TRKB. (A) The left panel shows confocal images for DRG neurons in bright field, 488, 561 nm and all 3 merged channels of CAPS1 and TAC-1 staining. N = 2 animals, n = 92 cells. The graph to the right quantifies CAPS1 fluorescence intensity in TAC-1 positive and negative neurons. (B) The right panel shows confocal images of DRG neurons in bright field, 488 nm, 561 nm and all 3 channels merged. The graph to the right shows CAPS1 fluorescence intensity in TRKB positive neurons compared to TRKB negative neurons. N = 2 animals, n = 34 cells. Mann Whitney significance test was applied, ns p > 0.05. \* p < 0.05. All error bars are SEM.

<sup>38</sup> 13.5% ± 1.9 SEM of all E19.5 DRG neurons express substance P, this fraction gets bigger as the mice develop in age (Hall et al., 1997).

## III.6.2 CAPS2 Isoform Localization into DRG Subtypes

DRG neurons were co-stained against CAPS2 and iB<sub>4</sub>. Images were acquired in similar fashion as the previous experiment. There was a striking difference in CAPS2 localization, for instance, its fluorescence signal was four times higher in peptidergic neurons compared to non-peptidergic neurons (Figure 52). Almost 80% of peptidergic neurons expressed CAPS2. Based on our previous data that indicate that CAPS2 is found in half of DRG neurons, this experiment accordingly states that this 50% are the peptidergic neurons. To further verify and strengthen these findings, we co-stained neurons against CAPS2 and anti-NK-1r or anti-TRKB. The percentage of NK-1r expressing cells in vitro was  $\sim 25\% \pm 0.5$  SEM (Figure 53 A), which was very close to the endogenous in vivo expression levels (Hall et al., 1997). Of those neurons that were positive for NK-1r, 60% expressed CAPS2 (Figure 53 B). About 60% of peptidergic neurons were TRKB positive (Figure 53 A) of which 80% expressed CAPS2 (Figure 53 B). This data set reinforces the idea that CAPS2 expression is restricted to peptidergic neurons and led us to hypothesize that the 50% LDCV stimulated secretion profile observed in WT neurons might be regulated by CAPS2 that is found in  $\sim 50\%$  of DRG neurons. The next experiments were designed to investigate this possibility.

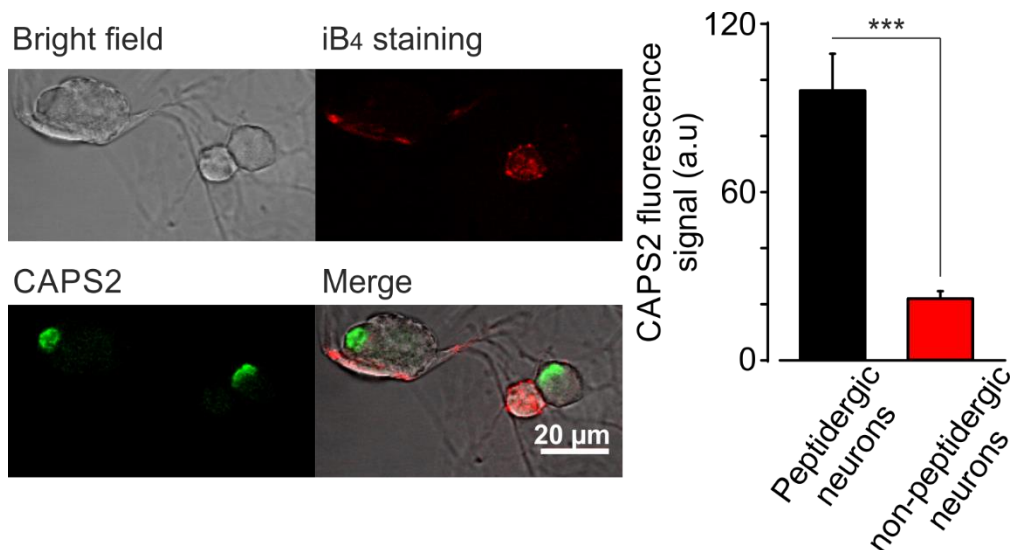


**Figure 52 CAPS2 with iB<sub>4</sub> staining.**

Embryonic WT DRG neurons were fixed with 4% PFA for 20 min then stained against CAPS2 and iB<sub>4</sub>-Alexa 561. Alexa 488 secondary goat anti-rabbit antibody was used against CAPS2 antibody. The left panel shows confocal acquired images of DRG neurons in bright field, 561, 488 nm and merged channels. The graph to the right shows CAPS2 fluorescence signal distribution among peptidergic and non-peptidergic DRG neurons. N = 2 animals, n = 57 cells. Mann Whitney significance test was applied, n\*\*\* p < 0.001. All error bars are SEM

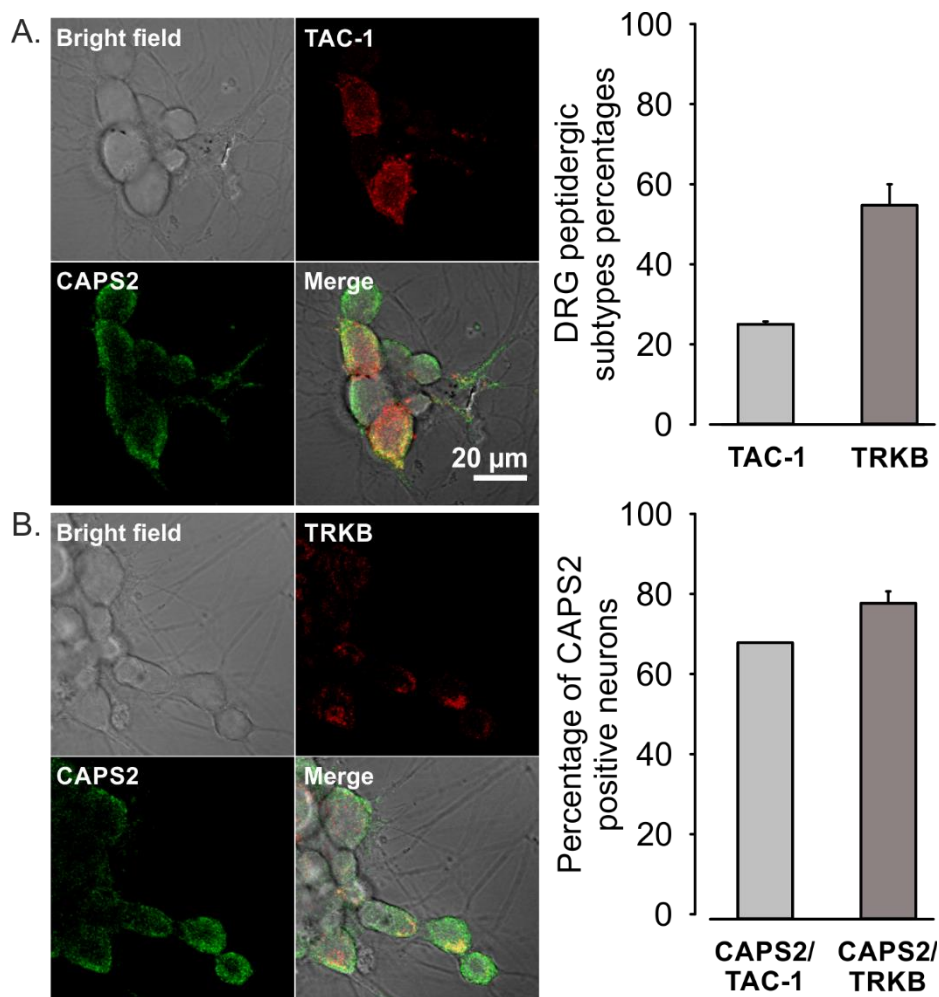


**Figure 53 CAPS2 localization into peptidergic subtypes neurons.**

Embryonic WT DRG neurons were fixed with 4% PFA for 20 min then stained against CAPS2 and stained either against TAC-1 or TRKB. (A) The left panel shows confocal images for DRG neurons in bright field, 488, 561 nm and all 3 channels merged of CAPS2 and TAC-1 staining. The graph on the upper right shows the percentages of DRG neurons that are either TAC-1 or TRKB positive neurons. N= 2 animals, n = 156 cells for TAC-1 and n = 95 cells for TRKB. (B) The lower left panel shows confocal images for DRG neurons in bright field, 488, 561 nm and all 3 channels merged of CAPS2 and TRKB staining. The graph on the lower right shows the percentage of CAPS2 positive neurons of TAC-1 or TRKB subtype. N = 2 animals, n = 34 for TAC-1 and n = 53 cells for TRKB. All error bars are SEM.

## III.7 LDCV Secretion in Peptidergic and Non-Peptidergic Neurons

To verify our hypothesis we assessed which neuron subtype can secrete LDCVs. We took advantage of the fact that iB<sub>4</sub> stains living cells without affecting their physiological properties and measured LDCV release from peptidergic and non-peptidergic neurons.

### III.7.1 CAPS2 Mediates LDCV Secretion

DRG neurons from two week old WT mice were transfected with NPY-Venus and labelled with iB<sub>4</sub> according to the previously described protocol (Figure 54 A). Cells were washed with warmed extracellular solution at 34 °C. LDCV secretion was recorded in TIRFM dual-view setting which was necessary to eliminate spectral overlaps coming from the bright signal of Alexa-561

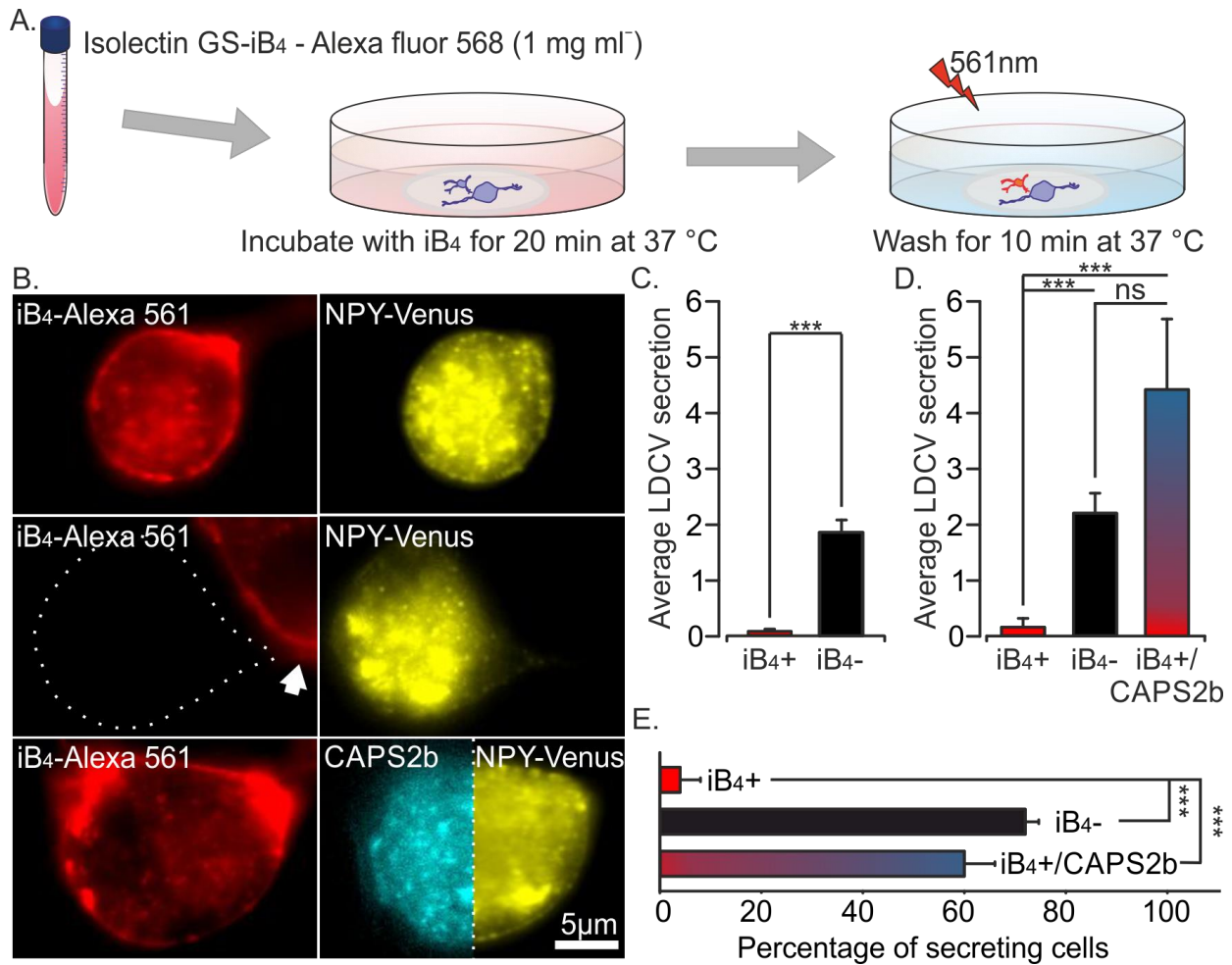


**Figure 54 Examining secretion in peptidergic and non-peptidergic DRG neuron subpopulations.**

(A) Schematic diagram explaining iB<sub>4</sub>-Alexa 568 staining of DRG neurons. Cells are incubated in extracellular solution in the presence of 1 mg.ml<sup>-1</sup> of iB<sub>4</sub>-Alexa 568 for 20 min at 37 °C then washed for 10 min with continual perfusion. iB<sub>4</sub>+ neurons were visualized with 561 nm laser. (B) Imaging of iB<sub>4</sub> positive non-peptidergic unmyelinated DRG neurons. The top panels show a non-peptidergic DRG neuron transfected with NPY-Venus while the middle panels show a peptidergic neuron, outlined with white dotted line, the white arrow points out an adjacent non-peptidergic DRG neuron. The bottom panel shows a non-peptidergic DRG neuron co-expressing NPY-Venus and CAPS2b-mTFP. (C) Average LDCV secretion in iB<sub>4</sub>+ non-peptidergic neurons (N = 4, n = 34) compared to iB<sub>4</sub>- peptidergic neurons (N = 4, n = 30). (D) Average LDCV secretion of iB<sub>4</sub> non-peptidergic DRG neurons overexpressing CAPS2b (N = 3, n = 20) compared to iB<sub>4</sub>+ non-peptidergic (N = 3 n = 19) and iB<sub>4</sub>- peptidergic neurons (N = 3, n = 14). (E) Percentage of iB<sub>4</sub> non-peptidergic DRG neurons overexpressing CAPS2b secreting cells compared to iB<sub>4</sub>- iB<sub>4</sub>+ DRG neurons. 2 weeks old mice were used for these experiments. Error bars in (C, D & E) are SEM and \*\*\*p < 0.001 Mann Whitney test; \*\*\*p < 0.001 one way ANOVA; \*\*\*p < 0.001 one way ANOVA, respectively.

that is coupled to the isolectin product. Measurements from four cultures showed that LDCV secretion occurs almost exclusively in peptidergic neurons. Out of 34 non-peptidergic recorded neurons only 2 cells secreted. We then overexpressed CAPS2b in WT adult DRG neurons and repeated the previous experiment and we measured LDCV secretion from non-peptidergic transfected neurons. All of the sudden, these silent cells started to secrete (Figure 54 D) and the percentage of secreting cells elevates from almost nil to 60% (Figure 54 E). Although, non-peptidergic neurons express CAPS1, it seems the presence of this isoform is not sufficient to allow LDCV secretion. Therefore, CAPS2 is required for the priming of LDCV secretion from the soma of WT DRG neurons.

### **III.8 Establishing DRG/S neuron Co-Culture**

In order to assess the function of CAPS isoforms in mediating synaptic transmission, we established DRG/S neuron co-culture. DRG neurons do not form autaptic synapses, neither in vivo nor in cultures (Ransom et al., 1977a). DRG neurons that are located outside the spinal cord, form synapses with S neurons by extending their axons mainly to the dorsal horn neurons (Barber and Vaughn, 1986; Zeilhofer et al., 2012) and to lesser extent the large axons are extended to the ventral horn neurons (Molander and Grant, 1987). The establishment of this sophisticated co-cultures involved extensive optimization to enhance cell survival and synapse formation rate in vitro.

#### **III.8.1 DRG/S neuron Survival in Vitro**

The first challenge was to maintain S neurons living in culture along with DRG neurons. Initially it was difficult to keep S neurons in culture for longer than four days but changes in the culture conditions helped keep S neurons alive for at least nine days in vitro (Figure 55). Neurons grew processes which was an indication that they are in good health condition. We then tested whether these neurons form synapses in vitro under these culture preparation conditions.



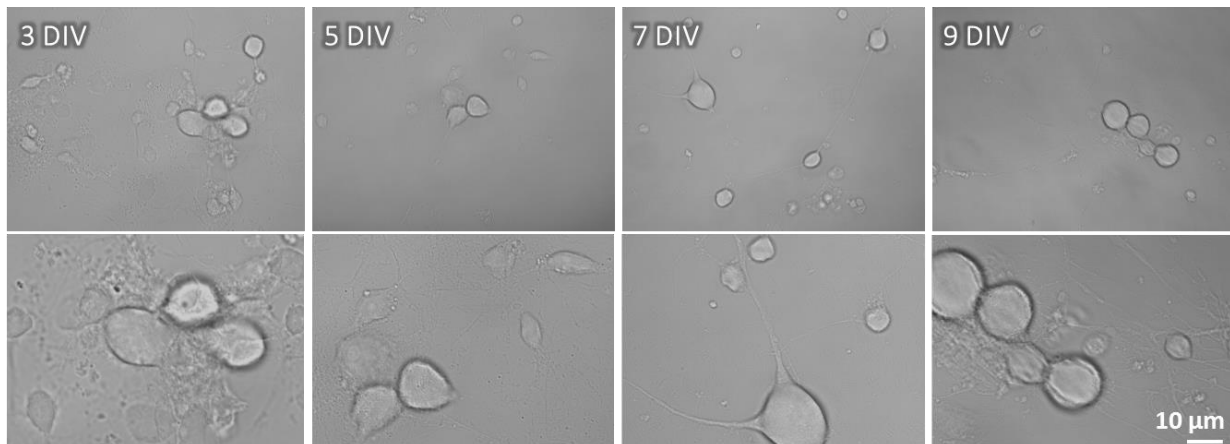


**Figure 55 DRG/S neuron co-cultured neurons morphology over time.**

WT DRG neurons were co-cultured with WT S neurons in culture. Morphology and health state of these cells were monitored at DIV 3, 5, 7 and 9 using confocal microscope.

### III.8.2 Synapses Form between DRG and S neurons<sup>39</sup>

To check whether synapses do form in vitro, Mr. Ali Harb performed preliminary experiments in which DRG neurons were co-cultured with S neurons and kept in culture for four days. The co-cultured neurons were fixed with 4% PFA and stained against MAP-2 to mark neurons (Caceres et al., 1986; Fischer et al., 1986) and synaptophysin to mark synapses between neurons (Jahn et al., 1985; Regnier-Vigouroux et al., 1991; Wiedenmann et al., 1985). The red spots opposing the S neuron suggest that synapses start forming between the two types of neurons at day four in vitro (Figure 56). This experiment confirmed that synapses form but whether these synapses are functional remained unknown.

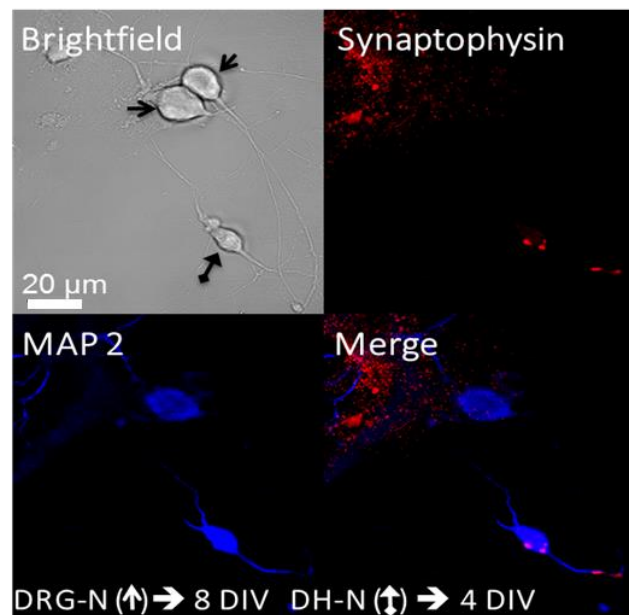


**Figure 56 Marking synapses between DRG neurons and S neurons.**

WT DRG/S neuron culture were fixed with 4% PFA and stained as MAP-2 (1:1000) shown in blue and against synaptophysin (1:1000) shown in red. The upper two arrows on the bright field image indicate a DRG neuron while the lower arrow points to S neuron. The red dotted staining on the S neuron soma and neurite are synapses formed between DRG and spinal neurons.

<sup>39</sup> This experiment was carried out by Mr. Ali Harb during his Masters II.

### III.8.3 Synapses are Functionally Connected<sup>40</sup>

To investigate synapse functionality, field electrode stimulation was ruled out as it would stimulate all cells in proximity. Taking advantage that some DRG neurons are touch sensitive through specialized mechanoreceptors (Abraira and Ginty, 2013; Lumpkin and Bautista, 2005); co-cultured DRG/S neuron were loaded with Fluo 4 AM and DRG neurons were mechanically stimulated in hope that they would have mechanoreceptors which respond to the stimulus. After several trials, we were able to find one

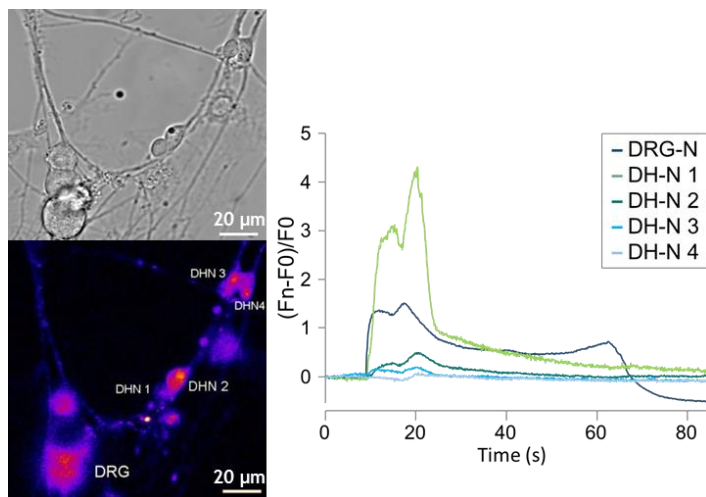


**Figure 57 DRG/S neuron Synapses are functional.**

DRG/S neuron co-cultured cells were loaded with Fluo 4 AM. One DRG neuron was poked with glass pipette to depolarize the cells and induce an increase of the intracellular calcium concentration. The bright field image shows One DRG neuron and next to it our smaller dorsal horn neurons (DHN). The graph on the right displays the change in Fluo4 fluorescence intensity over time.

DRG neuron that responded first steep increase in Fluo 4 fluorescence. In contrast, the S neurons displayed a delayed answer to the stimuli indicating that they were not directly activated by the touch but instead received their input over synaptic transmission from the DRG neurons (Figure 57). Attempts to directly mechanically stimulate S neurons were unsuccessful (data not shown). Therefore we conclude that DRG neurons form functional synapses with S neurons in our culture conditions. To further understand the development of the synapses, we did an extensive study involving hundreds of cells and counting thousands of synapses to understand when these synapses start to form in our co-culture conditions.

### III.8.4 Characterizing Synapses over Time

DRG neurons of Synaptobrevin-mRFP knockin (Matti et al., 2013) were co/cultured with WT S neurons and fixed with 4% PFA for ten minutes instead of the usual twenty minutes to maintain the synapses integrity. The SybKI signal allowed tracing of the processes back to DRG neurons and distinguish them from S neurons. The co-cultured neurons were stained against bassoon to label presynapses (Brandstatter et al., 1999; Richter et al., 1999; tom Dieck et al., 1998)

<sup>40</sup> This experiment was carried out by Dr. Ute Becherer.



## RESULTS

---

and PSD95<sup>41</sup> to label postsynapses (Cho et al., 1992; Hunt et al., 1996). Co-cultured neurons were fixed and stained at different time point and synapses were counted (Figure 58 A). We counted two types of synapses, those that we called mature synapses that included all three signals from SybKI, Bassoon and PSD95 and non-active synapses that encompass the signal of bassoon and PSD95 near a process that is labelled with SybKI signal. Analysing thousands of synapses, showed that mature synapses start to form at day three in vitro and increase as they stay longer while immature synapses number remain the same. As the cells grow older in culture, DRG neurons tend to survive but S neurons number declines (Figure 58 B). Next, we wanted to understand where these synapses are located. In automated fashion, we measured the distances from individual synapses on processes back to DRG neurons and S neurons (Figure 58 C). Synapses form in significantly closer proximity to S neurons compared to DRG neurons. Thus, TIRFM recordings should be performed closer to S neurons to pick up synaptic activity (Figure 58 D). To further ensure a good quality of the culture, we made sure that the density of astrocytes remained consistent. This experiment enabled us to firmly control the parameters of establishing synapses between DRG and S neurons. To achieve a count of 80 synapses per 0.5 mm<sup>2</sup>, an average number of 3.5 DRG neurons, 5 S neurons and 3.6 astrocytes are needed per 0.5 mm<sup>2</sup> that should be maintained in culture for 9 DIV. Now that synapses between DRG and S neurons are fully controlled in our co-culture settings, studying CAPS isoforms effect on synaptic transmission became feasible.

---

<sup>41</sup> Post synaptic density 95

# RESULTS

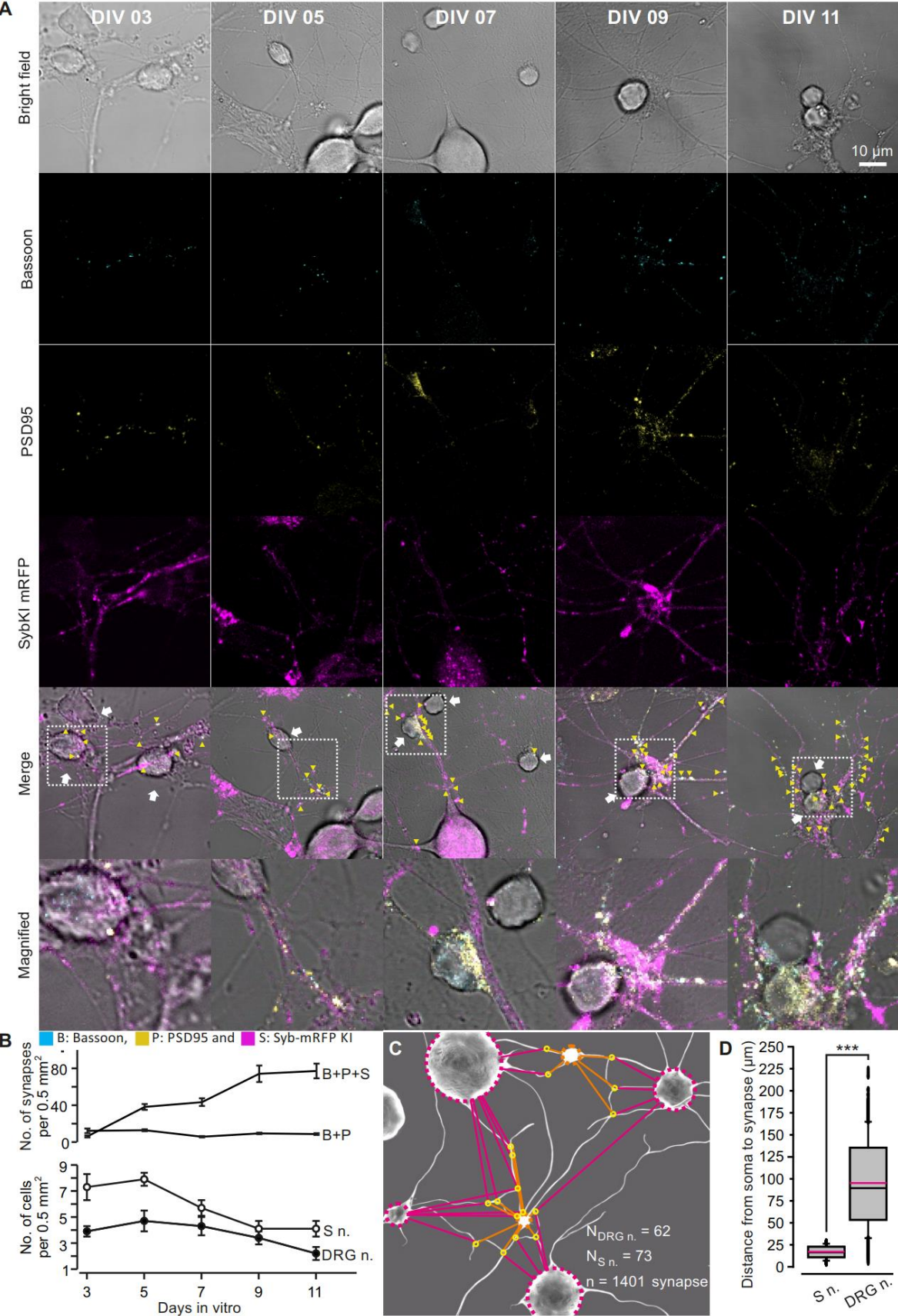


Figure 58 Synapse formation over time.

## RESULTS

---

**Continuing Figure 58...** Co-cultured Synaptobrevin-mRFP Knock-In (SybKI) DRG neurons with WT S neurons were fixed with 4% PFA at DIV 03, 05, 07, 09 and 11. To identify fully functional synapses, neurons were stained against presynaptic marker Bassoon and postsynaptic marker PSD-95. Synaptobrevin-mRFP in DRG neurons allowed the identification of heterotypic synapses that were formed between DRG and S neurons and not homotypic synapses in between two S neurons.

(A) From top to bottom bright field and confocal images of Bassoon (cyan), PSD-95 (yellow) and SybKI (magenta) labelling. The fifth row of images corresponds to the overlay of all 4 channels. White arrows point at S neurons and yellow arrows indicate synapses in which Bassoon, PSD-95 and SybKI signals co-localize. The last row is a magnified portion of the images row 5 delineated by a stippled line. (B) Synapses in which Bassoon, PSD-95 and SybKI signal co-localized (top), as well as DRG and S neurons (bottom) were counted manually and plotted against the number of DIV. The data was normalized to the acquired surface area. (C) Schematic representation of the analysis method used to measure the distance from each heterotypic synapse to the nearest DRG and S neuron cell body of neurons that were maintained for 9 days in co-culture. (D) Box plot of the distance between heterotypic synapses and neuronal cell bodies at DIV 9. Pink and black lines in the box correspond to the average and median distances, respectively. Note that heterotypic synapses were preferentially formed closer to S neurons than to DRG neurons. The data originated from two separated cultures. In total DRG neurons were isolated from 2 adult mice while S neurons were isolated from 12 P0 mice. Several DRG and S neurons were analyzed and hundreds of synapses were counted: DIV 03,  $n_{\text{DRG neurons}} = 75$ ,  $n_{\text{S neurons}} = 139$  and  $n_{\text{synapses}} = 286$ ; DIV 05,  $n_{\text{DRG neurons}} = 84$ ,  $n_{\text{S neurons}} = 157$  and  $n_{\text{synapses}} = 258$ ; DIV 07,  $n_{\text{DRG neurons}} = 82$ ,  $n_{\text{S neurons}} = 109$  and  $n_{\text{synapses}} = 845$ ; DIV 09,  $n_{\text{DRG neurons}} = 62$ ,  $n_{\text{S neurons}} = 73$  and  $n_{\text{synapses}} = 1401$  and DIV 11,  $n_{\text{DRG neurons}} = 31$ ,  $n_{\text{S neurons}} = 58$  and  $n_{\text{synapses}} = 1120$ . A total of 343 DRG neurons, 536 S neurons and 4704 synapse were counted.

### III.9 CAPS1 Localization at Synapses

CAPS2 is present in half of the DRG neuronal population and is responsible for the secretion of LDCVs in these neurons. We speculated that CAPS1 play an essential role in mediating synaptic transmission. If CAPS1 is involved in synaptic transmission by promoting priming of synaptic vesicles in DRG neurons then CAPS1 should be localized to synapses. To test this hypothesis, we performed an immunostaining of the DRG/S neuron co-culture with anti CAPS1 antibody and anti synaptophysin which is specifically localized to synapses (Jahn et al., 1985; Regnier-Vigouroux et al., 1991; Wiedenmann et al., 1985). To avoid confounding results, the culture included DRG neurons that were isolated from WT mice and S neurons that were isolated from CAPS dKO mice (Figure 59 E). With this configuration a co-localisation of both proteins can only occur at heterologous synapses formed between DRG and S neurons and not at inter S neuron synapses. Figure 59 A shows that CAPS1 is aggregating at discrete spots along the neurites partially co-localizing with synaptophysin. The co-localization analysis with Manders coefficient showed that a large fraction of CAPS1 is not localized to synapses (Figure 59 B) but rather that it was spread along the neurites. Additionally, only about 40% of synaptophysin is localized to CAPS1 because more than 60% of synapses were formed in between S neurons inherently devoid of

## RESULTS

CAPS (Figure 59 C). This indicates that nearly all synapses between DRG and S neuron contained CAPS1. Furthermore, CAPS1 fluorescence signal was 2.5 fold higher at synapses in comparison to extra synaptic regions (Figure 59 D, F). Therefore, CAPS1 is not only localized to but also enriched at synapses suggesting a possible role in synaptic transmission.

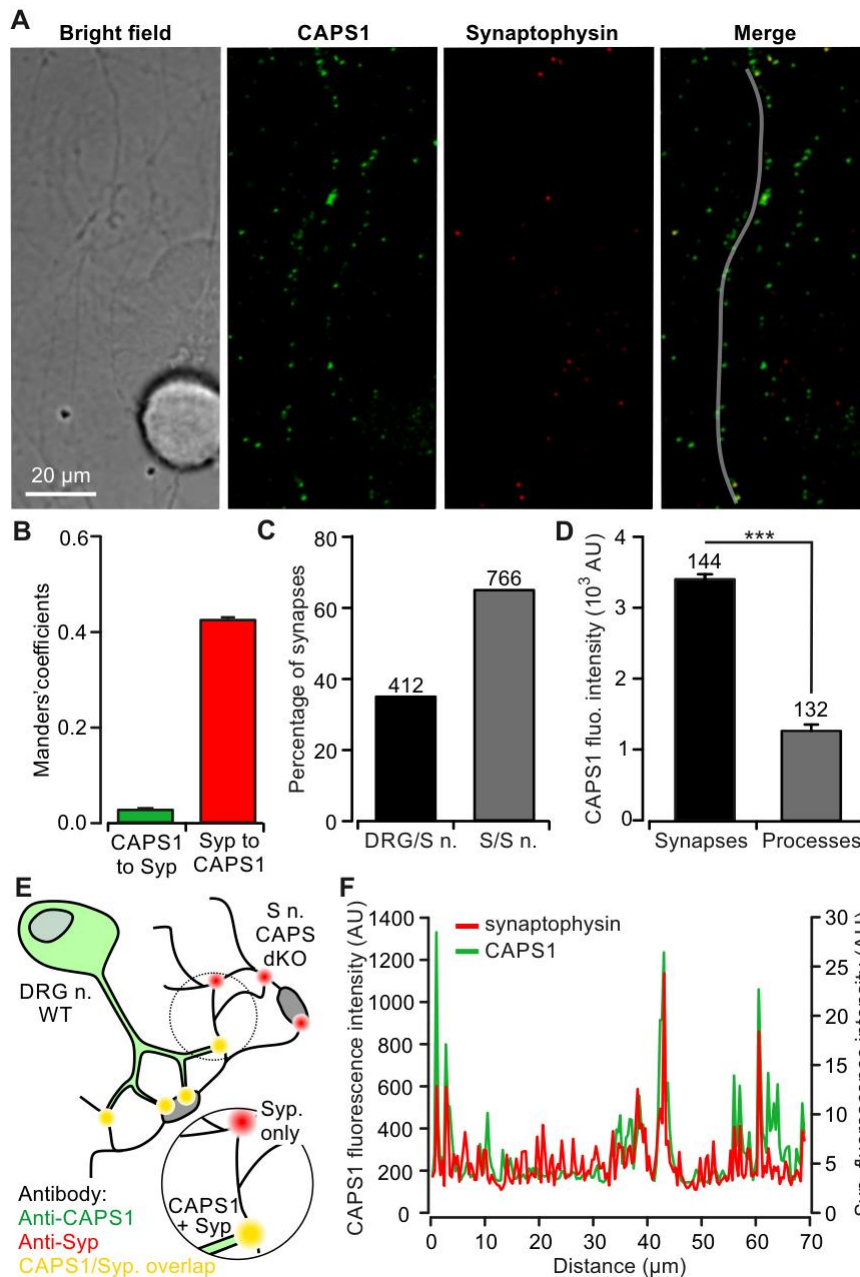


**Figure 59 CAPS1 colocalization at synapses in co-cultured DRG/S neuron.**

(A) Co-cultured P0 WT DRG neurons with E18 CAPS dKO S neurons that were fixed with 4% paraformaldehyde at DIV 7 and stained with antibodies directed against CAPS1 and synaptophysin. This culture condition ensured that CAPS1 labelling would be exclusively localized to DRG and not S neurons. (A) From left to right bright field, and confocal maximal intensity projected images (MIP) of CAPS1 (green) and synaptophysin (red) labeling. The last panel depicts the overlay of both confocal channels. (B) Graph showing Manders' coefficients of CAPS1 positive pixels co-localizing with synaptophysin or of synaptophysin positive pixel co-localizing with CAPS1 in green and red, respectively. (C) Percentage of heterotypic synapses between DRG/S neurons compared to homotypic S/S neurons. A total of 1178 synapse were analyzed, 412 where heterotypic while 766 were homotypic. (D) Average fluorescence intensity of CAPS1 labeling measured at 144 synapse and 135 nearby positions on the DRG neuron neurites. (E) Schematic



### III.10 Measuring Synaptic Transmission via V-GLUT mNectarine

We initially decided to measure synaptic transmission by tagging VGLUT with a pH sensitive fluorescent protein. Fusion of fluorescent protein with synaptic vesicle associated proteins like, synaptophysin, Synaptobrevin, synaptotagmin and VGLUT is a common procedure to measure synaptic vesicle fusion (Miesenbock et al., 1998; Sankaranarayanan and Ryan, 2000). We were limited in the choice of the options of fluorescent proteins because CAPS was tagged with mTFP and NPY with Venus so we selected the pH sensitive mNectarine (Johnson et al., 2009). The mNectarine was cloned to the N-terminal part of VGLUT so that it faces the luminal side of the vesicle (See *Appendix VI.4*). Because of its pH sensitive characteristics, mNectarine signal was not visible at all in acidic environment of vesicles. This was one major disadvantage, because we would not know which cells were transfected. Measurements would be carried blindly, hoping that the cell was

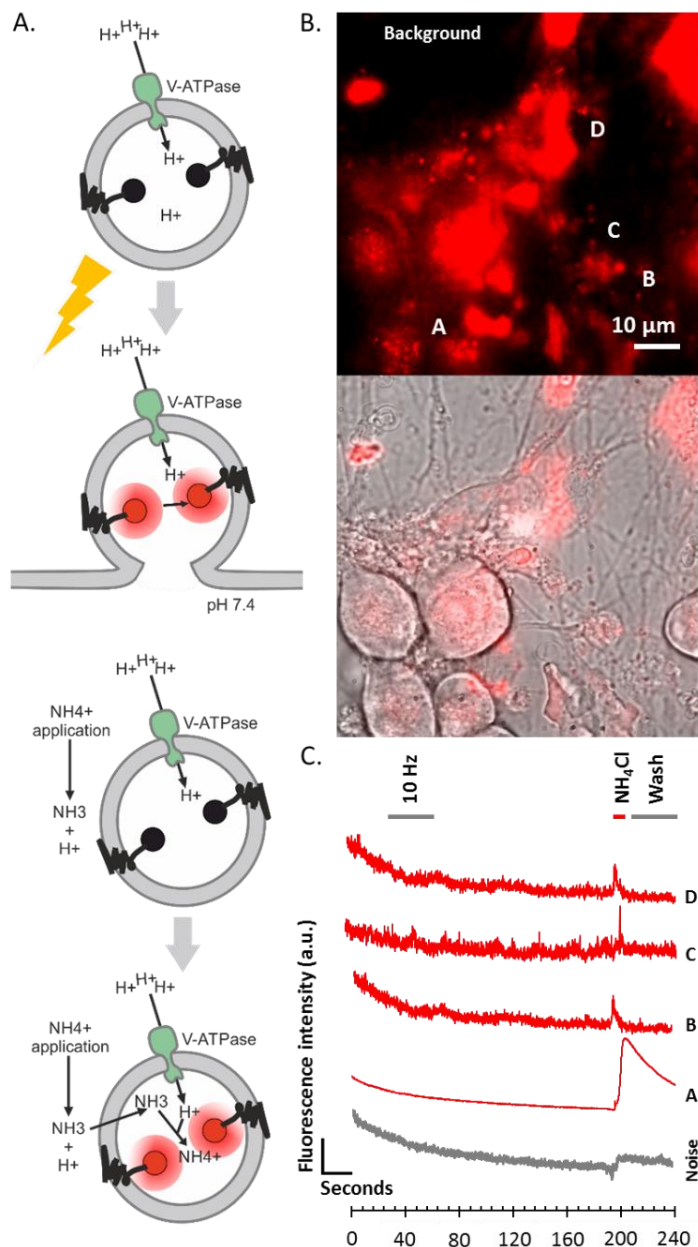


**Figure 60 Measuring synaptic transmission with vGlut-mNectarine.** (A) Vesicles that are labelled with vGlut-mNectarine shows no fluorescence but once secretion is induced, pH elevates pushing the mNectarine to fluoresce. Upon NH<sub>4</sub>Cl application, NH<sub>3</sub> goes inside vesicles chelating proton ions and elevating pH inside the vesicles which pushes mNectarine to fluoresce serving as a method to reveal all synapses in transfected cells. (B) The first panel shows vGlut-mNectarine signal imaged at 561 nm laser and the second panel shows an overlay of the red channel with the bright field. (C) Measuring synaptic transmission in transfected cells after inducing secretion with 4 V at 10 Hz electrical stimulus. The graph displays the fluorescence intensity as a function of time.

## RESULTS

transfected. Then at the end of the experiment the cells were superfused with  $\text{NH}_4\text{Cl}$  to deprotonate the content of vesicles and reveal the transfected cells and synapses (Figure 60 A). The production of this virus passed through a year of optimization to enhance its transfection efficacy. It required a special bacteria to produce the DNA without unwanted genetic recombination. Stbl3 a chemically competent *E. coli* were designed for cloning huge plasmid DNA with direct repeats found in lentiviral expression vectors. This bacteria is used to reduce the frequency of homologous recombination of long LTRs and often yield ten folds higher DNA compared to the conventional DH5 $\alpha$  cells. Once transfected it was almost impossible to see the signal in transfected cells and it required high laser power which also increase autofluorescence (Figure 60 B). Cells were randomly stimulated and no clear response was evident as the noise was very high which made this measurements very complicated (Figure 60 C). One layer of complexity was unintentionally added to this set of experiments as we were trying to measure synaptic transmission at 5 DIV. We didn't know at that time the optimal time point to measure synaptic transmission. We eventually decided to drop this method and replace it by the well-established synaptophysin-pHluorin lentiviral driven expression system.

### III.11 Measuring Synaptic Transmission via Synaptophysin-pHluorin

SypHy held a major advantage over VGLUT-mNectarine because the signal is slightly visible in transfected cells (Royle et al., 2008). Upon vesicle fusion or  $\text{NH}_4\text{Cl}$  application and therefore pH elevation, an increase in fluorescence is recorded (Figure 61). SypHy has been established as a powerful tool to record synaptic transmission, as it has an excellent signal to noise ratio and high transfection efficacy<sup>42</sup>. Furthermore,

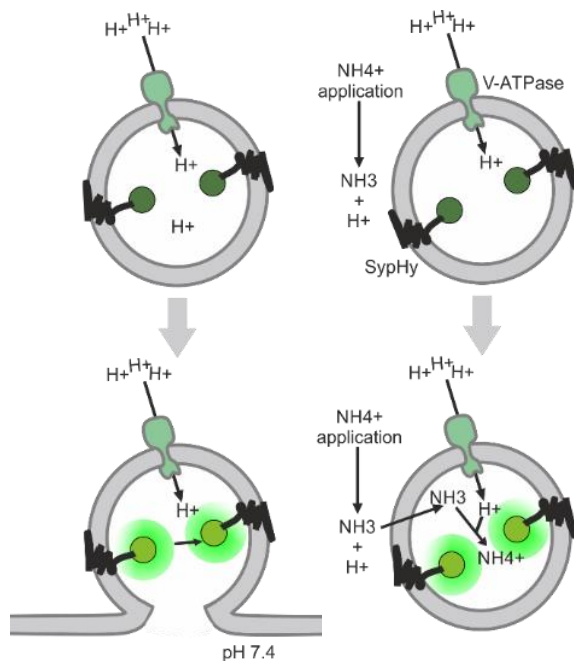


**Figure 61  $\text{NH}_4\text{Cl}$  mode of action on SypHy.**

SypHy is slightly fluorescent at acidic pH, once the vesicle fuses with the membrane, the pH elevates which increase the fluorescent of SypHy. Upon  $\text{NH}_4\text{Cl}$  application, the  $\text{NH}_3$  diffuses into the membrane and deprotonates the lumen of vesicles by binding the  $\text{H}^+$  ions inside hence achieving maximal SypHy fluorescence intensity.

<sup>42</sup> The transfection efficacy was about 70% in conventional means of virus production and this percentage is increased till +90% in ultra-centrifuged viral batches.

## RESULTS

its specificity of marking synaptic vesicles was well documented in the literature (Granseth et al., 2006; Kwon and Chapman, 2011; Li et al., 2011; Miesenbock et al., 1998; Royle et al., 2008). Stimulation protocols were extensively tested (see *Materials and Methods* chapter) and adjusted to evoke robust SV secretion with minimal possible stress to cells. We then used this methodology to test the effect of CAPS isoforms on synaptic transmission. We hypothesized that CAPS1 is preferentially localized to synapses because it is a priming factor of SV secretion.

### III.11.1 CAPS1 Mediates SV Secretion in DRG/S neuron Co-Culture

DRG neurons of WT, CAPS1 and 2 dKO, CAPS1 KO and CAPS2 KO genotypes were transfected with SypHy, co-cultured with WT S neurons and measured as previously described. Raw data of the exemplary measurements are displayed in figure 62. Individual synapses exhibited different maximal responses upon  $\text{NH}_4\text{Cl}$  application as shown in figure 57 B. For this reason we

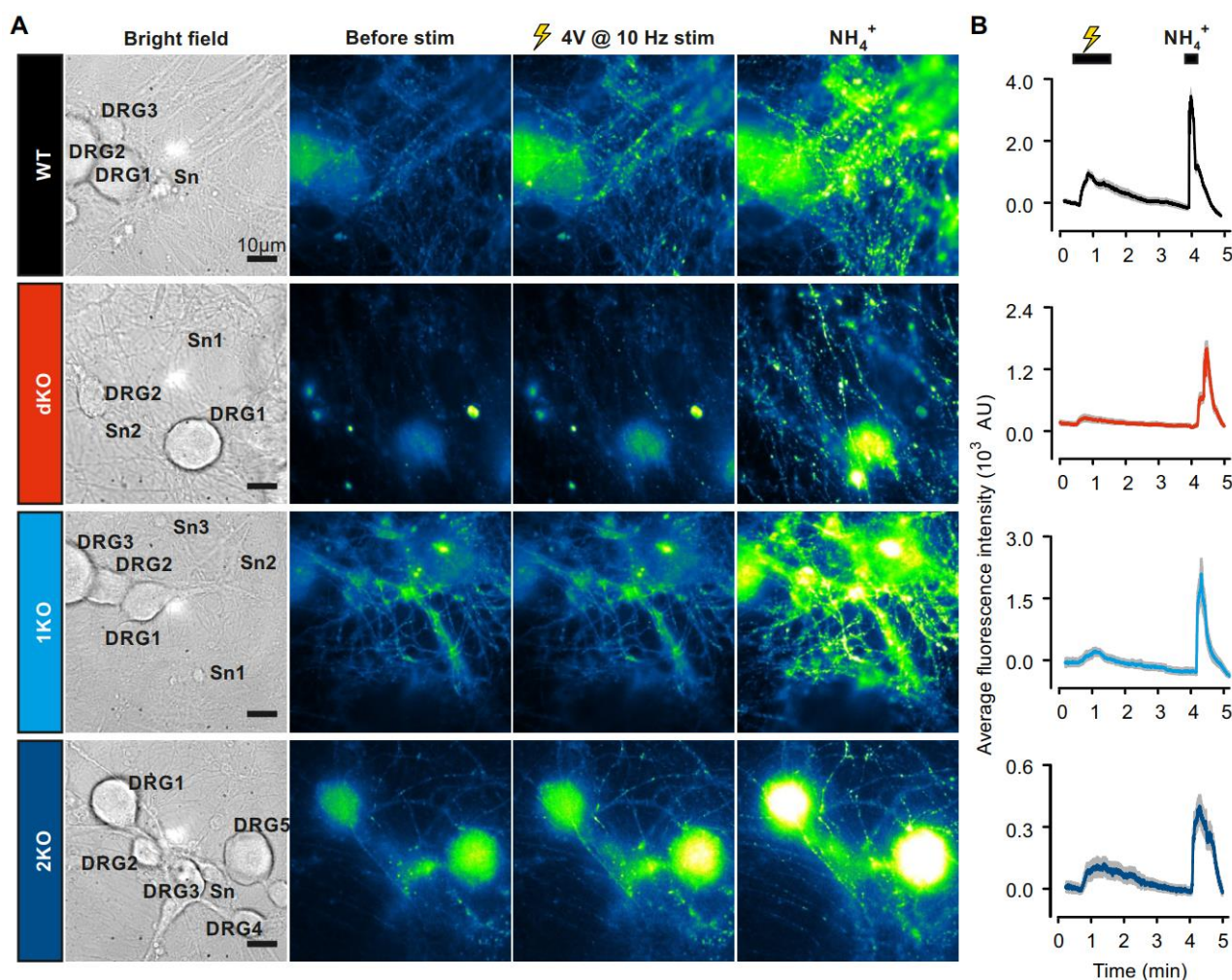
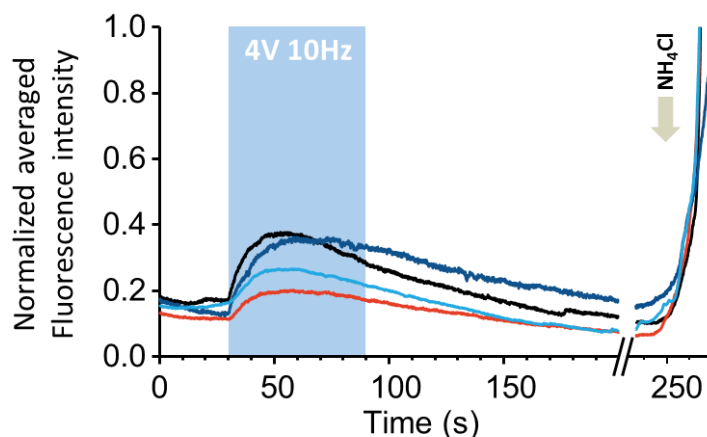


Figure 62 Exemplary traces of averaged synapses from individual recordings of DRG/S neuron co-cultures.

## RESULTS

**Continuing Figure 62...** (A) Embryonic DRG neurons of WT, dKO, 1KO or 2KO were co-cultured with WT S neurons. The first column consists of bright field images of the different co-cultures, the second column shows *semi*-TIRF images before applying the stimulus and the third column display the same cells after the stimulus. The forth column shows the application of  $\text{NH}_4\text{Cl}$ . (B) Shows the averaged traces from all synapses per one recording. Error bars are SEM.

normalized all the synapses to their individual maximal response upon 40 mM  $\text{NH}_4\text{Cl}$  application (Figure 62). Figure 63 shows that the response to 10 Hz depolarization train was maximal in WT neurons and reduced to 38.5% in dKO neurons. Similarly, deletion of CAPS1 reduced the peak SypHy response to 58%. In contrary, deletion of CAPS2 had little effect on the maximum increase of SypHy fluorescence. Hence, in DRG neurons synaptic transmission appears to be promoted exclusively by CAPS1 while CAPS2 seems to be responsible for LDCV release. We noticed that the average time course of SypHy fluorescence intensity change of many cells elicited by field electrode stimulation was different depending on the genotype. The question was then whether CAPS2 might have an indirect effect on synaptic transmission.



**Figure 63 Synaptic transmission in DRG/S neuron co-culture.**

This graph shows the normalized to individual maximal intensity averaged synapses of WT DRG/WT S neurons (black trace), dKO DRG-WT S neurons (red trace), 1KO DRG-WT S neurons (light blue trace) and 2KO DRG-WT S neurons (navy blue trace). WT set: N = 32 cell, n = 209 synapse, dKO set: N = 35 cell, n = 252 synapse, 1KO set: N = 38 cell, n = 270 synapse and 2KO set: N = 155 synapse. SEM were too small to be displayed.

### III.11.2 A Role for CAPS2 in Synaptic Transmission?

The average time course of fluorescence intensity change can be influenced by two parameters: the fluorescence intensity change of each individual synapse due to spontaneous activity or the time point at which they react in delayed fashion within the stimulus range. In the latter case, the unsynchronized response to a stimulus would result in a reduced but broader average peak. To investigate whether CAPS isoform had an effect on the synchronization of synaptic transmission to the stimulus, we measured the delay between the stimulus and the change of fluorescence intensity at each synapse. We pooled all synapses that responded with a fluorescence increase during immediately upon stimulation. In WT control DRG neurons they represent 80% of



## RESULTS

all synapses (Figure 64). In CAPS2 KO neurons the proportion of synapses that were synchronous with the stimulus decreased slightly to 70% while in CAPS dKO and in CAPS2 KO neurons the percentage of synchronous synapses raised significantly to more than 90%. In WT control neurons the unsynchronized released occurred not only with a delay after the onset of stimulus but also and to a similar extent before the stimulus. This finding is intriguing because DRG neurons in co-culture with S neurons are not spontaneously active in vitro (Ransom et al., 1977a).  $Ca^{2+}$  concentration measurements

performed to test the field electrodes show virtually no calcium variation prior field electrode stimulation (Figure 42). The asynchronous synaptic transmission prior stimulus was not changed in CAPS1 KO neurons when compared to WT neurons. However, SV exocytosis ensuing after the onset of stimulus was increased from 11% in WT neurons to 18% in CAPS1 KO neurons. In contrast, in CAPS dKO and CAPS2 KO cells, the unsynchronized response was reduced to less than 5% whether the response occurred prior to or after stimulation. Taken together synaptic transmission in WT and in CAPS1 KO neurons was considerably more unsynchronized in comparison to transmission in CAPS dKO and CAPS2 KO neurons. We hypothesize that stimulation of peptidergic DRG neurons, which expressed CAPS2 (Figure 52), induced the release of a variety of neuropeptides, which in turn activated their respective presynaptic receptors inducing asynchronous synaptic activity.

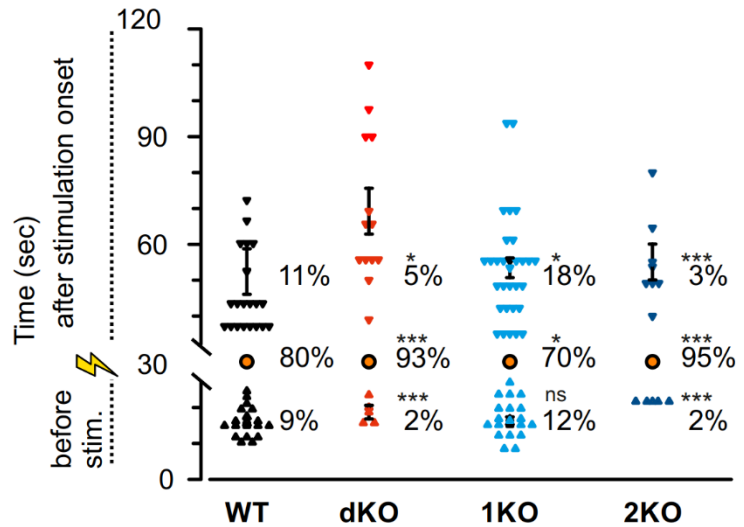


**Figure 64 Synaptic transmission synchronicity.**

The graph shows synaptic responses synchronicity in different sets plotted against time. Synaptic activity was divided into three groups that includes the synapses that responded before the stimulus, the synapses that responded at the stimulus and the synapses that responded in delayed fashion. WT set: N = 32 cell, n = 209 synapse, dKO set: N = 35 cell, n = 252 synapse, 1KO set: N = 38 cell, n = 270 synapse and 2KO set: N = 155 synapse. Error bars are SEM and Mann Whitney test significance test was applied, ns non-significant, \* p < 0.5, \*\* p < 0.01 and \*\*\*p < 0.001.

### III.12 CAPS2 Indirectly Modulates Synapses

To test whether CAPS2-mediated secretion peptides affects synaptic transmission, three peptide antagonists were used to block the major peptides secreted by peptidergic neurons (Figure 65). We selected the antagonists based on their selective characteristics reported in the literature. We chose the most effective and specific blockers available. For instance, the potent and selective TRKB inhibitor Cyclotraxin B was used at 10  $\mu$ M to alter BDNF related physiological processes such as neuronal differentiation and synaptic plasticity (Cazorla et al., 2010; Thibault et al., 2014). L-703,606 oxalate salt hydrate was used as a non-peptide NK-1 tachykinin receptor antagonist at 10  $\mu$ M (Cascieri et al., 1992; Fong et al., 1992; Greenwood-Van Meerveld et al., 2014; Martinez et al., 2015). The third peptide antagonist was Olcegepant to block the binding of CGRP to its receptor (Dasgupta et al., 2014; Russo et al., 2009). Olcegepant is known to be not stable for long in aqueous solution and can be toxic for cells if incubated with for more than 50 min, for these reasons, it was incubated for shorter amount of time at a low concentration (10 nM) (Doods et al., 2000; Nitzan-Luques et al., 2013) (Figure 65). The three peptide blockers were also added to the extracellular solution and the cells were continually perfused during the experiment to ensure

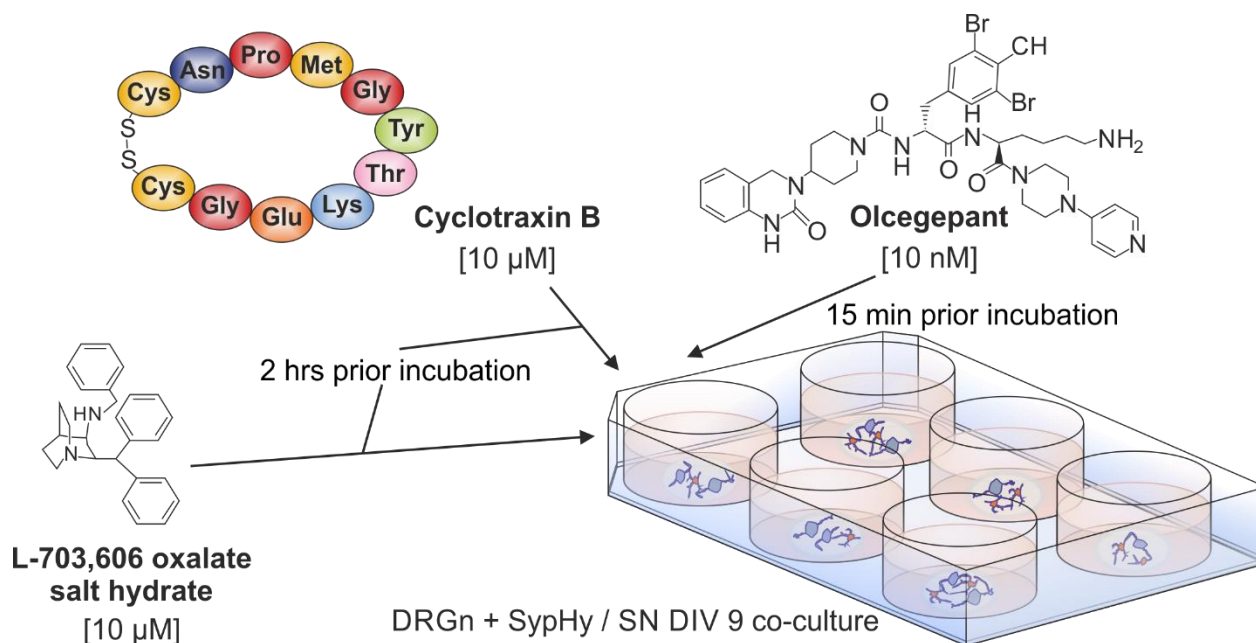


**Figure 65 Blocking CGRP, substance P and BDNF.**

The non-peptides antagonists Olcegepant and oxalate salt hydrate were used to block CGRP and substance P binding to their receptors. The peptide antagonist Cyclotraxin B was used to block the binding of BDNF to TRKB receptors. The cells were pre-incubated with Cyclotraxin B and oxalate salt hydrate at 10  $\mu$ M for 2 hrs. Olcegepant was incubated for shorter time, about 15 min prior to measurements. During the experiment, the cells were continuously perfused with extracellular solution containing the three antagonists to ensure effective blocking of the receptors of interest.

## RESULTS

effective blocking. Synaptic transmission was measured in WT with or without peptide blocker treatment. We were expecting to see more synchronized synaptic activity coupled to the stimulus but the results were far more surprising. Figure 8A shows two exemplary recordings in which WT neurons were treated or not (control) by the antagonists. The images are overlays of two successive DRG neurites pictures acquired during field electrode stimulation (white) and during 40 mM

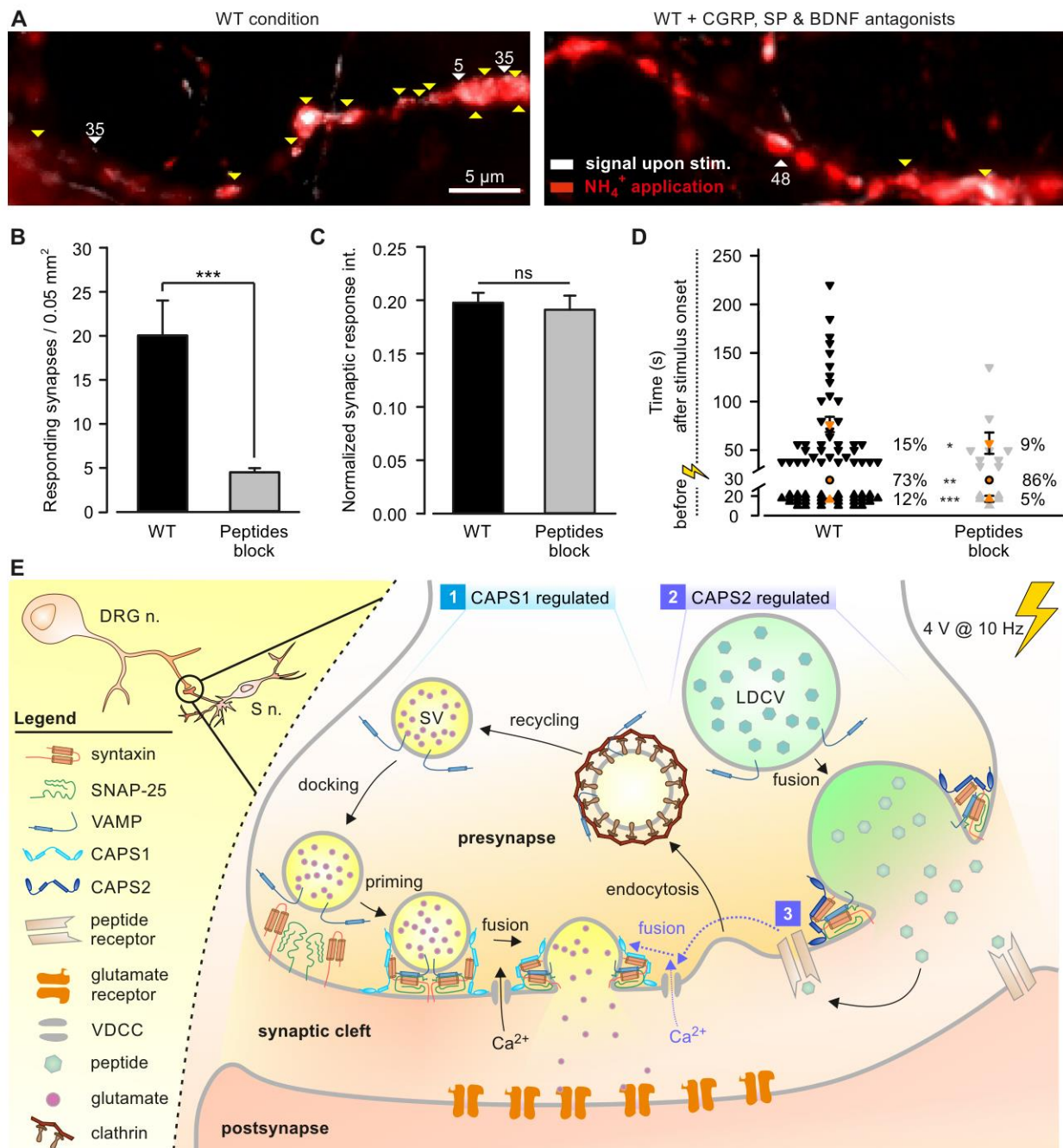


Figure 66 Peptides antagonists reduce active synapses and synchronize them.

## RESULTS

**Continuing Figure 66...** Synaptic transmission was measured in WT DRG/S neurons co-culture that were pre-incubated or not (control) with a cocktail of peptide antagonists containing 10 nM Olcegepant to block CGRP receptors, 10  $\mu$ M L-703,606 oxalate salt hydrate as a non-peptide NK-1 tachykinin receptor antagonist and 1  $\mu$ M Cyclotraxin B to inhibit BDNF binding to TRKB. Cells were stimulated via field electrode at 10 Hz for 1 min and after a period of recovery they were superfused with  $\text{NH}_4\text{Cl}$  like in Figure 7. Co-cultures were made with 2 adult mice for DRG neurons and 12 P0 mice for S neurons. Number of cells was 29 and 50 for control and peptide block, respectively. Total number of counted synapses was 241 and 101 for control and for peptides blocking condition, respectively. Error bars are SEM and Mann Whitney significance test was applied, ns non-significant, \*  $p < 0.5$ , \*\*  $p < 0.01$  and \*\*\*  $p < 0.001$ . (A) Representative overlay of the maximum intensity projection of SypHy epifluorescence images of DRG/S neurons acquired prior to (white) and during superfusion with  $\text{NH}_4\text{Cl}$  (red). The white image reveals only active synapses while the red image depicts all SypHy labeled synapses. Control condition is displayed on the left while cells pre-incubated with the blockers are shown on the right. Yellow arrows indicate the synapses that were synchronized with the initiation of the stimulus. White arrows point to uncoupled synapses responding before or after stimulus. The associated numbers correspond to the delay in seconds. (B) Peptide antagonist pretreatment (grey) reduces the average number of active synapses in comparison to control (black). (C) Average synaptic SypHy responses normalized to SypHy fluorescence upon  $\text{NH}_4\text{Cl}$  application in control compared to cells treated with peptides antagonist reveals that the number of SV secreted at each active synapse was not affected by the antagonists. (D) Similarly to the deletion of CAPS2, peptide blocker treatment synchronizes the synaptic activity to the stimulus. Density dot plot showing the time point of activity and the percentage of synapses that were either synchronized to the stimulus or that responded before or after the stimulus. The time point of response of each asynchronized synapse is shown by individual symbol whereas all the synchronized synapses are shown as one orange circle. Orange dash are the average time point of asynchronized response  $\pm$  SEM. (E) Model of CAPS1 and CAPS2 function in DRG neurons. Our data indicates that SV exocytosis is promoted by CAPS1 and LDCVs are primed by CAPS2. Peptidergic cargo released by LDCVs indirectly affects synaptic transmission through binding to their receptors which might activate  $\text{Ca}^{2+}$  channels or other proteins leading to  $[\text{Ca}^{2+}]_i$  increase and finally SV fusion.

$\text{NH}_4^+$  application that renders all synapses visible (red). In control neurons a large majority of synaptic sites were active as can be recognized by the large overlap of red and white pixels. In contrast, in neurons treated with inhibitors only few red synaptic sites were also marked white. This reveals that only few synapses were active upon depolarization. Overall, nearly 5 times less treated synapses responded to the stimulus as in control (Figure 66 B). For responding synapses the change in fluorescence intensity of SypHy was nearly identical whether the cells were treated or not (Figure 66 C). This indicates that the number of released SV at responding synapse was independent of the treatment. More importantly, exocytosis of SV was significantly better synchronized to the stimulus upon peptide antagonist treatment when compared to untreated control cells (Figure 66 D). In control neurons only 73% of synapses exhibited fluorescence upon depolarization whereas in treated neurons this percentage immediately rose to 86% (\*\*  $p < 0.01$ ). Synchronization of synaptic response was essentially due to reduction by a factor greater than 2 of the percentage of synapses that were active before the stimulus when comparing control and treated neurons (\*\*\*  $p < 0.001$ ). In summary, blocking the effect of CGRP, substance P and BDNF via antagonist treatment, reproduced the effect of CAPS2 deletion on unsynchronized synaptic activity. Therefore, we can conclude that while CAPS1 directly promotes SV exocytosis, CAPS2 indirectly modulates synaptic transmission via control of neuropeptide release contained in LDCVs.

## IV. Discussion

Regulation of vesicle release literature had a strong boost in the late 1980s when SNARE proteins were first introduced as major elements in regulating membrane fusion (Brunger, 2005; Fasshauer, 2003; Hong, 2005; Jahn and Scheller, 2006; Trimble et al., 1988; Wilson et al., 1989). It is widely accepted that alterations in the components of the SNARE machinery hinders or even abolish vesicle secretion. Many proteins interact with SNARE proteins either prior or subsequent to the formation of SNARE complexes (Fiebig et al., 1999; Nicholson et al., 1998) mediating together membrane fusion. Accumulating evidence proposes that CAPS regulates the release machinery. CAPS is well conserved in evolution. One CAPS isoform (UNC-31) exists in *C. elegans*, whereas two isoforms, CAPS1 and CAPS2 are expressed in vertebrates. CAPS is believed to mediate exocytosis in an ATP-dependent step by binding to the vesicle membrane and cell membrane (Grishanin et al., 2004). More recent findings indicated that CAPS affects fusion pore formation (Eckenstaler et al., 2016). It is well known that mutations in CAPS disturb the function of the nervous system, reinforcing the importance of this key player in vesicle fusion. For instance, CAPS1 deletion is lethal (Speidel et al., 2003), while CAPS2 deletion is not lethal but mutations are often associated with autism (Bonora et al., 2014; Sadakata et al., 2007a). Reviewing twenty years of literature concerning CAPS isoforms adds enough complexity about the nature of the now-accepted different functions of this protein (Table 3). We aimed to evaluate separately the two isoforms, investigate their localization and test their effect on LDCV and SV secretion machinery. We believe this is the first time someone has approached the function of CAPS isoforms through suggesting that the different localization of both isoforms in brain and DRG tissues (Speidel, D. et al., 2003; Sadakata et al., 2006) might imply different functions. Through the course of this discussion we will provide compelling arguments showing that CAPS isoforms play differential roles in mediating secretion of LDCVs and SVs in DRG neurons. The first experiments aimed to identify whether CAPS is found and later to localize CAPS into DRG neurons subtypes.

### **IV.1 CAPS1 is Localized to all DRG Neurons while CAPS2 is Localized to the Peptidergic Subtypes**

Localizing CAPS into DRG neurons was not easy, as no good commercial anti-CAPS1 or CAPS2 antibodies were not available at the time I started my work. It was necessary to identify whether these isoforms were present in DRGs, for this purpose, we made RT-PCR as a first approach to address this issue. The presence of glial cells and fibroblast in complete DRGs contaminates the observed signal and limits the significance of the conclusions. Nevertheless, RT-PCR remains a common practice to screen for mRNAs in complete glands. For example full adrenal glands have been used to investigate the content of chromaffin cells (Bruder et al., 2007; Nguyen Truong et al., 2014); although they contain other cell types such as fibroblasts (Kirshner et al., 1989; O'Connor et al., 2007) and endothelial cells (Banerjee et al., 1985). A more precise method would ultimately be single cell PCR on individual DRG neurons. Previous single cell PCR and RNA sequencing showed that these cells are highly heterogeneous (Usoskin et al., 2015) and it is therefore very difficult to screen for proteins at individual cell level. Because using RT-PCR was a quick and a more convenient approach, we used it to investigate the presence of CAPS isoforms at the mRNA level in DRG neurons. RT-PCR semi-quantitative results showed that CAPS1 is highly expressed at the mRNA level in DRGs and to lesser extent CAPS2 which was consistent with what was previously described (Sadakata et al., 2006). Next we wanted to verify the existence of CAPS at the protein level, to show that the detected mRNA is being translated into protein. We also wanted to check the developmental expression of CAPS isoforms through time. For this reason, we isolated DRGs from embryonic and adult mice. Results showed that both isoforms are present in embryonic DRG neurons. These isoforms were differentially regulated during development. CAPS1 expression level tripled between the E18 and P7 while CAPS2 levels merely increased over this time period. This was not surprising if we took into consideration our later findings that show CAPS1 is preferentially localized at synapses and the fact that synapses between DRG neurons and spinal neurons start to form at P5-P6 and continues maturation over a period of time extending up to P40 in mice (Ashrafi et al., 2014; Betley et al., 2009). Our findings were consistent with what was shown of CAPS developmental expression in brain (Speidel et al., 2005). With new commercially available CAPS1 antibody and in house made CAPS2 antibody, we were able to investigate the cellular and subcellular localisation of CAPS isoform. ICC experiment



## DISCUSSION

showed that CAPS1 and/or 2 were present in all DRG neurons. Later on, it was possible to purify antibodies specific against CAPS2 from the previous serum. Double ICC experiments showed that CAPS1 is found in all DRG neurons while CAPS2 in 45% of the population. This data confirmed the immunohistochemistry results of Sadakata et al., (2007). They also agree with findings in other regions of the nervous system where it has been shown that CAPS1 was almost expressed in all brain cells while CAPS2 was expressed in sub-regions like cerebellum, cortex, hippocampus and olfactory bulb (Speidel et al., 2003). Further, using various markers (iB4, anti TRKB, anti NK-1r, anti CAPS1 and anti CAPS2) we were able to differentiate between peptidergic and not peptidergic neurons. We found that CAPS1 was uniformly localized between the two types while CAPS2 was almost localized to all peptidergic medium and large neurons (Figure 67). To further verify this finding, we stained against peptidergic subtypes like NK-1r and TRKB and found that CAPS2

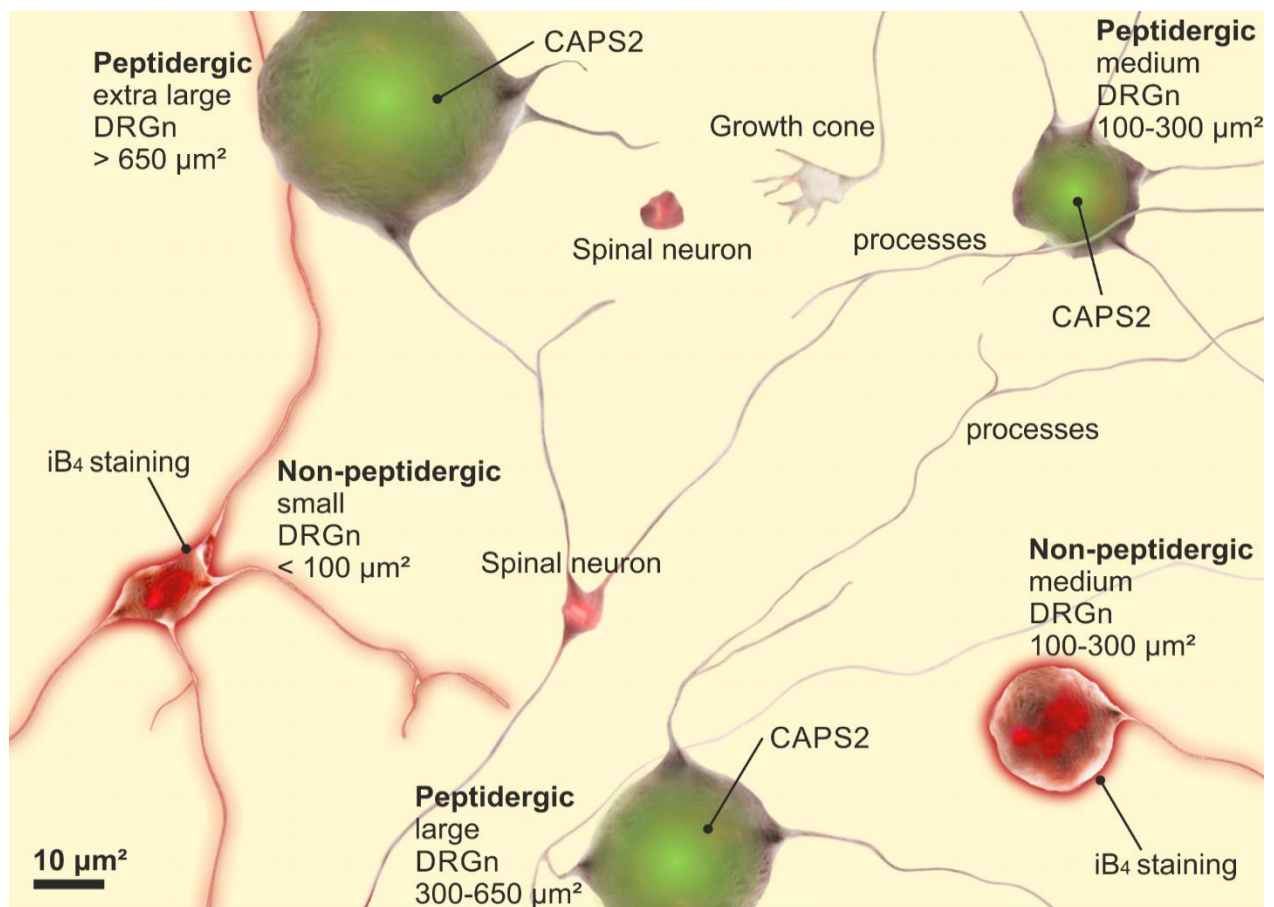


**Figure 67 CAPS localization into peptidergic and non-peptidergic neurons.**

DRG neurons were classified according to peptidergic and non-peptidergic neurons using iB4 labeling. Peptidergic neurons were exclusively large and extra-large in size and some were of medium sized cells. Non-peptidergic neurons on the other hand were either exclusively small sized cells or of medium size. CAPS2 was localized to peptidergic neurons while CAPS1 was expressed randomly among peptidergic and non-peptidergic neurons.

Image courtesy: This image was generated together with the help of Mr. Abed Shaib.

localizes to these neurons. This confirms that CAPS2 indeed is localized to peptidergic neurons. Interestingly, CAPS2 had a remarkable subcellular cytoplasmic localization, which we failed to identify due to time constraints (see *Appendix VI.6*). Additionally, CAPS1 distribution was not uniform among different DRG neurons. Some cells exhibited a stronger CAPS1 fluorescence signal compared to other cells. We tried to identify which subtype of these cells had higher CAPS1 endogenous expression levels. CAPS1 didn't preferentially localize to cells that were positive with TRKB, rather some NK-1r positive neurons exhibited high CAPS1 expression. We showed that peptide secretion of WT neurons is not modulated by CAPS1. The elevation of CAPS1 isoform in a fraction of peptidergic NK-1r subtype could be explained by the fact that upon nerve injury, some larger neurons start to secrete substance P that usually do not produce it (Lee et al., 1985; Szucs et al., 1999; Weissner et al., 2006). *In vivo*, substance P secreting neurons represent  $13.5\% \pm 1.9$  of DRG population (Hall et al., 1997), and this percentage increases to 25% in our DRG neuron culture. These newly-secreting substance P stressed neurons need to transmit this information to the higher order of CNS dorsal horn neurons (Swett and Woolf, 1985; Yoon et al., 1996). To do so, CAPS1 might be upregulated to mediate SV secretion which is in line of our working model. After the adequate input, the spinal neurons in return will trigger central sensitization (Khasabov et al., 2002).

### IV.2 CAPS2 is the Priming Factor for LDCV Secretion

Our data showed that CAPS2 and not CAPS1 is responsible for priming LDCVs in DRG neurons. It is well documented that CAPS1 is essential for calcium-mediated LDCV exocytosis (Ann et al., 1997; Berwin et al., 1998; Grishanin et al., 2004; Renden et al., 2001; Speese et al., 2007; Tandon et al., 1998). Similarly, CAPS2 has been shown to have a priming function and that its function is redundant with CAPS1; for instance, both CAPS1 (Liu et al., 2008) and CAPS2 primes LDCV secretion in chromaffin cells (Liu et al., 2011). Similarly, CAPS1 (Eckenstaler et al., 2016; Farina et al., 2015; Sadakata et al., 2013) as well as CAPS2 (Sadakata and Furuichi, 2009; Shinoda et al., 2011) can prime LDCV secretion in hippocampal neurons. Consistently, both CAPS isoforms have similar function in regulating LDCV release in cerebellum (Sadakata and Furuichi, 2009). Unlike the previously cited cell types, in DRG neurons CAPS isoforms not only exert distinct functions but also their subcellular localization was different. CAPS2 and not CAPS1



## DISCUSSION

is intensely localized to the cytoplasm where it primes LDCVs, while CAPS1 is localized to synapses where it primes SVs. The question is whether the differential function of CAPS isoforms is due to specific interaction with the two organelles or whether the localization is dictating the function of the isoform. We showed that LDCV release is promoted to a similar extent upon overexpressing either isoform in WT neurons; it appears that support priming. Moreover, our data shows that both isoforms can rescue the CAPS1 and 2 dKO secretion phenotype. We think that flooding the cells with viral-driven overexpression overcomes the specific localisation of both isoforms and thereby evens their function. In consistence, and while keeping in mind that CAPS1 is in all DRG neurons, overexpressing CAPS2 in non-peptidergic non-secreting CAPS2-missing neurons, secretion is induced (see Figure 54). In line with these findings, CAPS 2 KO DRG peptidergic neurons exhibited no LDCV secretion (*data not shown*). Munc13 exhibits a similar phenotype to CAPS1, for example it does not prime LDCV release in chromaffin cells but upon

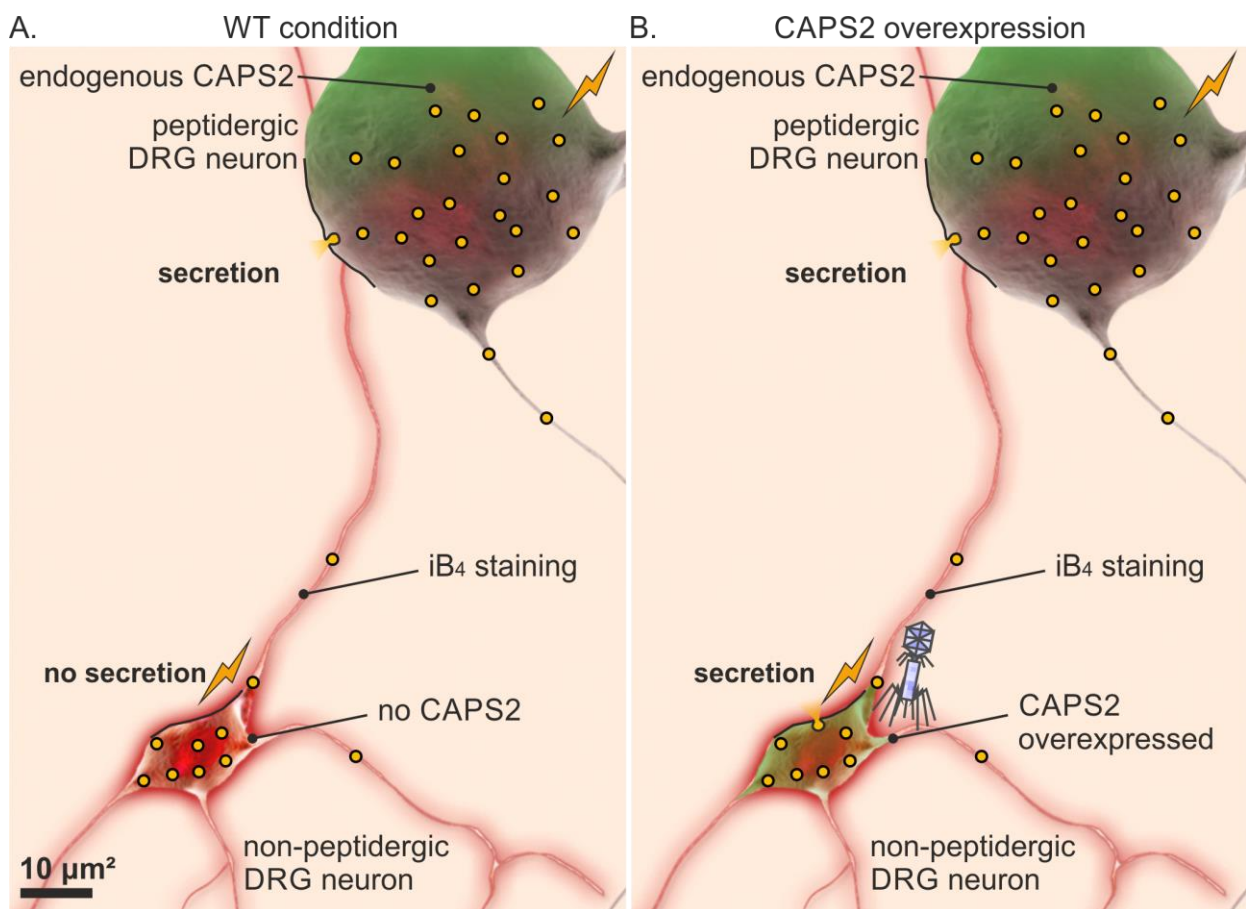


**Figure 68 CAPS2 primes LDCV release.**

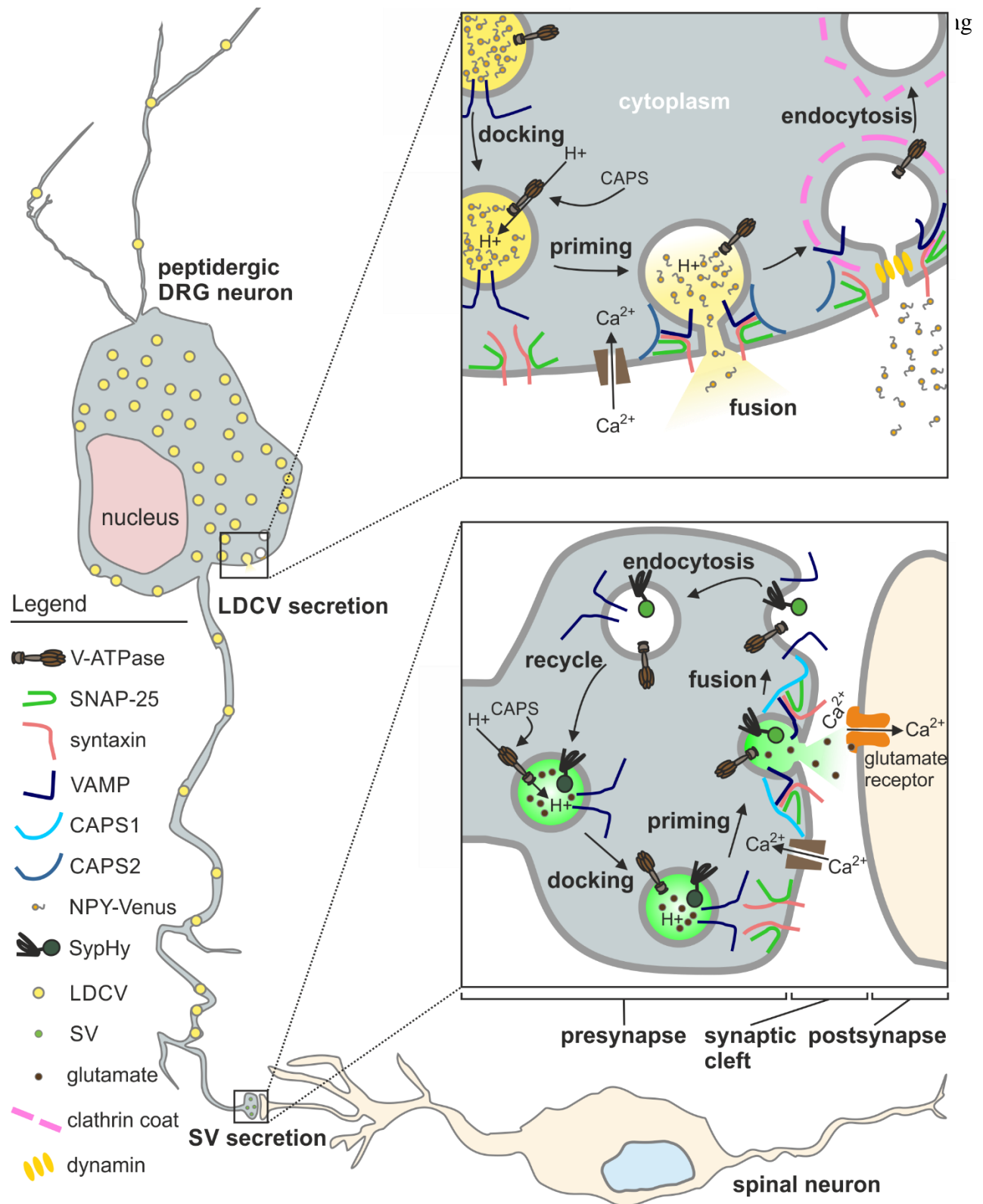
DRG peptidergic neurons endogenously expressing CAPS2 can secrete LDCVs upon stimulating with 4 V at 100 Hz while non-peptidergic neurons cannot secrete LDCVs using the same stimulus. This phenotype can be reversed upon overexpressing CAPS2 in non-peptidergic neurons driving them to secrete LDCVs.

Image courtesy: This image was generated together with the help of Mr. Abed Shaib.

over expressing it, the secretion is increased (Man et al., 2015). Therefore, we hypothesize that both isoforms can prime LDCVs but that due to its somatic localization, CAPS2 is conferring to the DRG neurons the ability to secrete LDCVs. Our CAPS priming model allows the possibility of extending it to other cell types. For instance, Farina et al., (2015) showed that CAPS1 primes LDCV fusion at synapses in hippocampal neurons. They also showed that CAPS1 was localized to synapses while CAPS2 was merely present. This fits well our theory that both CAPS isoforms can prime LDCVs, it depends on the availability. An important question remains unsolved as how would CAPS2 switch the non-peptidergic non-secreting DRG neurons into peptidergic secreting neurons? Or simply, CAPS2 derives secretion from non-peptidergic neurons without affecting the nature of these cells.

### IV.3 CAPS1 Primes SV Secretion

To study CAPS effect on synaptic transmission we extensively studied the synapse formation between the co-cultured neurons to ensure optimal close-to-physiological conditions for the experiments. DRG neurons can be grown with other cell types like skin cells (Koizumi et al., 2004; Malin et al., 2007; Reynolds et al., 1997; Taherzadeh et al., 2003) and higher order CNS neurons (Gu and MacDermott, 1997; Shepherd et al., 1997). We co-cultured DRG neurons with S neurons allowing them to form synapses (Joseph et al., 2010). This co-culture system has been used by only very few groups (Cao et al., 2009; Hendrich et al., 2012; Joseph et al., 2011; Ohshiro et al., 2007; Yu et al., 2015) and to the best of my knowledge none were using neurons from mice. It was important to focus on the synapses that form between DRG neurons and S neurons and exclude all the synapses between S neurons. To do so, we initially infected the DRG neurons with adenovirus encoding for Life Act-Ruby and added later the S neurons. The processes originating from infected DRG neurons were nicely labelled with red and can be differentiated from S neurons processes (see *Appendix VI.7*). But this approach was limited by the transfection efficacy of the adenovirus whereby not all DRG neurons would be transfected and therefore excluding some synapses between DRG neurons and S neurons. For this reason, we decided to use the SybKI mice (Matti et al., 2013) to prepare the DRG neurons co-cultured with WT S neurons. This way, all DRG processes were labelled and we could study exclusively the synapses between DRGs and S neurons. Through these co-cultures, we confirmed that synapses do form between these neurons.



**Figure 69 CAPS differential role model.**

CAPS2 is localized to peptidergic DRG neurons and is responsible for priming LDCV secretion. CAPS1 is found at all DRG neurons and primes SV secretion at synapses with spinal neurons. Our data also indicate that CAPS regulates the intravesicular pH by making it more acidic probably by interacting with the proton pumps.

high number of synapses with good cell quality suitable for electrophysiological experiments. Further, we also confirmed that these synapses are not only linked but also active. We loaded the cells with calcium sensitive dye and we stimulated single DRG neuron neighboring S neurons and monitored the fluorescence intensity. We did not use the field electrode stimulation as it will stimulate all cell simultaneously; rather we took advantage from the fact that cultured DRG neurons maintain the ability to sense thermal (Cesare and McNaughton, 1996; Reid and Flonta, 2001), chemical (Jordt et al., 2004; Peier et al., 2002) and mechanical stimuli (McCarter et al., 1999). We proved that these synapses were functionally connected after trying out several different chemical and mechanical stimulating methods. In these well-adjusted co-culture conditions we measured SV fusion using the SyHy based imaging technique. We compared exocytosis from WT with CAPS1 KO, CAPS2 KO or CAPS dKO DRG neurons. Unlike peptide release, measurement of SV fusion showed that CAPS1 and not CAPS2 mediates neurotransmitter release (Figure 69). Knocking out both CAPS isoforms dramatically reduced SV fusion as compared to WT. While CAPS2 KO didn't have any effect on the scale of SV fusion, CAPS1 KO induced a strong decrease in SV fusion. This data is consistent with our ICC experiments where we showed that CAPS2 was concentrated in DRG cell bodies while CAPS1 was localized to synapses. This idea is partially supported by a recent paper published by Farina et al. (2015) where they show that CAPS1 is present at synapses in hippocampal neurons and that CAPS1 primes LDCVs there. Our findings contradict with an older paper that showed synaptic vesicles secretion in hippocampal neurons requires both CAPS1 and CAPS2 (Jockusch et al., 2007). This notion gets puzzling when combined with the fact that CAPS2 is weakly present at synapses. Together with the LDCV secretion results, these data also indicate that priming can be fulfilled by either isoform in our system, depending on the isoform availability and since CAPS1 is localized to synapses, it simply primes SVs.

### **IV.4 CAPS2 Indirectly Affects Synaptic Transmission through Peptide Release**

An interesting phenomena was evident while acquiring the synaptic transmission data whereby some synapses showed unsynchronized synaptic activity, while the activity of other synapses were tightly coupled to the stimulus. In depth analysis showed that synaptic activity in dKO DRG neurons was less coupled to the stimulus when compared to the WT genotype. Complementary to this, DRG neurons of CAPS2 KO genotype showed a very similar behavior of

unsynchronized synaptic activity to dKO DRG neurons. Conversely, CAPS1 KO DRG neurons showed synaptic activity that was precisely synchronised to the stimulus as described in WT DRG neurons. Altogether, this data infers that CAPS2 is somehow affecting indirectly synaptic transmission. Our LDCV secretion data shows that LDCV secretion occurs at a low rate when the neurons were stimulated at 10 Hz frequency. Secreted peptides at the cell body or synapses (De Camilli and Jahn, 1990; Navone et al., 1989; Scarfone et al., 1988) find their way to peptides receptors on the presynaptic membrane, inducing an autocrine feedback on synaptic transmission (Figure 70). For instance, it was shown that CGRP receptors are present in CGRP containing nerve terminals (Nuki et al., 1994). In hippocampal neurons BDNF does not act on TRKB receptors postsynaptically, rather presynaptically modulating long term potentiation (Xu et al., 2000). In accordance, NPY was described to have presynaptic activity through multiple NPY receptors that

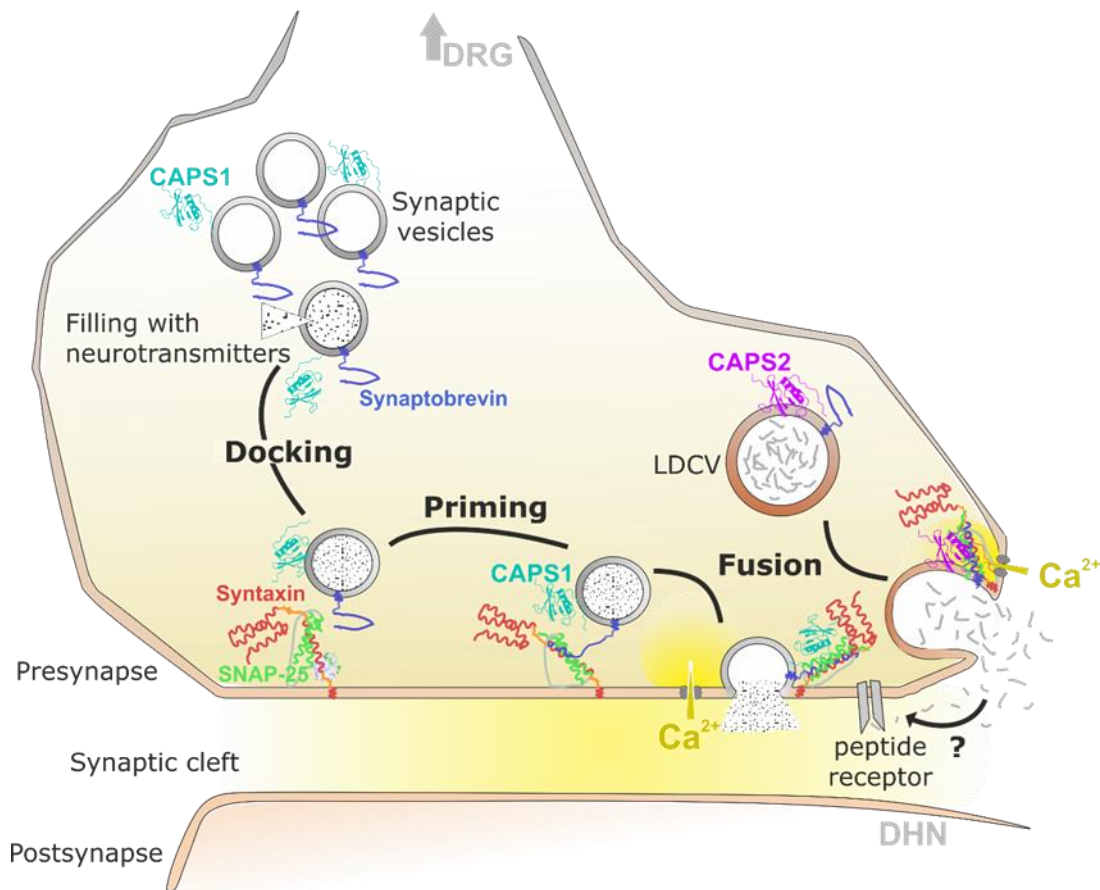


**Figure 70 CAPS2 indirect effect on synaptic transmission model.**

The electrical stimulation used to induce SV secretion is strong enough to induce LDCV secretion as well. The secreted peptides at or near the synaptic cleft find their way to the peptide-receptor on presynapses. Therefore depolarizing the membrane to the level of inducing later SV secretion. This model explains the asynchronous synaptic transmission that is less coupled to the main stimulus. While CAPS1 regulates SV exocytosis, CAPS2 is responsible for regulating LDCV exocytosis. The cargo released from LDCVs affects SV secretion, hence CAPS2 indirectly affects synaptic transmission.

coexist on pre- and postsynapses (Chen and van den Pol, 1996; Obrietan and van den Pol, 1996). Once the peptides are released, their effect is reported to be slower than small sized neurotransmitters such as GABA, glutamate and acetylcholine (Schlicker and Kathmann, 2008). Perhaps, this could explain the delayed asynchronous synaptic responses. To provide more cues elucidating any possible indirect role of CAPS2, we decided to use a cocktail of non-peptide and peptide antagonists for the major peptides secreted by DRG neurons. Blocking the effect of CGRP, substance P and BDNF induced a synchronization of the synapses with the stimulus suggesting that there were no or little other exterior effectors to the synaptic transmission. This evidence supports the idea that CAPS2 can regulate the synaptic activity through the secretion of peptide contained in LDCVs. The effect of these peptides antagonists was even more pronounced on the number of active synapses in control compared to the condition in which the neurons were treated with peptide antagonists as their number was significantly reduced from  $20 \pm 4$  to  $5 \pm 0.3$  synapse per  $0.05 \text{ mm}^2$  area. This lasting decrease in synaptic transmission could be due to the fact that the absence of these peptides led to an alteration of calcium concentration, subsequently generating long term depression (Malenka and Nicoll, 1999). Retrograde signalling involving peptides, messengers, conventional transmitters and lipid messengers in neurons often regulates presynaptic plasticity (Regehr et al., 2009). These substances can be either released from the neuron cell bodies or processes targeting presynaptic structures leading to the modification of synaptic transmission in the form of a long-lasting effect (Castillo, 2012; Regehr et al., 2009; Tao and Poo, 2001). Even though there is a wide agreement that these messengers trigger LTD and/or LTP, the mechanisms and main effectors underlying such changes are unknown (Futai et al., 2007; Gottmann, 2008).

## V. Conclusion and Perspectives

CAPS is a complex multi-domain protein that is known to be a strong priming factor in several species. Recent evidence indicates that CAPS might be implicated in several functions with contradicting roles among different species and within the same species in different cells (Ann et al., 1997; Berwin et al., 1998; Eckenstaler et al., 2016; Elhamdani et al., 1999; Farina et al., 2015; Grishanin et al., 2004; Jockusch et al., 2007; Liu et al., 2011; Liu et al., 2008; Renden et al., 2001; Sadakata and Furuichi, 2009; Sadakata et al., 2013; Shinoda et al., 2011; Speese et al., 2007; Speidel et al., 2005; Tandon et al., 1998; Vogl et al., 2015). Through this thesis, we managed to demonstrate that CAPS isoforms play differential role in regulating secretion of LDCVs and SVs in murine DRG neurons. We showed that CAPS2 is localized to peptidergic neurons and is the priming factor for LDCVs while CAPS1 has no function in LDCV exocytosis from DRG neuron somata. We also showed that CAPS1 is localized to synapses and is responsible for mediating synaptic transmission by direct priming of SVs while CAPS2 had no direct effect. Finally, we produced evidence indicating that CAPS2 indirectly affects synaptic transmission by regulating peptide release near synapses.

Our findings provides a probable understanding of pain generation in DRG neurons by suggesting a molecular switch for pain synthesis. We propose that CAPS2 might be the molecular switch that converts non-peptidergic DRG neurons into neurons that are capable of neuropeptide release. By overexpressing the ‘absent’ CAPS2 in non-peptidergic neurons, they start to release peptides. It is known that in response to chronic pain injury, the number of peptidergic neurons is increased. We speculate that CAPS2 expression in these neurons is activated hence pushing these non-peptidergic neurons to secrete. It is unclear though what triggers the change of non-peptidergic neurons to peptidergic neurons. To address this important issue, an experiment should be carried out by which one would overexpress CAPS2b and stain with iB4 together with CGRP, BDNF, NK-1r and chromogranin A. The idea is to find a non-peptidergic neuron overexpressing CAPS2 and check whether it has any of the peptides inside LDCVs. In order to conduct this experiment properly, CAPS2b should be overexpressed slowly using a Lentiviral system to give the cells the necessary time for all the possible molecular changes that CAPS2 might induce. In addition to the



expression speed, additional complexity lies in the transfection efficacy of CAPS-Semileki Forest virus in DRG neurons which was as low as 20%. It would be very difficult to find a fixed transfected cell that would be stained with iB<sub>4</sub> and the other peptidergic subtypes.

Collectively, we can conclude that CAPS isoforms play differential roles due to its differential localization. A lot of questions were answered during this thesis<sup>†</sup> and a lot of answers still wait to be uncovered. For instance, the localization signal that sends CAPS1 to synapses and keeps CAPS2 in somata of DRG neurons, remains unknown<sup>43</sup>. It is still unclear whether CAPS2 pushes non-peptidergic neurons to become peptidergic neurons hence the secretion, or it only derives secretion of LDCVs in non-peptidergic neurons once expressed. Furthermore, it is interesting to investigate the expression of CAPS2 upon nerve constriction and chronic pain generation in vivo models.

<sup>†</sup>**NB:** This thesis book did not include the identification of Munc13 isoforms. Dr. Benjamin Cooper kindly provided us with Munc13-eGFP KI mice. We identified two isoforms of Munc13 expressed in DRG neurons, munc13-2 and munc13-3. We also investigated the region that is responsible for CAPS1 localization to synapses. Primary results favored our speculated region of interest which is also found in munc13-1. Data was not included in this thesis awaiting further experiments to support our initial conclusions and other functional experiments. It is worth mentioning that with the help of Mr. Ali Harb, we managed to patch adult DRG neurons and induce secretion by depolarizing single cells.

---

<sup>43</sup> Experiments that attempt to provide evidence about the localization signal of CAPS isoforms were performed but are not covered in the course of this book.

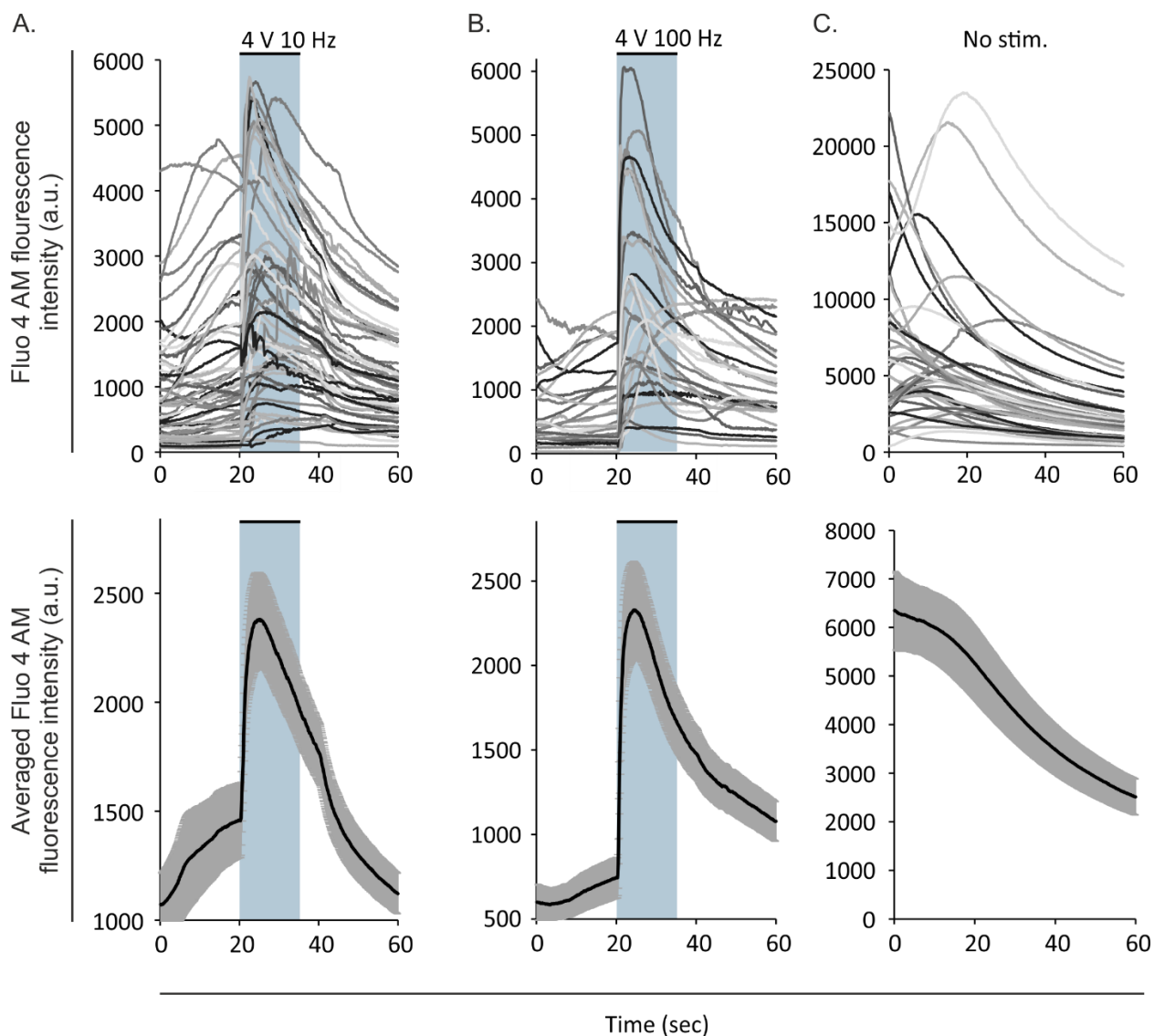


## **VI. Appendix**

<b>VI.1</b> Stimulating Hippocampal Neurons	Page 114
<b>VI.2</b> CAPS2 Negative Control	Page 115
<b>VI.3</b> CAPS1 Negative Control	Page 116
<b>VI.4</b> NPY-Venus is loaded correctly into LDCVs	Page 116
<b>VI.5</b> VGLUT-mNectarine structure	Page 118
<b>VI.6</b> LDCV Size in Peptidergic and Non-Peptidergic Neurons – STED	Page 118
<b>VI.7</b> Golgi Staining	Page 120
<b>VI.8</b> Life Act-Ruby Experiment	Page 120
<b>VI.9</b> List of Antibodies	Page 122

## VI.1 Stimulating Hippocampal Neurons

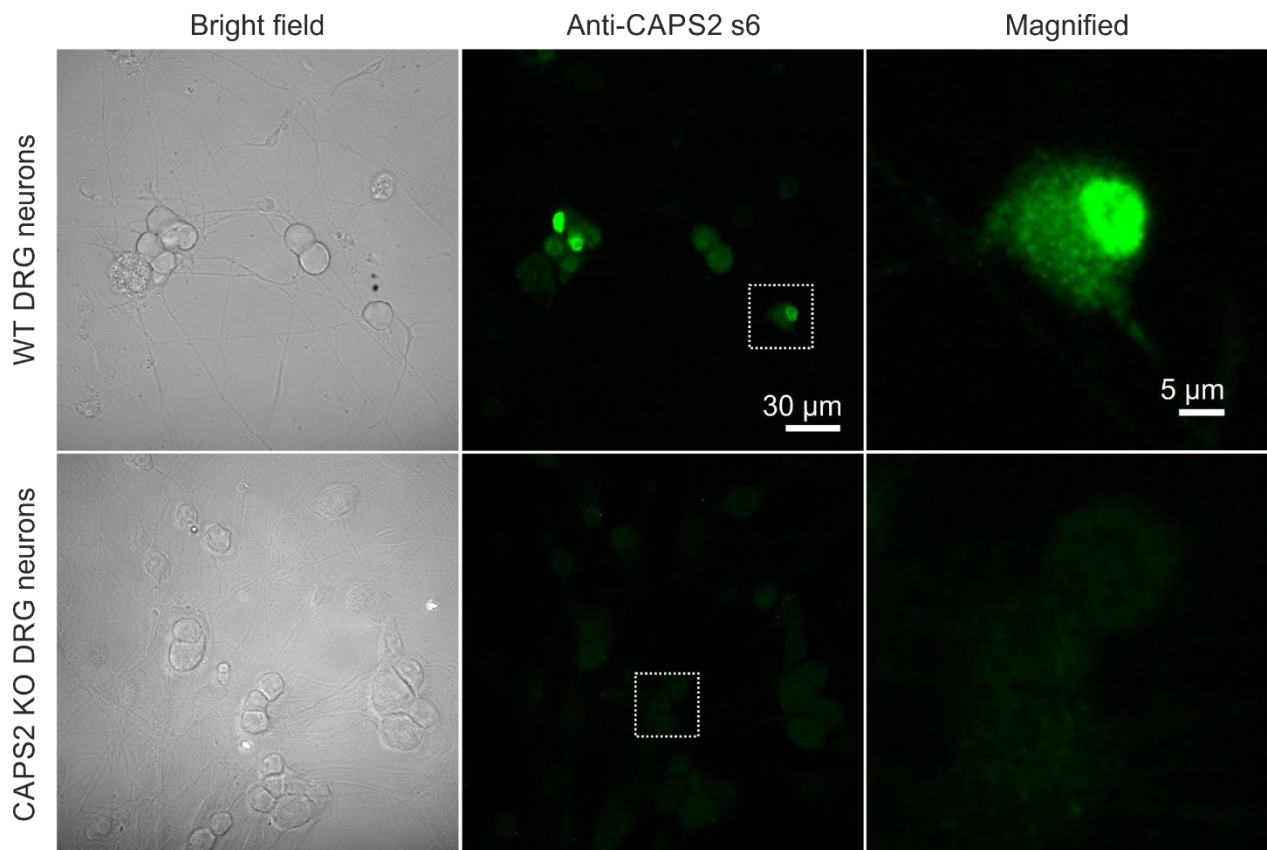
Hippocampal neurons were loaded with Fluo 4 AM and were incubated for 20 min before recording. The cells were washed by continual perfusion at 37 °C. Hippocampal neurons were stimulated through the field electrode with different frequencies while measuring fluorescence intensity in epifluorescence at 488 nm. (A) Top graph shows the response of neurons to the application of a stimulus of 4 V at 10 Hz,  $n = 69$  cells were stimulated out of which 55 cells responded. The lower graph shows the average of Fluo 4 fluorescence intensities. (B) The upper graph shows the application of 4 V at 100 Hz stimulus response curves,  $n = 38$  cells were stimulated out of which 29 cells responded. The lower graph shows the average of Fluo 4 fluorescence intensities. (C) The upper graph shows the fluorescence intensity fluctuations without any



stimulation serving as a control. The lower graphs shows the averaging of Fluo 4 fluorescence intensities.

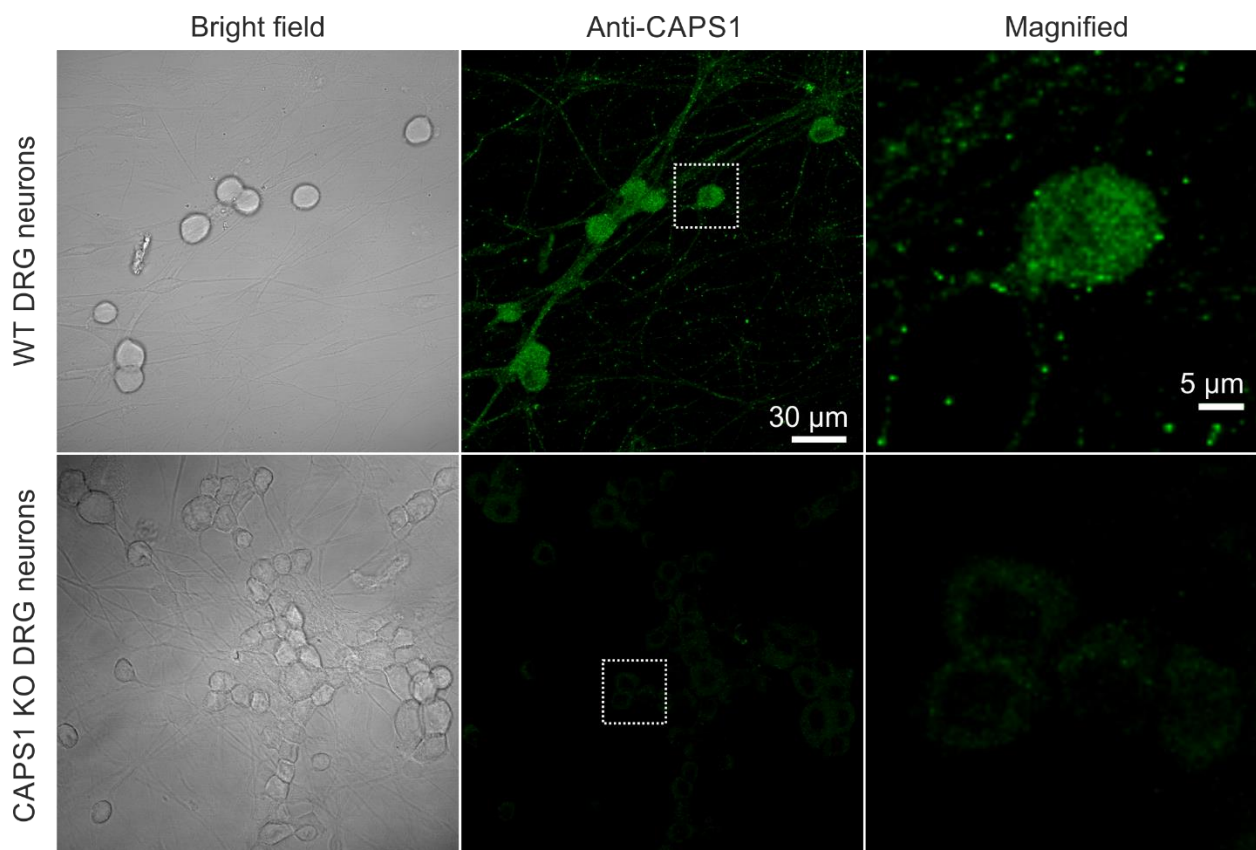
## VI.2 CAPS2 Negative Control

Anti-CAPS2 Serum 6 was tested with CAPS2 KO control to ensure there is no cross reactivity with CAPS1. Embryonic WT DRG neurons were stained against CAPS2 (1:1000) and the signal was revealed via staining with goat anti-rabbit secondary antibody coupled to Alexa 488. The cells fluorescence was measured via confocal microscopy. Results showed staining in WT cells while absence of the signal was evident in CAPS2 KO cells. It is worth to note that anti-CAPS2 serum 6 staining always had some background noise in CAPS2 KO cells, even with higher dilutions, but the signal in WT was significantly higher exhibiting staining pattern in subcellular compartments.



### VI.3 CAPS1 Negative Control

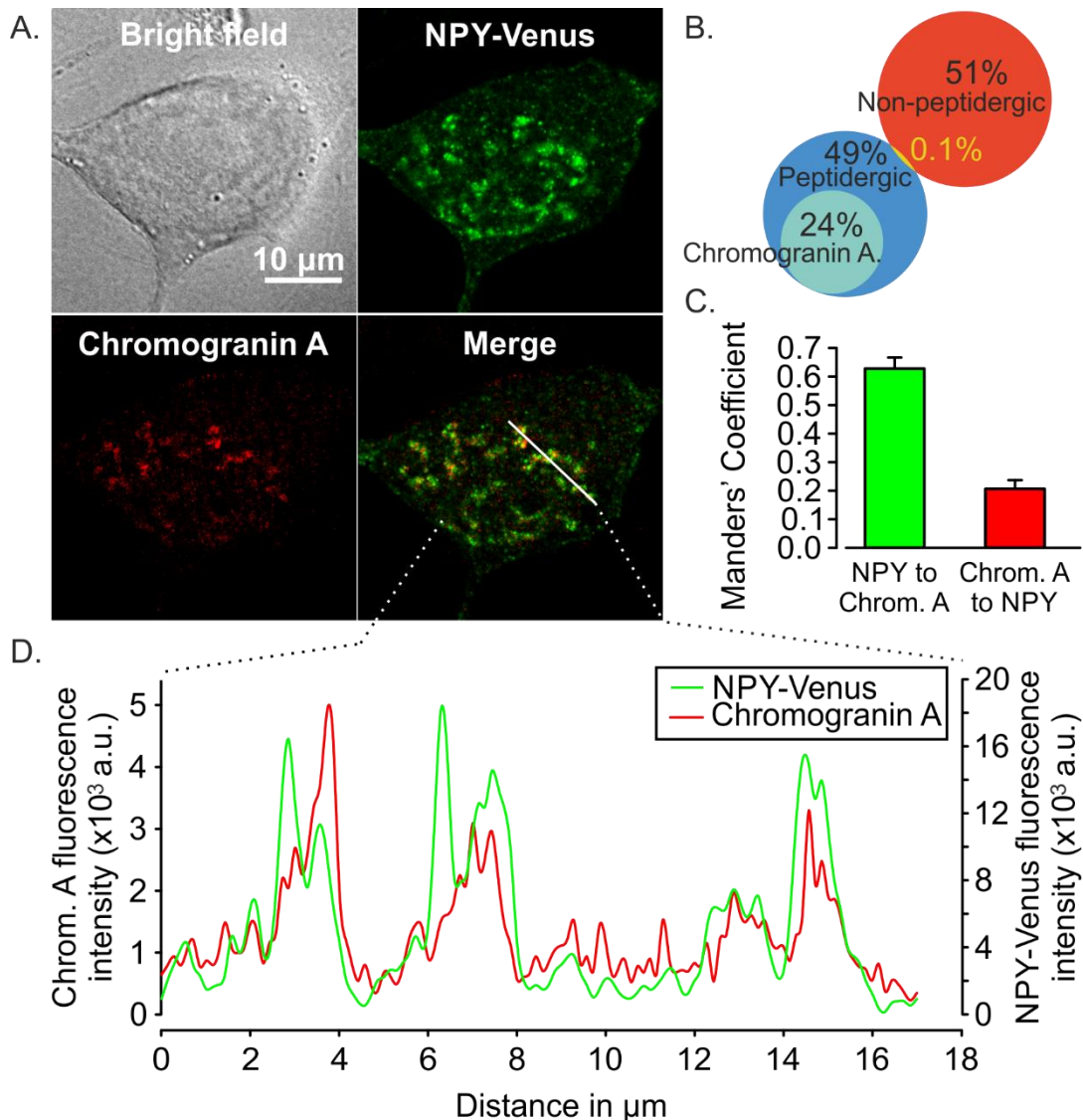
Similar control involving CAPS1 KO cells were performed to ensure the specificity of SynapticSystems anti-CAPS1 antibody (1:1000) and no cross-reactivity with CAPS2. The results below shows total absence of punctae staining in CAPS1 KO cells (lower panel in the figure below).



### VI.4 NPY-Venus is loaded correctly into LDCVs

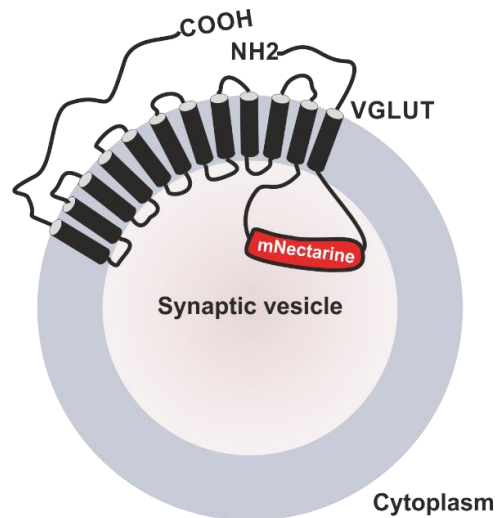
NPY-Venus is commonly used for labeling LDCVs with a pH-sensitive fluorescent protein (Ramamoorthy et al., 2011). NPY-Venus was cloned into a second generation pRR1.sin.cPPT.CMV.WPRE Lentiviral vector in order to drive its expression in DRG neurons. Although, Lentiviruses are gentle and express slowly the encoded protein for long term without stressing the cells and ensure high survival rate after transfection (Dull et al., 1998; Vigna and Naldini, 2000), it was critical to test if NPY-Venus is loaded correctly into LDCVs upon a viral overexpression in DRG neurons. To do so, DRG neurons were transfected with the Lentivirus

encoding for NPY-Venus and left for 7 days in culture, then fixed with 4% PFA and permeabilized with 0.2% triton for 1 h to ensure that LDCV membranes are permeabilized. The primary polyclonal antibody against Chromogranin A (*ab15160*) from Abcam was used in dilution 1/200 and incubated overnight. Goat anti Rabbit coupled to Alexa 561 was used against the primary antibody in dilution 1/2000 and stacks of confocal images were acquired. (A) This panel includes a bright field image showing single DRG neuron, NPY-Venus imaged at 514 and assigned to a false green color, Chromogranin A signal imaged at 561 nm in red and the merger of the channels. (B) Percentage of Chromogranin A positive cells. (C) Manders' coefficient showing the colocalization from NPY to Chromogranin A and the opposite. (D) Line scan analysis to show colocalization of NPY with Chromogranin A at individual vesicles. N = 2 adult mice and n = 46 cells.



## VI.5 VGLUT-mNectarine structure

VGLUT-mNectarine was cloned into a second generation Lentivirus pLenti2g-VGLUT-mNectarine. The mNectarine was inserted near the N-terminal part of VGLUT towards the lumen of the vesicle.



## VI.6 LDCV Size in Peptidergic and Non-Peptidergic Neurons – STED

To test if NPY-Venus is loaded in similar vesicles in peptidergic and non-peptidergic neurons we decided to measure their size with STED microscopy (Ms Angelina Staudt made the staining of the cultures and Dr. Ute Becherer acquired and analysed the STED images). NPY-Venus transfected DRG neurons were stained with iB<sub>4</sub>-Alexa641 to identify peptidergic and non-peptidergic neurons (see Figure 3). Because STED beam bleaches Venus extremely fast, we fixed the DRG neurons with 4% PFA at DIV 7 and performed an immuno-labelling against Venus with anti GFP antibody (Life Technology, G10362, at a dilution of 1:20) and anti-rabbit secondary antibody (Abberior STAR red). We acquired first a stack of 5 images in confocal mode at 561 nm to visualize the IB<sub>4</sub> signal (top row: maximum intensity projection). Then we visualized the LDCVs in a single section of the cells at 647 nm in confocal (middle row) and STED (bottom row). STED allowed us to clearly identify individual vesicles as can be seen on the enlarged portion of the images.

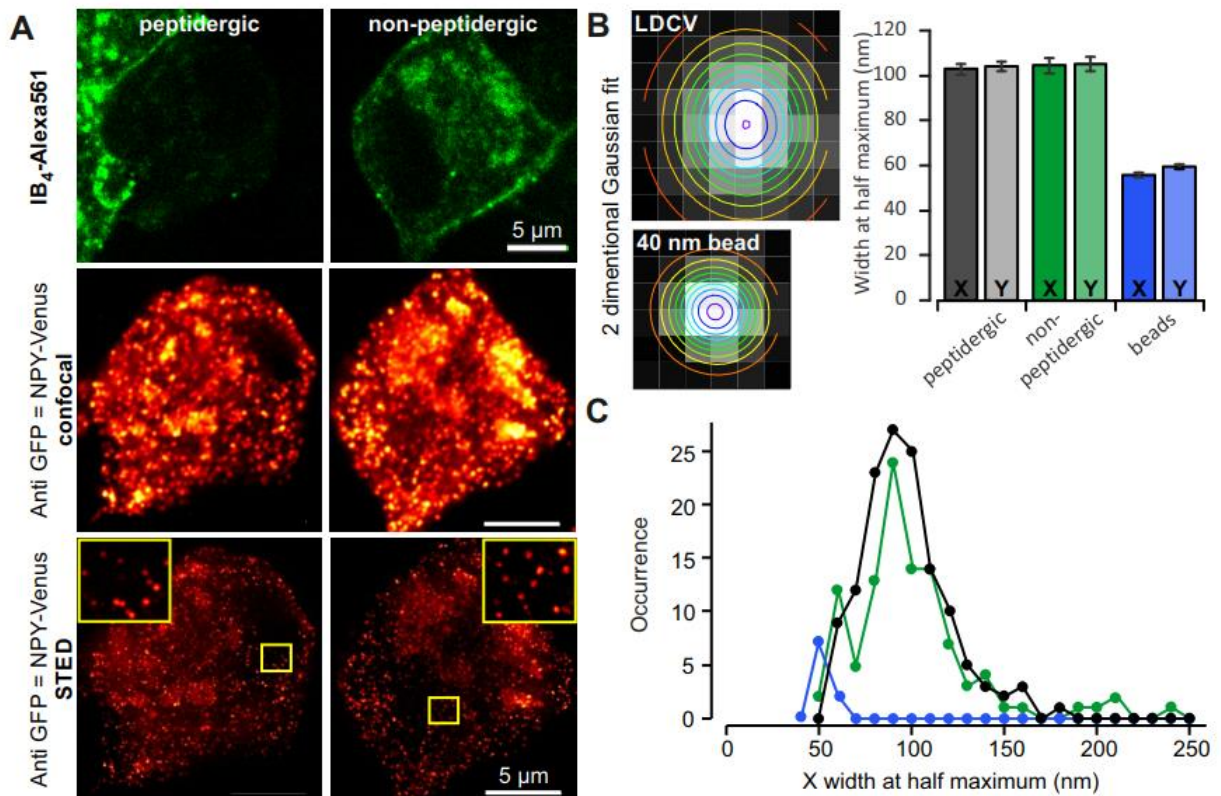


(A) Vesicles labeled with NPY-Venus had a diameter of  $103 \pm 2$  nm in both DRG neuron subtypes. Individual vesicle images were cut out of the image of the cell (top picture), imported in Igor (Wavemetrics) and fitted by equation 1 where  $A$  is the amplitude,  $cor$  the cross-correlation term that lays between -1 and 1,  $x_o$ ,  $y_o$  are the center coordinates and  $x_{width}$ ,  $y_{width}$  are the x and y half width at half maximum of the vesicle displayed in (B).

$$(1) f(x) = A \cdot \exp \left[ \frac{-1}{2(1-cor^2)} \left( \left( \frac{x-x_o}{x_{width}} \right)^2 + \left( \frac{y-y_o}{y_{width}} \right)^2 - \frac{2 \cdot cor \cdot (x-x_o)(y-y_o)}{x_{width} \cdot y_{width}} \right) \right]$$

In the graph we displayed the X and Y full width at half maximum of vesicles from peptidergic and non-peptidergic neurons. To insure that we had the resolution to be able to distinguish variations in vesicle size we imaged 40 nm large crimson red beads (Invitrogen, bottom picture) with the same STED settings as the used to image DRG neurons. Their apparent size was  $55.6 \pm 1.1$  nm well below the size of NPY-Venus labelled vesicles ( $n = 10$ ).

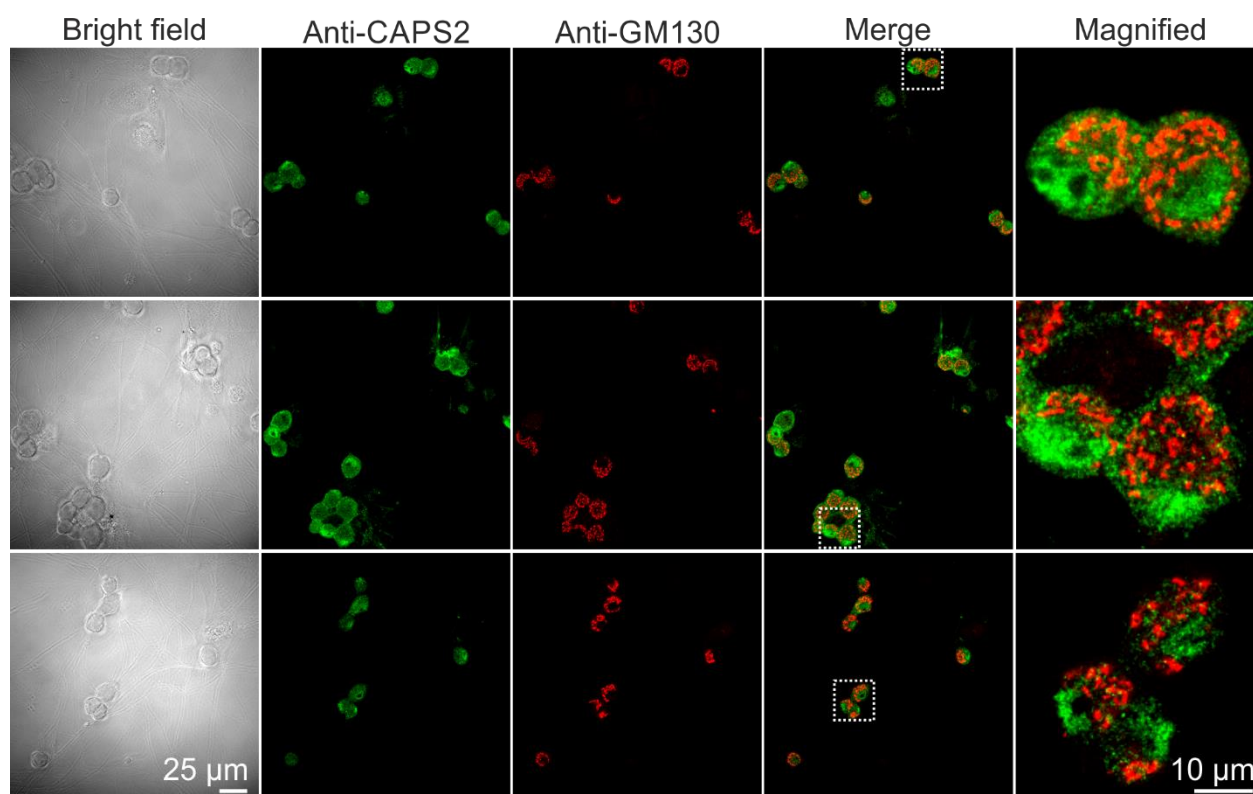
(C) The size distribution of NPY-Venus labeled vesicles show that they represent one population whether in peptidergic or non-peptidergic neurons.  $n_{neurons} = 7$  and  $6$ ,  $n_{LDCVs} = 135$  and  $105$  for peptidergic and non-peptidergic, respectively.





## VI.7 Golgi Staining

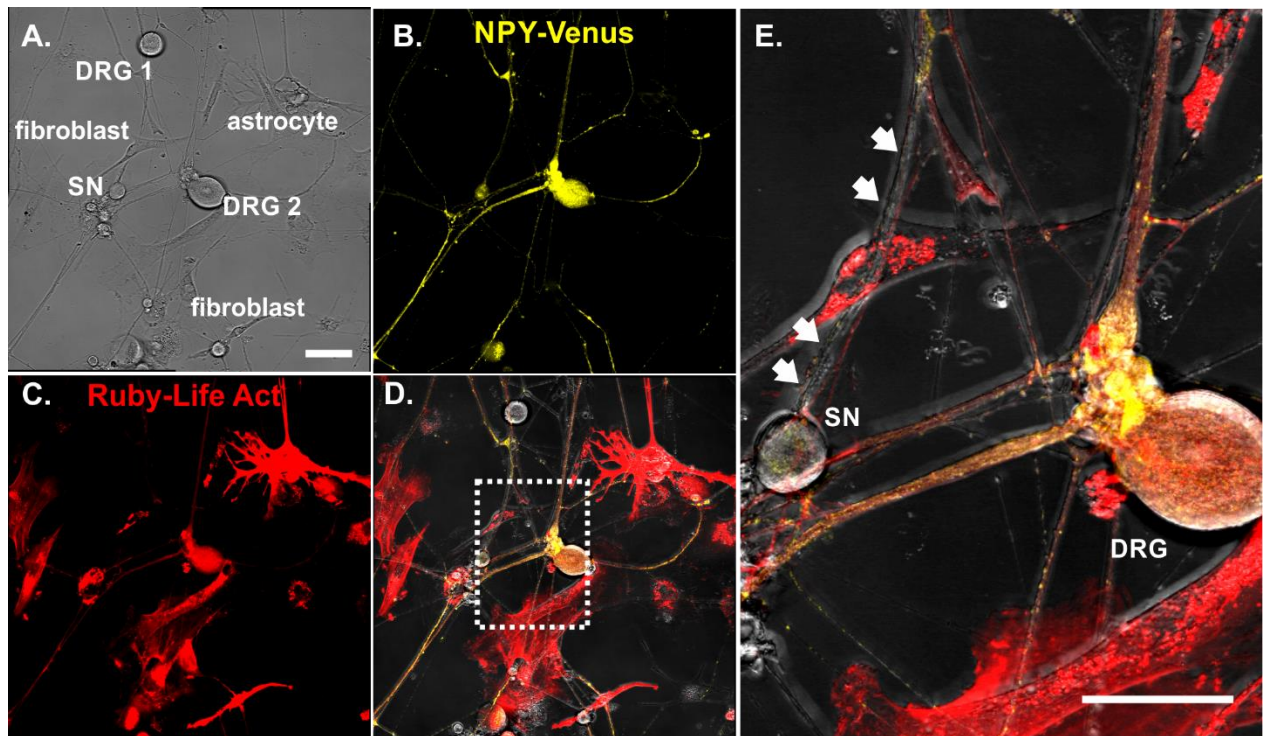
In the hopeful efforts to determine CAPS2 subcellular localization, we co-stained with CAPS2 purified serum 6 antibody and with anti-GM130 antibody, a *cis-Golgi* marker from Abcam (ab52649). Results showed there is no correlation between CAPS2 signal and *cis-Golgi* compartments. Further staining against other *Golgi* compartments were not successful. Unfortunately, it remains unknown at what subcellular compartment CAPS2 signal is enriched.



## VI.8 Life Act-Ruby Experiment

DRG neurons were double transfected by an Adenovirus that was kindly provided by Prof. Peter Lipp, encoding for Life Act tagged to Ruby fluorescent protein and a Lentivirus encoding for NPY-Venus. S neurons were added on the second day and images were acquired after 16 hrs using confocal microscope. (A) Bright field image composed of four stitched images with 12% overlap. (B) NPY-Venus signal imaged at 514 nm. (C) Life Act-Ruby imaged at 561 nm

wavelength. (D) Merged image that is magnified in (E.), the white arrows point to a process that originates from S neurons. Scale bar is 20  $\mu$ m.



## VI.9 List of Antibodies

Antibody	Host	Immunogen	Manufacturer & catalog no.	Working dilution
<i>Primary antibody</i>				
<b>CAPS1</b>	Rabbit	Recombinant protein (aa 18-107 of mouse CAPS 1)	Synaptic systems (No 262 013)	1:1000
<b>CAPS2</b>	Rabbit	Exon 1 of CAPS2e	Provided by M. Jung	1:1500
<b>Synaptophysin1 (monoclonal)</b>	Mouse	Clone 7.2	Synaptic systems (No. 101 011)	1:1000
<b>Bassoon</b>	Rabbit	Recombinant protein aa 330 – C terminal (rat)	Synaptic systems (No 141 003)	1:300
<b>PSD95 (monoclonal)</b>	Mouse	Fusion protein aa 77-299 (human)	NeuroMab (Clone K28/43)	1:500
<b>eGFP</b>	Rabbit	Full length protein	Life technologies (G10362)	1:20
<b>Chromogranin A</b>	Rabbit	Recombinant fragment from the C-terminal (human)	Abcam (ab15160)	1:1000
<b>B-actin</b>	Mouse	Monoclonal, clone AC-15	Sigma Aldrich (A1978)	1:5000
<i>Secondary antibody - Life Technologies, Invitrogen</i>				
<b>Alexa 488</b>		goat anti-mouse	A-11001	1:2000
<b>Alexa 647</b>		goat anti- mouse	A-21235	1:2000
<b>Alexa 488</b>		goat anti-rabbit	A-11008	1:2000
<b>Alexa 647</b>		goat anti-rabbit	A-21244	1:2000
<b>Fab fragments</b>		goat anti-mouse (IgG H&L)	Biomol: Rockland, (810-1102)	1:50
<b>STAR Red</b>		goat anti-rabbit (IgG)	Abberior (2-0012-011-9)	1:100

**Table 4** List of used antibodies.

## Publications

### **CAPS2 primes regulated peptide release while CAPS1 directly promotes synaptic transmission in murine dorsal root ganglion neurons**

Shaib AH., Harb A., Shaaban A., Klose M., Staudt A., Mohrmann R., Rettig J. and Becherer U.

(Manuscript in preparation)

### **Large dense core vesicle exocytosis from mouse dorsal root ganglion neurons is regulated by NPY**

Bost A., Shaib AH., Schwartz A., Niemeyer B., and Becherer U.

Neuroscience. Elsevier. December 2016.

### **Comparative analysis of the development of swarming communities of *Bacillus Subtilis* in case of Pta and ComXP mutant strains**

Hamze K., Zeaiter Z., Lakkis G., Shaib A., Kobaissi A.

International Journal of Scientific & Technology Research, Volume 4, Issue 11, November 2015. ISSN 2277-8616

## VII. References

- Abbe, E. (1873). Beiträge zur theorie des mikroskops und der mikroskopischen wahrnehmung (Contributions to the theory of the microscope and microscopic observations). *Arkiv Mikroskop Anat.*
- Abraira, V.E., and Ginty, D.D. (2013). The sensory neurons of touch. *Neuron* 79, 618-639.
- Adams, L.A., Ang, L.C., and Munoz, D.G. (1993). Chromogranin A, a soluble synaptic vesicle protein, is found in cortical neurons other than previously defined peptidergic neurons in the human neocortex. *Brain Res* 602, 336-341.
- Alberts, B., D. Bray, J. Lewis, M. Raff, K. Roberts, and J. D. Watson (1989). *Molecular Biology of the Cell*. New York: Garland Publishing.
- Alberts B, J.A., Lewis J (2002). *Molecular Biology of the Cell*. New York: Garland Science.
- Ann, K., Kowalchuk, J.A., Loyet, K.M., and Martin, T.F. (1997). Novel Ca<sup>2+</sup>-binding protein (CAPS) related to UNC-31 required for Ca<sup>2+</sup>-activated exocytosis. *J Biol Chem* 272, 19637-19640.
- Applegate, M.D., and Landfield, P.W. (1988). Synaptic vesicle redistribution during hippocampal frequency potentiation and depression in young and aged rats. *J Neurosci* 8, 1096-1111.
- Araque, A., Parpura, V., Sanzgiri, R.P., and Haydon, P.G. (1999a). Tripartite synapses: glia, the unacknowledged partner. *Trends Neurosci* 22, 208-215.
- Araque, A., Sanzgiri, R.P., Parpura, V., and Haydon, P.G. (1999b). Astrocyte-induced modulation of synaptic transmission. *Can J Physiol Pharmacol* 77, 699-706.
- Ashrafi, S., Betley, J.N., Comer, J.D., Brenner-Morton, S., Bar, V., Shimoda, Y., Watanabe, K., Peles, E., Jessell, T.M., and Kaltschmidt, J.A. (2014). Neuronal Ig/Caspr recognition promotes the formation of axoaxonic synapses in mouse spinal cord. *Neuron* 81, 120-129.
- Axelrod, D. (1981). Cell-substrate contacts illuminated by total internal reflection fluorescence. *J Cell Biol* 89, 141-145.
- Balkowiec, A., and Katz, D.M. (2002). Cellular mechanisms regulating activity-dependent release of native brain-derived neurotrophic factor from hippocampal neurons. *J Neurosci* 22, 10399-10407.
- Banerjee, D.K., Ornberg, R.L., Youdim, M.B., Heldman, E., and Pollard, H.B. (1985). Endothelial cells from bovine adrenal medulla develop capillary-like growth patterns in culture. *Proc Natl Acad Sci U S A* 82, 4702-4706.
- Barabas, M.E., Kossyrev, E.A., and Stucky, C.L. (2012). TRPA1 is functionally expressed primarily by IB4-binding, non-peptidergic mouse and rat sensory neurons. *PLoS One* 7, e47988.
- Barber, R.P., and Vaughn, J.E. (1986). Differentiation of dorsal root ganglion cells with processes in their synaptic target zone of embryonic mouse spinal cord: a retrograde tracer study. *J Neurocytol* 15, 207-218.
- Basarsky, T.A., Parpura, V., and Haydon, P.G. (1994). Hippocampal synaptogenesis in cell culture: developmental time course of synapse formation, calcium influx, and synaptic protein distribution. *J Neurosci* 14, 6402-6411.
- Bauerfeind, R., Ohashi, M., and Huttner, W.B. (1994). Biogenesis of secretory granules and synaptic vesicles. Facts and hypotheses. *Ann N Y Acad Sci* 733, 233-244.

- Beattie, E.C., Stellwagen, D., Morishita, W., Bresnahan, J.C., Ha, B.K., Von Zastrow, M., Beattie, M.S., and Malenka, R.C. (2002). Control of synaptic strength by glial TNF $\alpha$ . *Science* 295, 2282-2285.
- Becherer, U., and Rettig, J. (2006). Vesicle pools, docking, priming, and release. *Cell Tissue Res* 326, 393-407.
- Belanger, M., and Magistretti, P.J. (2009). The role of astroglia in neuroprotection. *Dialogues Clin Neurosci* 11, 281-295.
- Bennett, M.K., and Scheller, R.H. (1994). A molecular description of synaptic vesicle membrane trafficking. *Annu Rev Biochem* 63, 63-100.
- Berwin, B., Floor, E., and Martin, T.F. (1998). CAPS (mammalian UNC-31) protein localizes to membranes involved in dense-core vesicle exocytosis. *Neuron* 21, 137-145.
- Betley, J.N., Wright, C.V., Kawaguchi, Y., Erdelyi, F., Szabo, G., Jessell, T.M., and Kaltschmidt, J.A. (2009). Stringent specificity in the construction of a GABAergic presynaptic inhibitory circuit. *Cell* 139, 161-174.
- Bichara, M., Pinet, I., Schumacher, S., and Fuchs, R.P. (2000). Mechanisms of dinucleotide repeat instability in *Escherichia coli*. *Genetics* 154, 533-542.
- Blaschko, H.M., E. (1967). Catecholamines. Springer-Verlag Berlin, Heidelberg and New York.
- Bolte, S., and Cordelieres, F.P. (2006). A guided tour into subcellular colocalization analysis in light microscopy. *J Microsc* 224, 213-232.
- Bonora, E., Graziano, C., Minopoli, F., Bacchelli, E., Magini, P., Diquigiovanni, C., Lomartire, S., Bianco, F., Vargiolu, M., Parchi, P., *et al.* (2014). Maternally inherited genetic variants of CADPS2 are present in autism spectrum disorders and intellectual disability patients. *EMBO Mol Med* 6, 795-809.
- Bost, A., Shaib, A.H., Schwarz, Y., Niemeyer, B.A., and Becherer, U. (2017). Large dense-core vesicle exocytosis from mouse dorsal root ganglion neurons is regulated by neuropeptide Y. *Neuroscience*.
- Bradbury, E.J., Burnstock, G., and McMahon, S.B. (1998). The expression of P2X3 purinoreceptors in sensory neurons: effects of axotomy and glial-derived neurotrophic factor. *Mol Cell Neurosci* 12, 256-268.
- Brandstatter, J.H., Fletcher, E.L., Garner, C.C., Gundelfinger, E.D., and Wassle, H. (1999). Differential expression of the presynaptic cytomatrix protein bassoon among ribbon synapses in the mammalian retina. *Eur J Neurosci* 11, 3683-3693.
- Brewer, G.J., and Cotman, C.W. (1989). Survival and growth of hippocampal neurons in defined medium at low density: advantages of a sandwich culture technique or low oxygen. *Brain Res* 494, 65-74.
- Bruder, E.D., Lee, J.J., Widmaier, E.P., and Raff, H. (2007). Microarray and real-time PCR analysis of adrenal gland gene expression in the 7-day-old rat: effects of hypoxia from birth. *Physiol Genomics* 29, 193-200.
- Brunger, A.T. (2005). Structure and function of SNARE and SNARE-interacting proteins. *Q Rev Biophys* 38, 1-47.
- Burry, R.W. (2011). Controls for immunocytochemistry: an update. *J Histochem Cytochem* 59, 6-12.
- Caceres, A., Banker, G.A., and Binder, L. (1986). Immunocytochemical localization of tubulin and microtubule-associated protein 2 during the development of hippocampal neurons in culture. *J Neurosci* 6, 714-722.
- Cao, D.S., Yu, S.Q., and Premkumar, L.S. (2009). Modulation of transient receptor potential Vanilloid 4-mediated membrane currents and synaptic transmission by protein kinase C. *Mol Pain* 5, 5.

- Cascieri, M.A., Ber, E., Fong, T.M., Sadowski, S., Bansal, A., Swain, C., Seward, E., Frances, B., Burns, D., and Strader, C.D. (1992). Characterization of the binding of a potent, selective, radioiodinated antagonist to the human neurokinin-1 receptor. *Mol Pharmacol* 42, 458-463.
- Castillo, P.E. (2012). Presynaptic LTP and LTD of excitatory and inhibitory synapses. *Cold Spring Harb Perspect Biol* 4.
- Cazorla, M., Jouvenceau, A., Rose, C., Guilloux, J.P., Pilon, C., Dranovsky, A., and Premont, J. (2010). Cyclothiazin-B, the first highly potent and selective TrkB inhibitor, has anxiolytic properties in mice. *PLoS One* 5, e9777.
- Cesare, P., and McNaughton, P. (1996). A novel heat-activated current in nociceptive neurons and its sensitization by bradykinin. *Proc Natl Acad Sci U S A* 93, 15435-15439.
- Chen, G., and van den Pol, A.N. (1996). Multiple NPY receptors coexist in pre- and postsynaptic sites: inhibition of GABA release in isolated self-innervating SCN neurons. *J Neurosci* 16, 7711-7724.
- Cho, K.O., Hunt, C.A., and Kennedy, M.B. (1992). The rat brain postsynaptic density fraction contains a homolog of the *Drosophila* discs-large tumor suppressor protein. *Neuron* 9, 929-942.
- Cisternas, F.A., Vincent, J.B., Scherer, S.W., and Ray, P.N. (2003). Cloning and characterization of human CADPS and CADPS2, new members of the Ca<sup>2+</sup>-dependent activator for secretion protein family. *Genomics* 81, 279-291.
- Coons, A.H., Creech, H. J. & Jones, R. N. (1941). Immunological properties of an antibody containing a fluorescent group. *Proc Soc Expt Biol Med* 47, 200-202.
- Craig, A.D. (2009). How do you feel--now? The anterior insula and human awareness. *Nat Rev Neurosci* 10, 59-70.
- Dasgupta, B., Kozlowski, E., Schroeder, D.R., Torrente, J.R., Xu, C., Pin, S., Conway, C.M., Dubowchik, G.M., Macor, J.E., and Vrudhula, V.M. (2014). Serendipitous oxidation product of BIBN4096BS: a potent CGRP receptor antagonist. *Bioorg Med Chem Lett* 24, 2744-2748.
- De-Miguel, F.F., and Trueta, C. (2005). Synaptic and extrasynaptic secretion of serotonin. *Cell Mol Neurobiol* 25, 297-312.
- De Camilli, P., and Jahn, R. (1990). Pathways to regulated exocytosis in neurons. *Annu Rev Physiol* 52, 625-645.
- De Duve, C. (1963). The lysosome. *Sci Am* 208, 64-72.
- de Kock, C.P., Wierda, K.D., Bosman, L.W., Min, R., Koksma, J.J., Mansvelder, H.D., Verhage, M., and Brussaard, A.B. (2003). Somatodendritic secretion in oxytocin neurons is upregulated during the female reproductive cycle. *J Neurosci* 23, 2726-2734.
- Doods, H., Hallermayer, G., Wu, D., Entzeroth, M., Rudolf, K., Engel, W., and Eberlein, W. (2000). Pharmacological profile of BIBN4096BS, the first selective small molecule CGRP antagonist. *Br J Pharmacol* 129, 420-423.
- Dull, T., Zufferey, R., Kelly, M., Mandel, R.J., Nguyen, M., Trono, D., and Naldini, L. (1998). A third-generation lentivirus vector with a conditional packaging system. *J Virol* 72, 8463-8471.
- Dykes, I.M., Lanier, J., Eng, S.R., and Turner, E.E. (2010). Brn3a regulates neuronal subtype specification in the trigeminal ganglion by promoting Runx expression during sensory differentiation. *Neural Dev* 5, 3.
- Eckenstaler, R., Lessmann, V., and Brigadski, T. (2016). CAPS1 effects on intragranular pH and regulation of BDNF release from secretory granules in hippocampal neurons. *J Cell Sci* 129, 1378-1390.



- Elhamdani, A., Martin, T.F., Kowalchuk, J.A., and Artalejo, C.R. (1999).  $\text{Ca}^{2+}$ -dependent activator protein for secretion is critical for the fusion of dense-core vesicles with the membrane in calf adrenal chromaffin cells. *J Neurosci* 19, 7375-7383.
- Faisal A. Al-Allaf, O.E.T., Lia Paola Zambetti, Viktoria Tchetchelnitski, and Huseyin Mehmet (2012). Remarkable stability of an instability-prone lentiviral vector plasmid in *Escherichia coli* Stbl3.
- Faissner, A., Pyka, M., Geissler, M., Sobik, T., Frischknecht, R., Gundelfinger, E.D., and Seidenbecher, C. (2010). Contributions of astrocytes to synapse formation and maturation - Potential functions of the perisynaptic extracellular matrix. *Brain Res Rev* 63, 26-38.
- Fang, Z., Forslund, N., Takenaga, K., Lukanidin, E., and Kozlova, E.N. (2006). Sensory neurite outgrowth on white matter astrocytes is influenced by intracellular and extracellular S100A4 protein. *J Neurosci Res* 83, 619-626.
- Farina, M., van de Bospoort, R., He, E., Persoon, C.M., van Weering, J.R., Broeke, J.H., Verhage, M., and Toonen, R.F. (2015). CAPS-1 promotes fusion competence of stationary dense-core vesicles in presynaptic terminals of mammalian neurons. *Elife* 4.
- Fasshauer, D. (2003). Structural insights into the SNARE mechanism. *Biochim Biophys Acta* 1641, 87-97.
- Fiebig, K.M., Rice, L.M., Pollock, E., and Brunger, A.T. (1999). Folding intermediates of SNARE complex assembly. *Nat Struct Biol* 6, 117-123.
- Fischer, I., Shea, T.B., Sapirstein, V.S., and Kosik, K.S. (1986). Expression and distribution of microtubule-associated protein 2 (MAP2) in neuroblastoma and primary neuronal cells. *Brain Res* 390, 99-109.
- Fletcher, T.L., De Camilli, P., and Banker, G. (1994). Synaptogenesis in hippocampal cultures: evidence indicating that axons and dendrites become competent to form synapses at different stages of neuronal development. *J Neurosci* 14, 6695-6706.
- Fong, T.M., Huang, R.R., and Strader, C.D. (1992). Localization of agonist and antagonist binding domains of the human neurokinin-1 receptor. *J Biol Chem* 267, 25664-25667.
- Frick, M., Eschertzhuber, S., Haller, T., Mair, N., and Dietl, P. (2001). Secretion in alveolar type II cells at the interface of constitutive and regulated exocytosis. *Am J Respir Cell Mol Biol* 25, 306-315.
- Fujita, Y., Xu, A., Xie, L., Arunachalam, L., Chou, T.C., Jiang, T., Chiew, S.K., Kourtesis, J., Wang, L., Gaisano, H.Y., *et al.* (2007).  $\text{Ca}^{2+}$ -dependent activator protein for secretion 1 is critical for constitutive and regulated exocytosis but not for loading of transmitters into dense core vesicles. *J Biol Chem* 282, 21392-21403.
- Fullmer, J.M., Riedl, M.S., Higgins, L., and Elde, R. (2004). Identification of some lectin IB4 binding proteins in rat dorsal root ganglia. *Neuroreport* 15, 1705-1709.
- Futai, K., Kim, M.J., Hashikawa, T., Scheiffele, P., Sheng, M., and Hayashi, Y. (2007). Retrograde modulation of presynaptic release probability through signaling mediated by PSD-95-neurologin. *Nat Neurosci* 10, 186-195.
- Gartner, A., and Staiger, V. (2002). Neurotrophin secretion from hippocampal neurons evoked by long-term-potential-inducing electrical stimulation patterns. *Proc Natl Acad Sci U S A* 99, 6386-6391.
- Gehlert, D.R. (1999). Role of hypothalamic neuropeptide Y in feeding and obesity. *Neuropeptides* 33, 329-338.
- Goers, L., Freemont, P., and Polizzi, K.M. (2014). Co-culture systems and technologies: taking synthetic biology to the next level. *J R Soc Interface* 11.

- Gottmann, K. (2008). Transsynaptic modulation of the synaptic vesicle cycle by cell-adhesion molecules. *J Neurosci Res* 86, 223-232.
- Granseth, B., Odermatt, B., Royle, S.J., and Lagnado, L. (2006). Clathrin-mediated endocytosis is the dominant mechanism of vesicle retrieval at hippocampal synapses. *Neuron* 51, 773-786.
- Green, E.L. (1941). Genetic and Non-Genetic Factors Which Influence the Type of the Skeleton in an Inbred Strain of Mice. *Genetics* 26, 192-222.
- Greenwood-Van Meerveld, B., Mohammadi, E., Tyler, K., Pietra, C., Bee, L.A., and Dickenson, A. (2014). Synergistic effect of 5-hydroxytryptamine 3 and neurokinin 1 receptor antagonism in rodent models of somatic and visceral pain. *J Pharmacol Exp Ther* 351, 146-152.
- Grishanin, R.N., Kowalchuk, J.A., Klenchin, V.A., Ann, K., Earles, C.A., Chapman, E.R., Gerona, R.R., and Martin, T.F. (2004). CAPS acts at a pre-fusion step in dense-core vesicle exocytosis as a PIP2 binding protein. *Neuron* 43, 551-562.
- Grosshans, B.L., Ortiz, D., and Novick, P. (2006). Rabs and their effectors: achieving specificity in membrane traffic. *Proc Natl Acad Sci U S A* 103, 11821-11827.
- Gu, J.G., and MacDermott, A.B. (1997). Activation of ATP P2X receptors elicits glutamate release from sensory neuron synapses. *Nature* 389, 749-753.
- Gu, Y., Chen, Y., Zhang, X., Li, G.W., Wang, C., and Huang, L.Y. (2010). Neuronal soma-satellite glial cell interactions in sensory ganglia and the participation of purinergic receptors. *Neuron Glia Biol* 6, 53-62.
- Guenard, V., Gwynn, L.A., and Wood, P.M. (1994). Astrocytes inhibit Schwann cell proliferation and myelination of dorsal root ganglion neurons in vitro. *J Neurosci* 14, 2980-2992.
- Guo, A., Vulchanova, L., Wang, J., Li, X., and Elde, R. (1999). Immunocytochemical localization of the vanilloid receptor 1 (VR1): relationship to neuropeptides, the P2X3 purinoceptor and IB4 binding sites. *Eur J Neurosci* 11, 946-958.
- Gustafsson, M.G. (2000). Surpassing the lateral resolution limit by a factor of two using structured illumination microscopy. *J Microsc* 198, 82-87.
- Gustafsson, M.G. (2005). Nonlinear structured-illumination microscopy: wide-field fluorescence imaging with theoretically unlimited resolution. *Proc Natl Acad Sci U S A* 102, 13081-13086.
- Gustafsson, M.G.L.A., D.A.; Sedat, J.W (1997). US patent 5671085, cols. 23–25.
- Hall, A.K., Ai, X., Hickman, G.E., MacPhedran, S.E., Nduaguba, C.O., and Robertson, C.P. (1997). The generation of neuronal heterogeneity in a rat sensory ganglion. *J Neurosci* 17, 2775-2784.
- Hanson, P.I., Roth, R., Morisaki, H., Jahn, R., and Heuser, J.E. (1997). Structure and conformational changes in NSF and its membrane receptor complexes visualized by quick-freeze/deep-etch electron microscopy. *Cell* 90, 523-535.
- Heikkinen, A., Pihlajaniemi, T., Faissner, A., and Yuzaki, M. (2014). Neural ECM and synaptogenesis. *Prog Brain Res* 214, 29-51.
- Heintzmann, R.C., C. (1998). Laterally modulated excitation microscopy: improvement of resolution by using a diffraction grating. *Proc SPIE* 3568, 185-195.

- Hendrich, J., Bauer, C.S., and Dolphin, A.C. (2012). Chronic pregabalin inhibits synaptic transmission between rat dorsal root ganglion and dorsal horn neurons in culture. *Channels (Austin)* 6, 124-132.
- Hong, W. (2005). SNAREs and traffic. *Biochim Biophys Acta* 1744, 120-144.
- Horie, H., and Kim, S.U. (1984). Improved survival and differentiation of newborn and adult mouse neurons in F12 defined medium by fibronectin. *Brain Res* 294, 178-181.
- Huang, L.Y., and Neher, E. (1996). Ca(2+)-dependent exocytosis in the somata of dorsal root ganglion neurons. *Neuron* 17, 135-145.
- Hunt, C.A., Schenker, L.J., and Kennedy, M.B. (1996). PSD-95 is associated with the postsynaptic density and not with the presynaptic membrane at forebrain synapses. *J Neurosci* 16, 1380-1388.
- Hunt, S.P., and Mantyh, P.W. (2001). The molecular dynamics of pain control. *Nat Rev Neurosci* 2, 83-91.
- Ibanez, C.F., and Ernfors, P. (2007). Hierarchical control of sensory neuron development by neurotrophic factors. *Neuron* 54, 673-675.
- Ishikawa, T., Miyagi, M., Ohtori, S., Aoki, Y., Ozawa, T., Doya, H., Saito, T., Moriya, H., and Takahashi, K. (2005). Characteristics of sensory DRG neurons innervating the lumbar facet joints in rats. *Eur Spine J* 14, 559-564.
- Jacobs, J.M., and Meyer, T. (1997). Control of action potential-induced Ca<sup>2+</sup> signaling in the soma of hippocampal neurons by Ca<sup>2+</sup> release from intracellular stores. *J Neurosci* 17, 4129-4135.
- Jahn, R., and Scheller, R.H. (2006). SNAREs--engines for membrane fusion. *Nat Rev Mol Cell Biol* 7, 631-643.
- Jahn, R., Schiebler, W., Ouimet, C., and Greengard, P. (1985). A 38,000-dalton membrane protein (p38) present in synaptic vesicles. *Proc Natl Acad Sci U S A* 82, 4137-4141.
- Jahn, R., and Sudhof, T.C. (1993). Synaptic vesicle traffic: rush hour in the nerve terminal. *J Neurochem* 61, 12-21.
- Jahr, C.E., and Jessell, T.M. (1985). Synaptic transmission between dorsal root ganglion and dorsal horn neurons in culture: antagonism of monosynaptic excitatory postsynaptic potentials and glutamate excitation by kynurenate. *J Neurosci* 5, 2281-2289.
- Jockusch, W.J., Speidel, D., Sigler, A., Sorensen, J.B., Varoqueaux, F., Rhee, J.S., and Brose, N. (2007). CAPS-1 and CAPS-2 are essential synaptic vesicle priming proteins. *Cell* 131, 796-808.
- Johnson, D.E., Ai, H.W., Wong, P., Young, J.D., Campbell, R.E., and Casey, J.R. (2009). Red fluorescent protein pH biosensor to detect concentrative nucleoside transport. *J Biol Chem* 284, 20499-20511.
- Johnson, J.L., Monfregola, J., Napolitano, G., Kiosses, W.B., and Catz, S.D. (2012). Vesicular trafficking through cortical actin during exocytosis is regulated by the Rab27a effector JFC1/Slp1 and the RhoA-GTPase-activating protein Gem-interacting protein. *Mol Biol Cell* 23, 1902-1916.
- Jordt, S.E., Bautista, D.M., Chuang, H.H., McKemy, D.D., Zygmunt, P.M., Hogestatt, E.D., Meng, I.D., and Julius, D. (2004). Mustard oils and cannabinoids excite sensory nerve fibres through the TRP channel ANKTM1. *Nature* 427, 260-265.
- Joseph, D.J., Choudhury, P., and Macdermott, A.B. (2010). An in vitro assay system for studying synapse formation between nociceptive dorsal root ganglion and dorsal horn neurons. *J Neurosci Methods* 189, 197-204.

- Joseph, D.J., Williams, D.J., and MacDermott, A.B. (2011). Modulation of neurite outgrowth by activation of calcium-permeable kainate receptors expressed by rat nociceptive-like dorsal root ganglion neurons. *Dev Neurobiol* 71, 818-835.
- Kang, H.K., and Cox, D.W. (1996). Tandem repeats 3' of the IGHA genes in the human immunoglobulin heavy chain gene cluster. *Genomics* 35, 189-195.
- Kettenmann, H., and Verkhratsky, A. (2011). [Neuroglia--living nerve glue]. *Fortschr Neurol Psychiatr* 79, 588-597.
- Khasabov, S.G., Rogers, S.D., Ghilardi, J.R., Peters, C.M., Mantyh, P.W., and Simone, D.A. (2002). Spinal neurons that possess the substance P receptor are required for the development of central sensitization. *J Neurosci* 22, 9086-9098.
- Kirshner, N., Corcoran, J.J., and Erickson, H.P. (1989). Synthesis of alpha 2-macroglobulin by bovine adrenal cortical cell cultures. *Am J Physiol* 256, C779-785.
- Klenchin, V.A., and Martin, T.F. (2000). Priming in exocytosis: attaining fusion-competence after vesicle docking. *Biochimie* 82, 399-407.
- Koizumi, S., Fujishita, K., Inoue, K., Shigemoto-Mogami, Y., Tsuda, M., and Inoue, K. (2004). Ca<sup>2+</sup> waves in keratinocytes are transmitted to sensory neurons: the involvement of extracellular ATP and P2Y<sub>2</sub> receptor activation. *Biochem J* 380, 329-338.
- Kubo, A., Katanosaka, K., and Mizumura, K. (2012). Extracellular matrix proteoglycan plays a pivotal role in sensitization by low pH of mechanosensitive currents in nociceptive sensory neurones. *J Physiol* 590, 2995-3007.
- Kuznetsov, S.A., Langford, G.M., and Weiss, D.G. (1992). Actin-dependent organelle movement in squid axoplasm. *Nature* 356, 722-725.
- Kwon, S.E., and Chapman, E.R. (2011). Synaptophysin regulates the kinetics of synaptic vesicle endocytosis in central neurons. *Neuron* 70, 847-854.
- Labrakakis, C., Gerstner, E., and MacDermott, A.B. (2000). Adenosine triphosphate-evoked currents in cultured dorsal root ganglion neurons obtained from rat embryos: desensitization kinetics and modulation of glutamate release. *Neuroscience* 101, 1117-1126.
- Lacor, P.N., Grayson, D.R., Auta, J., Sugaya, I., Costa, E., and Guidotti, A. (2000). Reelin secretion from glutamatergic neurons in culture is independent from neurotransmitter regulation. *Proc Natl Acad Sci U S A* 97, 3556-3561.
- Lang, T., Wacker, I., Wunderlich, I., Rohrbach, A., Giese, G., Soldati, T., and Almers, W. (2000). Role of actin cortex in the subplasmalemmal transport of secretory granules in PC-12 cells. *Biophys J* 78, 2863-2877.
- Lee, Y., Takami, K., Kawai, Y., Girgis, S., Hillyard, C.J., MacIntyre, I., Emson, P.C., and Tohyama, M. (1985). Distribution of calcitonin gene-related peptide in the rat peripheral nervous system with reference to its coexistence with substance P. *Neuroscience* 15, 1227-1237.
- Li, H., Foss, S.M., Dobryy, Y.L., Park, C.K., Hires, S.A., Shaner, N.C., Tsien, R.Y., Osborne, L.C., and Voglmaier, S.M. (2011). Concurrent imaging of synaptic vesicle recycling and calcium dynamics. *Front Mol Neurosci* 4, 34.
- Lin, R.C., and Scheller, R.H. (1997). Structural organization of the synaptic exocytosis core complex. *Neuron* 19, 1087-1094.

- Liu, T., Shang, S.J., Liu, B., Wang, C.H., Wang, Y.S., Xiong, W., Zheng, L.H., Zhang, C.X., and Zhou, Z. (2011). Two distinct vesicle pools for depolarization-induced exocytosis in somata of dorsal root ganglion neurons. *J Physiol* 589, 3507-3515.
- Liu, Y., Schirra, C., Edelmann, L., Matti, U., Rhee, J., Hof, D., Bruns, D., Brose, N., Rieger, H., Stevens, D.R., *et al.* (2010). Two distinct secretory vesicle-priming steps in adrenal chromaffin cells. *The Journal of cell biology* 190, 1067-1077.
- Liu, Y., Schirra, C., Stevens, D.R., Matti, U., Speidel, D., Hof, D., Bruns, D., Brose, N., and Rettig, J. (2008). CAPS facilitates filling of the rapidly releasable pool of large dense-core vesicles. *J Neurosci* 28, 5594-5601.
- Liu, Y., Schweitzer, E.S., Nirenberg, M.J., Pickel, V.M., Evans, C.J., and Edwards, R.H. (1994). Preferential localization of a vesicular monoamine transporter to dense core vesicles in PC12 cells. *J Cell Biol* 127, 1419-1433.
- Lodish H, B.A., Zipursky SL, et al. (2000). *Molecular Cell Biology*. New York: W H Freeman.
- Lowe, M. (2000). Membrane transport: tethers and TRAPPs. *Curr Biol* 10, R407-409.
- Lumpkin, E.A., and Bautista, D.M. (2005). Feeling the pressure in mammalian somatosensation. *Curr Opin Neurobiol* 15, 382-388.
- Malenka, R.C., and Nicoll, R.A. (1999). Long-term potentiation--a decade of progress? *Science* 285, 1870-1874.
- Malin, S.A., Davis, B.M., and Molliver, D.C. (2007). Production of dissociated sensory neuron cultures and considerations for their use in studying neuronal function and plasticity. *Nat Protoc* 2, 152-160.
- Man, K.N., Imig, C., Walter, A.M., Pinheiro, P.S., Stevens, D.R., Rettig, J., Sorensen, J.B., Cooper, B.H., Brose, N., and Wojcik, S.M. (2015). Identification of a Munc13-sensitive step in chromaffin cell large dense-core vesicle exocytosis. *Elife* 4.
- Manneville, J.B., Etienne-Manneville, S., Skehel, P., Carter, T., Ogden, D., and Ferenczi, M. (2003). Interaction of the actin cytoskeleton with microtubules regulates secretory organelle movement near the plasma membrane in human endothelial cells. *J Cell Sci* 116, 3927-3938.
- Mao, Y., Yan, R., Li, A., Zhang, Y., Li, J., Du, H., Chen, B., Wei, W., Zhang, Y., Sumners, C., *et al.* (2015). Lentiviral Vectors Mediate Long-Term and High Efficiency Transgene Expression in HEK 293T cells. *Int J Med Sci* 12, 407-415.
- Martin, T.F., and Kowalchuk, J.A. (1997). Docked secretory vesicles undergo Ca<sup>2+</sup>-activated exocytosis in a cell-free system. *J Biol Chem* 272, 14447-14453.
- Martinez, A.N., Ramesh, G., Jacobs, M.B., and Philipp, M.T. (2015). Antagonist of the neurokinin-1 receptor curbs neuroinflammation in ex vivo and in vitro models of Lyme neuroborreliosis. *J Neuroinflammation* 12, 243.
- Matti, U., Pattu, V., Halimani, M., Schirra, C., Krause, E., Liu, Y., Weins, L., Chang, H.F., Guzman, R., Olausson, J., *et al.* (2013). Synaptobrevin2 is the v-SNARE required for cytotoxic T-lymphocyte lytic granule fusion. *Nat Commun* 4, 1439.
- McCarter, G.C., Reichling, D.B., and Levine, J.D. (1999). Mechanical transduction by rat dorsal root ganglion neurons in vitro. *Neurosci Lett* 273, 179-182.
- McLeod, A.L., Krause, J.E., Cuello, A.C., and Ribeiro-da-Silva, A. (1998). Preferential synaptic relationships between substance P-immunoreactive boutons and neurokinin 1 receptor sites in the rat spinal cord. *Proc Natl Acad Sci U S A* 95, 15775-15780.

- Melli, G., and Hoke, A. (2009). Dorsal Root Ganglia Sensory Neuronal Cultures: a tool for drug discovery for peripheral neuropathies. *Expert Opin Drug Discov* 4, 1035-1045.
- Miesenbock, G., De Angelis, D.A., and Rothman, J.E. (1998). Visualizing secretion and synaptic transmission with pH-sensitive green fluorescent proteins. *Nature* 394, 192-195.
- MJ., C. (1965). *The Anatomy of the Laboratory Mouse*. Academic Press London.
- Molander, C., and Grant, G. (1987). Spinal cord projections from hindlimb muscle nerves in the rat studied by transganglionic transport of horseradish peroxidase, wheat germ agglutinin conjugated horseradish peroxidase, or horseradish peroxidase with dimethylsulfoxide. *J Comp Neurol* 260, 246-255.
- Molliver, D.C., Wright, D.E., Leitner, M.L., Parsadanian, A.S., Doster, K., Wen, D., Yan, Q., and Snider, W.D. (1997). IB4-binding DRG neurons switch from NGF to GDNF dependence in early postnatal life. *Neuron* 19, 849-861.
- Naora, H. (1951). Microspectrophotometry and cytochemical analysis of nucleic acids. *Science* 114, 279-280.
- Navone, F., Di Gioia, G., Jahn, R., Browning, M., Greengard, P., and De Camilli, P. (1989). Microvesicles of the neurohypophysis are biochemically related to small synaptic vesicles of presynaptic nerve terminals. *J Cell Biol* 109, 3425-3433.
- Nedergaard, M., and Verkhratsky, A. (2012). Artifact versus reality--how astrocytes contribute to synaptic events. *Glia* 60, 1013-1023.
- Nguyen Truong, C.Q., Nestvogel, D., Ratai, O., Schirra, C., Stevens, D.R., Brose, N., Rhee, J., and Rettig, J. (2014). Secretory vesicle priming by CAPS is independent of its SNARE-binding MUN domain. *Cell Rep* 9, 902-909.
- Nicholson, K.L., Munson, M., Miller, R.B., Filip, T.J., Fairman, R., and Hughson, F.M. (1998). Regulation of SNARE complex assembly by an N-terminal domain of the t-SNARE Sso1p. *Nat Struct Biol* 5, 793-802.
- Nitzan-Luques, A., Minert, A., Devor, M., and Tal, M. (2013). Dynamic genotype-selective "phenotypic switching" of CGRP expression contributes to differential neuropathic pain phenotype. *Exp Neurol* 250, 194-204.
- Nuki, C., Kawasaki, H., Takasaki, K., and Wada, A. (1994). Pharmacological characterization of presynaptic calcitonin gene-related peptide (CGRP) receptors on CGRP-containing vasodilator nerves in rat mesenteric resistance vessels. *J Pharmacol Exp Ther* 268, 59-64.
- O'Connor, D.T., Mahata, S.K., Mahata, M., Jiang, Q., Hook, V.Y., and Taupenot, L. (2007). Primary culture of bovine chromaffin cells. *Nat Protoc* 2, 1248-1253.
- Obrietan, K., and van den Pol, A.N. (1996). Neuropeptide Y depresses GABA-mediated calcium transients in developing suprachiasmatic nucleus neurons: a novel form of calcium long-term depression. *J Neurosci* 16, 3521-3533.
- Ohshiro, H., Ogawa, S., and Shinjo, K. (2007). Visualizing sensory transmission between dorsal root ganglion and dorsal horn neurons in co-culture with calcium imaging. *J Neurosci Methods* 165, 49-54.
- Okamoto, N., Hatsukawa, Y., Shimojima, K., and Yamamoto, T. (2011). Submicroscopic deletion in 7q31 encompassing CADPS2 and TSPAN12 in a child with autism spectrum disorder and PHPV. *Am J Med Genet A* 155A, 1568-1573.
- Ooij, C.v. (2009). Recipe for fluorescent antibodies. *Nature*.

- Park, Y., and Kim, K.T. (2009). Short-term plasticity of small synaptic vesicle (SSV) and large dense-core vesicle (LDCV) exocytosis. *Cell Signal* *21*, 1465-1470.
- Parpura, V., and Verkhratsky, A. (2012). Neuroglia at the crossroads of homeostasis, metabolism and signalling: evolution of the concept. *ASN Neuro* *4*, 201-205.
- Patapoutian, A., Peier, A.M., Story, G.M., and Viswanath, V. (2003). ThermoTRP channels and beyond: mechanisms of temperature sensation. *Nat Rev Neurosci* *4*, 529-539.
- Peier, A.M., Reeve, A.J., Andersson, D.A., Moqrich, A., Earley, T.J., Hergarden, A.C., Story, G.M., Colley, S., Hogenesch, J.B., McIntyre, P., *et al.* (2002). A heat-sensitive TRP channel expressed in keratinocytes. *Science* *296*, 2046-2049.
- Pevsner, J., Hsu, S.C., Braun, J.E., Calakos, N., Ting, A.E., Bennett, M.K., and Scheller, R.H. (1994). Specificity and regulation of a synaptic vesicle docking complex. *Neuron* *13*, 353-361.
- Pfrieger, F.W., and Barres, B.A. (1997). Synaptic efficacy enhanced by glial cells in vitro. *Science* *277*, 1684-1687.
- Piekut, D.T. (1985). Ultrastructural studies on the afferent synaptic input to oxytocin-containing neurons in the paraventricular nucleus of the hypothalamus. *J Ultrastruct Res* *90*, 71-79.
- Pierce, L.M., Rankin, M.R., Foster, R.T., Dolber, P.C., Coates, K.W., Kuehl, T.J., and Thor, K.B. (2006). Distribution and immunohistochemical characterization of primary afferent neurons innervating the levator ani muscle of the female squirrel monkey. *Am J Obstet Gynecol* *195*, 987-996.
- Poirier, M.A., Xiao, W., Macosko, J.C., Chan, C., Shin, Y.K., and Bennett, M.K. (1998). The synaptic SNARE complex is a parallel four-stranded helical bundle. *Nat Struct Biol* *5*, 765-769.
- Pysh, J.J., and Wiley, R.G. (1974). Synaptic vesicle depletion and recovery in cat sympathetic ganglia electrically stimulated in vivo. Evidence for transmitter secretion by exocytosis. *J Cell Biol* *60*, 365-374.
- Quintana, A., Schwindling, C., Wenning, A.S., Becherer, U., Rettig, J., Schwarz, E.C., and Hoth, M. (2007). T cell activation requires mitochondrial translocation to the immunological synapse. *Proc Natl Acad Sci U S A* *104*, 14418-14423.
- Ramamoorthy, P., Wang, Q., and Whim, M.D. (2011). Cell type-dependent trafficking of neuropeptide Y-containing dense core granules in CNS neurons. *J Neurosci* *31*, 14783-14788.
- Ransom, B.R., Christian, C.N., Bullock, P.N., and Nelson, P.G. (1977a). Mouse spinal cord in cell culture. II. Synaptic activity and circuit behavior. *J Neurophysiol* *40*, 1151-1162.
- Ransom, B.R., Neale, E., Henkart, M., Bullock, P.N., and Nelson, P.G. (1977b). Mouse spinal cord in cell culture. I. Morphology and intrinsic neuronal electrophysiologic properties. *J Neurophysiol* *40*, 1132-1150.
- Regehr, W.G., Carey, M.R., and Best, A.R. (2009). Activity-dependent regulation of synapses by retrograde messengers. *Neuron* *63*, 154-170.
- Regnier-Vigouroux, A., Tooze, S.A., and Huttner, W.B. (1991). Newly synthesized synaptophysin is transported to synaptic-like microvesicles via constitutive secretory vesicles and the plasma membrane. *EMBO J* *10*, 3589-3601.
- Reid, G., and Flonta, M.L. (2001). Physiology. Cold current in thermoreceptive neurons. *Nature* *413*, 480.



- Renden, R., Berwin, B., Davis, W., Ann, K., Chin, C.T., Kreber, R., Ganetzky, B., Martin, T.F., and Broadie, K. (2001). *Drosophila* CAPS is an essential gene that regulates dense-core vesicle release and synaptic vesicle fusion. *Neuron* 31, 421-437.
- Reynolds, M., Alvares, D., Middleton, J., and Fitzgerald, M. (1997). Neonatally wounded skin induces NGF-independent sensory neurite outgrowth in vitro. *Brain Res Dev Brain Res* 102, 275-283.
- Richter, K., Langnaese, K., Kreutz, M.R., Olias, G., Zhai, R., Scheich, H., Garner, C.C., and Gundelfinger, E.D. (1999). Presynaptic cytomatrix protein bassoon is localized at both excitatory and inhibitory synapses of rat brain. *J Comp Neurol* 408, 437-448.
- Rizo, J., and Rosenmund, C. (2008). Synaptic vesicle fusion. *Nat Struct Mol Biol* 15, 665-674.
- Rizo, J., and Xu, J. (2015). The Synaptic Vesicle Release Machinery. *Annu Rev Biophys* 44, 339-367.
- Robert D. Burgoyne, A.M. (1993). Regulated exocytosis. *Biochem J* 293, 305-316.
- Royle, S.J., Granseth, B., Odermatt, B., Drevier, A., and Lagnado, L. (2008). Imaging phluorin-based probes at hippocampal synapses. *Methods Mol Biol* 457, 293-303.
- Russo, A.F., Kuburas, A., Kaiser, E.A., Raddant, A.C., and Recober, A. (2009). A Potential Preclinical Migraine Model: CGRP-Sensitized Mice. *Mol Cell Pharmacol* 1, 264-270.
- Ryan, S., Blyth, P., Duggan, N., Wild, M., and Al-Ali, S. (2007). Is the cranial accessory nerve really a portion of the accessory nerve? Anatomy of the cranial nerves in the jugular foramen. *Anat Sci Int* 82, 1-7.
- Sadakata, T., and Furuichi, T. (2009). Developmentally regulated Ca<sup>2+</sup>-dependent activator protein for secretion 2 (CAPS2) is involved in BDNF secretion and is associated with autism susceptibility. *Cerebellum* 8, 312-322.
- Sadakata, T., Itakura, M., Kozaki, S., Sekine, Y., Takahashi, M., and Furuichi, T. (2006). Differential distributions of the Ca<sup>2+</sup>-dependent activator protein for secretion family proteins (CAPS2 and CAPS1) in the mouse brain. *J Comp Neurol* 495, 735-753.
- Sadakata, T., Kakegawa, W., Shinoda, Y., Hosono, M., Katoh-Semba, R., Sekine, Y., Sato, Y., Tanaka, M., Iwasato, T., Itohara, S., *et al.* (2013). CAPS1 deficiency perturbs dense-core vesicle trafficking and Golgi structure and reduces presynaptic release probability in the mouse brain. *J Neurosci* 33, 17326-17334.
- Sadakata, T., Mizoguchi, A., Sato, Y., Katoh-Semba, R., Fukuda, M., Mikoshiba, K., and Furuichi, T. (2004). The secretory granule-associated protein CAPS2 regulates neurotrophin release and cell survival. *J Neurosci* 24, 43-52.
- Sadakata, T., Sekine, Y., Oka, M., Itakura, M., Takahashi, M., and Furuichi, T. (2012). Calcium-dependent activator protein for secretion 2 interacts with the class II ARF small GTPases and regulates dense-core vesicle trafficking. *FEBS J* 279, 384-394.
- Sadakata, T., Washida, M., Iwayama, Y., Shoji, S., Sato, Y., Ohkura, T., Katoh-Semba, R., Nakajima, M., Sekine, Y., Tanaka, M., *et al.* (2007a). Autistic-like phenotypes in *Cadps2*-knockout mice and aberrant CADPS2 splicing in autistic patients. *J Clin Invest* 117, 931-943.
- Sadakata, T., Washida, M., Morita, N., and Furuichi, T. (2007b). Tissue distribution of Ca<sup>2+</sup>-dependent activator protein for secretion family members CAPS1 and CAPS2 in mice. *J Histochem Cytochem* 55, 301-311.
- Saeed, A.W., and Ribeiro-da-Silva, A. (2012). Non-peptidergic primary afferents are presynaptic to neurokinin-1 receptor immunoreactive lamina I projection neurons in rat spinal cord. *Mol Pain* 8, 64.

- Sankaranarayanan, S., and Ryan, T.A. (2000). Real-time measurements of vesicle-SNARE recycling in synapses of the central nervous system. *Nat Cell Biol* 2, 197-204.
- Scarfone, E., Dememes, D., Jahn, R., De Camilli, P., and Sans, A. (1988). Secretory function of the vestibular nerve calyx suggested by presence of vesicles, synapsin I, and synaptophysin. *J Neurosci* 8, 4640-4645.
- Schafer, M.K., Mahata, S.K., Stroth, N., Eiden, L.E., and Weihe, E. (2010). Cellular distribution of chromogranin A in excitatory, inhibitory, aminergic and peptidergic neurons of the rodent central nervous system. *Regul Pept* 165, 36-44.
- Schlicker, E., and Kathmann, M. (2008). Presynaptic neuropeptide receptors. *Handb Exp Pharmacol*, 409-434.
- Schonn, J.S., Maximov, A., Lao, Y., Sudhof, T.C., and Sorensen, J.B. (2008). Synaptotagmin-1 and -7 are functionally overlapping Ca<sup>2+</sup> sensors for exocytosis in adrenal chromaffin cells. *Proc Natl Acad Sci U S A* 105, 3998-4003.
- Scott, A., Hasegawa, H., Sakurai, K., Yaron, A., Cobb, J., and Wang, F. (2011). Transcription factor short stature homeobox 2 is required for proper development of tropomyosin-related kinase B-expressing mechanosensory neurons. *J Neurosci* 31, 6741-6749.
- Scott, B.S. (1977). Adult mouse dorsal root ganglia neurons in cell culture. *J Neurobiol* 8, 417-427.
- Segond von Banchet, G., Pastor, A., Biskup, C., Schlegel, C., Benndorf, K., and Schaible, H.G. (2002). Localization of functional calcitonin gene-related peptide binding sites in a subpopulation of cultured dorsal root ganglion neurons. *Neuroscience* 110, 131-145.
- Shaner, N.C., Lin, M.Z., McKeown, M.R., Steinbach, P.A., Hazelwood, K.L., Davidson, M.W., and Tsien, R.Y. (2008). Improving the photostability of bright monomeric orange and red fluorescent proteins. *Nat Methods* 5, 545-551.
- Shepherd, I.T., Luo, Y., Lefcort, F., Reichardt, L.F., and Raper, J.A. (1997). A sensory axon repellent secreted from ventral spinal cord explants is neutralized by antibodies raised against collapsin-1. *Development* 124, 1377-1385.
- Shinoda, Y., Sadakata, T., Nakao, K., Katoh-Semba, R., Kinameri, E., Furuya, A., Yanagawa, Y., Hirase, H., and Furuichi, T. (2011). Calcium-dependent activator protein for secretion 2 (CAPS2) promotes BDNF secretion and is critical for the development of GABAergic interneuron network. *Proc Natl Acad Sci U S A* 108, 373-378.
- Sieburth, D., Madison, J.M., and Kaplan, J.M. (2007). PKC-1 regulates secretion of neuropeptides. *Nat Neurosci* 10, 49-57.
- Silverman, J.D., and Kruger, L. (1990). Selective neuronal glycoconjugate expression in sensory and autonomic ganglia: relation of lectin reactivity to peptide and enzyme markers. *J Neurocytol* 19, 789-801.
- Sivilotti, L., and Woolf, C.J. (1994). The contribution of GABAA and glycine receptors to central sensitization: disinhibition and touch-evoked allodynia in the spinal cord. *J Neurophysiol* 72, 169-179.
- Slezak, M., and Pfrieder, F.W. (2003). New roles for astrocytes: regulation of CNS synaptogenesis. *Trends Neurosci* 26, 531-535.
- Snider, W.D., and McMahon, S.B. (1998). Tackling pain at the source: new ideas about nociceptors. *Neuron* 20, 629-632.
- Sollner, T., Bennett, M.K., Whiteheart, S.W., Scheller, R.H., and Rothman, J.E. (1993). A protein assembly-disassembly pathway in vitro that may correspond to sequential steps of synaptic vesicle docking, activation, and fusion. *Cell* 75, 409-418.

- Speese, S., Petrie, M., Schuske, K., Ailion, M., Ann, K., Iwasaki, K., Jorgensen, E.M., and Martin, T.F. (2007). UNC-31 (CAPS) is required for dense-core vesicle but not synaptic vesicle exocytosis in *Caenorhabditis elegans*. *J Neurosci* 27, 6150-6162.
- Speidel, D., Bruederle, C.E., Enk, C., Voets, T., Varoqueaux, F., Reim, K., Becherer, U., Fornai, F., Ruggieri, S., Holighaus, Y., *et al.* (2005). CAPS1 regulates catecholamine loading of large dense-core vesicles. *Neuron* 46, 75-88.
- Speidel, D., Salehi, A., Obermueller, S., Lundquist, I., Brose, N., Renstrom, E., and Rorsman, P. (2008). CAPS1 and CAPS2 regulate stability and recruitment of insulin granules in mouse pancreatic beta cells. *Cell Metab* 7, 57-67.
- Speidel, D., Varoqueaux, F., Enk, C., Nojiri, M., Grishanin, R.N., Martin, T.F., Hofmann, K., Brose, N., and Reim, K. (2003). A family of Ca<sup>2+</sup>-dependent activator proteins for secretion: comparative analysis of structure, expression, localization, and function. *J Biol Chem* 278, 52802-52809.
- Stucky, C.L., and Lewin, G.R. (1999). Isolectin B(4)-positive and -negative nociceptors are functionally distinct. *J Neurosci* 19, 6497-6505.
- Sudhof, T.C. (2004). The synaptic vesicle cycle. *Annu Rev Neurosci* 27, 509-547.
- Sutton, R.B., Fasshauer, D., Jahn, R., and Brunger, A.T. (1998). Crystal structure of a SNARE complex involved in synaptic exocytosis at 2.4 Å resolution. *Nature* 395, 347-353.
- Swett, J.E., and Woolf, C.J. (1985). The somatotopic organization of primary afferent terminals in the superficial laminae of the dorsal horn of the rat spinal cord. *J Comp Neurol* 231, 66-77.
- Szucs, P., Polgar, E., Spigelman, I., Porszasz, R., and Nagy, I. (1999). Neurokinin-1 receptor expression in dorsal root ganglion neurons of young rats. *J Peripher Nerv Syst* 4, 270-278.
- Taherzadeh, O., Otto, W.R., Anand, U., Nanchahal, J., and Anand, P. (2003). Influence of human skin injury on regeneration of sensory neurons. *Cell Tissue Res* 312, 275-280.
- Takeda, Y., Chou, K.B., Takeda, J., Sachais, B.S., and Krause, J.E. (1991). Molecular cloning, structural characterization and functional expression of the human substance P receptor. *Biochem Biophys Res Commun* 179, 1232-1240.
- Tandon, A., Bannykh, S., Kowalchuk, J.A., Banerjee, A., Martin, T.F., and Balch, W.E. (1998). Differential regulation of exocytosis by calcium and CAPS in semi-intact synaptosomes. *Neuron* 21, 147-154.
- Tang, Y., Garson, K., Li, L., and Vanderhyden, B.C. (2015). Optimization of lentiviral vector production using polyethylenimine-mediated transfection. *Oncol Lett* 9, 55-62.
- Tao, H.W., and Poo, M. (2001). Retrograde signaling at central synapses. *Proc Natl Acad Sci U S A* 98, 11009-11015.
- Thibault, K., Lin, W.K., Rancillac, A., Fan, M., Snollaerts, T., Sordoullet, V., Hamon, M., Smith, G.M., Lenkei, Z., and Pezet, S. (2014). BDNF-dependent plasticity induced by peripheral inflammation in the primary sensory and the cingulate cortex triggers cold allodynia and reveals a major role for endogenous BDNF as a tuner of the affective aspect of pain. *J Neurosci* 34, 14739-14751.
- Tiscornia, G., Singer, O., and Verma, I.M. (2006). Production and purification of lentiviral vectors. *Nat Protoc* 1, 241-245.
- Todd, A.J. (2010). Neuronal circuitry for pain processing in the dorsal horn. *Nat Rev Neurosci* 11, 823-836.

- Todd, A.J., Puskas, Z., Spike, R.C., Hughes, C., Watt, C., and Forrest, L. (2002). Projection neurons in lamina I of rat spinal cord with the neurokinin 1 receptor are selectively innervated by substance p-containing afferents and respond to noxious stimulation. *J Neurosci* 22, 4103-4113.
- tom Dieck, S., Sanmarti-Vila, L., Langnaese, K., Richter, K., Kindler, S., Soyke, A., Wex, H., Smalla, K.H., Kampf, U., Franzer, J.T., *et al.* (1998). Bassoon, a novel zinc-finger CAG/glutamine-repeat protein selectively localized at the active zone of presynaptic nerve terminals. *J Cell Biol* 142, 499-509.
- Toonen, R.F., Kochubey, O., de Wit, H., Gulyas-Kovacs, A., Konijnenburg, B., Sorensen, J.B., Klingauf, J., and Verhage, M. (2006). Dissecting docking and tethering of secretory vesicles at the target membrane. *EMBO J* 25, 3725-3737.
- Trimble, W.S., Cowan, D.M., and Scheller, R.H. (1988). VAMP-1: a synaptic vesicle-associated integral membrane protein. *Proc Natl Acad Sci U S A* 85, 4538-4542.
- Tuchscherer, M.M., and Seybold, V.S. (1985). Immunohistochemical studies of substance P, cholecystokinin-octapeptide and somatostatin in dorsal root ganglia of the rat. *Neuroscience* 14, 593-605.
- Usoskin, D., Furlan, A., Islam, S., Abdo, H., Lonnerberg, P., Lou, D., Hjerling-Leffler, J., Haeggstrom, J., Kharchenko, O., Kharchenko, P.V., *et al.* (2015). Unbiased classification of sensory neuron types by large-scale single-cell RNA sequencing. *Nat Neurosci* 18, 145-153.
- van de Bospoort, R., Farina, M., Schmitz, S.K., de Jong, A., de Wit, H., Verhage, M., and Toonen, R.F. (2012). Munc13 controls the location and efficiency of dense-core vesicle release in neurons. *J Cell Biol* 199, 883-891.
- Vigna, E., and Naldini, L. (2000). Lentiviral vectors: excellent tools for experimental gene transfer and promising candidates for gene therapy. *J Gene Med* 2, 308-316.
- Vitale, N., Chasserot-Golaz, S., Bailly, Y., Morinaga, N., Frohman, M.A., and Bader, M.F. (2002). Calcium-regulated exocytosis of dense-core vesicles requires the activation of ADP-ribosylation factor (ARF)6 by ARF nucleotide binding site opener at the plasma membrane. *J Cell Biol* 159, 79-89.
- Vogl, C., Cooper, B.H., Neef, J., Wojcik, S.M., Reim, K., Reisinger, E., Brose, N., Rhee, J.S., Moser, T., and Wichmann, C. (2015). Unconventional molecular regulation of synaptic vesicle replenishment in cochlear inner hair cells. *J Cell Sci* 128, 638-644.
- Wake, H., Ortiz, F.C., Woo, D.H., Lee, P.R., Angulo, M.C., and Fields, R.D. (2015). Nonsynaptic junctions on myelinating glia promote preferential myelination of electrically active axons. *Nat Commun* 6, 7844.
- Walent, J.H., Porter, B.W., and Martin, T.F. (1992). A novel 145 kd brain cytosolic protein reconstitutes Ca(2+)-regulated secretion in permeable neuroendocrine cells. *Cell* 70, 765-775.
- Wang, H., Rivero-Melian, C., Robertson, B., and Grant, G. (1994). Transganglionic transport and binding of the isolectin B4 from *Griffonia simplicifolia* I in rat primary sensory neurons. *Neuroscience* 62, 539-551.
- Wang, H., and Zylka, M.J. (2009). Mrgprd-expressing polymodal nociceptive neurons innervate most known classes of substantia gelatinosa neurons. *J Neurosci* 29, 13202-13209.
- Weissner, W., Winterson, B.J., Stuart-Tilley, A., Devor, M., and Bove, G.M. (2006). Time course of substance P expression in dorsal root ganglia following complete spinal nerve transection. *J Comp Neurol* 497, 78-87.
- Wiedenmann, B., Lawley, K., Grund, C., and Branton, D. (1985). Solubilization of proteins from bovine brain coated vesicles by protein perturbants and Triton X-100. *J Cell Biol* 101, 12-18.

- Wilson, D.W., Wilcox, C.A., Flynn, G.C., Chen, E., Kuang, W.J., Henzel, W.J., Block, M.R., Ullrich, A., and Rothman, J.E. (1989). A fusion protein required for vesicle-mediated transport in both mammalian cells and yeast. *Nature* 339, 355-359.
- Woolf, C.J., and Ma, Q. (2007). Nociceptors--noxious stimulus detectors. *Neuron* 55, 353-364.
- Xu, B., Gottschalk, W., Chow, A., Wilson, R.I., Schnell, E., Zang, K., Wang, D., Nicoll, R.A., Lu, B., and Reichardt, L.F. (2000). The role of brain-derived neurotrophic factor receptors in the mature hippocampus: modulation of long-term potentiation through a presynaptic mechanism involving TrkB. *J Neurosci* 20, 6888-6897.
- Yaksh, T.L., Hua, X.Y., Kalcheva, I., Nozaki-Taguchi, N., and Marsala, M. (1999). The spinal biology in humans and animals of pain states generated by persistent small afferent input. *Proc Natl Acad Sci U S A* 96, 7680-7686.
- Yang, Z., Li, H., Chai, Z., Fullerton, M.J., Cao, Y., Toh, B.H., Funder, J.W., and Liu, J.P. (2001). Dynamin II regulates hormone secretion in neuroendocrine cells. *J Biol Chem* 276, 4251-4260.
- Yoon, Y.W., Na, H.S., and Chung, J.M. (1996). Contributions of injured and intact afferents to neuropathic pain in an experimental rat model. *Pain* 64, 27-36.
- Yu, H., Pan, B., Weyer, A., Wu, H.E., Meng, J., Fischer, G., Vilceanu, D., Light, A.R., Stucky, C., Rice, F.L., *et al.* (2015). CaMKII Controls Whether Touch Is Painful. *J Neurosci* 35, 14086-14102.
- Zeilhofer, H.U., Wildner, H., and Yevenes, G.E. (2012). Fast synaptic inhibition in spinal sensory processing and pain control. *Physiol Rev* 92, 193-235.
- Zhang, C., and Zhou, Z. (2002). Ca(2+)-independent but voltage-dependent secretion in mammalian dorsal root ganglion neurons. *Nat Neurosci* 5, 425-430.
- Zhao-Wen, W. (2008). *Molecular Mechanisms of Neurotransmitter Release*. Springer-Verlag.
- Zhou, K.M., Dong, Y.M., Ge, Q., Zhu, D., Zhou, W., Lin, X.G., Liang, T., Wu, Z.X., and Xu, T. (2007). PKA activation bypasses the requirement for UNC-31 in the docking of dense core vesicles from *C. elegans* neurons. *Neuron* 56, 657-669.

